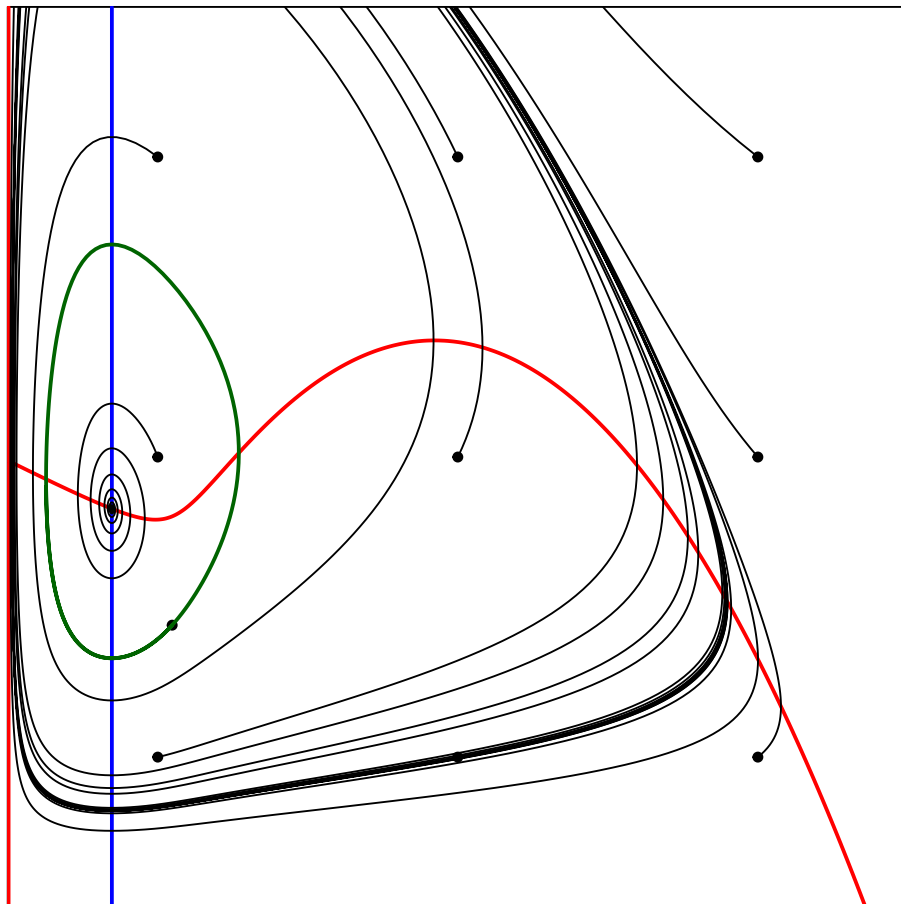


# Biological Modeling of Populations

## 2025



Rob J. de Boer

Theoretical Biology & Bioinformatics

Utrecht University



Ebook publicly available at [tbb.bio.uu.nl/rdb/books/bm.pdf](https://tbb.bio.uu.nl/rdb/books/bm.pdf) and [books/bmAnswers.pdf](https://tbb.bio.uu.nl/rdb/books/bmAnswers.pdf). The figure on the cover depicts a phase plane with nullclines (in red and blue), trajectories (black), and an unstable limit cycle (green), and was made with the R-script <https://tbb.bio.uu.nl/rdb/bm/models/hyper.R>.

© Utrecht University, 2025: Feel free to use material from this book but please cite its source.



# Contents

<b>1</b>	<b>Preface</b>	<b>1</b>
<b>2</b>	<b>Introduction</b>	<b>3</b>
2.1	The simplest possible model for a huge problem . . . . .	3
2.2	Exponential growth and decay . . . . .	5
2.3	Summary . . . . .	6
2.4	Exercises . . . . .	7
<b>3</b>	<b>Density dependence</b>	<b>11</b>
3.1	Negative density dependence . . . . .	12
3.2	Logistic growth and our assumptions . . . . .	15
3.3	Non-linear density-dependence . . . . .	17
3.4	Positive density dependence . . . . .	20
3.5	Summary . . . . .	21
3.6	Exercises . . . . .	22
<b>4</b>	<b>Stability and return time</b>	<b>29</b>
4.1	Stability defined by the local slope of the growth function . . . . .	29
4.2	Linearization . . . . .	30
4.3	Return time . . . . .	32
4.4	Basins of attraction . . . . .	33
4.5	Summary . . . . .	34
4.6	Exercises . . . . .	34
<b>5</b>	<b>Killing and consumption</b>	<b>37</b>
5.1	Bacteria in chemostats . . . . .	38
5.2	Replicating resources . . . . .	42
5.3	Horizontal and vertical nullclines . . . . .	45
5.4	Summary . . . . .	47
5.5	Exercises . . . . .	48
<b>6</b>	<b>The basic reproductive ratio <math>R_0</math></b>	<b>53</b>
6.1	The SIR model . . . . .	53
6.2	The SEIR model . . . . .	55
6.3	Fitness in consumer-resource models . . . . .	56
6.4	Summary . . . . .	57
6.5	Exercises . . . . .	58
<b>7</b>	<b>Functional response</b>	<b>61</b>
7.1	Monod functional response . . . . .	62
7.2	Sigmoid functional response . . . . .	67
7.3	2-dimensional functional response functions . . . . .	72

7.4	Summary . . . . .	77
7.5	Exercises . . . . .	77
<b>8</b>	<b>Modeling chains</b>	<b>83</b>
8.1	A 3-dimensional Lotka-Volterra chain . . . . .	84
8.2	Chains with saturating interacting terms . . . . .	85
8.3	Other famous chain models . . . . .	87
8.4	Summary . . . . .	89
8.5	Exercises . . . . .	89
<b>9</b>	<b>Competition</b>	<b>93</b>
9.1	Competitive exclusion . . . . .	93
9.2	Adding explicit resource dynamics . . . . .	95
9.3	The Lotka-Volterra competition model . . . . .	98
9.4	Several consumers on two resources . . . . .	100
9.5	Essential Resources . . . . .	103
9.6	Summary . . . . .	104
9.7	Exercises . . . . .	105
<b>10</b>	<b>Co-existence in large communities</b>	<b>111</b>
10.1	Niche space models . . . . .	111
10.2	Stability and Persistence . . . . .	115
10.3	Random assembly . . . . .	117
10.4	Neutral coexistence . . . . .	122
10.5	Cross-feeding . . . . .	122
10.6	Summary . . . . .	124
10.7	Exercises . . . . .	124
<b>11</b>	<b>Maps</b>	<b>129</b>
11.1	Stability . . . . .	129
11.2	Deriving a map mechanistically . . . . .	132
11.3	Eggs produced during the season . . . . .	135
11.4	Summary . . . . .	136
11.5	Exercises . . . . .	136
<b>12</b>	<b>Bifurcation analysis</b>	<b>137</b>
12.1	Hopf bifurcation . . . . .	137
12.2	Transcritical bifurcation . . . . .	140
12.3	Saddle node bifurcation . . . . .	140
12.4	Pitchfork bifurcation . . . . .	142
12.5	Period doubling cascade leading to chaos . . . . .	143
12.6	Summary . . . . .	146
12.7	Exercises . . . . .	146
<b>13</b>	<b>Numerical exercises</b>	<b>149</b>
13.1	Grind . . . . .	149
13.2	Numerical exercises . . . . .	150
<b>14</b>	<b>Make a model</b>	<b>155</b>
14.1	Exercises . . . . .	155
<b>15</b>	<b>Appendix: mathematical prerequisites</b>	<b>157</b>
15.1	Phase plane analysis . . . . .	157

---

15.2 Linearization . . . . .	159
15.3 Convenient functions . . . . .	162
15.4 Scaling . . . . .	163
15.5 The resource nullcline with a sigmoid functional response . . . . .	164
15.6 A few useful mathematical formulas . . . . .	165
15.7 Parameter estimation . . . . .	167
15.8 Gillespie algorithm . . . . .	169
15.9 Kinetic proofreading . . . . .	170
15.10 Tilman diagrams: the 4-dimensional Jacobian . . . . .	171
15.11 Exercises . . . . .	173



# Chapter 1

## Preface

This book is an introduction into modeling populations in biology. We will make mathematical models for populations of bacteria, cells, hosts with parasites, and predators with their prey. Models are formulated in terms of ordinary differential equations (ODEs), and we will see that these ODEs for different biological systems often resemble one another. The book covers the material of a course given to undergraduate biology students at Utrecht University, and aims at teaching these students how to make and use simple mathematical models in biological research. There are several other textbooks on this subject, and some unique features of this particular book are: (1) an emphasis on “parameter free” models and phase plane analysis, (2) the usage of the epidemiological concept of an  $R_0$  (or fitness) to simplify parameter conditions, and (3) a mechanistic “graphical” approach for model development.

The last point is most important. Rather than just explaining the classic models, we will attempt to devise a model ourselves by translating the relevant biological processes, like immigration, birth, death, infection and killing, into intuitive graphs depicting how each process depends on the population densities. These graphs are subsequently translated into simple mathematical functions, and by collecting these functions into a system of differential equations we obtain a “mechanistic” mathematical model that explicitly depends on its underlying biological processes. Finally, we will compare our “mechanistic” model with the typically more “phenomenological” classic models covered in other textbooks.

What is the reason for this rather laborious procedure for explaining models to students? I think it is important that biologists can identify each term in a mathematical model with an underlying biological process for which they have some knowledge, or at least some intuition. For example, one often needs biological insight to know how, or even whether, birth, death and interaction rates depend on the population size, as the results obtained with a model are likely to depend on these assumptions. By identifying differences between models based upon different assumptions we learn to become critical readers of mathematical models, and learn to be careful with the necessary assumptions one has to make when modeling an interesting biological system.

A second emphasis of this book is on phase plane analysis, which means that we sketch nullclines and trajectories, either by hand or by computer. Phase plane analysis allows one to visualize the potential steady states of a model, and to determine their stability (again by hand or by computer software). Phase plane analysis is a relatively simple technique that is easily accessible to motivated biology students. Most pictures in this book are made an R-software package called Grind, which is good at drawing nullclines, finding steady states, and numerical integration.

During the course students work extensively with Grind, and the R-scripts used for making the figures in this book are available on the website [tbb.bio.uu.nl/rdb/bm/models/](http://tbb.bio.uu.nl/rdb/bm/models/).

Because the parameter values of biological models are typically unknown, there is a strong emphasis in this book on analyzing models with free parameters. This has the enormous advantage that the results will be general, and that we do not run the risk of ignoring possibilities that may occur for different parameter settings. Most pictures in this book therefore have no numbers along the axes (except for zero and one); rather they have parameter expressions for the points of interest. Such expressions in terms of parameters will be simplified using the epidemiological concept reproduction ratio,  $R_0$ , and the ecological concept “critical resource density”,  $R^*$ . Simplification typically increases our understanding of the underlying biology.

The expected audience of this book is students of biology and ecology. Too many biologists treat a mathematical model as a “black box” that is too difficult to understand. A main objective of this course is to open the black box and teach biology students how to develop simple mathematical models themselves. This allows for a much better understanding, and for a healthy critical attitude toward the existing models in the field. This course therefore only covers simple caricature models that are designed to capture the essentials of the biological problem at hand. Such simple models can be completely understood, and therefore allow for excellent insight and provide new ideas about the biological problem (May, 2004). Other areas of theoretical biology are about large-scale simulation models that are designed to summarize the existing knowledge about a particular system, like the metabolism of a whole cell, or the nutrient flow in a complete ecosystem. Investigators use such large models for predicting the behavior of the biological system, e.g., when circumstances are changing. Simple caricature models cannot predict what *will* happen, but importantly they are much better at predicting what *could* happen. Although large-scale models are not covered in this book, the material covered in this course should also be useful for students interested in developing large realistic models. First, small modules within the large models should be developed by the same mechanistic process that we here use for simple models. Second, it is a sobering lesson to let oneself be surprised by the sometimes unexpected behavior of simple toy models. This lesson is equally important for scholars developing large-scale models by combing many such simple models.

Readers are expected to be familiar with phase space analysis, i.e., should know how to sketch nullclines and solve simple algebraic equations. We provide a set of tutorials on [tbb.bio.uu.nl/rdb/bm/videos.html](http://tbb.bio.uu.nl/rdb/bm/videos.html) that can be used to catch up on these topics. During the course we will use Jacobi matrices for performing stability analysis, and this will be explained in the beginning of the course using the accompanying ebook by Panfilov *et al.* (2025). The course comes with a set of webpages that can be reached via the home page [tbb.bio.uu.nl/rdb/bm/](http://tbb.bio.uu.nl/rdb/bm/). The ebooks used in this course can be downloaded from [tbb.bio.uu.nl/rdb/books/](http://tbb.bio.uu.nl/rdb/books/) (the answers to the exercises of this book are in the file [books/bmAnswers.pdf](#)).

Finally, this book originated from a theoretical ecology course given decades ago by Paulien Hogeweg at Utrecht University. She taught me the strength of phase plane analysis and simple caricature models. After I started teaching this course its contents and presentation have evolved, and have been adapted to the questions, and the comments from numerous students attending this course.

## Chapter 2

# Introduction

This course is an introduction into theoretical biology for biology students. We will teach you how to make and analyze mathematical models, with the ultimate aim that you can critically judge the contributions the assumptions of existing models, and that you can devise useful novel models whenever you need them in your future biological research. Mathematical models are used in all areas of biology, and they are typically formulated in ordinary differential equations (ODEs). We will analyze such models by hand by sketching nullclines and computing steady states, and by letting a computer perform numerical integration and phase plane analysis. A major emphasis of this course is to develop differential equations by following a graphical procedure, depicting each biological process as a function of its relevant variable(s). Experience with devising mathematical models will help you to understand and evaluate models proposed by others.

This first chapter introduces some basic concepts underlying modeling with differential equations. You will become familiar with the notion of a “solution”, “steady state”, “half life”, and the “expected life span”. Concepts like solution and steady state are important because a differential equation describes the *change* of the population size, rather than its *actual size*. We will start with simple models that are only convenient to introduce these concepts. To keep models general they typically have free parameters, i.e., parameters are letters instead of numbers. Later models in the course are more challenging and more interesting.

### 2.1 The simplest possible model for a huge problem

Consider the amount of plastic,  $P$ , floating in the oceans. Since plastic decays very slowly,  $P$  increases more or less proportionally with the daily amount of plastic,  $k$ , that is dumped into the oceans. A current estimate for the world-wide dumping rate is 8 millions tons of plastic per year, i.e.,  $k = 2.17 \times 10^4$  ton per day. Knowing  $k$  we write the following mathematical model,

$$\frac{dP}{dt} = k , \tag{2.1}$$

which says that the variable  $P$  increases at a rate  $k$  per time unit (here per day). In this ODE  $P$  is a variable that changes over time, and the “dimension” of  $P$  is tons of plastic in the oceans. Formally one should write  $dP(t)/dt = k$ , because the variable  $P$  is a function of time, but for simplicity  $P(t)$  is abbreviated to  $P$ . The parameter  $k$  in this Eq. (2.1) here is a constant, with

dimension tons of plastic per day. Actually,  $k$  should also be increasing over time, as we have been dumping more and more plastics, but for simplicity we here consider a time period over which  $k$  is relatively constant (see the last question).

This equation is so simple that one can derive its general *solution*

$$P(t) = P(0) + kt , \quad (2.2)$$

where  $P(0)$  is the amount of plastic that was already in the ocean at the time we started dumping  $k$  tons per day. Plotting  $P(t)$  over time therefore gives a straight line with slope  $k$ , intersecting the vertical axis at  $P(0)$ . The slope of this line is  $k$ , which is indeed the derivative defined by Eq. (2.1). Thus, the differential equation Eq. (2.1) gives the “rate of change”, and the solution of Eq. (2.2) gives the “population size at time  $t$ ”. Note that the solution depends on both the initial condition,  $P(0)$ , and the parameter,  $k$ .

Typically, differential equations are too complicated for solving them explicitly, and their general solutions are not available. In this course we will therefore not consider the integration methods required for obtaining solutions of ODEs. However, having a solution one can easily check it by taking the derivative with respect to time. For example, the derivative of Eq. (2.2) with respect to time is  $\partial_t[P(0) + kt] = k$ , which is indeed the right hand side in Eq. (2.1). Summarizing, the solution in Eq. (2.2) gives the amount of plastic at time  $t$ , and Eq. (2.1) gives its daily rate of change. Note that if we were to take measures reducing the amount of plastic that streams into the ocean, we would only need to change the value of the parameter  $k$ . The model remains the same.

We can change the model by making it somewhat more realistic, e.g., by accounting for the fact that plastic in the ocean is decaying slowly, i.e., with a very long half-life. Defining a rate of decay,  $d$ , the model becomes

$$\frac{dP}{dt} = k - dP , \quad (2.3)$$

where the parameter  $d$  defines the rate at which individual plastic molecules decay.  $d$  has a dimension per day (or per unit of time), and therefore is called a “rate”. In the ODE this can be checked by observing that the term  $dP$  should have the same dimension “tons per day” as  $k$  (otherwise they cannot be subtracted from another). Biological examples of Eq. (2.3) would be red blood cells produced by bone marrow, shrimps being washed onto a beach, daily intake of vitamins, and so on. The  $k$  parameter then defines the inflow, or production, and the  $d$  parameter is a death rate. Although this seems a straightforward extension of Eq. (2.1), it is much more difficult to obtain the solution

$$P(t) = \frac{k}{d} \left(1 - e^{-dt}\right) + P(0)e^{-dt} , \quad (2.4)$$

which is depicted in Fig. 2.1a. The term on the right corresponds to the exponential loss of the initial value,  $P(0)$ . The term on the left is more complicated, but when evaluated at long time scales, i.e., for  $t \rightarrow \infty$ , the term  $(1 - e^{-dt})$  will approach one, and one obtains the “steady state”  $\bar{P} = k/d$ . We conclude that the solution of Eq. (2.4) ultimately approaches the steady state  $\bar{P} = k/d$ , which is ultimate amount of plastic in the oceans when we keep on dumping  $k$  tons per day. Note that this predicted steady state value is independent of the initial condition  $P(0)$ .

Fortunately, we do not always need a solution to understand the behavior of a model. The same steady state can also directly be obtained from the differential equation. Since a steady state means that the rate of change of the population is zero we set

$$\frac{dP}{dt} = k - dP = 0 \quad \text{to obtain} \quad \bar{P} = \frac{k}{d} . \quad (2.5)$$

which is the same value as obtained above from the solution for  $t \rightarrow \infty$ . Note that a steady state also gives a population size, and therefore provides some insight in the behavior of the model. For instance, the steady state  $\bar{P} = k/d$  predicts that if we were to half the amount of plastic that we dump in the oceans the world-wide burden of plastic would also half. The decay rate only determines how slowly this halved burden would be approached. If we could double the decay rate by using plastics with a shorter half-life, the steady state would also be halved, and would be approached two-fold faster.

## 2.2 Exponential growth and decay

Above we have already used the term half-life, and having the model of Eq. (2.3) we can precisely define what we mean by this. Consider the situation that we completely abandon the usage of plastic, and the current amount of plastic,  $P(0)$ , is slowly decaying. To study this we do not need to change the model, we just set  $k = 0$ , to be left with  $dP/dt = -dP$ . This is the famous equation for exponential decay of radioactive particles, with the almost equally famous solution  $P(t) = P(0)e^{-dt}$ , saying that ultimately, i.e., for  $t \rightarrow \infty$ , the amount of plastic,  $P(t)$ , will approach zero. Plotting the natural logarithm of  $P(t)$  as a function of time would give a straight line with slope  $-d$  per day (because  $\ln[P(0)e^{-dt}] = \ln[P(0)] - dt$ ). This exponential decay equation allows us to introduce two important concepts: the half-life and the expected life span. The half-life is defined as the time it takes to loose half of the initial population, and is defined by the solution,  $P(t) = P(0)e^{-dt}$ , i.e.,

$$\frac{P(0)}{2} = P(0)e^{-dt} \quad \text{which simplifies into} \quad \ln \frac{1}{2} = -dt \quad \text{or} \quad t = \frac{\ln 2}{d}. \quad (2.6)$$

Since  $\ln 2 \simeq 0.69$  the half life is approximately  $0.69/d$  days. Note that the dimension is correct: a half life indeed has dimension time because  $d$  is a rate with dimension  $\text{day}^{-1}$ . The other concept is expected life span: if radioactive particles or biological individuals have a probability  $d$  to die per unit of time, their expected life span is  $1/d$  time units. This is like throwing a die. If the probability to throw a four is  $1/6$ , the expected waiting time to get a four is six trials. Finally, note that this exponential decay model has only one steady state,  $\bar{P} = 0$ , and that this state is stable because it is approached at infinite time. A steady state with a population size of zero is often called a “trivial” steady state.

The opposite of exponential decay is exponential growth

$$\frac{dN}{dt} = rN \quad \text{with the solution} \quad N(t) = N(0)e^{rt}, \quad (2.7)$$

where the parameter  $r$  is known as the “natural rate of increase”. The solution can easily be checked: the derivative of  $N(0)e^{rt}$  with respect to  $t$  is  $rN(0)e^{rt} = rN(t)$ . Biological examples of this equation are the growth of mankind, the exponential growth of a pathogen in a host, the growth of a tumor, and so on. Similar to the half life defined above, one can define a doubling time for populations that are growing exponentially:

$$2N(0) = N(0)e^{rt} \quad \text{gives} \quad \ln 2 = rt \quad \text{or} \quad t = \ln[2]/r. \quad (2.8)$$

This model also has only one steady state,  $\bar{N} = 0$ , which is unstable because any small perturbation above  $N = 0$  will initiate unlimited growth of the population. To obtain a non-trivial (or non-zero) steady state population size in populations maintaining themselves by reproduction one therefore needs density dependent birth or death rates. This is the subject of the next chapter.

In replicating biological populations, this natural rate of increase of  $dN/dt = rN$  should obviously be a composite of birth and death rates. A more natural model for a biological population that grows exponentially therefore is

$$\frac{dN}{dt} = (b - d)N \quad \text{with solution} \quad N(t) = N(0)e^{(b-d)t}, \quad (2.9)$$

where  $b$  is a birth rate with dimension  $t^{-1}$ , and  $d$  is the death rate with the same dimension. Writing the model with explicit birth and death rates has the advantage that the parameters of the model are strictly positive (which will be true for all parameters in this course). Moreover, one now knows that the “generation time” or “expected life span” is  $1/d$  time units. Since every individual has a birth rate of  $b$  new individuals per unit of time, and has an expected life span of  $1/d$  time units, the expected number of offspring of an individual over its entire life-span is  $R_0 = b/d$  (see Chapter 6). We will use this  $R_0$  as the maximum “fitness” of an individual, i.e., the life-time number of offspring expected under the best possible circumstances. In epidemiology the  $R_0$  is used for predicting the spread of an infectious disease: whenever  $R_0 < 1$  a disease will not be able to spread in a population because a single infected host is expected to be replaced by less than one newly infected host (Anderson & May, 1991); see Chapter 6.

Biological examples of Eq. (2.9) are mankind, the exponential growth of algae in a lake, and so on. Similarly, the natural rate of increase  $r = b - d$  yields a “doubling time” of  $t = \ln[2]/r$  time units. A famous example of the latter is the data from Malthus (1798) who investigated the birth records of a parish in the United Kingdom, and found that the local population had a doubling time of 30 years. Solving the natural rate of increase  $r$  per year from  $30 = \ln[2]/r$  yields  $r = \ln[2]/30 = 0.0231$  per year, which is sometimes expressed as a growth rate of 2.31% per year. More than 200 years later the global human growth rate is still approximately 2% per year. Exponential growth therefore seems a fairly realistic model to describe the growth of the quite complicated human population over a period of several centuries.

In this book we will give solutions of differential equations whenever they are known, but for most interesting models the solution is not known. We will therefore not explain how these solutions are obtained (see textbooks like the one by Adler (1997) for an overview of methods of integration). You can also use symbolic software like Mathematica to find the explicit solution of some of the differential equations used here.

Finally, it is important to realize that most models introduced in this book require a number of “unrealistic assumptions”: (1) all individuals within a population are equal, (2) each populations is well-mixed and can therefore be described with a single density, (3) population sizes are so large that we never have populations containing less than one member, and (4) typically parameters are constants that do not vary over time. We will see that such “unrealistic” models nevertheless help us to think clearly about the biology described by the model (May, 2004).

## 2.3 Summary

An ordinary differential equation (ODE) describes the rate of change of a population. The actual population size is given by the solution of the ODE, which is generally not available. To find the population size one can compute the steady state(s) of the model (the ODE), and/or solve the ODEs numerically on a computer, which gives the model behavior. Steady states are derived by setting the rate of change to zero, and solving for the actual population size. Doubling times and half-lives are solved from the solution of the exponential growth (or decay)

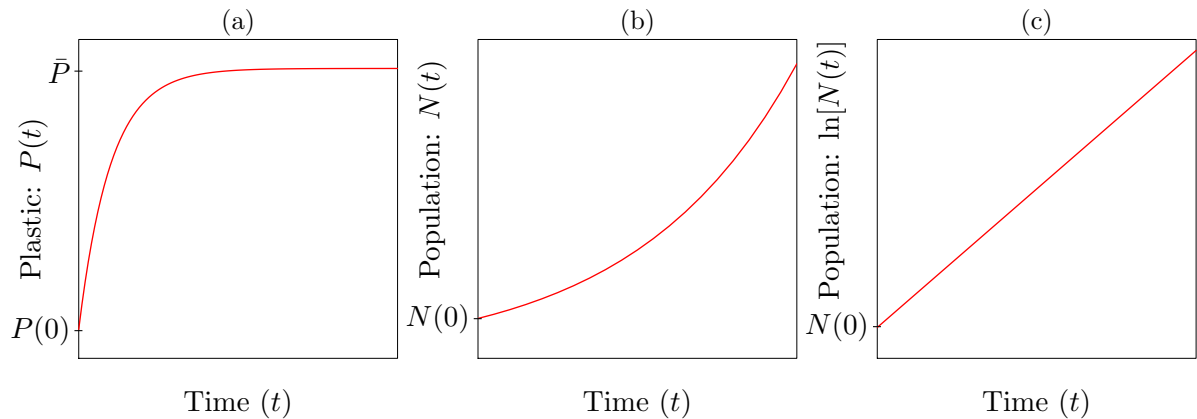


Figure 2.1: Population growth. Panel (a) depicts the solution of Eq. (2.4). Panels (b) and (c) depict exponential growth on a linear, and a logarithmic vertical axis, respectively. A differential equation describes the slope of the solution for each value of the variable(s), i.e., in Panel (b) the slope of the  $N(t) = N(0)e^{rt}$  curve for each value of  $N(t)$  is  $dN/dt = r$ . This figure was made with the model `intro.R`.

equation  $N(t) = N(0)e^{rt}$ . The fitness,  $R_0$ , of a population is the expected number of offspring of one individual over one generation, under the best possible circumstances.

## 2.4 Exercises

### Question 2.1. Red blood cells

Red blood cells are produced in the bone marrow at a rate of  $m$  cells per day. They have a density independent death rate of  $d$  per day.

- Which differential equation from this chapter would be a correct model for the population dynamics of red blood cells?
- Suppose you donate blood. Sketch your red blood cell count predicted by this model in a time plot.
- Suppose a sportsman increases his red blood cell count by receiving blood. Sketch a time plot of his red blood cell count.

### Question 2.2. Pesticide on apples

During their growth season apples are frequently sprayed with pesticide to prevent damage by insects. By eating apples you accumulate this pesticide in your body. An important factor determining the concentration of pesticide is their half life in the human body. An appropriate mathematical model is

$$\frac{dP}{dt} = \sigma - \delta P,$$

where  $\sigma$  is the daily intake of pesticide, i.e.,  $\sigma = \alpha A$  where  $A$  is the number of apples that you eat per day and  $\alpha$  is the amount of pesticide per apple, and  $\delta$  is the daily rate at which the pesticide decays in human tissues.

- Sketch the amount of pesticide in your body,  $P(t)$ , as a function of your age, assuming you eat the same number of apples throughout your life.
- How much pesticide do you ultimately accumulate after eating apples for decades?
- Suppose you have been eating apples for decades and stop because you are concerned about the unhealthy effects of the pesticide. How long does it take to reduce your pesticide level by 50%?

- d. Suppose you start eating two apples per day instead of just one. How will that change the model, and what is the new steady state? How long will it now take to reduce pesticide levels by 50% if you stop eating apples?
- e. What is the decay rate if the half-life is 50 days?

### Question 2.3. ATP

Although this book is not about modeling molecular biology, one can consider molecules as populations that are interacting via chemical reactions, and hence undergo population dynamics. A famous example is the turnover of ATP, the molecule providing energy to cells when it is hydrolyzed. The human body requires the hydrolysis of at least 60 kg of ATP per day to meet its energy needs, i.e., about our body weight per day, but the total amount of ATP in all cells of a 60 kg individual is about 60 g only. Since the total amount of ATP remains close to this steady state value, one would write

$$\frac{dA}{dt} = p - \delta A = 0 ,$$

where  $A$  is the total amount of ATP,  $p$  is the daily production of ATP by phosphorylation of ADP, and  $\delta$  is the daily turnover rate of ATP.

- a. What is the dimension of the production parameter  $p$ ?
- b. What is the steady state,  $\bar{A}$ , according to this model, and what does this tell you about the ratio  $p/\delta$ ?
- c. Knowing that we hydrolyze  $\delta A = 60 \times 10^3$  g of ATP per day, what would your estimate be for the turnover rate of ATP?

### Question 2.4. Bacterial growth

Every time you brush your teeth, bacteria enter your blood circulation. Since this a nutritious environment for them they immediately start to grow exponentially. Fortunately, we have neutrophils in our blood that readily kill bacteria upon encountering them. A first model would be:

$$\frac{dB}{dt} = rB - kNB ,$$

where  $B$  and  $N$  are the number of bacteria and neutrophils measured in a ml of blood,  $r$  is the growth rate of the bacteria (per hour), and  $k$  is the rate at which bacteria are killed by neutrophils.

- a. What is the doubling time of the bacteria in the absence of neutrophils?
- b. Neutrophils are short-lived cells produced in the bone marrow, and chemotherapy can markedly reduce the neutrophil counts in the peripheral blood. What is the critical number of neutrophils that is required to prevent rampant bacterial infections after chemotherapy?
- c. What is the dimension of the parameters  $r$  and  $k$ ?
- d. The  $kNB$  term is called a mass-action term because it is proportional to both the bacterial and the neutrophil densities. A disadvantage of such a term is that each neutrophil is assumed to kill an unrealistically large number of bacteria per hour,  $kB$ , if the bacterial density becomes very large. Later in the course we will use saturation functions to allow for maximum killing rates per killer cell. An example of such a model would be

$$\frac{dB}{dt} = rB - \frac{kNB}{h + B} ,$$

where the total number of bacteria killed per hour approaches  $kN$  when  $B \rightarrow \infty$  (please check this). What is now the dimension of  $k$ ?

- e. What is now the critical number of neutrophils that is required to prevent bacterial infections after chemotherapy? Can you sketch this?
- f. What is the dimension of  $h$ , and how would you interpret that parameter?

## Extra questions

### Question 2.5. Physics: a cup of tea

Newton's law of cooling describes that the rate of heat loss of a body is proportional to the difference in the temperatures between the body and its environment, and can be written as

$$\frac{dT}{dt} = c(T_E - T) ,$$

where  $T$  is the temperature of the object, e.g., a cup of tea, and  $T_E$  is the (constant) temperature of the environment. We have learned in this chapter that the solution is a function  $T(t)$  that has  $c(T_E - T(t))$  as its derivative. Note that this model is identical to Eq. (2.3) when we write  $k = cT_E$  and  $d = c$ , and hence that the solution is given by Eq. (2.4).

- What is the steady state temperature of the object?
- What is the dimension of the parameter  $c$ ?
- How many parameters does the model have?

### Question 2.6. Physics: acceleration

Consider the famous equation for velocity and acceleration,  $x(t) = \frac{1}{2}at^2 + v(0)t$ , and let us derive this from the ODEs,

$$\frac{dx}{dt} = v \quad \text{and} \quad \frac{dv}{dt} = a ,$$

where  $x$  is the total distance covered,  $v$  is the velocity, and  $a$  is the time derivative of the velocity, which is defined as the "acceleration". This is actually a simpler system than the model for Newton's law of cooling because the variables  $x$  and  $v$  only appear in the left hand sides of their ODEs, i.e., we do not need to find a function with a derivative depending on itself. Indeed, integrating  $dv/dt$  readily gives  $v(t) = at + v(0)$ , where the integration constant  $v(0)$  is the velocity at time zero, and integrating  $dx/dt = at + v(0)$  gives  $x(t) = \frac{1}{2}at^2 + v(0)t$ .

- Check the dimensions of the velocity,  $v$ , and the acceleration,  $a$ .
- In Eq. (2.1) we considered the case where we dump a fixed amount,  $k$ , of plastic in the oceans on a daily basis. Now consider the more realistic case where  $k(t)$  becomes a variable that increases linearly over time, i.e., write that  $dk/dt = a$ , where  $a$  is the slope with which  $k(t)$  increases. Starting at a time when  $k(0)$  tons of plastic was dumped per day, we write the solution  $k(t) = at + k(0)$ . What is the new ODE for the total amount of plastic in the oceans, and what is its solution?
- Do you expect the amount of plastic in the oceans to approach a (new) steady state?



## Chapter 3

# Density dependence

Populations change size by various biological processes, like migration, production, replication (birth), death and differentiation. Biological models tend to be complicated, and typically non-linear, because these processes often depend on the population size(s). This is a form of feedback that is called density dependence. In this chapter we will develop a number of models for the growth of a population, where at least one of these processes is regulated by the density of that population. Considering single populations, the models in the chapter will consist of only one ODE (i.e., they are one-dimensional), and what we will do is define functions describing how these biological processes depend on the population density. Using biological knowledge and intuition we will first sketch a reasonable curve describing this relationship (see Fig. 3.1). This curve is subsequently described with a simple mathematical function, and since we are aiming for non-dimensional functions, we can multiply such a function with the appropriate parameter of the model (and keep the dimensions of the model correct). This ultimately results in a model with density-dependent interaction terms each corresponding to a well-defined biological process. We will analyze the model by identifying steady states and by numerical integration. These results can then be compared with data and the corresponding classic models in the literature.

We have seen in Chapter 2 that non-replicating populations that are maintained by a fixed source term, and have a density-independent death rate, e.g., Eq. (2.3), will ultimately approach a stable steady state where the source balances the death. If such a population is perturbed it will return to the same steady state at a rate determined by the death rate (the inverse of this rate is called the “return time”, which we will address later in Chapter 4). This demonstrates that stable population densities can come about without having any regulation or feedbacks in the system. This is not true for the replicating population that we considered in Chapter 2 because the only steady state of Eq. (2.9) is  $N = 0$ . Whenever  $b > d$ , i.e., if the fitness  $R_0 > 1$ , this  $\bar{N} = 0$  equilibrium is unstable (see Chapter 4). If  $R_0 < 1$  the equilibrium is stable, and the population will ultimately go extinct (i.e., for  $t \rightarrow \infty$  the solution  $N(0)e^{(b-d)t} \rightarrow 0$  when  $d > b$ ). One could argue that Eq. (2.9) also has a steady state when  $b = d$ , but this is a untenable condition because the birth rate and the death rate would have to stay exactly the same over long time scales. (Technically speaking, one is solving for the variables, and not for the parameters).

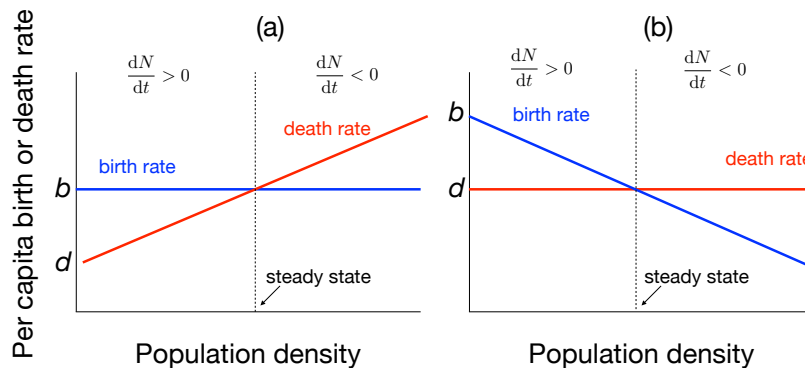


Figure 3.1: Examples of linear relationships between *per capita* birth and death rates and the population density. When the birth rate exceeds the death rate the population will grow ( $dN/dt > 0$ ). Steady states correspond to the intersection points where the birth rate equals the death rate.

### 3.1 Negative density dependence

At high population densities the availability of essential resources is typically low, and this is expected to result in a lower fecundity and/or higher death rates (see Fig. 3.1). This is called negative density dependence since both processes reduce the net population growth rate. Numerous examples from microorganisms and ecology illustrate that fecundity tends to decline with the population density (see Fig. 3.2 and Walker *et al.* (2009)). Similarly the contact inhibition of proliferation of cells growing in a monolayer, or as a tissue, plays a role in limiting the population size until the resource “space” is filled up (Wieser & Oesch, 1986). At high population densities, one also expects the death rates of cells or organisms to be high (although several microorganisms have evolved mechanisms to survive long periods of starvation (Phaiboun *et al.*, 2015)). Let us start by adding negative density-dependence to the birth and death processes of our basic models.

#### Density dependent death

If the death rate were to increase with the population size, the simplest model would be to have a linear increase of the *per capita* death rate with the population size (see Fig. 3.1a). A linear increase need not be realistic, as one could argue that death rates increase steeply at high densities, or alternatively that the death rate should approach a maximum at the highest densities. Choosing for a linear increase of the *per capita* death rate would therefore be “natural” first choice because it is a compromise between the two alternatives, and is definitely the simplest possible extension of the density-independent death rate,  $d$ , in Eq. (2.3) and Eq. (2.9).

By adding a linear increase to the normal death rate,  $d$ , we obtain a simple mathematical function,  $F(N) = d + cN$ , for the graph in Fig. 3.1a, where  $d$  is the normal death rate that is approached when the population size is small, and where  $c$  is the slope with which the death rate increases with  $N$ . Since  $cN$  should be a rate that can be added to the death rate  $d$ , the dimension of  $c$  should be per time unit per individual, and the dimension of  $F(N)$  is a rate that should replace the  $d$  parameter in Eq. (2.3) and Eq. (2.9). It is therefore much simpler to define a non-dimensional function,  $f(N)$ , that we can multiply with the original death rate,  $d$ , i.e.,

define  $df(N) = F(N)$ , and solve

$$f(N) = \frac{F(N)}{d} = 1 + \frac{cN}{d} = 1 + \frac{N}{k}, \quad (3.1)$$

where  $k = d/c$  has same dimension as  $N$ . Now we can preserve the original death rate of the model, and multiply the parameter  $d$  in Eq. (2.3) and Eq. (2.9) with  $f(N)$ . Thanks to this simplification the exact interpretation of the new density-dependence parameter,  $k$ , is the population size at which the death rate had doubled (i.e., when  $N = k$  the *per capita* death rate is  $2d$ ). This is an intuitive parameter with a simple dimension that one can easily explain to an audience, and estimate from experimental data (see Fig. 3.2a). Finally, because  $f(N) = 1$  when  $N \rightarrow 0$  the minimum *per capita* death rate,  $d$ , and maximum generation time,  $d^{-1}$ , remain exactly the same.

For the replicator population of Eq. (2.9), the full model becomes

$$\frac{dN}{dt} = \left[ b - d \left( 1 + \frac{N}{k} \right) \right] N. \quad (3.2)$$

At low population sizes the expected life span of the individuals remains  $1/d$  time units, and they always have a birth rate  $b$  per time unit. Since the  $R_0$  is a maximum fitness, it is computed for an individual under optimal conditions, which here means  $N \rightarrow 0$ . The fitness of individuals obeying Eq. (3.2) therefore equals  $R_0 = b/d$ . To search for steady states of Eq. (3.2) one sets  $dN/dt = 0$ , cancels the trivial  $N = 0$  solution, and solves from the remainder that

$$b - d = \frac{dN}{k} \quad \text{that} \quad \bar{N} = k \frac{b - d}{d} = k(R_0 - 1) \quad (3.3)$$

is the non-trivial steady state population size. In ecology such a steady state is called the “carrying capacity”. A negative feedback in the form of a linearly increasing density-dependent death rate is therefore sufficient to have a carrying capacity. Here, the carrying capacity depends strongly on the fitness of the population, i.e., doubling  $(R_0 - 1)$  doubles the steady state population size, whatever the magnitude of  $R_0$ .

For a population that is maintained by a source, i.e.,  $dN/dt = s - dN$ , the full model becomes

$$\frac{dN}{dt} = s - d \left( 1 + \frac{N}{k} \right) N, \quad \text{with steady states} \quad \bar{N} = \frac{-dk \pm \sqrt{dk(dk + 4s)}}{2d}. \quad (3.4)$$

Because the square root term is positive and larger than  $dk$ , the positive root of this quadratic equation corresponds to a meaningful steady state, and the negative root has to be ignored. Because this population has no birth rate the  $R_0$  is not defined.

### Density dependent birth

Now that we have learned how one can add density-dependent effects to the death terms of a model, we turn to adding negative density-dependence to the birth or source terms of Eq. (2.9) and Eq. (2.3). For the replicator model the *per capita* birth rate should decrease with the population size (evidence supporting a decreasing birth rate in two “natural” populations is shown in Fig. 3.2). The simplest functional relationship between a decreasing *per capita* birth rate and the population size is again a linear one, and the graph in Fig. 3.1b can mathematically be described as  $F(N) = b - cN$ , where  $b$  is the birth rate at low population densities and  $c$  is the slope of the line. Simplifying this into a non-dimensional function we write

$$f(N) = \frac{F(N)}{b} = 1 - \frac{cN}{b} = 1 - \frac{N}{k}, \quad (3.5)$$

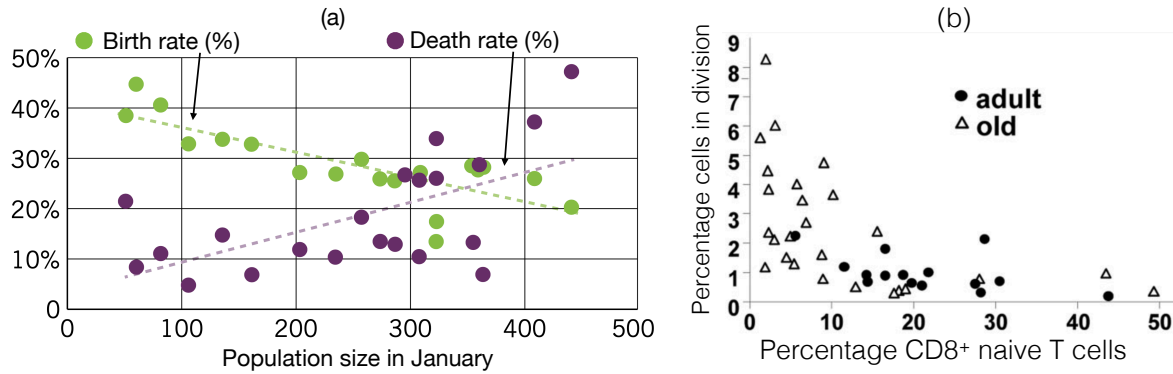


Figure 3.2: Density dependence in “natural” populations. Panel (a): Heck cattle have been introduced to the Oostvaardersplassen in the Netherlands as a semi-natural population of grazers. The population was started with a small group of animals in 1983, and after approximately 20 years the density approached a carrying capacity of 300–400 cattle. Ecologists have measured birth and death rates over the years (Figure taken from an article in NRC Handelsblad on 11 December 2010). Panel (b): naive CD8<sup>+</sup> T cells start dividing when their densities are low. The horizontal axis depicts the percentage of naive CD8<sup>+</sup> T cells present in young and old Rhesus macaques, and the vertical axis depicts the percentage of naive CD8<sup>+</sup> T cells that have recently divided (Cicin-Sain *et al.*, 2007).

and multiply the original birth rate parameter,  $b$ , by this non-dimensional function such that the model becomes

$$\frac{dN}{dt} = \left[ b \left( 1 - \frac{N}{k} \right) - d \right] N . \quad (3.6)$$

The dimension of the parameter  $k$  is again biomass, or individuals, and its exact interpretation now is that  $k$  defines the population size where the birth rate becomes zero (which is again intuitive and measurable). Because  $f(N)$  will become negative whenever  $N > k$ , which would give a negative birth rate, it is technically better to define  $f(N) = \max(0, 1 - N/k)$ , where the function  $\max()$  returns the maximum of its arguments. Because the steady state will always correspond to a density with a non-zero birth rate, we proceed with Eq. (3.5) for reasons of simplicity.

Since at low densities  $f(N) \rightarrow 1$ , the interpretation of the parameter  $b$  remains the maximum birth rate, implying that the fitness of individuals obeying Eq. (3.6) remains  $R_0 = b/d$  (which is a natural result because at a sufficiently low population size the density-dependence should have no effect). The steady states of Eq. (3.6) are  $N = 0$  and solving

$$b - d = \frac{bN}{k} \quad \text{yields} \quad \bar{N} = k \left( 1 - \frac{d}{b} \right) = k \left( 1 - \frac{1}{R_0} \right) . \quad (3.7)$$

A negative feedback in the form of a linear density-dependent *per capita* birth rate therefore also allows for a carrying capacity. When  $R_0 \gg 1$ , this carrying capacity approaches the value of  $k$ , and becomes fairly independent of the fitness (which differs from the result obtained with density-dependent death).

Similarly, the source term in a  $dN/dt = s - dN$  model could suffer from the negative density-dependence. An example would be the production of red blood cells in the bone marrow, which is increased when interstitial cells in the kidney increase their production of *erythropoietin* (EPO) when they suffer from too low oxygen levels. Although the effect of EPO is non linear (Schirm *et al.*, 2013) we could start with multiplying  $s$  with Eq. (3.5) to obtain

$$\frac{dN}{dt} = s \left( 1 - \frac{N}{k} \right) - dN \quad (3.8)$$

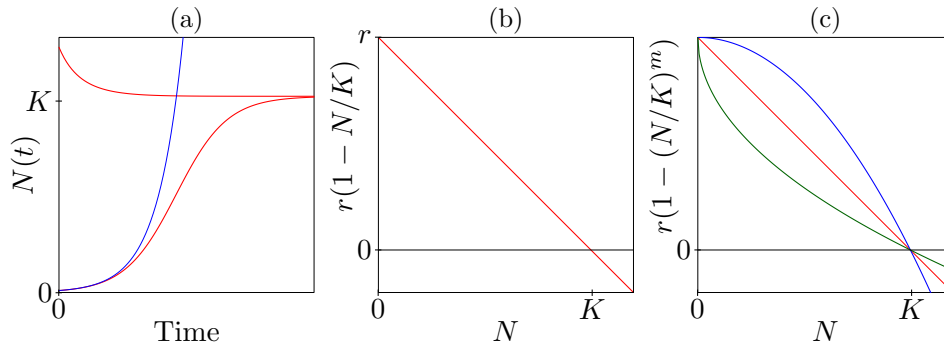


Figure 3.3: Logistic growth. The heavy red lines in Panel (a) depicts the behavior of Eq. (3.10) starting at a low and a high density, respectively. The light blue line starts at the same low density and shows the corresponding exponential growth curve, because we have set  $K \rightarrow \infty$ . Panel (b) depicts the *per capita* growth rate of Eq. (3.10). Panel (c) shows that one can easily extend Logistic growth with a non-linear density-dependence, i.e., the heavy lines depict Eq. (3.11) for  $m = 0.5$  (green) and  $m = 2$  (blue). This figure was made with the model `logist.R`.

where the production rate  $s$  (e.g., in cells  $\text{day}^{-1}$ ) decreases linearly with the red blood cell density  $N$ . The interpretation of  $k$  remains the population size at which the production is zero. For red blood cells this may sound unrealistic as their production by the bone marrow is probably not completely stopping at high red blood cell, or low EPO, densities. The model may nevertheless behave realistically around normal steady state densities. The equilibrium state obtained by solving  $dN/dt = 0$  is  $\bar{N} = sk/(dk + s)$  (which is a saturation function of the source  $s$ ), and by substituting  $\bar{N}$  into  $f(N)$  we observe that at steady state the total production equals

$$sf(\bar{N}) = s\left(1 - \frac{\bar{N}}{k}\right) = s\left(1 - \frac{s}{dk + s}\right) = \frac{dks}{dk + s} \quad \text{cells day}^{-1}, \quad (3.9)$$

which is of the form  $\frac{ab}{a+b}$ , and hence is a saturation function of  $dk$  and of  $s$ . When  $dk \rightarrow \infty$  the production at steady state approaches  $s$  cells  $\text{day}^{-1}$ , and when  $s \rightarrow \infty$  it approaches  $dk$  cells  $\text{day}^{-1}$ .

## 3.2 Logistic growth and our assumptions

Having derived a number of models for population growth we should start comparing them with existing models. The density-dependent models for replicating populations, Eq. (3.2) and Eq. (3.6), are both of the form  $dN/dt = \alpha N - \beta N^2$ , where  $\alpha$  and  $\beta$  are parameter combinations of the original birth and death rates,  $b$  and  $d$ , and the density-dependence parameter  $k$  (see the exercises). Both models are therefore mathematically identical to the classic “logistic equation”:

$$\frac{dN}{dt} = rN(1 - N/K), \quad \text{with solution} \quad N(t) = \frac{K}{1 + e^{-rt}(K/N(0) - 1)}, \quad (3.10)$$

with a natural rate of increase of  $r = b - d$ , and a carrying capacity that is directly defined by the parameter  $K$  (these equations are identical because  $\alpha = r$  and  $\beta = r/K$  in the logistic growth model). The behavior of the three models for a replicating population is therefore the identical: starting from a small initial population the growth is first exponential, and will approach zero when the population size approaches the carrying capacity (see Fig. 3.3a). Starting from a large initial population, i.e., from  $N(0) > K$ , the population size will decline until the carrying capacity is approached. Logistic growth is often employed to describe population growth in

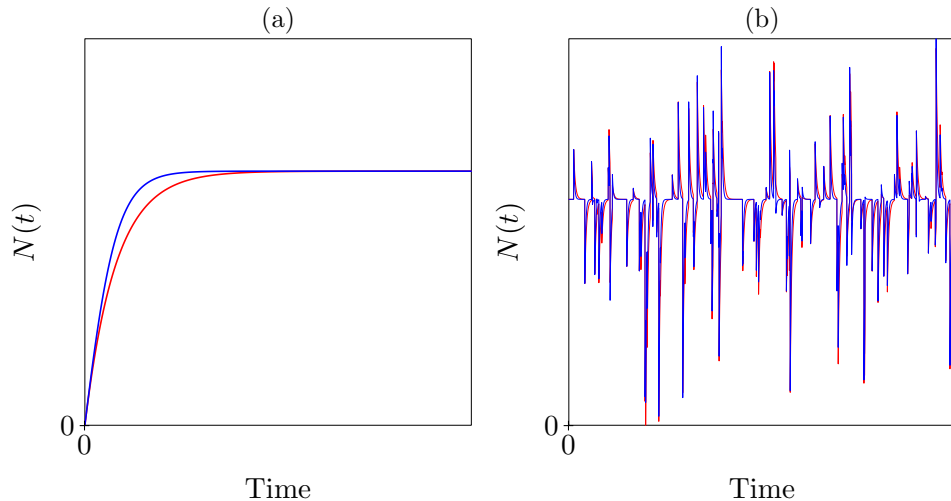


Figure 3.4: Populations with density-dependence either on the production (i.e., obeying Eq. (3.8); red lines), or on the death rate (i.e., obeying Eq. (3.4); blue lines). In Panel (b) we add noise sampled from a normal distribution with mean zero and 2.5% standard deviation to the population size  $N(t)$  of both models at random selected time points. This figure was made with the model `source.R`. Note that the two panels are scaled somewhat differently.

many biological disciplines (ranging from ecology, epidemiology, virology, to cell biology), and by deriving Eq. (3.10) ourselves we have learned that is is indeed an excellent choice for populations having a linear density-dependence on their *per capita* birth and/or death rate. Eq. (3.10) is more convenient than the models we derived ourselves because the carrying capacity is defined by just one of its parameters. However, because Eq. (3.10) has no explicit death rate, we cannot define a life span, and hence the  $R_0$  is not defined. Finally, one can extend Eq. (3.10) to allow for a non-linear density-dependence (Richards, 1959),

$$\frac{dN}{dt} = rN(1 - (N/K)^m), \quad \text{with solution} \quad N(t) = \frac{K}{[1 - (1 - [K/N(0)]^m)e^{-rmt}]^{1/m}}, \quad (3.11)$$

see Ram *et al.* (2019) for a derivation of this solution. The meaning of  $r$  and  $K$  remain the same and  $m$  can be used to define a concave or convex dependence of the *per capita* growth rate on the population density (Fig. 3.3c). We provide this solution because it is known, and because this would be a convenient function to fit to data from populations that are expanding to a carrying capacity (Ram *et al.*, 2019). The estimated value of  $m$  would reveal the shape of the density dependence (i.e., linear, convex or concave). This model cannot reveal whether the birth rates, the death rates, or both depend on the population density, however.

The two density-dependent models for populations that are maintained by a source, i.e., Eqs. (3.4) and (3.8), are mathematically not identical, and their steady states are defined by quite different parameter expressions. Thus, the effect of changing a parameter like the source,  $s$ , on the steady state of the population depends on the biological process that depends (most strongly) on the population density. In Fig. 3.4 we depict the behavior of both models in the presence and absence of noise. The two models are given the same source and death rates, and the  $k$  value of the model with density-dependent death is set to such a value that both models have the same steady state (see the R-script `source.R`). Thus, at low densities the two populations have the same initial growth rate, and at high densities they approach the same steady state (see Fig. 3.4a where the red line depicts the population with density-dependent production, and the blue curve is the population with density-dependent death). We observe that the population with density-dependent death approaches the steady state somewhat ear-

lier than the population with density-dependent production. In the presence of noise, i.e., by frequently adding a randomly drawn small value to  $N$  (with mean zero and 2.5% standard deviation), we observe that the (red) population with density-dependent production is somewhat more sensitive to noise than the (blue) population with density-dependent death (Fig. 3.4b). The difference between the two models is small, but this depends on the value of the density-dependence parameter,  $k$ , i.e., when  $k \gg s/d$  the models will approach the same behavior, and the smaller  $k$  the more different the behavior. Although the difference is small, we have to conclude that the sensitivity of the steady state to changes in the external circumstances, e.g., noisy changes in parameter values and/or population densities, depends to the biological choices we make when developing the model. Thus, whenever possible, we better employ our biological knowledge when devising a model, and if it remains unknown which biological process depends most on the density, it is best to develop several models to test the sensitivity of the results on these assumptions (Ganusov, 2016). Because, the same is true for the assumption on the linear shape of  $f(N)$ , we expand our analysis to the shape of  $f(N)$  in the next section.

### 3.3 Non-linear density-dependence

Above we have considered *per capita* birth and death rates that were linear functions of the population density. Although this is generally taken to be sufficient, as one typically models replicating populations with logistic growth, it would in most cases be more realistic to let production, birth and death rates only be density-dependent when the resources become limiting, i.e., at the high population densities (see the blue concave curve in Fig. 3.3c). Populations that grow spatially by extending their boundaries would be an exception, because they are already faced with high competitor densities at low population numbers (and even then their density dependence is not expected to be linear; see the exercises). Thus, we need general functions that allow us to define non-linear relationships, and it would be convenient to have functions that are non-dimensional. Above we already used the simple decreasing non-dimensional function  $f(x) = 1 - (x/k)^n$ , which is linear when  $n = 1$ , concave when  $n > 1$ , and convex when  $n < 1$  (see Fig. 3.3c), and where  $x = k$  is the population density at which  $f(x) = 0$ . Because  $f(x) < 0$  when  $x > k$  one should formally use

$$f(x) = \max(0, 1 - [x/k]^n) , \quad (3.12)$$

which indeed provides a simple tunable function to generally describe decreasing effects.

Having a decreasing function,  $0 \leq f(x) \leq 1$ , one can also define an non-dimensional increasing function,  $g(x) = 1 - f(x) = [x/k]^n$  to have a linear ( $n = 1$ ), convex ( $n > 1$ ), or concave ( $n < 1$ ) function that equals one when  $x = k$ . To define increasing functions with a plateau, one could define  $f(x) = \min(1, [x/k]^n)$ , but since this has a discontinuity at  $x = k$ , it is more convenient to use a Hill function, or an exponential function, i.e.,

$$f(x) = \frac{x^n}{h^n + x^n} \quad \text{or} \quad f(x) = 1 - e^{-\ln[2]x/h} , \quad (3.13)$$

to define a saturated ( $n = 1$ ) or sigmoid ( $n > 1$ ) saturation function; see Page 162. Both functions are generally used to formulate saturated and/or sigmoid density dependent effects. The functions in Eq. (3.13) are zero when  $x = 0$ , increase with  $x$ , they are half-maximal,  $f(x) = 0.5$ , when  $x = h$ , and they approach their maximum,  $f(x) = 1$ , when  $x \rightarrow \infty$ . Having increasing functions  $0 \leq f(x) < 1$ , one can again define decreasing non-dimensional functions by defining  $g(x) = 1 - f(x)$ , e.g.,

$$g(x) = \frac{1}{1 + (x/h)^n} \quad \text{and} \quad g(x) = e^{-\ln[2]x/h} , \quad (3.14)$$

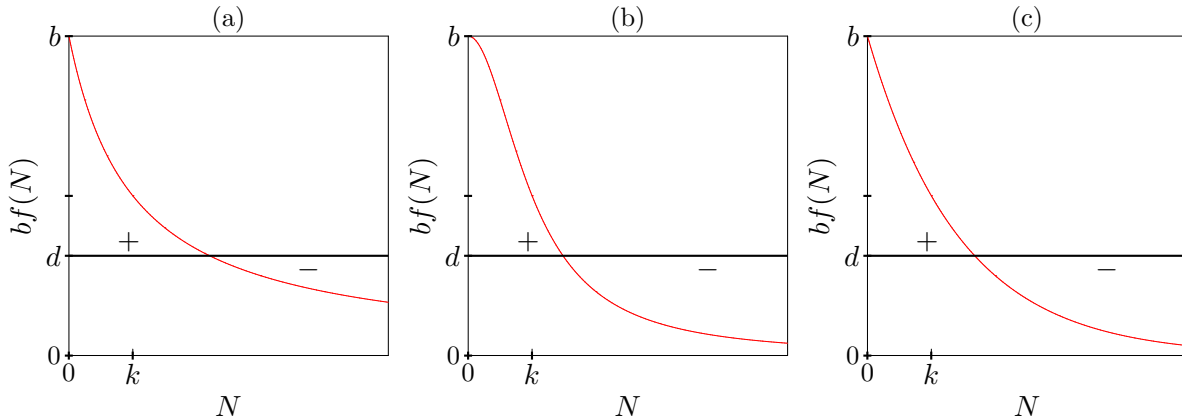


Figure 3.5: Density dependent birth rates based upon examples taken from Eq. (3.16). The declining red curves in Panels (a)–(c) correspond to *per capita* birth rate,  $bf(N)$ , where the density dependence is defined by one of the three functions in Eq. (3.16). The horizontal black lines depict the density independent *per capita* death rate of Eq. (3.15). The intersects therefore correspond to steady states.

which no longer need the somewhat cumbersome  $\max()$  function of Eq. (3.12); see Page 162.

Because all functions in Eqs. (3.12–3.14) are dimensionless, and remain bounded between zero and one, i.e.,  $0 \leq f(x) < 1$ , one can easily multiply any parameter in a model (corresponding to some biological process) with  $f(x)$ , to define non-linear density dependent effects of any population onto any biological process. For down-regulatory effects, i.e., decreasing functions, one can use either the simple Eq. (3.12), or the Hill function or exponential function of Eq. (3.14). A minor technical difference is that the  $h$  parameters of Eq. (3.14) “naturally” define the value of  $x$  where  $g(x) = 0.5$ , whereas the  $k$  parameter in Eq. (3.12) most “naturally” defines the value of  $x$  where  $f(x) = 0$ . For positive effects approaching a maximum one typically uses one of the functions in Eq. (3.13), and for effects without a maximum one could resort to the simple  $f(x) = (x/h)^n$ . We will illustrate this with a few examples below.

### Non-linear negative density-dependent birth

For a replicating population with density dependent growth we can now generalize Eq. (3.5) into

$$\frac{dN}{dt} = (bf(N) - d)N, \quad (3.15)$$

and use one of the several candidates from Eq. (3.12) or Eq. (3.14) to choose a decreasing density dependent function,  $f(N)$ . For instance, the linear density dependent birth rate depicted in Fig. 3.2a would speak in favor of using the linear  $f(N) = 1 - N/k$  from Eq. (3.12). For non-linear examples we here sample from Eq. (3.14), e.g.,

$$f(N) = \frac{1}{1 + N/k}, \quad f(N) = \frac{1}{1 + [N/k]^2} \quad \text{and} \quad f(N) = e^{-\ln[2]N/k}, \quad (3.16a,b,c)$$

and depict their shape and the steady state they would give in Fig. 3.5. Because in a well-mixed population, the birth rate probably remains close to its maximal value as long as the population size is sufficiently small, the sigmoid function of Eq. (3.16b), and the concave  $f(N) = 1 - (N/k)^2$  of Eq. (3.12) seem most realistic for most non-spatial models.

Each of the three models in Fig. 3.5 has a single non-trivial steady state (see Table 3.1), and this steady state is always stable (see Fig. 3.5). The latter can be seen graphically because at

Function	$f(0)$	$f(k)$	$f(\infty)$	$R_0$	Carrying capacity	Eq.
$f(N) = \max(0, 1 - N/k)$	1	0	0	$b/d$	$\bar{N} = k(1 - 1/R_0)$	(3.5)
$f(N) = \max(0, 1 - [N/k]^m)$	1	0	0	$b/d$	$\bar{N} = k \sqrt[m]{1 - 1/R_0}$	(3.12)
$f(N) = 1/(1 + N/k)$	1	0.5	0	$b/d$	$\bar{N} = k(R_0 - 1)$	(3.14)
$f(N) = 1/(1 + [N/k]^2)$	1	0.5	0	$b/d$	$\bar{N} = k\sqrt{R_0 - 1}$	(3.14)
$f(N) = e^{-\ln[2]N/k}$	1	0.5	0	$b/d$	$\bar{N} = (k/\ln[2]) \ln[R_0]$	(3.14)

Table 3.1: Properties of several non-linear functions defining a density dependent birth rate in the model  $dN/dt = (bf(N) - d)N$ .

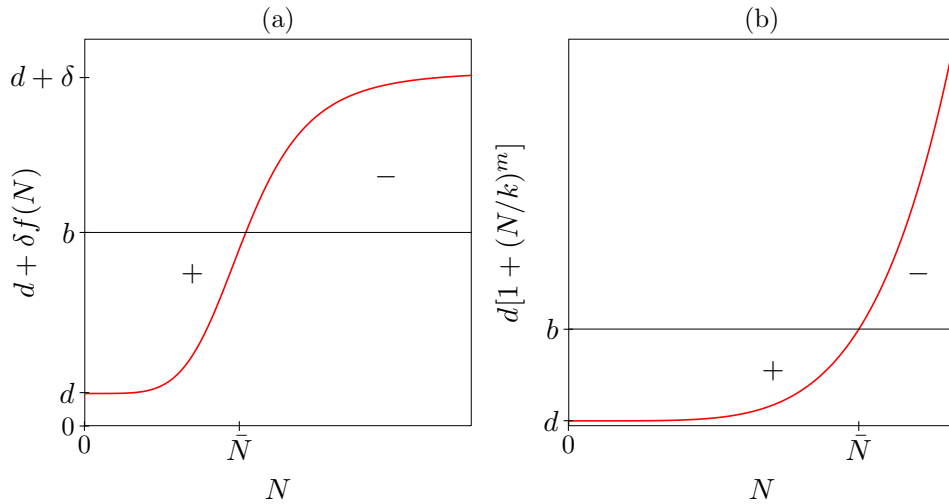


Figure 3.6: Non-linear density-dependent death rates. Panel (a) uses the Hill function  $f(N) = N^m/(h^m + N^m)$  and depicts the *per capita* death rate defined by Eq. (3.17). Panel (b) illustrates the *per capita* death rate defined by Eq. (3.18) for  $m = 5$ . The horizontal black lines denote an arbitrary density-independent birth rate, such that the intersections correspond to a steady state level. This figure was made with the model `death.R`.

the steady state, where  $dN/dt = 0$ , increasing the population size to a value slightly above its steady state value brings the population density into a region where  $dN/dt < 0$  (as indicated by the  $-$  signs in Fig. 3.5), whereas decreasing the population to a value slightly below the steady state value increases  $dN/dt$  (see the  $+$  signs).

Since all these functions are bounded between zero and one, i.e.,  $0 \leq f(N) < 1$ , the fitness in these models is always  $R_0 = b/d$ . Although the different functions may reflect quite a different biology, the models that result from incorporating them have a very similar behavior. For instance, starting with a small population the population size plotted in time will always look like a sigmoid function. In other words, finding a population with a sigmoid population growth tells us very little about the shape of its underlying density dependent regulation. Table 3.1 shows for some of these models how their carrying capacity depends on the fitness  $R_0$ .

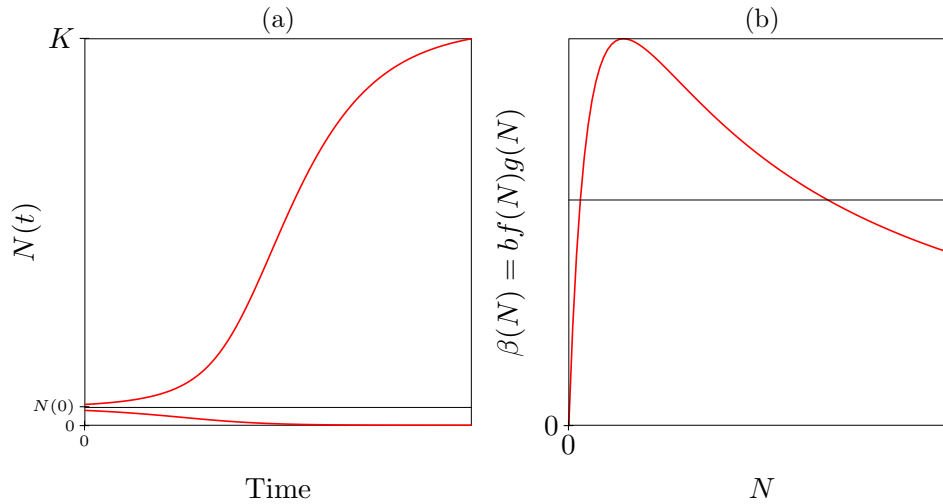


Figure 3.7: Positive density-dependence on the reproduction leads to an Allee effect. Panel (a) shows that a population based up Eq. (3.19a) has a critical density (depicted by the horizontal line) above which it increases until the carrying capacity is approached, and below which it declines. The heavy red line in Panel (b) depicts the *per capita* birth rate as a function of the population density, and the horizontal black line depicts the *per capita* death rate. Densities at which these line intersect are steady state (because the birth rate balances the death rate). The steady state at a low density is the unstable critical density and the one at a high density is the stable carrying capacity. This figure was made with the model `allee.R`.

### Non-linear density-dependent death

One could use an increasing Hill-function to define a *per capita* death rate that increases with the population density, i.e., write

$$\frac{dN}{dt} = [b - d - \delta f(N)]N, \quad (3.17)$$

where  $\delta$  is an additional death rate that is due to competition, and comes on top of the normal death rate experienced at low densities (when  $f(N) \rightarrow 0$ ). A steep sigmoid Hill-function would allow one to define a population density,  $h$ , at which the competition starts to severely increase the death rate, until the maximum *per capita* death rate,  $d + \delta$  is approached. Since it remains unclear whether such a maximum death rate is desirable, one could also use a power function to define a *per capita* death rate that keeps on increasing with the population density, e.g.,

$$\frac{dN}{dt} = (b - d[1 + (N/k)^m])N \quad (3.18)$$

which has a linear increase in the death rate when  $m = 1$ , and a faster than linear increase when  $m > 1$ . The interpretation of  $k$  remains the same as in Eq. (3.2), i.e., when  $N = k$  the death rate has doubled. Having a fitness  $R_0 = b/d$  the steady state is  $\bar{N} = k \sqrt[m]{R_0 - 1}$ . Fig. 3.1a shows that this steady state is stable for  $m = 1$ . Confirm for yourself that this is true for all values of  $m$  by sketching the same picture for  $m = 1/2$  and  $m = 2$  (see Fig. 3.6b and the exercises).

## 3.4 Positive density dependence

Now that we learned to use saturation functions we are ready to start modeling positive feedbacks. Replicating populations not only face competition at high densities, they may also suffer

from a lack of conspecifics at low densities. Examples would be sexual reproduction where individuals need to encounter partners or gametes (Berec *et al.*, 2007), growing tumors that by inducing angiogenesis increase their own growth rate, cooperating predators like wolves or spoonbills, and microorganism that improve their own environment (Kramer *et al.*, 2009).

Modeling population growth with sexual reproduction basically means that we have to extend our current model with density dependent birth and/or death with an additional function describing the probability at which individuals are expected to encounter mates. A mechanistic approach would be to define a function,  $g(N)$ , for the probability that there is at least one mate in an individual's neighborhood, and multiply the birth rate with that probability. This can be defined as a Poisson process, where  $g(N) = 1 - e^{-\lambda N}$  is one minus the probability that there are no mates in the neighborhood of a particular female. Knowing that such an exponential function closely resembles the increasing Hill-function  $g(N) = N/(h + N)$  (see Fig. 15.4), we can also use a somewhat more phenomenological model, and define  $h$  as the population density where the probability of finding a mate is one half. Having either of these two functions defining the mating we extend Eq. (3.15) and/or Eq. (3.18) with  $g(N)$  to obtain

$$\frac{dN}{dt} = (bf(N)g(N) - d)N \quad \text{or} \quad \frac{dN}{dt} = (bg(N) - d[1 + (N/k)^m])N, \quad (3.19a,b)$$

where  $f(N)$  is one of the declining functions defined by Eqs. (3.12) to (3.14).

We study the effect of a positive density-dependence by numerically solving Eq. (3.19a) with  $f(N) = 1/(1 + N)$  and  $g(N) = N/(h + N)$ , starting with either a low, or a somewhat higher, initial population density (Fig. 3.7a). The small population declines and goes extinct, whereas the somewhat larger population expands and approaches carrying capacity. The horizontal black lines depict the critical density that the population needs to expand. Populations that would accidentally drop below this density are expected to go extinct. The *per capita* birth rate,

$$\beta(N) = b \frac{1}{1 + N} \frac{N}{h + N}, \quad (3.20)$$

is depicted by the red line in Fig. 3.7b. At low densities, i.e., when  $N \rightarrow 0$ , this approaches the increasing line  $\beta(N) \simeq (b/h)N$  because the birth rate is maximal and it is difficult to find mates (i.e.,  $f(N) \simeq 1$  and  $g(N)$  is small). At high densities the red line decreases, i.e.,  $\beta(N) \rightarrow 0$  when  $N \rightarrow \infty$ , because of competition (i.e.,  $f(N)$  is small and  $g(N) \simeq 1$ ). The horizontal black line depicts a density-independent death rate, and we see that this line intersects the birth-rate curve at two population densities. The lower density is the unstable steady state above which the population can grow (see Eq. (3.19a)), and the higher density is the carrying capacity. Because the net *per capita* population growth is negative at low densities this is called a “strong” Allee effect, which implies that a population of zero individuals is a stable steady state. Eq. (3.19a) therefore has three steady states, of which  $N = 0$  and  $N = K$  (where  $K$  is the carrying capacity) are stable. Having alternative steady states is due to the fact that this model has a positive feedback (May, 1977).

### 3.5 Summary

The growth of populations typically involves feedbacks that are called density dependence (or homeostasis). In replicating populations, negative density-dependence allows for a carrying capacity, i.e., a stable steady state population size. A negative density-dependence can be implemented as a feedback on the birth rate, and/or the death rate. The most convenient approach

to implement feedback functions in mathematical models is to define non-dimensional functions describing a particular biological feedback, and to multiply the corresponding parameter of the model with that function. The most general model describing the growth of a replicating population is the Logistic growth equation. Density-dependence can have a linear, a concave or convex shape, and can be positive or negative. A Hill-function is convenient tool for defining increasing or decreasing non-linear saturation functions. Positive feedbacks allow for multiple steady states.

### 3.6 Exercises

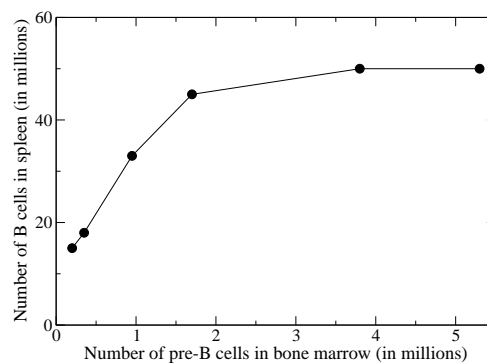
#### Question 3.1. Carrying capacity

What do you expect for the individual well-being in a human population that is approaching its carrying capacity:

- Do you expect the individual birth rate to be small or large?
- Do you expect the individual death rate to be small or large?
- In which population would you prefer to live: a small expanding population, or in one that is approaching carrying capacity?
- Optimists like Julian Simon advised the American government by saying that “every human being represents hands to work, and not just another mouth to feed” (Cohen, 1995). We can investigate this proposal by arguing that the carrying capacity  $K$  in Eq. (3.10) increases with the population size. Test a simple example, e.g.,  $K = k\sqrt{N}$ , and see how this influences the result. Do you still expect a carrying capacity where the individual well-being is at its minimum?

#### Question 3.2. Homeostasis

B cells are lymphocytes that can produce antibodies. They circulate via blood and lymph. Novel (naive) B are produced in the bone marrow by pre-B cells that divide, mature, and egress. Agenes *et al.* (1997) at the Pasteur Institute were breeding mice with different numbers of pre-B cells in the bone marrow to study how the number of circulating naive B cells (e.g., those in the spleen) depends on this source from the marrow. They found the following:



A simple model for the naive B cell population is  $dB/dt = m - dB$  where  $m$  is the bone marrow production, and  $1/d$  is the average life span of naive B cells. We have learned above that the rate of naive B cell production,  $m$ , is proportional to the number of pre-B cells in the bone marrow, e.g.,  $m = \alpha P$ , where  $P$  is the number of pre-B cells that was being changed in the mice. The investigators allowed the mice to mature and we can therefore assume that their observations correspond to the steady state,  $\bar{B}$ , of our simple model. Thus, in terms of this model, the data graph should correspond to  $m \propto P$  on the horizontal axis, and  $\bar{B}$  on the vertical axis.

- a. Is the simple model compatible with the data?
- b. If not, how would you extend the model?
- c. Do the data require homeostasis, i.e., density dependent regulation?
- d. Is  $dB/dt = m - dB$  accounting for homeostasis?

### Question 3.3. Overfishing herring

With this question we aim to increase our insights into setting sustainable limits of harvesting populations. As an example we consider the quota defined to achieve sustainable fisheries of herring in the North Sea. For simplicity assume that the dynamics of the herring population in the North Sea can be described by a simple logistic growth model, i.e.,  $dN/dt = rN(1 - N/K)$ . Although this is clearly a gross oversimplification we will learn something insightful from this exercise.

- a. Sketch the population growth  $dN/dt = f(N)$  as a function of the population size  $N$ . What is the maximum of the function  $f(N)$ ?
- b. What is the long-term optimal population size for the fishermen, and what would then be the maximum harvest (i.e., the maximum number of fish captured per unit of time)?
- c. Add this maximum harvest explicitly to the logistic growth equation to model a situation where the fishermen have adopted this policy for a long time. Sketch the new growth equation as a function of  $N$  for the new situation. Do you expect this to be sustainable? What would be a more durable quota for fishing herring?
- d. Study the effect of noise on the sustainability of harvesting the population with a fixed quota. For example, consider a carrying capacity that fluctuates due to weather conditions changing on a weekly time scale (you may use the file `herring.R` for this).
- e. It is well known that harvesting a fraction of the population works much better than defining a fixed total quota (or a total catch limit). Defining a quota on the yearly investment on catching fish, i.e., on the fraction  $f$  that fishermen can maximally harvest, would change the model into  $dH/dt = rH(1 - H/K) - fH$ . What is economically speaking the optimal value of  $f$ ? Is that lower than the fixed quota  $Q = rk/4$ ? Hint: compute the new steady state,  $\bar{H}$ , and then the expected harvest,  $f\bar{H}$ , and finally compute its maximum by taking the derivative  $\partial_f$ .
- f. Is this indeed more sustainable? What is now the effect of a noisy carrying capacity?

### Question 3.4. Biofilm

Bacteria often reside in self-organized environments known as biofilms. The bacterial cells become embedded in a matrix of self-produced extracellular polymeric substances, which act like a biological “glue” enabling the microbes to colonize a wide range of surfaces. Once integrated into biofilms, bacterial cells can better withstand environmental challenges. Production of a protective biofilm by the bacteria therefore classifies as positive density dependence, and one way to implement this into an equation for bacterial growth would be to write a hill function,  $F(B)$ , for the positive effect of the biofilm on the birth rate, e.g.,

$$\frac{dB}{dt} = [bF(B) - d(1 + eB)]B, \quad \text{where} \quad F(B) = \frac{B}{h + B}$$

and where we also allow for a carrying capacity by having negative density dependence in the death rate. When  $B = h$  the effect of the biofilm on the birth rate is half-maximal.

- a. Sketch the *per capita* birth rate and the *per capita* death rate in one graph.
- b. Sketch the population birth rate and death rate in one graph. Hint: realize that these are of the form  $y = \frac{ax^2}{b+x}$  and  $y = ax + bx^2$ , respectively, and that the former approaches  $y = \frac{a}{b}x^2$  when  $x \rightarrow 0$ , and  $y = ax$  when  $x$  is large, and that the latter approaches  $y = ax$  when  $x \rightarrow 0$ , and  $y = bx^2$  when  $x$  is large. If you need further assistance in drawing these functions use the `biofilm.R` model on the website.
- c. How many steady states do you expect for these bacteria, and which of them are stable? How would you call this?

d. Can you write a similar model where the biofilm reduces the death rate?

**Question 3.5. Stem cells (requires nullclines)**

Consider a population of stem cells that are dividing and dying at a fixed rate. The stem cells are located on a surface (or substrate) at the border of a tissue, and this substrate provides the stem cells a signal that inhibits their differentiation. Thus, as long as the cells remain in contact with the substrate they remain stem cells, whereas cells that detach differentiate and mature into the cell type defining the tissue. Let there be room on the substrate for about  $K$  cells, i.e., let there be  $K$  “binding sites”. When a stem cell divides, one of the daughter cells will remain attached to the surface, while the other daughter will only stay attached when the site next to it is empty. Thus, describing the number of stem cells on the surface with the variable  $S$ , the probability that this neighboring site is empty is approximately  $1 - S/K$ .

- Write a model for this population of stem cells. Do we need density dependent birth or death rates to have a stable carrying capacity?
- What is the carrying capacity, and why is it smaller than the number of sites  $K$ ?
- What would be the corresponding equation for the differentiated cells?
- Sketch the production rate of differentiated cells as a function of the number of stem cells.
- Sketch the nullclines.

**Question 3.6. Regression to the mean (computer)**

To establish whether or not populations are regulated by density dependent effects it is typically best to measure *per capita* birth and death rates at different population densities, and plot these as a function of the population size (e.g., Fig. 3.2). Alternatively, one can take a long time series of sequential population densities,  $N_t$ , and study how the *per capita* rate of change between subsequent time points, i.e.,  $(N_{t+\Delta} - N_t)/N_t$ , depends on the previous population density,  $N_t$ . Although the second method comes with a well-known problem (Shenk *et al.*, 1998), it is nevertheless still being used to detect density-dependence in time-series data (Freckleton *et al.*, 2006). The problem is illustrated by the following R-script (called `regMean.R` on the website):

```
n <- 100; data <- rnorm(n,1,0.1); hist(data)
N <- data[1:(n-1)]; r <- (data[2:n]-N)/N
plot(N,r,type="p")
lm(r~N,as.data.frame(cbind(N,r)))
```

Artificial data is generated by drawing  $n = 100$  times from a normal distribution with  $\mu = 1$  and  $\sigma = 0.1$ . The *per capita* rate of increase,  $r$ , is computed by subtracting two subsequent data points, and dividing by the former. The relationship is plotted and quantified by linear regression (by a call to `lm()`).

- What do you expect for the relationship between  $r$  and  $N_t$  in this random data set?
- What do you find, and how can this be?
- Can a time-series provide solid evidence for density dependent effects? The Freckleton *et al.* (2006) paper provides an excellent discussion on this topic.

**Question 3.7. Fitting Logistic growth to the Gause data from 1934**

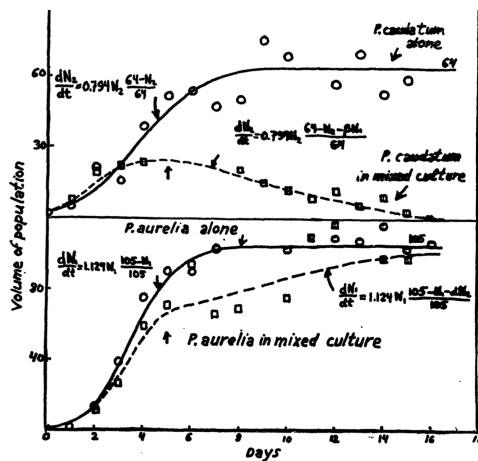


Figure 1 from Gause (1934).

In his classic experiments Gause (1934) was growing two species of *Paramecium* either in isolation, or in combination. The solid lines in the figure on the left suggest that the growth curve of *P. aurelia* and *P. caudatum* in isolation can very reasonably be described by a logistic growth equation, and in Gause's own handwriting one can read the parameter values he estimated for the logistic function (i.e.,  $r = 0.794$  per day with  $K = 64$  for *P. caudatum* and  $r = 1.129$  per day with  $K = 105$  for *P. aurelia*). We here fit this data ourselves to gain some experience in fitting models to data, and to study if all parameters can indeed be identified from this data. First, read Section 15.7 in the Appendix for some background on parameter fitting.

- The data of the individual experiments (circles) is available in the files `aurelia1.txt` and `caudatum1.txt` in the directory `tbb.bio.uu.nl/rdb/bm/models/data`. The file `gause1.R` allow you to read these files and fit the general logistic equation,  $dN/dt = rN(1 - N/K)$ , to the data (and perform an F-test). The script rounds Gause's estimates into an initial guess, i.e., sets `p <- c(r=1, K=100)`, and subsequently fits the model to both data sets using  $N(0)$ ,  $r$  and  $K$  as free parameters (note that we have to set column names to  $N$  because the model returns a column called  $N$ , whereas the corresponding columns in the data are called  $A$  or  $C$ ). Do you obtain a good fit and do your estimates agree with Gause's estimates?
- Why do we ultimately refrain from estimating the initial condition (i.e., why do we go from 6 to 4 free parameters)?
- Do the growth rates,  $r$ , and the carrying capacities,  $K$ , differ between both species? What are the confidence ranges on the parameters?
- Fitting the data with a shared growth rate (i.e., with a 3-parameter model) obviously decreases the quality of the fit somewhat (i.e., increases the SSR). Use an F-test to study whether or not the 4-parameter model is significantly better than the 3-parameter model.
- What would be your conclusion on the parameters of both species?
- If you enjoyed this question and are sufficiently familiar with Lotka-Volterra competition models, you could proceed with also fitting the competition experiments (see the similar question in Chapter 9).

## Extra questions

### Question 3.8. Habitat destruction

Levins (1969) and Levins & Culver (1971) proposed a “metapopulation” model in which one just counts the presence or absence of a single species in a large area with many small patches of suitable habitats (think of butterflies that are either present or absent in distinct suitable habitats). Instead of modeling the population size, the model describes the fraction,  $0 \leq P \leq 1$ , of patches occupied by this species. Empty patches can become occupied by colonization (at rate  $c$ ) from occupied patches. As the species may locally go extinct in any individual patch (at rate  $e$ ), only a fraction of the patches will actually be occupied (i.e.,  $P < 1$ ). Since the number of migrants arriving in a patch should be proportional to the number of occupied patches,  $P$ , in the environment, and because arrival only leads to a novel colonization if migrants land on an empty patch (which occurs with a probability  $1 - P$ ), they write for their pristine (undisturbed) environment

$$\frac{dP}{dt} = cP(1 - P) - eP. \quad (3.21)$$

- a. What is the non-trivial steady state of this model, and do you recognize this from the other models in this chapter?
- b. What fraction of the patches is “empty” at the steady state (i.e., in what fraction of the patches is the species absent)?

Now suppose that a random fraction of the habitats is destroyed and that only a fraction  $\alpha < 1$  is still suitable (i.e., a fraction  $\Delta = 1 - \alpha$  was destroyed). This changes the model into

$$\frac{dP}{dt} = cP(\alpha - P) - eP . \quad (3.22)$$

- c. What is the non-trivial steady state in an environment where a fraction  $\alpha < 1$  of the patches is left over?
- d. At what fraction of  $\alpha$  is a species expected to go extinct?
- e. Now consider a rare species occupying only 1% of the patches in the pristine environment, i.e., suppose  $\bar{P} = 0.01$  (with 99% empty patches), and suppose that a random fraction,  $\Delta = 1 - \alpha$ , of the habitats is destroyed. At what fraction of habitats  $\alpha$  is this particular species expected to go extinct? Give a biological interpretation in terms of the fraction of habitats,  $\Delta$ , that can be destroyed before the species is expected to go extinct. Do you think this is an artificial or a potentially realistic result?

### Question 3.9. Red blood cells (partly Grind)

Red blood cell (RBC) production in the bone marrow is increased when erythrocyte numbers in the periphery are low. Mechanistically, this works via the hormone *erythropoietin* (EPO) that is produced by renal epithelial cells when the blood provides insufficient oxygen to them. In a normal steady state little EPO is produced. This process has been modeled extensively (Belair *et al.*, 1995; Schirm *et al.*, 2013), and typically this involves steep sigmoid curves because the production of EPO is sharply up-regulated at low RBC counts. EPO is not the only regulator, i.e., in the complete absence of EPO there is still some production of RBC. On average the human body produces  $3 \times 10^9$  new erythrocytes per kg of body weight per day, and RBC have an expected life span of about 120 days. Hence at steady state there would be  $\bar{B} = 120 \times 3 \times 10^9 = 3.6 \times 10^{11}$  RBC.

Since little EPO is produced under normal conditions we assume that in the absence of EPO the production,  $s_0$ , is about one third of the normal production, i.e.,  $s_0 = 10^9$  RBC  $\text{kg}^{-1} \text{d}^{-1}$ , and assume that this can be increased up to 10-fold at maximum EPO concentrations. Because the bone marrow of the long bones becomes fatty in the elderly, the total amount of bone marrow that is producing erythrocytes decreases with age, which means the maximum production rate declines. Nevertheless, the number of peripheral red blood cells remains fairly constant when we age. Let us try to combine all of this in a mathematical model, to study whether or not that model yields the homeostasis suggested by the observation that the RBC count hardly decreases in the elderly.

- a. Define a steep sigmoid function,  $E = f(B)$ , for the concentration of EPO as a function the RBC density in the blood.
- b. Define a function defining the rate of RBC production as a function of the EPO concentration  $E$ . How would the rate of RBC production depend on the RBC count? You may need R to plot this.
- c. Write a mathematical model describing the dynamics of the number of RBC in the blood, and determine all of its parameters such that you can run in it Grind.
- d. What is the expected steady state RBC density in people with a kidney disease that disables the production of EPO? Run the model in Grind to compute the steady state in the presence of EPO (see the model `epo.R`).
- e. Does this model explain the observation that erythrocyte numbers are fairly independent of the age of an individual?

### Question 3.10. Generalized logistic growth

We have seen in this chapter that the famous logistic growth model of Eq. (3.10) is obtained when the *per capita* birth and/or death rate depend linearly on the population size. In Eq. (3.11) we have generalized the logistic growth model by raising the density-dependent term to the  $m^{\text{th}}$  power.

- Verify that Eq. (3.10) is indeed obtained when both the *per capita* birth and the death rate depend linearly on the population size.
- Consider a population obeying Eq. (3.11), and assume that only the birth rate is density dependent (i.e., the death rate is a constant). What would the *per capita* birth rate function look like? Would this be realistic for  $m = 0.5$  and  $m = 2$ , and for any value of  $m$ ?
- Consider the same population, and now assume that only the death rate is density dependent. What would the *per capita* death rate function look like? Would this be realistic for  $m = 0.5$  and  $m = 2$ , and for any value of  $m$ ?

**Question 3.11. Life stages (requires nullclines)**

Consider an insect population consisting of larvae ( $L$ ) and adults ( $A$ ). Adults give birth to larvae (in an asexual manner), and these larvae later mature into adults. Adults have a density independent mortality, i.e., a given expected life span. Larvae compete with adults and have a mortality that is dependent on the density of adults (use a simple term for this).

- Make a model consisting of two ODEs for the growth of such a population.
- Sketch nullclines and determine the stability of all steady states.
- Assume that the dynamics of the larvae is much faster than that of adults, i.e., make a “quasi steady state” assumption for the larvae. Hint: A QSSA for the larvae means that one solves  $L$  from  $dL/dt = 0$ . The quasi steady state expression for  $L$  is subsequently substituted into  $dA/dt$ , which is correct whenever  $L$  changes much more rapidly than  $A$ .
- Write the new ODE for the adults. Does this equation look familiar to you?
- What model is obtained when we make the quasi steady state assumption for the adults?
- Which of the two assumptions do you think is most realistic?

**Question 3.12. Seedlings over-shadowed by adult plants (requires nullclines)**

Make the seedling question in Chapter 14 and analyze your model, or the one provided in the answers of Chapter 14, by sketching nullclines for all qualitatively different situations.

- Sketch the nullclines, the vector field, and determine the stability of the steady state.
- Will there always be a non-trivial steady state? Give a mathematical and an intuitive answer.
- Will that state always be stable?
- Does this model allow for homeostasis?

**Question 3.13. Tumor growth**

Consider a spatial model for a small melanoma growing as a flat disk. Assume that the tumor cells are dividing only at the tumor boundary because of a lack of blood supply inside, and that cell death occurs uniformly throughout the tumor mass. A first approximation would be that the total biomass is proportional to the area of this circle, i.e.,  $A = c\pi r^2$ , where  $r$  is its radius and  $c$  is a constant scaling from area to biomass. Since reproduction takes place at the border, realize that the circumference of the circle is given by  $2\pi r$ . Thus, if  $N$  is the total number of cells in the tumor, the number of cells at the surface is proportional to  $\sqrt{N}$ .

- Write a growth model for the total number of cells in the tumor.
- What are the steady states?
- Sketch the per capita growth as a function of the tumor mass. Does this look okay?

**Question 3.14. The Fisher equation (Grind)**

To spatially model a population that is growing logistically on a one-dimensional spatial domain one can just add a diffusion term, and write a partial differential equation (PDE) like,

$$\frac{\partial N}{\partial t} = rN\left(1 - \frac{N}{K}\right) + D\frac{\partial^2 N}{\partial x^2},$$

where the parameter  $D$  is a diffusion constant. This is called a reaction-diffusion equation.  $N$  is actually a function of time and space, which should formally be written as  $N(x, t)$ . This equation was introduced by the famous Ronald Fisher in 1937 (to describe the spatial spread of an advantageous allele). To study such a PDE numerically one needs to discretize it into something like

$$\frac{dN_i}{dt} = rN_i \left(1 - \frac{N_i}{K}\right) + D(N_{i-1} + N_{i+1} - 2N_i), \quad \text{for } i = 1, 2, \dots, n$$

where  $i$  defines a location of a (small) compartment in space, and  $D$  now describes the movement of individuals between neighboring compartments. Note that  $D$  should be sufficiently small, i.e., one needs to define many small compartments to accurately describe the PDE.

- a. This model is available in the website as the file `fisher.R`. Study how such a vector of equations can be defined in R, and realize that we have wrapped the boundaries, i.e., individuals move from  $N_1$  to  $N_n$  and vice versa.
- b. What is the behavior of the model?
- c. What do you expect will happen if the model is extended with an Allee effect?

## Chapter 4

# Stability and return time

In the previous chapter we have seen several numerical examples of populations approaching a steady state. Such a stable steady state is an attractor of the system, and in most examples this corresponded to the carrying capacity of the population. We have also argued that for replicating populations the trivial steady state,  $N = 0$ , is unstable whenever the maximal *per capita* birth rate exceeds the minimal *per capita* death rate, i.e., whenever  $R_0 > 1$ , because the population will expand following a positive perturbation. Technically, we need the solution of the ODE to see which attractor is approached when  $t \rightarrow \infty$ , but in this chapter we will determine the stability of a steady state by simplifying the differential equation around a steady state. By doing so we will be able to define the “return time” of a stable steady state as the typical time it would take the population to return to the steady state after a small disturbance. Steady states with a long return time are sensitive to perturbations and are said to have a low resilience. Populations having several stable steady states, e.g., those with an Allee effect (see Eq. (3.19)), will have an unstable steady state defining the boundary between the basins of attraction of the alternative attractors.

### 4.1 Stability defined by the local slope of the growth function

In the previous chapter we emphasized that is typically most convenient to sketch biologically defined *per capita* functions for birth and death rates, and subsequently multiply these with the population size to obtain a function defining the net growth,  $dN/dt = f(N)$ , of the population. Having defined such a growth function one can plot it as a function of the population size, i.e., plot  $f(N)$  as a function of  $N$  (see Fig. 4.1). The values of  $N$  at which  $f(N) = 0$  then define the steady states because  $dN/dt = 0$ . The growth function the classic logistic model,  $f(N) = rN(1 - N/K)$ , is a parabola that is zero when  $N = 0$  or  $N = K$ , and has its maximum at  $N = K/2$  (see the blue line in Fig. 4.1a). To check the stability of the non-trivial steady state,  $\bar{N} = K$ , one can study what happens when the steady state population size is somewhat increased. Increasing  $N$  from its non-trivial steady value  $\bar{N}$  results in a negative value of  $f(N)$ , implying that the population will decrease after it was increased by a perturbation. Similarly, a decrease of the population size will result in an increase, because  $f(N) > 0$  when  $N \lesssim K$ . This suggests that the steady state is stable because  $f(N)$  provides a negative feedback on small perturbations around the steady state.

We can generalize this approach by plotting several of the growth functions introduced in the

previous chapter. For example, for the generalized logistic growth model,  $f(N) = rN(1 - (N/K)^m)$ , the steady states remain to be localized at  $\bar{N} = 0$  and  $\bar{N} = K$ , and the only qualitative changes is that the maximum is shifted to the right for  $m = 2$  and to the left for  $m = 1/2$  (see Fig. 4.1a). The carrying capacity  $\bar{N} = K$  therefore remains a stable steady state. For the non-replicating population with a density dependent production, i.e.,  $f(N) = s(1 - N/k) - dN$  from Eq. (3.8), we observe that  $f(N)$  is a straight line starting at  $f(0) = s$ , and intersecting the horizontal axis as  $\bar{N} = K = \frac{sk}{s+dk}$  (see the red line in Fig. 4.1b). The growth function of Eq. (3.4), i.e.,  $f(N) = s - d(1 + N/k)N$  is depicted as a blue line in Fig. 4.1b, and is a parabola having its maximum at  $N = -k/2$  and intersecting the horizontal axis at

$$\bar{N} = K = \frac{-dk + \sqrt{dk(dk + 4s)}}{2d}.$$

By the same approach we infer that the steady state of the two non-replicating populations is also stable because of a negative feedback that decreases population growth when the population were to increase.

Importantly, note that we only need the local slope  $\partial_N f(N)$  in the point  $N = \bar{N}$  to infer the stability of the steady state (where we use the “partial”,  $\partial$ , notation to explicitly define what derivative we take, e.g.,  $\partial_x x^2 = 2x$ ,  $\partial_y xy = x$ , and  $\partial_t N(t) = dN(t)/dt$ ). Thus, we see that a steady state of an equation,  $dN/dt = f(N)$ , is stable whenever  $f'(\bar{N}) < 0$  (where we use the shorthand  $f'$  to denote its derivative,  $\partial_N f$ , and  $f'(\bar{N})$  for the derivative in the steady state). Similarly, one can see that a steady state is unstable when  $f'(\bar{N}) > 0$  because that corresponds to a positive feedback where an increase in the population from its steady state value leads to a further increase of the population. An example of an unstable steady state is the origin of Fig. 4.1a, where  $f(N)$  has a positive slope in the trivial steady state  $\bar{N} = 0$ .

## 4.2 Linearization

The fact that one can read the stability of a steady state by the local slope, or derivative, of the growth function is not a lucky coincidence. Mathematically one can linearize any continuous function  $f(x)$  around any particular value, e.g.,  $\bar{x}$ , by its local derivative  $\partial_x f(\bar{x})$  in that point:

$$f(x) \simeq f(\bar{x}) + \partial_x f(\bar{x})(x - \bar{x}) = f(\bar{x}) + f'h, \quad (4.1)$$

where  $h = x - \bar{x}$  is a small distance in the  $x$ -direction, and  $f' = \partial_x f(x)$  is the derivative of  $f(x)$  with respect to  $x$  at the value  $x = \bar{x}$  (see Fig. 15.3 in the Appendix, and the accompanying Ebook (Panfilov *et al.*, 2025)). For example, one can linearize the function  $f(x) = 2x^2$  by its derivative  $f'(x) = 4x$ , and approximate the value of  $f(x)$  at  $x = 3.1$  by writing,  $f(3.1) \simeq f(3) + 4 \times 3 \times 0.1 = 2 \times 9 + 1.2 = 19.2$ , and see that this is close to the true value  $f(3.1) = 19.22$ . To apply this to our stability analysis one rewrites  $f(N)$  into  $f(\bar{N} + h)$  where  $\bar{N}$  is the steady state population size and  $h$  is considered to be a small disturbance of the population density from the steady state, i.e.,  $h = N - \bar{N}$ . Following Eq. (4.1) one rewrites  $dN/dt$  into

$$\frac{dN}{dt} = f(N) \simeq f(\bar{N}) + \partial_N f(\bar{N})(N - \bar{N}) = 0 + \lambda h, \quad (4.2)$$

because  $f(\bar{N}) = 0$ , and where we have defined  $\lambda = \partial_N f(\bar{N})$  as the local derivative of  $f(N)$  at  $N = \bar{N}$ , and  $h = N - \bar{N}$  as the distance to the steady state. Because the sum of two derivatives is the derivative of the sum, and  $d\bar{N}/dt = 0$ , we can apply the following trick

$$\frac{dN}{dt} = \frac{dN}{dt} - \frac{d\bar{N}}{dt} = \frac{d(N - \bar{N})}{dt} = \frac{dh}{dt}, \quad (4.3)$$

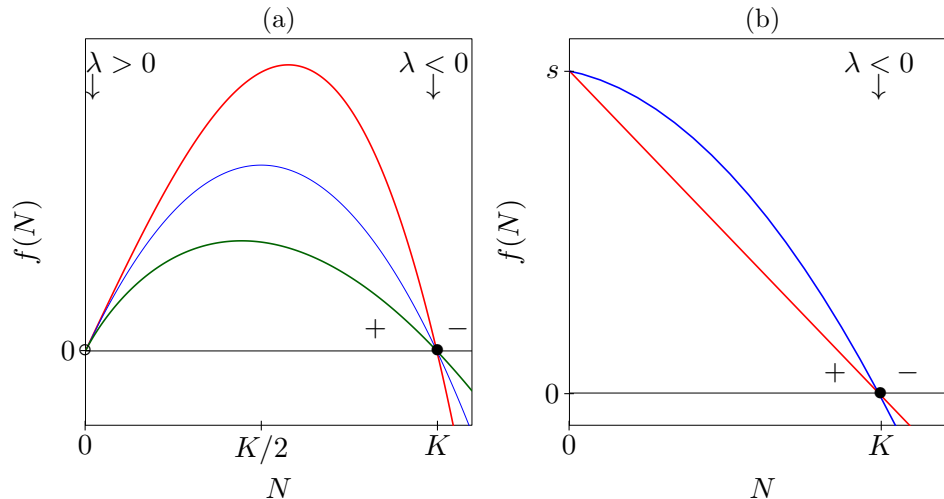


Figure 4.1: The stability of a steady state is determined by the local derivative (slope) of the growth function at the steady state. We plot the population growth rate,  $dN/dt = f(N)$ , as a function of the population size  $N$ . Panel (a) depicts the generalized logistic growth model,  $f(N) = rN[1 - (N/K)^m]$  for  $m = 0.5$  (green),  $m = 1$  (blue), and  $m = 2$  (red). The blue line is the characteristic logistic parabola. Panel (b) shows the population growth of Eq. (3.8), modeling density dependent production, i.e.,  $f(N) = s(1 - N/k) - dN$  as a red line, and the density dependent death of Eq. (3.4), i.e.,  $f(N) = s - d(1 + N/k)N$  as a blue line. The  $k$  parameters of the latter two models have been scaled such that both models have the same steady state  $K$ . The carrying capacities depicted in Panel (a) are all stable because  $\partial_N f(N) = \lambda = -mr < 0$  when  $\bar{N} = K$ . Indeed, increasing the population size in the carrying capacities results in  $f(N) < 0$ , which is a negative feedback. In Panel (a) the trivial steady states are unstable because  $\partial_N f(N) = \lambda = r > 0$  when  $\bar{N} = 0$ . At the steady state  $\bar{N} = K$  in Panel (b),  $\lambda = -d - s/k < 0$  for the straight red line corresponding to Eq. (3.8), and  $\lambda = -d(1 + 2K/k) < 0$  for the blue parabola corresponding to Eq. (3.4).  $N = 0$  is not a steady state in Panel (b). Note that the dimension of the slopes,  $\lambda$ , are  $\text{time}^{-1}$  in each case. This figure was made with the model `logist.R`.

to obtain

$$\frac{dh}{dt} = \lambda h \quad \text{with solution} \quad h(t) = h(0)e^{\lambda t}, \quad (4.4)$$

for the behavior of the distance,  $h$ , to the steady state. Thus, whenever the local tangent  $\lambda$  at the equilibrium point is positive, small disturbances,  $h$ , grow. Whenever  $\lambda < 0$  they decline, and the equilibrium point is stable.

This readily confirms the intuitive approach explained in Fig. 4.1 where we used the slope,  $\lambda = f'(\bar{N})$ , to determine whether or not a steady state is stable. For example, for the logistic equation,  $f(N) = rN(1 - N/K)$ , one obtains  $\lambda = r - 2rN/K$ . At the carrying capacity, i.e., at  $N = K$ , the local tangent is  $\lambda = -r$ , and at  $N = 0$  we obtain  $\lambda = r$  (see Fig. 4.1a), confirming that  $N = K$  is a stable steady state, and that  $N = 0$  is an unstable steady state. Similarly, for the non-replicating populations in Fig. 4.1b, we obtain that at the carrying capacity where  $f(K) = 0$ ,  $\lambda = -d - s/k < 0$  for the straight red line corresponding to Eq. (3.8), and  $\lambda = -d(1 + 2K/k) < 0$  for the blue parabola corresponding to Eq. (3.4). Since both slopes are negative, local perturbations of size  $h(0)$ , die out at a rate defined by Eq. (4.4).

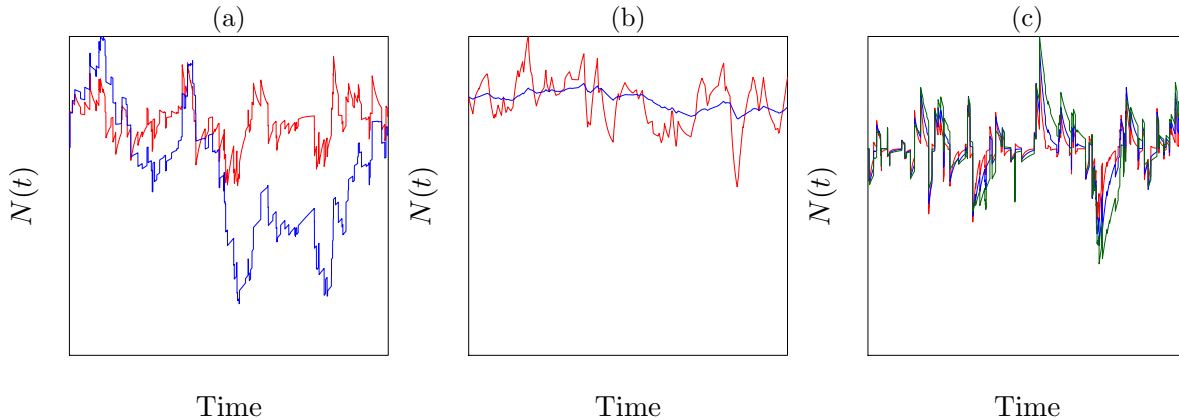


Figure 4.2: The return time to a steady state depends on the parameters and the density-dependent functions. Panels (a) and (b) depict a classic  $r$ -selected and  $K$ -selected population where the natural rate of increase of the  $r$ -selected species (in red) is 10-fold larger than that of the  $K$ -selected species (in blue). In Panel (a) we add noise sampled from a normal distribution with mean zero and 5% standard deviation to the population size  $N(t)$  of both models at randomly selected time points, and observe that the red  $r$ -selected species varies considerably less and remains closer to the carrying capacity. In Panel (b) we draw random values for the carrying capacity from a normal distribution with 5% standard deviation at randomly selected time points, and observe that the red  $r$ -selected species varies considerably more, as it more rapidly approaches the new carrying capacities. Panel (c) depicts the generalized logistic growth model of Eq. (3.11) for  $m = 0.5$  (green),  $m = 1$  (blue), and  $m = 2$  (red), where we add noise sampled from a normal distribution with mean zero and 5% standard deviation to the population size  $N(t)$  of at randomly selected time points, and observe that the (red) species with the steepest slope  $\lambda$  at the carrying capacity has the shortest return time. This figure was made with the models `logist3.R`.

### 4.3 Return time

Note that the slopes in Fig. 4.1 do have a different steepness, i.e., that the  $\lambda$ s differ. Since  $\lambda$  in Eq. (4.4) define the rate at which perturbations die out, the stability of a steady state can be expressed as a “Return time”

$$T_R = -\frac{1}{\lambda}, \quad (4.5)$$

i.e., the more negative  $\lambda$  the faster perturbations die out. Note that the dimension of  $T_R$  is correct: because  $\lambda$  is a rate with dimension “time<sup>-1</sup>”,  $T_R$  indeed has the dimension “time”. For example, consider the return time of the logistic growth equation around its carrying capacity. Above we derived that at  $\bar{N} = K$  the tangent  $\lambda = -r$ . This means for return time of the logistic growth equation that  $T_R = 1/r$ , i.e., the larger  $r$  the shorter the return time. Thus, populations that grow fast are more resistant to perturbations, which sounds intuitive.

The paradigm of  $r$ -selected and  $K$ -selected species in ecology is built upon this  $T_R = 1/r$  (see Fig. 4.2a for an example). An  $r$ -selected species with a 10-fold higher rate of increase than a  $K$ -selected species varies much less when we put additive white noise on the population size (Fig. 4.2a). However, if we introduce fluctuations in the environment corresponding to better and worse periods with a higher or smaller maximum population size by making the carrying capacity,  $K$ , a noisy parameter, we see that the  $r$ -selected species varies most (see Fig. 4.2b). Due to its faster growth rate the  $r$ -selected species traces these fluctuations, whereas a slower growing species lags behind and “averages” more over these periods.

Thus, the natural rate of increase,  $r$ , in the logistic equation plays an important role in the resilience of the carrying capacity to perturbations. The three growth functions of the generalized

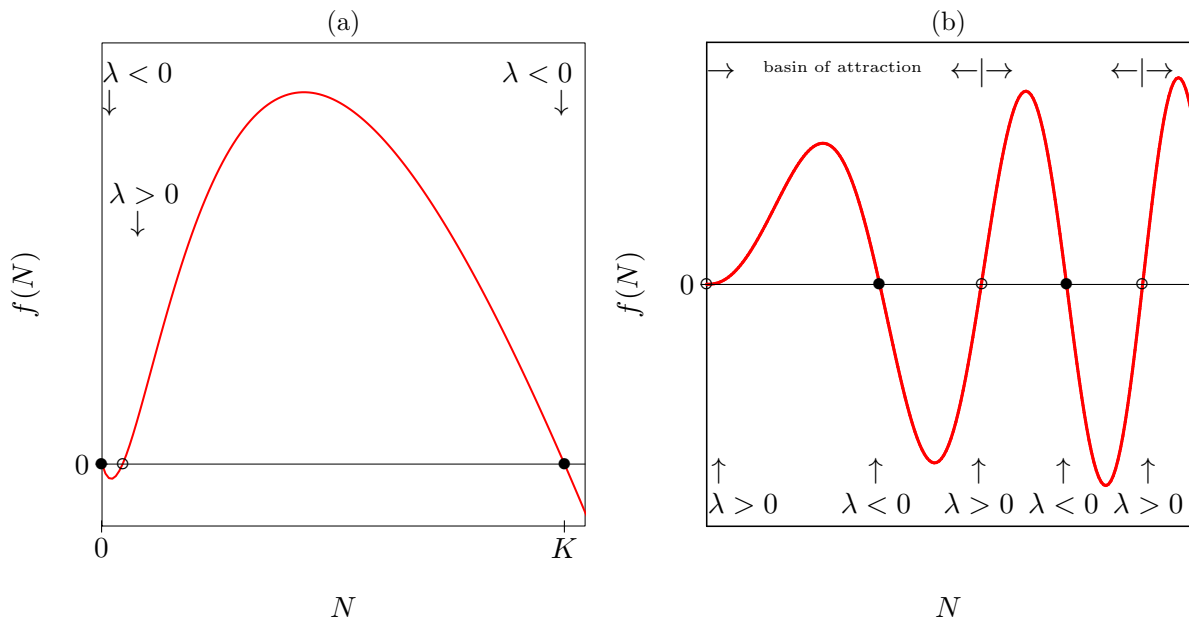


Figure 4.3: The stability of a steady state is determined by the local derivative (slope) of the growth function at the steady state. We plot the population growth rate,  $dN/dt = f(N)$ , as a function of the population size  $N$ . Panel (a) depicts the growth rate of a population with an Allee effect, i.e.,  $f(N) = (bf(N)g(N) - d)N$ , see Eq. (3.19a). Panel (b) depicts an arbitrary growth function to illustrate that each unstable steady state defines the boundary of the basin of attraction of a stable steady state.

logistic equation in Fig. 4.1a, reveal that the shape of the density dependence also plays a role. The derivative of  $f(N) = rN(1 - (N/K)^m)$  with respect to  $N$  is  $f'(N) = r - (m+1)r(N/K)^m$ , which at the carrying capacity becomes  $f'(K) = \lambda = -mr$ . A population with a concave,  $m > 1$ , density-dependence therefore has a shorter return time than a population with a linear ( $m = 1$ ), or convex ( $m < 1$ ) density-dependence (see Fig. 4.2c). Thus, carrying capacities are more stable when competition starts at relative high population densities, i.e., when  $m > 1$ . Similarly, the two non-replicating populations, with the same source,  $s$ , and expected life span,  $1/d$ , and the same carrying capacity,  $K$ , also have slightly different return times (see Fig. 3.4b). The growth curves in Fig. 4.1b reveal that the model with density-dependent death has a steeper slope,  $\lambda$ , at the steady state than the model with density-dependent production. The time series in Fig. 3.4b confirm this results in the expected difference in the return time.

We will return to the subject of return time later when we consider models composed of several ODEs. The slope  $\lambda$  will then be replaced by the largest eigenvalue,  $\lambda_{\max}$ , but Eq. (4.5) will have the same form, i.e.,  $T_R = \frac{-1}{\lambda_{\max}}$ .

## 4.4 Basins of attraction

In the previous chapter we saw that positive density-dependence can give rise to an Allee-effect, meaning that a population needs to be sufficiently large before it can grow. The growth function of that model is depicted in Fig. 4.3a, which confirms that this population has three steady states where  $f(\bar{N}) = 0$ . The local derivative,  $\lambda$ , has a positive slope at the critical population size, demonstrating that this is an unstable steady state. Since starting values below this unstable state all approach the stable point  $N = 0$ , and trajectories starting above

it all approach the carrying capacity, the unstable point separates the “basins of attraction” of the two stable steady states. This concept of a basin of attraction is further illustrated by the example function in Fig. 4.3b. Note that the return time has no bearing on a basin of attraction: return times are only defined in the neighborhood of a steady state where the linearization remains a good approximation. The concepts of “robustness” and “resilience” do involve the size of a basin of attraction. Steady states with a small basin of attraction have a low robustness because perturbations may push the population into approaching an alternative attractor. Thus, resilience can have two fairly unrelated interpretations: (1) the return time to an attractor after a small perturbation, and (2) the size of the basin of attraction, i.e., the robustness to larger perturbations.

## 4.5 Summary

Plotting the population growth function  $dN/dt = f(N)$  as a function of the population size,  $N$ , reveals the steady states, and from the slope in the steady state one can determine the stability of the steady state. A steady state is stable when the local derivative,  $\partial_N f(\bar{N}) = \lambda$ , of the growth function is negative, and it is unstable whenever  $\lambda > 0$ . When the slope is computed by taking the derivative, i.e., by linearization, one obtains a parameter expression that can be used to define the return time,  $T_R = -1/\lambda$ , quantifying how rapidly the population re-approaches the steady state following a small disturbance. Basins of attraction have borders defined by unstable steady states, or repellers, and steady states with a small basin of attractions are not resilient because sufficiently large disturbances that breach their basin boundary let the system approach an alternative attractor.

## 4.6 Exercises

### Question 4.1. Density dependent death

Consider a replicating population where most of the death is due to competition with other individuals, i.e., let  $f(N) = cN$  in a model where  $dN/dt = (b - f(N))N$ .

- Sketch the *per capita* death rate as a function of  $N$ .
- Sketch the *per capita* net growth rate as a function of  $N$ .
- Compute the steady states.
- Why is the  $R_0$  not defined?
- What is the return time in the non-trivial steady state?

### Question 4.2. Return time

- Compute the return time around the carrying capacities of the “logistic growth” models with an explicit density-dependent birth or death rate, i.e.,  $dN/dt = bN[1 - N/k] - dN$  and  $dN/dt = bN - dN[1 + N/k]$ . Which parameter do you expect to be the dominant factor in the return time after a small perturbation of the population at its carrying capacity.
- Compute the return time around the carrying capacities of the non-replicating population  $dN/dt = s - dN$ .
- Why are these return times independent of  $k$  and  $s$ ?
- Would adding negative density dependence to the model of the non-replication population, e.g.,  $dN/dt = s(1 - N/k) - dN$ , shorten the return time?

### Question 4.3. Whales

Make the whales question in Chapter 14 to develop a simple model for a population of whales

in the oceans. The main feature of this model is that females face difficulties find a male at low population densities, which is expected to give rise to an Allee effect. Use either your own model, or the model that is provided in the answers of Chapter 14, to confirm that this gives an Allee effect. To keep the (graphical) analysis simple, separately consider density-dependent birth and density-dependent death.

- a. Write an appropriate ODE for each of these two cases
- b. Sketch both the total and the *per capita* birth and death rates as a function of the population size (you probably want to use the file `whales.R`).
- c. Sketch the net growth of the whale population as a function of the population size, and indicate the basins of attraction of the steady states.



## Chapter 5

# Killing and consumption

In Chapter 3 we have written models for density-dependent population growth by allowing the birth rate to decline as a function of the population density, and/or the death rate to increase with the population density. Such models tend to be simplifications because density-dependent effects typically operate indirectly via other populations, and not by direct contacts between the individuals. For example, we have written a model for density-dependent production of red blood cells with a production term that decreases as a function of the density of red blood cells. In reality this depends on the production of EPO produced by cells in the kidney, which in turn depends on their oxygenation, which finally depends on the red blood cell density. Another example is the density-dependent growth of a population of bacteria, which typically operates via the depletion of resources, or via the production of toxins, at high bacterial densities. An example where direct competition would be a true mechanism is the slowing down of cell-division by “contact inhibition” when cells become surrounded by other cells in cell cultures or tissues.

To explicitly allow for the factors mediating the density-dependence we have to extend our models with variables representing these factors. Classic examples are bacteria or algae consuming nutrients required for their growth and maintenance. Because at high population densities the resource availability decreases by this consumption, one naturally obtains a density-dependence that will ultimately limit the total population size. A first example would be a population of cells growing in a closed environment, requiring a certain nutrient for successful cell division. If this nutrient becomes freely available upon cell death, one could write a conservation equation for the resource,  $R_T = R + cN$ , where  $R_T$  is the fixed total density of resource in the closed environment,  $cN$  is the total amount of resource contained in the  $N$  cells of the population, and  $R$  is the amount of resources that is freely available. Writing the rate of cell-division as a saturation function of the available resource density, with a maximum division or birth rate,  $b$ , one would obtain something like,

$$\frac{dN}{dt} = \frac{bRN}{h + R} - \delta N = \frac{b(R_T - cN)N}{h + R_T - cN} - \delta N = bN \left( 1 - \frac{h}{h + R_T - cN} \right) - \delta N, \quad (5.1)$$

where  $h$  the resource density at which the cells divide at half their maximal rate, and  $\delta$  is the death rate of the cells. Thus, we again an ODE where the population birth is limited directly by the population density, but note that none of the models in Chapter 3 resembles Eq. (5.1); see the exercises.

To generally extend our model with a dynamic resource that is limiting population growth, we need to add an ODE for the resource, with a production and a loss term, we need to define a

functional form for the consumption rate, and we need to define how the birth and/or death rate of the population depends on the amount of resources consumed. We will treat each of these terms separately, and, whenever needed, sketch functions to define the form of interaction terms.

## 5.1 Bacteria in chemostats

First consider bacteria growing in a well-mixed chemostat with a fixed influx of fluid containing nutrients, and a constant outflow of fluid containing nutrients and bacteria.<sup>1</sup> In the absence of bacteria one would write  $dR/dt = s - wR$ , where  $R$  (for resource) is the concentration of the nutrient in the chemostat,  $s$  is the rate of influx (e.g., in moles per hour), and  $w$  is the rate of efflux (then also per hour), and  $1/w$  is the average residence time in the chemostat. Some time after initializing the chemostat, the nutrient concentration approaches the steady state  $\bar{R} = s/w$ .

When the maximum nutrient levels remain sufficiently low, e.g., if the source  $s$  is small, one can safely assume that the rate at which bacteria take up nutrients remains proportional to  $R$ , and hence a sketch of the *per capita* consumption rate as a function of  $R$ , is expected to be a straight line through the origin with some slope, say  $a$ . Writing  $N$  for the density of bacteria, and  $a$  for the rate of uptake of nutrients per bacterium per hour, one would write

$$\frac{dR}{dt} = s - wR - aRN . \quad (5.2)$$

If the division rate of the bacteria is limited by nutrients, and if this were to remain proportional to their *per capita* uptake,  $aR$ , at these low nutrient levels, one would write

$$\frac{dN}{dt} = caRN - (w + d)N = caRN - \delta N , \quad (5.3)$$

where  $caR$  is the *per capita* birth rate,  $w$  remains the rate of wash-out from the chemostat,  $d$  is the death rate of the bacteria (per hour), and  $\delta = w + d$ . Seeding a chemostat at steady state,  $\bar{R} = \frac{s}{w}$ , with some bacteria will lead to bacterial growth whenever their  $R_0 = \frac{ca\bar{R}}{\delta} = \frac{cas}{\delta w} > 1$ .

The properties of this 2-dimensional model can be analyzed by sketching nullclines and computing the steady state(s). Starting with the latter we observe that in the presence of bacteria, the steady state resource density is solved by setting  $dN/dt = 0$  in Eq. (5.3). Cancelling the trivial  $N = 0$  solution that we already considered above, this leads to  $\bar{R} = \frac{\delta}{ca}$ . This calculation also reveals that the  $dN/dt = 0$  nullcline consists of two straight lines in the phase plane, one corresponding to the line  $N = 0$ , and the other to the line  $R = \frac{\delta}{ca}$ . To proceed with the steady state we next solve  $N$  from  $dR/dt = 0$  in Eq. (5.2),

$$N = \frac{s}{aR} - \frac{w}{a} \quad \text{which, after substituting } R = \frac{\delta}{ca}, \text{ gives } \bar{N} = \frac{sc}{\delta} - \frac{w}{a} . \quad (5.4)$$

The former expression gives the  $dR/dt = 0$  nullcline, and the latter the ‘‘carrying capacity’’ of the bacteria in a chemostat with source  $s$  and loss rate  $\delta = w + d$ . The model therefore has two steady states: the trivial  $(\bar{R}, \bar{N}) = (\frac{s}{w}, 0)$  and the non-trivial  $(\bar{R}, \bar{N}) = (\frac{\delta}{ca}, \frac{sc}{\delta} - \frac{w}{a})$ .

To study the stability of these steady state we perform phase plane analysis. Since the  $dR/dt = 0$  nullcline is expressed as a function  $N = f(R) = \frac{s}{aR} - \frac{w}{a}$ , and the  $dN/dt = 0$  nullclines are straight

<sup>1</sup>Note that this also applies to bacteria living in a gut microbiome, because they also depend on a external influx of nutrients, and are being washed out with the excrement; see Chapter 10. The gut is not well mixed, however.

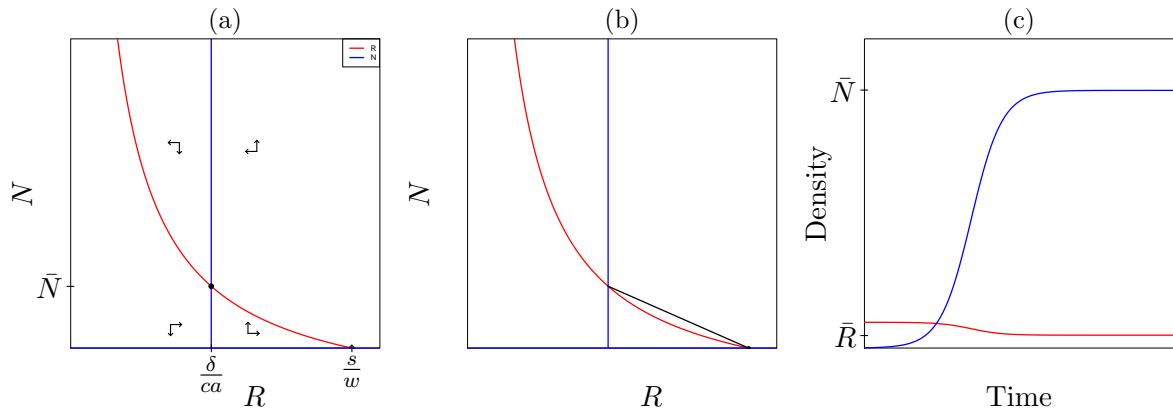


Figure 5.1: Bacterial growth in a chemostat. In Panels (a) and (b) the curved red lines depict the  $dR/dt = 0$  nullcline, and the straight blue lines the  $dN/dt = 0$  nullcline. They intersect in a stable steady state (as indicated by the solid symbol) located at  $(R, N) = (\bar{R}, \bar{N})$ . The black line in Panel (b) is a trajectory corresponding to the introduction of a few bacteria into a chemostat at the trivial steady state ( $R = s/w$ ). Panel (c) depicts this trajectory as a time plot, and illustrates that the bacterial growth curve looks like a sigmoidal logistic growth process. This figure was made with the model `chemo.R`.

lines at fixed  $R = \bar{R}$  or  $N = 0$  values, we define the vertical axis of the phase plane by the bacteria and the horizontal axis by the resource (see Fig. 5.1a) The  $dR/dt = 0$  nullcline,  $N = \frac{s}{aR} - \frac{w}{a}$ , has a vertical asymptote when  $R = 0$ , a horizontal asymptote  $N = -\frac{w}{a}$  when  $R \rightarrow \infty$ , and intersects the horizontal axis at the trivial resource density,  $R = s/w$  (see Fig. 5.1a). For the vector field one could start close to the origin,  $(R, N) \simeq (0, 0)$ , where  $dR/dt > 0$  because  $s > wR$ , and where  $dN/dt < 0$  because  $caR < \delta$  (see the arrows in the bottom-left corner). Flipping the horizontal arrows at the  $dR/dt = 0$  nullcline, and the vertical arrows at the  $dN/dt = 0$  nullcline, the vector field can be completed for every qualitatively different region in the phase space. One may double-check that  $dR/dt < 0$  and  $dN/dt > 0$  in the upper-right corner, where  $s < dR - aRN$  and  $caR > \delta$ . Finally, note that the location of the bacterial nullcline,  $R = R^* = \frac{\delta}{ca}$ , corresponds to the critical resource required for bacterial growth (Tilman, 1980, 1982), and that the nullclines will only intersect when  $\frac{s}{w} > R^*$ .

In Fig. 5.1a the steady state  $(\frac{s}{w}, 0)$  without bacteria is unstable because the vertical vectors are pointing away from it (actually, it is a saddle-point because the horizontal vectors are pointing towards it). Indeed, introducing bacteria into this state is expected to lead to bacterial growth (because  $\frac{s}{w} > R^*$ ). To determine the stability of the non-trivial steady state we have to linearize the system to compute the Jacobi matrix. Following the accompanying Ebook (Panfilov *et al.*, 2025), we write the two ODEs in Eq. (5.2) and (5.3) as two normal functions,  $f(R, N) = s - wR - aRN$  and  $g(R, N) = caRN - \delta N$ , determine their partial derivatives, and subsequently substitute the steady state values:

$$J = \begin{pmatrix} \frac{\partial_R f}{\partial_R g} & \frac{\partial_N f}{\partial_N g} \end{pmatrix}_{|(\bar{R}, \bar{N})} = \begin{pmatrix} -w - a\bar{N} & -a\bar{R} \\ ca\bar{N} & ca\bar{R} - \delta \end{pmatrix} = \begin{pmatrix} -w - a\bar{N} & -\delta/c \\ ca\bar{N} & 0 \end{pmatrix} = \begin{pmatrix} -\alpha & -\beta \\ +\gamma & 0 \end{pmatrix}, \quad (5.5)$$

where  $\alpha, \beta$  and  $\gamma$  are arbitrary positive values. Since the trace of this Jacobi matrix,  $\text{tr} = -\alpha < 0$ , and its determinant,  $\det = 0 - -\beta\gamma = \beta\gamma > 0$ , both eigenvalues will be negative (i.e., have a negative real part). We therefore conclude that the non-trivial steady state is stable. Note that we can also read of the signs of this Jacobian from the vector field. The local effect of  $R$  on  $dR/dt = f(R, N)$  is given by the negative arrow on the right side of the steady state, the negative effect of  $N$  on  $dR/dt = f(R, N)$  is given by the negative arrow above the steady state, the positive effect of  $R$  on  $dN/dt = g(R, N)$  is given by the positive arrow on the right

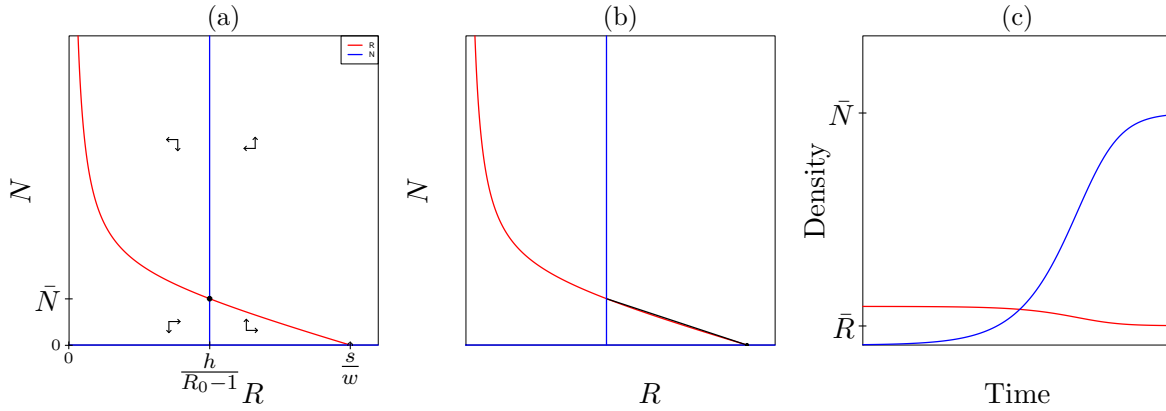


Figure 5.2: Bacteria with a Monod saturated growth function. In Panels (a) and (b) the curved red lines depict the  $dR/dt = 0$  nullcline, and the straight blue lines the  $dN/dt = 0$  nullcline. They intersect in a stable steady state (as indicated by the solid symbol) located at  $(R, N) = (\bar{R}, \bar{N})$ . The black line in Panel (b) is a trajectory corresponding to the introduction of a few bacteria into a chemostat at the trivial steady state ( $R = s/w$ ). Panel (c) depicts this trajectory as a time plot, and illustrates that the bacterial growth curve looks like a sigmoid logistic growth process. This figure was made with the model `chemoMonod.R`.

side of the steady state, and the null effect of  $N$  on  $dN/dt = g(R, N)$  is revealed by the fact that  $g(R, N) = 0$  above the steady state (see the section on the graphical Jacobian in the accompanying Ebook (Panfilov *et al.*, 2025)). A population that is maintained by a resource that is maintained by a source, and with a linear functional response (leading to mass-action consumption and birth terms), is therefore expected to have a stable steady state (the carrying capacity) whenever its  $R_0 > 1$ .

## Saturated consumption

Actually it has been known for a long time (Monod, 1949) that the division rate of bacteria approaches a maximum at high nutrient densities, and that this is limited by the rate at which a bacterium can consume nutrients. Thus, the division rate of bacteria is typically proportional to their consumption rate. The saturation at high nutrient densities is modeled with a Hill function,  $f(R) = \frac{R}{h+R}$ , which in this literature has been coined as the Monod saturation function. Allowing for saturation and assuming that the rate at which bacteria divide is proportional to the rate at which they take up nutrients, one would write

$$\frac{dR}{dt} = s - wR - \frac{aRN}{h+R} \quad \text{and} \quad \frac{dN}{dt} = \frac{caRN}{h+R} - (w+d)N = \frac{caRN}{h+R} - \delta N. \quad (5.6)$$

At the expense of one new parameter,  $h$ , representing the resource density at which the *per capita* consumption rate is half maximal, we now have a model that is also realistic at high resource densities. The fitness  $R_0$  of the bacteria can here be defined in two ways. First, one could invoke the maximum resource density,  $R = s/w$ , to compute a maximum division rate  $\frac{cas/w}{h+s/w} = \frac{cas}{wh+s}$ . With an expected residence time of  $1/\delta$  this would correspond to an  $R_0 = \frac{cas}{\delta(wh+s)}$ . Second, one could go for a much simpler definition of  $R_0$  by making use of the fact that the division rate approaches a maximum,  $ca$ , at infinite resource densities, which provides an  $R_0 = \frac{ca}{\delta}$ . The latter  $R_0$  is elegantly simple and will be used to clean up the expressions for the steady states.

Analyzing the behavior of the model by computing steady states and nullclines, we first observe that setting  $dN/dt = 0$ , and cancelling the trivial  $N = 0$  solution, again provides the steady

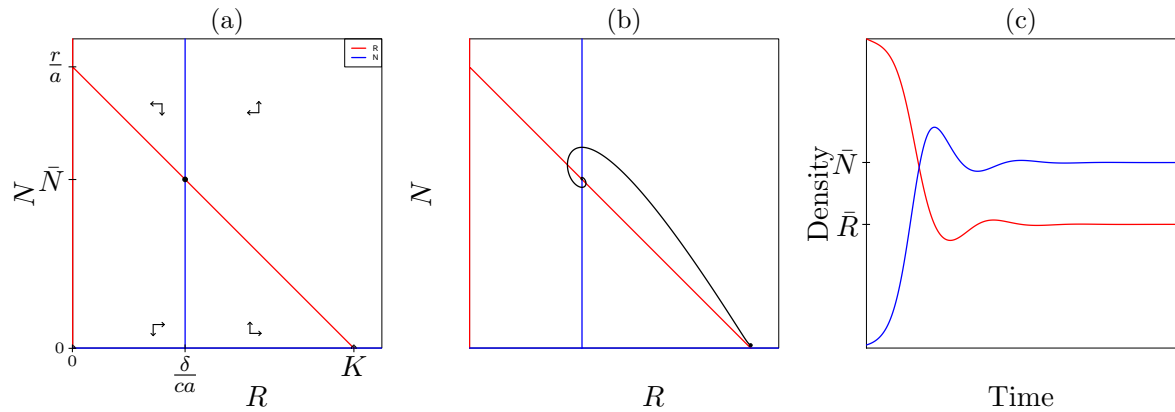


Figure 5.3: The Lotka-Volterra model. In Panels (a) and (b) the slanted red lines depict the  $dR/dt = 0$  nullcline, and the vertical blue lines the  $dN/dt = 0$  nullcline. They intersect in a stable steady state (as indicated by the solid symbol) located at  $(R, N) = (\bar{R}, \bar{N})$ . The predator nullcline is located at the critical prey density  $R^* = \frac{d}{ca} = \frac{K}{R_0}$ . The black line in Panel (b) is a trajectory, again corresponding to the introduction of a few consumers into the carrying capacity of the resource. Panel (c) depicts this trajectory as a time plot, and illustrates that the consumer growth curve looks like a sigmoid logistic growth process. This figure was made with the model `lotkaBM.R`.

state of the resource,  $\bar{R} = \frac{h\delta}{ca-\delta} = \frac{h}{R_0-1}$ , where  $R_0 = \frac{ca}{\delta}$ . The  $dN/dt = 0$  nullclines therefore remain to be two straight lines, one at  $N = 0$  and the other at  $R = R^* = \bar{R}$  (see Fig. 5.2). To find the steady state of the bacteria we need to substitute the  $R$  in the  $dR/dt = 0$  equation with  $\bar{R} = \frac{h\delta}{ca-\delta}$ . Starting with the consumption term, one obtains

$$\frac{a\bar{R}N}{h + \bar{R}} = \frac{aN}{h/\bar{R} + 1} = \frac{aN}{h\frac{ca-\delta}{h\delta} + 1} = \frac{a\delta N}{ca - \delta + \delta} = \frac{\delta}{c} N, \quad (5.7)$$

and hence for the full model

$$s - \frac{wh\delta}{ca - \delta} - \frac{\delta}{c}N = 0 \quad \text{resulting in} \quad \bar{N} = \frac{cs}{\delta} - \frac{chw}{ca - \delta} = \frac{c}{\delta} \left( s - \frac{hw}{R_0 - 1} \right). \quad (5.8)$$

The  $dR/dt = 0$  nullcline can be found as follows

$$s - wR = \frac{aRN}{h + R} \quad \leftrightarrow \quad N = \frac{(h + R)(s - wR)}{aR} = \frac{h + R}{a} \left( \frac{s}{R} - w \right), \quad (5.9)$$

which is zero when  $R = -h$  or  $R = s/w$ . Because  $N \simeq \frac{hs}{aR}$  when  $R \rightarrow 0$ , this nullcline has a vertical asymptote when  $R \rightarrow 0$ . Because  $h + R \rightarrow R$  when  $R \gg h$ , and  $s/R - w \rightarrow -w$  when  $R \gg s$ , the nullcline approaches a slant asymptote with slope  $-\frac{w}{a}R$  when  $R \rightarrow \infty$  (see Fig. 5.2).<sup>2</sup> We observe that adding Monod saturation to the model hardly changes the phase plane. Since the local vector field around the non-trivial steady state yields the same graphical Jacobian as the last matrix in Eq. (5.5) we confirm that non-trivial steady state is stable. Note, that this is quite different from the situation where saturated consumption is added to a model with a replicating resource (see Chapter 7).

<sup>2</sup>The slant asymptote can be checked by observing that when  $R \gg h$ , the nullcline is solved from  $s - wR = aN$ , revealing the slant asymptote  $N = \frac{s-wR}{a}$ . We also provide a tutorial [tbb.bio.uu.nl/rdb/bm/clips/sketch](http://tbb.bio.uu.nl/rdb/bm/clips/sketch) on finding slant asymptotes.

## 5.2 Replicating resources

Next consider a population consuming a replicating resource (that itself would approach a steady state in the absence of consumption). This could be zooplankers grazing algae, or killer cells that divide after removing tumor cells. In Chapter 3 we have learned that logistic growth is a reasonable general model for a replicating resource with linear density dependent birth and/or death rates. Thus, starting by adopting logistic growth for the resource, and with the same mass-action consumption as above, one would write

$$\frac{dR}{dt} = rR(1 - R/K) - aRN, \quad \frac{dN}{dt} = caRN - \delta N. \quad (5.10)$$

This is the famous Lotka-Volterra model that was proposed independently by Lotka (1913) and Volterra (1926) as an ecological predator-prey model. Note that the ODE for the consumers is identical to Eq. (5.3). We will see in Chapter 6 that epidemiological models for an infection spreading in a population of susceptible hosts can also be described with Eq. (5.10) (when  $R$  are susceptible and  $N$  infected hosts,  $a$  is an infection rate, and  $c = 1$ ). Interpreting  $R$  has the size of a tumor (or an infection),  $caR$  as a *per capita* cell division rate, and  $N$  as the number of immune effector cells, the same model has also been used for modeling an immune response to a replicating threat (Nowak & May, 2000).

Because the Lotka-Volterra model is used so widely in theoretical biology we will analyze it in detail. Starting with the steady states we observe that in the absence of consumers the resource will either be zero, or approach the steady state  $\bar{R} = K$ . In the presence of consumers one solves  $\bar{R} = \frac{\delta}{ca}$  by setting  $dN/dt = 0$ , and substituting this into

$$r(1 - R/K) - aN = 0 \quad \text{yields} \quad \bar{N} = \frac{r}{a} \left(1 - \frac{\delta}{caK}\right) \quad (5.11)$$

for the non-trivial steady state of the consumers. The  $dN/dt = 0$  nullcline consists of the now familiar straight lines  $N = 0$  and  $R = \frac{\delta}{ca}$ , and the  $dR/dt = 0$  isocline is defined by  $R = 0$  and  $N = \frac{r}{a} \left(1 - \frac{R}{K}\right)$ . Depicted in a phase space with  $N$  on the vertical axis and  $R$  on the horizontal axis, the nullcline of the resource is a declining straight line, intersecting the vertical axis at  $N = r/a$  and the horizontal axis at  $R = K$  (see Fig. 5.3a). The location of the non-trivial consumer nullcline again defines the critical resource density,  $R^*$ , required for net growth of the consumers, and the non-trivial steady state only exists when  $R^* < K$  (see Fig. 5.3a).

The model has maximally three steady states,

$$(\bar{R}, \bar{N}) = (0, 0), \quad (K, 0) \quad \text{and} \quad \left(\frac{\delta}{ca}, \frac{r}{a} \left[1 - \frac{\delta}{caK}\right]\right). \quad (5.12)$$

The vector field in Fig. 5.3a reveals that the first two are unstable (saddle points). Defining  $f(R, N) = dR/dt$  and  $g(R, N) = dN/dt$ , computing the four partial derivatives, the Jacobian of the non-trivial steady state is defined as

$$J = \begin{pmatrix} \partial_R f & \partial_N f \\ \partial_R g & \partial_N g \end{pmatrix}_{|(\bar{R}, \bar{N})} = \begin{pmatrix} r - \frac{2r}{K}\bar{R} - a\bar{N} & -a\bar{R} \\ ca\bar{N} & ca\bar{R} - \delta \end{pmatrix} = \begin{pmatrix} -\frac{r\delta}{caK} & -\delta/c \\ ca\bar{N} & 0 \end{pmatrix} = \begin{pmatrix} -\alpha & -\beta \\ +\gamma & 0 \end{pmatrix}, \quad (5.13)$$

where  $\alpha, \beta$  and  $\gamma$  are arbitrary positive values. Since the trace of this Jacobi matrix,  $\text{tr} = -\alpha < 0$ , and its determinant,  $\det = 0 - -\beta\gamma = \beta\gamma > 0$ , both eigenvalues will be negative (i.e., have a negative real part), and the non-trivial steady state is stable. Note that the trajectory in Fig. 5.3b is spiraling inwards, meaning that for the parameters that were used to make this figure the

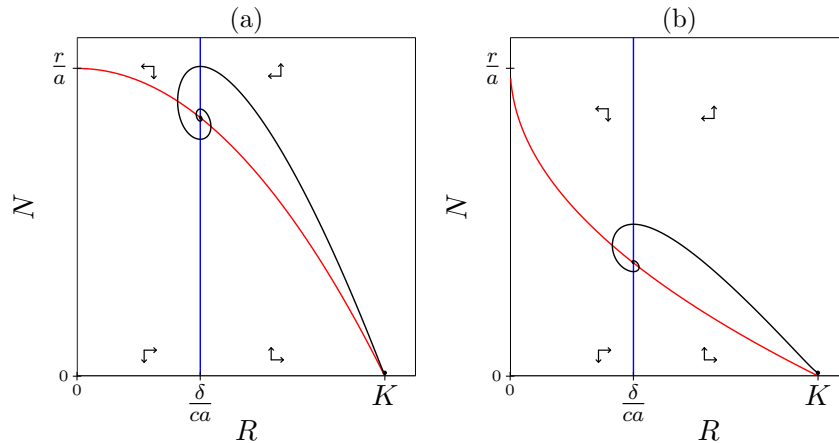


Figure 5.4: The “generalized” Lotka-Volterra model. In Panels (a) we set  $m > 1$  and in Panel (b)  $m < 1$ . The curved red lines depict the  $dR/dt = 0$  nullcline, and the straight blue lines the  $dN/dt = 0$  nullcline. Black lines are trajectories starting close to  $R = K$ . This figure was made with the model `lotkaBM.R`.

steady state is a stable spiral point (and that the eigenvalues are a complex pair with a negative real part).

The  $R_0$  of the resource is not defined because the logistic growth term collapsed birth and death into a net growth rate. Since  $dN/dt$  has separate birth and death terms, one can calculate an  $R_0$  for the predator. Because the *per capita* birth rate of the consumers,  $caR$ , is proportional to the prey density, we have to substitute the maximum prey density  $R = K$  into the birth rate,  $caR$  (because the  $R_0$  is calculated for the best possible circumstances; see Chapter 6). Doing so one arrives at  $R_0 = \frac{caK}{\delta}$ , and for this fitness  $R_0 = 1$  can indeed be used as an invasion criterion because the predator can only expand when  $caK > \delta$ . The expression of the fitness,  $R_0 = \frac{caK}{\delta}$ , and the location of the consumer nullcline,  $R^* = \frac{\delta}{ca}$ , resemble each other. This can be used to express  $R^*$  in terms of the  $R_0$ , i.e.,  $R^* = K/R_0$ , which says that the degree by which a predator exhausts its prey population is completely determined by its  $R_0$ . A predator with an  $R_0 = 10$  is therefore expected to deplete the prey density to 10% of its carrying capacity.

## Generalizing the Lotka-Volterra model

The Lotka-Volterra model assumed that the density-dependent terms of the resource are linear. What to expect for the consumption of replicating resources having a non-linear density-dependence? An approach to test this is to use the generalized form of the Logistic-growth equation (see Chapter 3), and write a “generalized” Lotka-Volterra model

$$\frac{dR}{dt} = rR(1 - (R/K)^m) - aRN, \quad \frac{dN}{dt} = caRN - \delta N, \quad (5.14)$$

which has identical  $dN/dt = 0$  nullclines. The non-trivial  $dR/dt = 0$  nullcline,  $N = \frac{r}{a}(1 - (R/K)^m)$ , is concave when  $m > 1$  and convex when  $m < 1$  (see Fig. 5.4). Because this does not affect the nature of the steady states in the phase plane, i.e., the local vector field in the neighborhood of the steady states remains the same, we conclude that similar model behavior is expected when resources have a non-linear density-dependence.

Generally the shape of the  $dR/dt = 0$  nullcline for a resource having a mass-action consumption

term reflects the *per capita* growth rate of the resource. Consider the more general form

$$\frac{dR}{dt} = [f(R) - aN] R , \quad (5.15)$$

where  $f(R)$  is an arbitrary function defining the *per capita* growth rate of  $R$ , and observe that the non-trivial nullcline can be written as  $N = f(R)/a$ . Thus, whenever the *per capita* growth rate of  $R$  is a monotonically declining function of  $R$ , we expect a declining “Lotka-Volterra like” nullcline of the resource in the phase space, provided we can cancel  $R$  from the consumption term (here the mass-action,  $aNR$ , term). We therefore expect more complicated nullclines for saturated consumption terms, e.g.,  $\frac{aNR}{h+R}$ , from which we cannot cancel  $R$ . This is explored in Chapter 7.

When should one expect the vertical  $dN/dt = 0$  nullcline that we obtained throughout in this chapter? The Lotka-Volterra model assumes that the birth rate of the consumers increases linearly with the *per capita* consumption,  $aR$ . This need not be true as a consumer’s birth rate may be a saturation function of its consumption; at a certain level of consumption the birth rate may slow down due to “diminishing returns”. Such a relationship, e.g., a *per capita* birth rate of

$$g(aR) = \beta \frac{aR}{H + aR} = \beta \frac{R}{h + R} , \quad (5.16)$$

where  $\beta$  is the maximum birth rate and  $h = H/a$ , would correspond to

$$\frac{dN}{dt} = \left[ \frac{\beta R}{h + R} - \delta \right] N , \quad (5.17)$$

with an  $R_0 = \beta/\delta$ . Since, one can cancel the  $N = 0$  solution after setting  $dN/dt = 0$ , we would still obtain a vertical nullcline (at  $R^* = \frac{h}{R_0 - 1}$ ). Rewriting Eq. (5.17) in a more general form like

$$\frac{dN}{dt} = [\beta f(R) - \delta] N , \quad (5.18)$$

one indeed obtains a vertical predator nullcline for any function  $f(R)$ . Summarizing, a vertical predator nullcline is obtained whenever one can cancel the consumer,  $N$ , from the consumer’s  $dN/dt = 0$  equation.

The nullcline will no longer be vertical when the consumer,  $N$ , remains present in the term between the square brackets of Eq. (5.18). This will be the case when the functional response is predator dependent, i.e., when one replaces  $f(R)$  by  $f(R, N)$ , or when the death rate is density dependent, e.g., when  $\delta$  is replaced by  $\delta(1 + \epsilon N^m)$ . Whenever this leads to a negative density-dependence, the predator nullcline will be slanted to the right, which changes the effect of the consumer on itself from zero to negative (see Fig. 5.5e). The graphical Jacobian of the non-trivial steady state of a Lotka-Volterra model with a negative density-dependence of the resource and the consumer will therefore be

$$J = \begin{pmatrix} - & - \\ + & - \end{pmatrix} \quad \text{with} \quad \text{tr} < 0 \quad \text{and} \quad \text{det} > 0 . \quad (5.19)$$

The steady state remains stable, and most of the conclusions drawn in this chapter seem robust to allowing for direct competition among the consumers. Conversely, in the next section we will see that allowing for positive density-dependence among the consumers, e.g., for cooperative hunting, can destabilize the steady state (see Fig. 5.5d), but only when the resource has little negative density-dependence (see Fig. 5.5f).

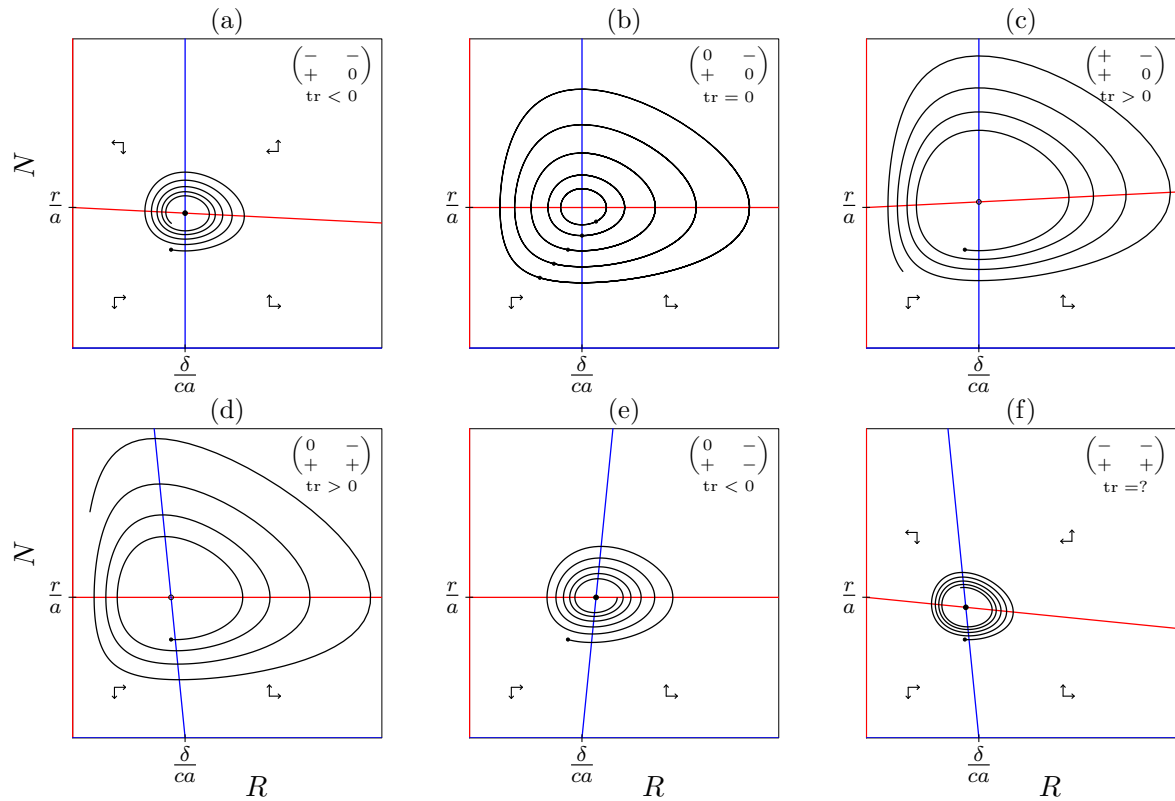


Figure 5.5: The Lotka-Volterra model with horizontal and slanted nullclines. Red lines depict the  $dR/dt = 0$  nullclines, blue lines the  $dN/dt = 0$  nullclines, and black lines trajectories. In Panels (a-c) the non-trivial consumer nullcline is a vertical line at  $R = \frac{\delta}{ca}$  (because  $\epsilon_N = 0$  in Eq. (5.23)), and in Panels (d) and (e) the non-trivial resource nullcline is a horizontal line at  $N = \frac{r}{a}$  (because  $\epsilon_R = 0$ ). Panel (a) depicts the classic Lotka-Volterra model with a resource nullcline that is slanted downwards (due to their negative density-dependence,  $\epsilon_R > 0$ , allowing for a carrying capacity). In Panel (b) the resource nullcline is horizontal and the consumer nullcline vertical. In Panel (c) the resource nullcline is slanted upwards (positive density-dependence,  $\epsilon_R < 0$ ). In Panel (d) the consumer nullcline is slanted leftwards (positive density-dependence,  $\epsilon_N < 0$ ). In Panel (e) the consumer nullcline is slanted rightwards ( $\epsilon_N > 0$ ). In Panel (f) illustrates that sufficient negative density-dependence of the resource,  $\epsilon_R > 0$ , can compensate for positive density-dependence of the consumer,  $\epsilon_N < 0$ , and allow for a stable steady state (if the trace is negative). The graphical Jacobian of the non-trivial steady state is provided in the upper right corner, the determinant of these matrices is always positive and the sign of the trace is indicated. The perpendicular nullclines in Panel (b) intersect in a steady state with neutral stability,  $\text{tr} = 0$  and  $\text{det} > 0$ , and the behavior of the model is cycles of neutral stability that are defined by the initial condition (bullets). This Figure was with the model `lotka0.R`.

### 5.3 Horizontal and vertical nullclines

The Lotka-Volterra model is sometimes written in a structurally unstable form without a negative density dependence of the resource:

$$\frac{dR}{dt} = rR - aRN, \quad \frac{dN}{dt} = caRN - \delta N, \quad (5.20)$$

which has the normal vertical  $dN/dt = 0$  nullcline at  $R = \frac{\delta}{ca}$  and a horizontal  $dR/dt = 0$  nullcline at  $N = \frac{r}{a}$  (see Fig. 5.5b). This model has limited biological relevance. The reason is that any small change of the model will lead to a qualitatively different type of behavior. The model is therefore said to be “structurally unstable”, and should not be used in biological research (the model is used in teaching examples because it is so elegantly simple). The non-trivial steady

state is given by the perpendicular intersection of the nullclines, i.e.  $(\bar{R}, \bar{N}) = (\frac{\delta}{ca}, \frac{r}{a})$ , and the Jacobian of this steady state is

$$J = \begin{pmatrix} r - a\bar{N} & -a\bar{R} \\ ca\bar{N} & ca\bar{R} - \delta \end{pmatrix} = \begin{pmatrix} 0 & -\delta/c \\ cr & 0 \end{pmatrix}. \quad (5.21)$$

Because  $\text{tr}(J) = 0$  the steady state has a “neutral” stability. The eigenvalues of this matrix are

$$\lambda_{\pm} = \pm \sqrt{-\delta r} = \pm i \sqrt{\delta r}; \quad (5.22)$$

see Page 165. Because the eigenvalues have no real part the steady state is not structurally stable: any small change of the system will slightly change the angle at which the nullclines intersect, and make the equilibrium either stable or unstable. The behavior of this model are cycles of neutral stability: any perturbation of the population densities leads to a new cycle (see Fig. 5.5b).

Thus, one should be careful with perfectly horizontal or vertical nullclines because they result in Jacobi matrices with a zero on the diagonal, and they are typically the result of ignoring (perhaps minor) density-dependent effects. The non-trivial steady state will have the biologically ill-defined neutral stability when the trace of the Jacobian is zero, i.e., when all diagonal elements are zero. Since biological populations are typically expected to have at least some effect on themselves, one should check the robustness of the results by slightly altering the slope of both horizontal and vertical nullclines. Generally, one tests for structural stability by making small changes to a model: the model is robust when small changes do not affect its results. Here we study the effect of the slope of the non-trivial nullclines of Eq. (5.20), by adding a small density-dependence to both ODEs,

$$\frac{dR}{dt} = rN - aRN - \epsilon_R R^2 \quad \text{and} \quad \frac{dN}{dt} = caRN - \delta N - \epsilon_N N^2. \quad (5.23)$$

We have seen above that neutral stability is obtained in the absence of density-dependence, i.e., when  $\epsilon_R = \epsilon_N = 0$ , leading to perpendicular nullclines (Fig. 5.5b). Any negative density-dependence,  $\epsilon > 0$ , leads to a stable steady states (Fig. 5.5a and e), whereas positive density-dependence,  $\epsilon < 0$ , tends to destabilize (Fig. 5.5c and d). This analysis shows that the non-trivial steady state is stable whenever at least one of the two populations has a negative density-dependence. When either the resource or the consumer has a negative density-dependence, and the other population a positive density-dependence, the sign of the trace will depend on the relative strength of the density-dependent effects.

Returning to the classic Lotka-Volterra model model with a carrying capacity of the resource, i.e., with  $\epsilon_R > 0$ , we observe in Fig. 5.5f that a small positive density-dependence of the consumer will lead to the graphical Jacobian

$$J = \begin{pmatrix} -\alpha & -\beta \\ \gamma & \delta \end{pmatrix} \quad \text{with} \quad \text{tr} = -\alpha + \delta \quad \text{and} \quad \det = -\alpha\delta + \beta\gamma. \quad (5.24)$$

This steady steady state will be stable when  $\delta \rightarrow 0$ , i.e., whenever the positive density-dependence of the consumer is sufficiently small (see Fig. 5.5f). We conclude that a vertical consumer nullcline is robust in a Lotka-Volterra model with a carrying capacity of the resource because slanting the consumer nullcline slightly leftwards or rightwards does not affect the stability of the steady state.

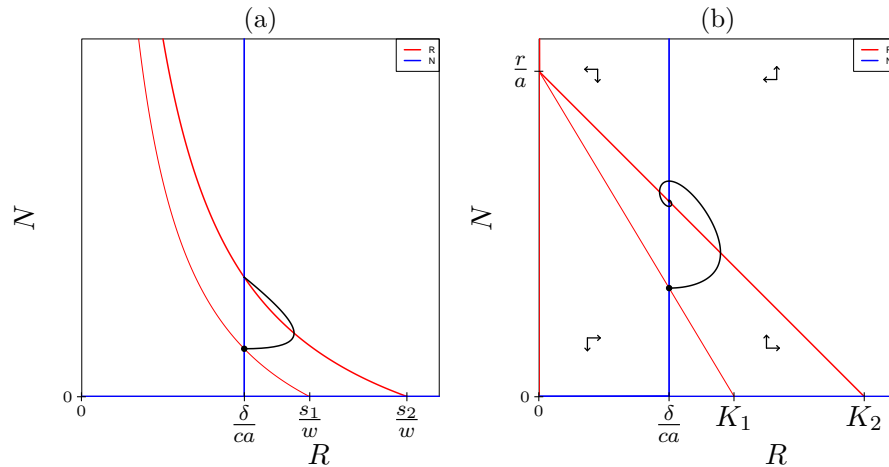


Figure 5.6: Enrichment of the resource increases the steady state of the consumer only. The red lines depict the  $dR/dt = 0$  nullcline and blue lines the  $dN/dt = 0$  nullcline. In Panel (a) we consider the chemostat of Eq. (5.2) for two different influx rates,  $s_1$  and  $s_2$ , of the resource. The trajectory corresponds to starting in the steady state with the low influx,  $s_1$ , and increasing the influx to the higher  $s_2$ . In Panel (b) we consider the Lotka-Volterra model of Eq. (5.10) for two different carrying capacities,  $K_1$  and  $K_2$ , of the resource. The trajectories corresponds to starting in the steady state with the low  $s_1$  or  $K_1$ , after increasing the influx to  $s_2$  (Panel a), or the carrying capacity to  $K_2$  (Panel b). Enrichment transiently increases both resource and consumer densities, but at the new steady state only the consumer is increased. Panel (a) was made with model `chemo.R` and Panel (b) with `lotkaBM.R`.

### Resource densities are determined consumers only

An unexpected consequence of vertical consumer nullclines located at  $R = \frac{\delta}{ca}$  is that the equilibrium density of the resource is determined by the parameters of the consumer, i.e.,  $\delta, c$  and  $a$  only, and is independent of its own parameters,  $s, w, r$  and/or  $K$  (see Fig. 5.6). This implies that the effect of increasing the inflow of resource (e.g., nutrients), or increasing the carrying capacity of the resource, increases the steady state of the consumer, and not that of the resource. In ecology this is known as the classic “Paradox of enrichment” (Rosenzweig, 1971), because eutrophication (enrichment) of 2-dimensional aquatic ecosystems comprised of algae,  $R$ , that are consumed by zooplankton,  $N$ , leads to an increase of the zooplankton densities, and not of the densities of the algae. Similar effects have been observed in 2-dimensional bacterial food chains (Kaunzinger & Morin, 1998). This unexpected property of these models is due to the fact that the consumers,  $N$ , cancel from the  $dN/dt = 0$  equation upon solving steady states. It is the steady state of the resource,  $\bar{R}$ , that is solved when setting  $dN/dt = 0$ . Which steady state is solved from which equation not only depends on the form of the equations, but also on the number of equations (see Chapter 8). As a consequence predictions for how populations are expected to change upon changing one of the parameters may crucially depend on the design of the model (De Boer, 2012), which is another form of non-robustness.

## 5.4 Summary

Consumer-resource models with a mass-action killing term tend to have a stable steady state where the consumer determines the density of the resource. Since we do not know beforehand which variable is solved from which equation, the general procedure for solving a steady state of a model with several ODEs, is to start with the most simple equations, and use the steady state

values that they provide for solving the more complex equations. Plotting the consumer on the vertical axis and the resource on the horizontal axis, the consumer nullcline is typically a vertical line located at the critical resource density,  $R^*$ , required for growth of the consumers, whereas the resource nullcline is a declining line intersecting the horizontal axis in the carrying capacity of the resource. Lotka-Volterra-like nullclines are obtained with replicating resources, when the consumption obeys a mass-action term (the birth rate of the consumer may be a saturation function of its consumption). The shape of the nullcline of the resource tends to reflect the *per capita* growth of the resource. Saturated consumption terms have little effect on the phase plane of a resource that is maintained by a source, but are expected to have a major effect when the resource is maintained by replication.

## 5.5 Exercises

### Question 5.1. Sketch the *per capita* birth rate

In Eq. (5.1) we considered a case of a population of cells in a closed environment containing a fixed amount,  $R_T$ , of nutrients. The cells consume nutrients as “building blocks” upon cell division, and the rate of cell division was a saturation function,  $\frac{bR}{h+R}$ , of the free nutrient availability,  $R = R_T - cN$ , where  $c$  is the amount of nutrient contained in a single cell.

- Sketch the *per capita* birth rate as a function of the population density  $N$  (hint: you may need to use the file `birth.R`).
- Which of the density dependent function from Chapter 3 would corresponds best with this concave shape?

### Question 5.2. Neutrophils

Let us return to the neutrophil project of Chapter 2 and complicate the model by giving the bacteria a carrying capacity,  $K$ , and allowing neutrophils to arrive from the bone marrow:

$$\frac{dB}{dt} = rB(1 - B/K) - kNB \quad \text{and} \quad \frac{dN}{dt} = s - dN ,$$

where  $k$  is the mass-action killing rate,  $s$  the source of neutrophils from the bone marrow, and  $d$  is the death rate of neutrophils. Note that in this model the neutrophil dynamics are independent of the bacteria.

- Sketch the nullclines for all qualitatively different situations, and determine the stability of all steady states.
- How would you define the parameter condition for immediate control in this model? (With immediate control we mean that  $dB/dt < 0$  upon invasion of a few bacteria.)
- In Chapter 2 we argued that neutrophils should have a maximum killing rate, and we wrote  $dB/dt = rB(1 - B/K) - \frac{kNB}{h+B}$ , where neutrophils maximally kill  $k$  bacteria per unit of time. Sketch the nullclines and determine the stability of all steady states of the model extended with this saturated killing rate. (Note that one can also write the saturation term as  $\frac{k'NB}{1+B/h}$  where  $k' = k/h$  to not change the dimension of the killing constant when extending the model, i.e., both  $k$  and  $k'$  are mass action killing rates.) Again, sketch the nullclines for all qualitatively different situations, and determine the stability of all steady states.
- For each of these situations, how would you now define the condition for immediate control?
- In reality neutrophils are rapidly released from a reservoir in the bone marrow during an inflammatory immune response. The model `neutrophils2.R` adds an equation for the bone marrow, and if you have time you may want to study that model.

### Question 5.3. Lotka-Volterra models

We have claimed that the Lotka-Volterra model is very general for the situation where a self-

replicating population is controlled by a population that exerts its control by a mass-action term, and which is stimulated to replicate as a function of this control term.

- Write an ODE model for a tumor that is controlled by natural killer cells that replicate when they encounter and kill tumor cells.
- Write an epidemiological model for a population of susceptible individuals that grow logistically in the absence of the infectious agent, with new infections occurring when infected individuals encounter susceptible individuals.
- Can you think of natural improvements of these models?

#### Question 5.4. Scaling

Read Section 15.4 in the Appendix and use this to scale the Lotka-Volterra predator-prey model by introducing non-dimensional population densities. Scale time by the natural rate of increase of the prey.

- Write a new model by scaling as many parameters as possible.
- How many parameters did you lose?
- What is the dimension of the remaining parameters?

#### Question 5.5. Desert

Consider the following model for a vegetation  $V$  in a desert. The growth of the vegetation is limited in the amount of water  $W$  in the soil:

$$\frac{dW}{dt} = a - bWV - cW \quad \text{and} \quad \frac{dV}{dt} = dWV - eV ,$$

where  $a$  is the rainfall dependent water uptake in the soil,  
 $b$  is the extra water uptake and evaporation by the vegetation,  
 $c$  is the normal evaporation,  
 $d$  is the water dependent growth of the vegetation,  
and  $e$  is the death rate of the vegetation.

For this exercise consider steady state situations.

- How much water does the soil contain if there is no vegetation?
- Suppose the rainfall increases two-fold because of a change in climate. How much water would the soil contain if there is still no vegetation?
- How much water would the soil contain if there is a vegetation?
- What would be the corresponding steady state of the vegetation?
- How much water would the soil contain if the rainfall increases two-fold in the presence of a vegetation?
- Draw the nullclines, and determine the stability of the steady states.
- How would the increased rainfall change these nullclines?

#### Question 5.6. Kingfishers

Make the question on Kingfishers in Chapter 14 and analyze your own model, or the models provided in the answers of Chapter 14, by phase plane analysis, i.e., sketch the nullclines, the vector field, and determine the stability of all steady states.

- Does this analysis suggest major improvements of the model?
- What would have happened if we had forgotten the spontaneous emigration?
- How does the phase plane change when we have a model where the immigration is a saturation function of the fish?

#### Question 5.7. Biotic and abiotic resources

Make a natural model for the following two situations:

- Consider an abiotic resource (like nitrate or phosphate) that flows in and out from a chemostat, and that is used by a consumer when it forms new material to divide. The birth rate of the consumer is a saturation function of the concentration of the resource, because at high resource concentrations the birth rate becomes limited by something else (e.g., another

resource). Because the resource is built into the cellular material of the consumers, the consumption of resource is proportional to the birth rate of the consumers. Assume that the consumers tend to flow out of the chemostat before they die.

- b. Consider a biotic resource, like a prey species that is being eaten by a consumer. The resource maintains itself by growth (i.e., replication) and has a carrying capacity in the absence of consumers. The carrying capacity of the resource is so low that the consumption term can safely be described by a mass-action term. The birth rate of the consumer is a saturation function of its consumption, because at high consumption levels the birth rate is also limited by other factors.
- c. Which equation differs most between the two situations, the resource or the consumer?

### Question 5.8. Evolution to self-extinction

Evolution can be detrimental because a normal process of adaptation can erode population sizes, and thereby raise the population's extinction risk (Rankin & Lopez-Sepulcre, 2005). Several models have shown that adaptation may drive populations to dangerously small numbers, making them vulnerable to stochasticity, either gradually (Matsuda & Abrams, 1994) or suddenly (Dercole *et al.*, 2002; Ferriere & Legendre, 2013). We study a simple example of 'Evolution to self-extinction' in the Lotka-Volterra model of Eq. (5.10) by asking what happens when the consumer keeps on evolving higher attack rates,  $a$ . Above we derived that the non-trivial state of the Lotka-Volterra model corresponds to

$$\bar{R} = \frac{\delta}{ca} \quad \text{and} \quad \bar{N} = \frac{r}{a} \left( 1 - \frac{\delta}{caK} \right),$$

which shows that the steady state of the resource is a declining function of the attack rate,  $a$ , and that the steady state of the consumer is a non-monotonic function of  $a$ .

- a. What is the minimal attack rate required for co-existence in Eq. (5.10)?
- b. Use the function curve() in R to plot  $\bar{R}$  and  $\bar{N}$  as a function of the attack rate.
- c. Will a new consumer with a higher attack rate always be able to invade into the non-trivial steady state of the Lotka-Volterra model?
- d. Is there an optimal attack rate? What do you expect to happen when consumers keep evolving higher attack rates?
- e. Why are we not observing that all resource-consumer systems (or host-parasite systems) go extinct?
- f. Is this different when the resource is maintained by a source, rather than by self-renewal?

### Extra questions

### Question 5.9. Cryptic oscillations

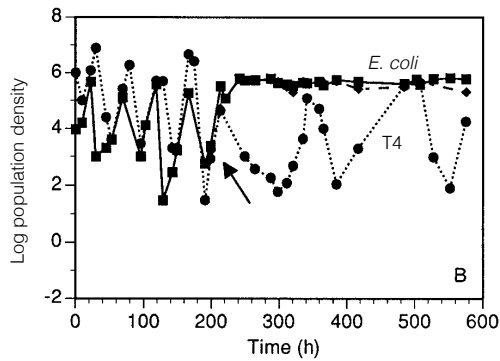


Fig. 3b from Bohannan & Lenski (1997).

The now classic experiments of Bohannan & Lenski (1997) demonstrated that when *E. coli* is cultured with its bacteriophage T4, the system can initially display predator-prey like oscillations, and later develop so-called “cryptic” oscillations where the phage densities continue to oscillate, but the *E. coli* densities become stable. The solid line in the Figure depicts the total population size of *E. coli* and the dotted lines that of the T4 phage. They study this in more detail in a later paper (Bohannan & Lenski, 1999), and this data is also discussed in Figure 4.6 of the excellent book of Weitz (2015). Finally, Yoshida *et al.* (2007) published a paper on cryptic oscillations in algae-zooplankton communities.

- Hypothesize why the *E. coli* becomes stable after about 200h of co-culture (i.e., at the arrow).
- How would you explain these cryptic oscillations after 200h, where the phages oscillate and the bacteria seem stable?
- Can you explain the difference in the average density of the phages in the period before and after the 200h point?
- If you have time, make a mathematical model and study it numerically to test your ideas and predictions.

### Question 5.10. Phages and bacteria (Grind)

Levin *et al.* (2013) and Jiang *et al.* (2013) describe several experiments in which they culture bacteria *in vitro* and infect them with phages to study the evolution of resistance. Some of their data are available on the website, and we ask you to fit the data to two different versions of their model. The first model is the system of delay differential equations (DDEs) that they present in their paper (Levin *et al.*, 2013), which consists of a resource,  $R$ , sensitive bacteria,  $B_0$ , resistant bacteria,  $B_1$ , infected bacteria,  $M$ , and phages,  $P$ , and where we have kept their notation of the parameters (i.e.,  $\delta$  is the infection rate, and  $v$  is the maximum consumption rate, and  $e$  is the amount of resources contained in a single bacterium),

$$\begin{aligned} \frac{dR(t)}{dt} &= -\frac{evR(t)}{K + R(t)} (B_0(t) + (1 - s)B_1(t)) , \\ \frac{dB_0(t)}{dt} &= \frac{vR(t)}{K + R(t)} B_0(t) - \delta B_0(t)P(t) , \\ \frac{dB_1(t)}{dt} &= \frac{vR(t)}{K + R(t)} (1 - s)B_1(t) , \\ \frac{dM(t)}{dt} &= \delta B_0(t)P(t) - \delta B_0(t - \lambda)P(t - \lambda) , \\ \frac{dP(t)}{dt} &= b\delta B_0(t - \lambda)P(t - \lambda) - \delta P(t)[B_0(t) + B_1(t)] , \end{aligned}$$

where we explicitly indicate that variables either depend on time,  $t$ , or on the time delay,  $t - \lambda$ , that is used to model the eclipse phase. Infected bacteria therefore burst after  $\lambda = 0.4$ h to give rise to  $b$  phages, where  $b$  is the burst size. The  $\delta P(t)[B_0(t) + B_1(t)]$  term in the last equation is the absorption of phages to bacteria, i.e., phages are absorbed by resistant bacteria, but cannot infect them. This model is provided on the website as the file `levin.R` with a parameter setting copied from Levin *et al.* (2013) (note that we have added the selection coefficient,  $s$ , to allow for a fitness cost of the resistance mechanism). The two data sets in Figure 2 of the Levin *et al.* (2013) paper are available on the website as the files `LevinPG13Fig2B0.csv` and `LevinPG13Fig2.csv`.

The first file contains the growth of (sensitive) bacteria in the absence of phages, and the second one provides the total densities of the bacteria and the phages after infection.

- Read the equations carefully and make sure that you understand the time delay.
- Plot the data with the `levin.R` script, and make sure you understand them.
- Fit the first data set to check their estimate for the consumption rate,  $v$ . Note that it makes no sense to check the  $e$  and  $k$  parameters because we have no information on the resource densities.
- Use your improved estimate of the consumption rate to fit the model to the infection data. Do you obtain a good fit, and what do you think of their parameter estimates?
- Time delays are notoriously difficult to solve numerically, and the DDE solver of the `deSolve` library is doing an excellent job here. We could nevertheless check whether or not the data suggest that this fixed time delay of  $\lambda = 0.4\text{h}$  is truly required, by changing the last two equations into ODEs:

$$\frac{dM(t)}{dt} = \delta B_0(t)P(t) - M(t)/\lambda \quad \text{and} \quad \frac{dP(t)}{dt} = bM(t)/\lambda - \delta P(t)[B_0(t) + B_1(t)] ,$$

where  $\lambda$  still defines the average length of the eclipse phase, but which is now exponentially distributed. This model is included in the same `levin.R` file in the function `odeModel`, and an example on how to fit the ODE model to the data is shown in the second half of the file. Do the data require the fixed time delay of the DDE model? Is it wise to allow for a fitness cost?

- Are there any other parameters that you would have added to the model?

### Question 5.11. Gillespie algorithm

Read Section 15.8 in the Appendix on simulating ODEs stochastically using discrete values of all variables. The Gillespie algorithm is illustrated with an R-script simulating the Lotka-Volterra predator-prey model of Eq. (15.32).

- Why do we write a Lotka-Volterra model with explicit birth and death rates for the prey (instead of logistic growth)?
- Actually, interpreting Eq. (15.32) as a predator/prey-model is somewhat stretched because we needed to assume that the killing of one prey creates exactly one new predator individual. How would the R-script have to change if one were to interpret  $R$  as tumor cells,  $N$  as killer cells,  $aRN$  as a killing event, and allow that killer cells can receive a signal to divide upon binding a tumor cell?
- How would the model have to change when one keeps track of the number of prey individuals eaten by a predator, and only allow predators to give birth after consuming a particular number of prey?
- One can study exponential decay with this model by setting  $b = N = 0$ . Can you determine the average half life of many Gillespie simulations and compare that to the expected value?

### Question 5.12. Return time

This is a challenging exercise that will show that one can also determine the return time around a steady state of a model composed of several ODEs, as it is defined by the largest eigenvalue, i.e.,  $T_R = \frac{-1}{\lambda_{\max}}$ . We recommend that you make this exercise by carefully reading the answer. In the answer we compute the return time of the non-trivial steady state of the Lotka-Volterra model and study how this depends on the mechanism of the density dependence of the prey. For reasons of simplicity we consider the case where the non-trivial steady state is a stable spiral point (and not a stable node), and first compute the return time of a general form of the Lotka-Volterra model, e.g.,

$$\frac{dR}{dt} = rR - \gamma R^2 - aRN \quad \text{and} \quad \frac{dN}{dt} = caRN - \delta N .$$

- Compute the return time of this general form.

- 
- b. What is the return time when we explicitly make the birth rate density dependent (e.g., replace  $rR - \gamma R^2$  with  $bR[1 - R/k] - dR$ )? Is the birth or the death rate determining the return time?
- c. Address the same questions for a Lotka-Volterra model with a density dependent death rate of the prey.
- d. Interpret your results.



## Chapter 6

# The basic reproductive ratio $R_0$

In this book we frequently use the fitness,  $R_0$ , of a population to simplify steady state values and the expressions for nullclines, which typically facilitates their biological interpretation. Analyzing competition in Chapter 9 we will see that the population with the largest  $R_0$ , and not necessarily the one with the largest carrying capacity, is typically expected to win the competitive exclusion. In our consumer-resource models we observed that the depletion of resource species is (at least partly) determined by the  $R_0$  of the consumer. We have defined  $R_0$  as a fitness, namely as the maximum number of offspring that is produced over the expected lifespan of an individual, in a situation without competition or predation, i.e., as the mean lifetime reproductive success of a typical individual (Heffernan *et al.*, 2005). The  $R_0$  plays a central role in epidemiology, where it is defined as the expected number of individuals that is successfully infected by a single infected individual during its entire infectious period, in a population that is entirely composed of susceptible individuals (Anderson & May, 1991; Diekmann *et al.*, 1990). Epidemics will grow whenever  $R_0 > 1$ . In order to provide a more general understanding of the basic reproductive ratio,  $R_0$ , we review some of the classic epidemiological approaches to define and calculate  $R_0$  in this chapter.

### 6.1 The SIR model

A basic model in epidemiology is the following “SIR” model, for Susceptible, Infected, and Recovered individuals, e.g.,

$$\frac{dS}{dt} = s - dS - \beta SI, \quad \frac{dI}{dt} = \beta SI - (\delta + r)I, \quad \text{and} \quad \frac{dR}{dt} = rI - dR, \quad (6.1)$$

where  $s$  defines the source of susceptibles,  $d$  is their death rate,  $\beta$  is an infection rate,  $\delta$  the death rate of infected individuals (with  $\delta \geq d$ ),  $r$  is a recovery rate, and where recovered individuals have the same death rate as susceptibles. The “virulence” of the pathogen can be defined by the additional death rate it inflicts on infected hosts, i.e., as  $\delta - d$ . Let us define a duration of infection with a time scale of days, i.e., let  $1/(\delta + r)$  be several days, and define  $\beta I$  and  $d$  as rates per day. This SIR model has several variations. First, if the time scale at which susceptible individuals are produced and die is much slower than that of the epidemic, one can simplify the first ODE into  $dS/dt = -\beta SI$  to study the initial phase of an epidemic. Second, note that in this version of the SIR model the subpopulation of recovered individuals does not feed back onto the dynamics of the other two subpopulations, which means that even if  $r > 0$ , recovered

individuals need not be considered when analyzing the establishment of an epidemic. Third, note that one can set  $r = 0$  to define an ‘‘SI’’ model of an endemic infection which no one recovers from. Finally, one often writes Eq. (6.1) with a frequency dependent transmission rate,

$$\frac{dS}{dt} = s - dS - \frac{\beta SI}{N}, \quad \frac{dI}{dt} = \frac{\beta SI}{N} - (\delta + r)I, \quad \text{and} \quad \frac{dR}{dt} = rI - dR, \quad (6.2)$$

where  $N = S + I + R$  to define that the infection rate is proportional to the fraction of infected individuals. This infection term is obtained when susceptible individuals are expected to meet some average number, say  $n$ , of other individuals every day, and a fraction  $I/N$  of them is infectious. Thus,  $\beta$  here combines the average infectivity per infectious person with the number of encounters  $n$ . This frequency dependent model is analyzed further in the exercises.

For understanding the derivation of the  $R_0$  we return to the SIR model with a mass action infection term. The disease-free steady state of Eq. (6.1) is defined as  $\bar{S} = s/d$  and  $\bar{I} = \bar{R} = 0$ , and the endemic equilibrium is defined as

$$\bar{S} = \frac{\delta + r}{\beta}, \quad \bar{I} = \frac{s}{\delta + r} - \frac{d}{\beta}, \quad \text{and} \quad \bar{R} = \frac{r}{d} \bar{I} = \frac{rs}{d(\delta + r)} - \frac{r}{\beta}, \quad (6.3)$$

which can only be present when  $\bar{I} > 0$ , i.e.,

$$\frac{s}{\delta + r} > \frac{d}{\beta} \quad \text{or} \quad \frac{s}{d} \frac{\beta}{\delta + r} > 1. \quad (6.4)$$

The  $R_0$  of the infection in Eq. (6.1) is defined by the rate,  $\beta S$ , at which new cases are produced per infected individual over its entire infectious period of  $1/(\delta + r)$  days, in a fully susceptible population  $\bar{S} = s/d$ .  $R_0$  is therefore defined as

$$R_0 = \beta \bar{S} \frac{1}{\delta + r} = \frac{s}{d} \frac{\beta}{\delta + r}. \quad (6.5)$$

Since the epidemic will only spread if an infected individual is replaced by more than one secondary case, we require  $R_0 > 1$ , which indeed corresponds to the condition derived in Eq. (6.4). Additionally, because the  $R_0$  is proportional to the number (or fraction) of susceptibles in the disease free equilibrium,  $\bar{S}$ , one can see that an epidemic will no longer be able to spread if  $\bar{S}$  is reduced by a factor  $R_0$ . This is what vaccination programs aim for, and because not all susceptibles need to be vaccinated, this is called ‘herd immunity’.

Thus, the condition for the existence of the endemic steady state is the same as the condition for the initial spread of the epidemic. This also means that we could have derived the same condition from the Jacobian of the disease-free steady state (because an epidemic will not take off when the uninfected steady state is stable). Since the recovered population does not affect the behavior of the model, we only need to consider the first two equations of Eq. (6.1) in the uninfected steady state ( $\bar{S} = s/d, \bar{I} = 0, \bar{R} = 0$ ), i.e.,

$$J = \begin{pmatrix} -d - \beta \bar{I} & -\beta \bar{S} \\ \beta \bar{I} & \beta \bar{S} - \delta - r \end{pmatrix} = \begin{pmatrix} -d & -\beta \bar{S} \\ 0 & \beta \bar{S} - \delta - r \end{pmatrix}. \quad (6.6)$$

Because this matrix is in a triangular form, the determinant is given by the multiplication of its diagonal elements, and because the determinant defines the product of the two eigenvalues (see Eq. (15.30)), the eigenvalues are  $\lambda_1 = \beta \bar{S} - \delta - r$  and  $\lambda_2 = -d$ .<sup>1</sup> The parameter condition  $R_0 > 1$  indeed corresponds to the transcritical bifurcation point,  $\lambda_1 = 0$ , where the infecteds start to grow, and the endemic steady state becomes positive.

<sup>1</sup>Note that the Jacobian of the full model would have been

$$J = \begin{pmatrix} -d - \beta \bar{I} & -\beta \bar{S} & 0 \\ \beta \bar{I} & \beta \bar{S} - \delta - r & 0 \\ 0 & r & -d \end{pmatrix} = \begin{pmatrix} -d & -\beta \bar{S} & 0 \\ 0 & \beta \bar{S} - \delta - r & 0 \\ 0 & r & -d \end{pmatrix},$$

## Expansion rate

Note that  $R_0$  is dimensionless, i.e., it is the expected number of secondary cases per infectious period. Since  $R_0$  is not a rate, it cannot define how fast the epidemic is expanding. Indeed the initial rate at which an epidemic is expected to grow is here defined by

$$\frac{dI}{dt} = \beta \bar{S} I - (\delta + r) I = \left( \frac{\beta s}{d} - \delta - r \right) I = \rho_0 I, \quad (6.7)$$

where the rate  $\rho_0$  is the initial *per capita* net growth rate of the infected individuals. Observe that this growth rate,  $\rho_0$ , corresponds to the largest eigenvalue of the Jacobi matrix in Eq. (6.6), and that applying the “invasion criterion”  $\rho_0 > 0$ , i.e.,  $\frac{\beta s}{d} > \delta + r$  or  $\frac{s}{d} \frac{\beta}{\delta + r} > 1$ , is again the same as requiring  $R_0 > 1$ . To study the relationship between  $\rho_0$  and  $R_0$  explicitly, we define  $L = 1/(\delta + r)$  as the length of the infectious period, and write

$$R_0 = \beta \bar{S} L \quad \text{and} \quad \rho_0 = \beta \bar{S} - \frac{1}{L} \quad \text{such that} \quad \beta \bar{S} = \rho_0 + \frac{1}{L} \quad \text{and} \quad R_0 = \rho_0 L + 1. \quad (6.8)$$

From the latter, one readily solves that

$$\rho_0 = \frac{R_0 - 1}{L} = (R_0 - 1)(\delta + r). \quad (6.9)$$

## Depletion of susceptibles

Finally, defining the disease free steady state as a carrying capacity,  $K = s/d$ , one can see that the ultimate degree of depletion of the susceptibles is fully determined by the  $R_0$ , i.e., in Eq. (6.3) we see that  $\bar{S} = K/R_0$ . Summarizing,  $R_0$  is a valuable and meaningful concept in epidemiology, there are several methods to compute an  $R_0$ , where the one that calculates the number of secondary cases produced during the infectious period of an infected individual seems the most intuitive.

## 6.2 The SEIR model

The definition of the  $R_0$  becomes more complicated in systems where the infection involves several stages. For instance, by adding a stage of exposed individuals,  $E$ , that are not yet infectious, one obtains the SEIR model

$$\frac{dS}{dt} = s - dS - \beta SI, \quad \frac{dE}{dt} = \beta SI - (\gamma + d)E, \quad \frac{dI}{dt} = \gamma E - (\delta + r)I, \quad \frac{dR}{dt} = rI - dR, \quad (6.10)$$

where the exposed individuals become infectious at a rate  $\gamma$  (and have the same death rate as the susceptibles). A general method for deriving the  $R_0$  for multi-stage models is the “next generation method” devised by Diekmann *et al.* 1990, and involves the definition of a matrix collecting the rates at which new infections appear in each compartment, and a matrix defining the loss and gains in each compartment. This method is general but its explanation would be too involved for the short summary in this chapter (if you are interested read any of the following: Heffernan *et al.* (2005) or Diekmann *et al.* (2012; 1990)). Eq. (6.10) is simple enough to define

---

with determinant  $-d \times (\beta \bar{S} - \delta - r) \times -d = \lambda_1 \times \lambda_2 \times \lambda_3$ . Hence the three eigenvalues are  $\lambda_2 = \beta \bar{S} - \delta - r$  and  $\lambda_1 = \lambda_3 = -d$ , which indeed leads to identical results. Ignoring the recovered population is indeed allowed.

the  $R_0$  by the more intuitive “survival” method. The initial rate at which an infected individual produces novel infections in the exposed population remains  $\beta\bar{S}$ , and this will occur over an infectious period of  $1/(\delta + r)$  time steps, i.e., we keep the  $\frac{\beta\bar{S}}{\delta+r}$  term, but since not all exposed individuals become infectious (i.e., only a fraction  $\gamma/(\gamma + d)$  are expected to survive and become infectious), we need to multiply this initial term with the fraction of individuals surviving the exposed period and obtain

$$R_0 = \frac{s}{d} \frac{\beta}{\delta + r} \frac{\gamma}{\gamma + d}. \quad (6.11)$$

We study the steady state by first solving  $\bar{E} = \frac{\delta+r}{\gamma}I$  from  $dI/dt = 0$ . Substituting that into  $dE/dt = 0$  yields  $\bar{S} = \frac{\gamma+d}{\gamma} \frac{\delta+r}{\beta}$ , which when substituted in  $dS/dt = 0$  gives

$$\bar{I} = \frac{s}{\beta\bar{S}} - \frac{d}{\beta} = \frac{\gamma}{\gamma+d} \frac{s}{\delta+r} - \frac{d}{\beta}, \quad (6.12)$$

which can only be positive when

$$\frac{\gamma}{\gamma+d} \frac{s}{\delta+r} > \frac{d}{\beta} \quad \text{or} \quad \frac{s}{d} \frac{\beta}{\delta+r} \frac{\gamma}{\gamma+d} > 1 \quad \text{or} \quad R_0 > 1, \quad (6.13)$$

confirming that the  $R_0$  derived by the survival method again corresponds to the parameter threshold at which the epidemic steady state becomes positive. The initial growth rate,  $r_0$ , of an epidemic in the SEIR model now depends on two ODEs,  $dE/dt$  and  $dI/dt$ , and can still be computed because these ODEs are linear around the disease-free steady state  $\bar{S} = s/d$ . Solving these ODEs and applying the invasion criterion  $dI/dt > 0$ , or deriving the largest eigenvalue of the Jacobian of the disease-free equilibrium, would therefore be alternative means to calculate the  $R_0$  of this SEIR model. For instance, considering  $S = \bar{S}$  and  $R = 0$  we could write the Jacobi matrix of the 2-dimensional system composed of just the exposed and infectious individuals,

$$J = \begin{pmatrix} \partial_E E' & \partial_I E' \\ \partial_E I' & \partial_I I' \end{pmatrix} = \begin{pmatrix} -(\gamma + d) & \beta\bar{S} \\ \gamma & -(\delta + r) \end{pmatrix}, \quad (6.14)$$

with a trace that is always negative and a determinant  $(\gamma + d)(\delta + r) - \gamma\beta\bar{S}$ . The epidemic will grow when this steady state is unstable, i.e., when

$$\det J < 0 \quad \text{or} \quad \frac{d}{s} \frac{\gamma+d}{\gamma} \frac{\delta+r}{\beta} - 1 < 0 \quad \Leftrightarrow \quad \frac{1}{R_0} < 1 \quad \Leftrightarrow \quad R_0 > 1,$$

where  $R_0$  is defined by Eq. (6.11). Summarizing, there are various ways to compute an  $R_0$  for infections involving multiple stages, where the next generation method (Diekmann *et al.*, 1990, 2012) is the most general (but is too involved to be explained here).

### 6.3 Fitness in consumer-resource models

In this book we have similarly defined the  $R_0$  of resource and consumer populations to facilitate the biological interpretations of otherwise more complicated expressions. For instance re-consider the Lotka-Volterra model with explicit birth and death rates for the resource,

$$\frac{dR}{dt} = bR(1 - R/k) - dR - aRN \quad \text{and} \quad \frac{dN}{dt} = caRN - \delta N, \quad (6.15)$$

with a carrying capacity  $\bar{R} = K = k(1 - d/b)$ . Using the survival method, the  $R_0$  of the resource is defined by the maximum number of offspring,  $b$  per day (note that the  $(1 - R/k)$  term can

only decrease the birth rate), over its expected life span of  $1/d$  days, i.e.,  $R_{0R} = b/d$ . One can also easily see that the resource population can only invade when the maximum birth rate,  $b$ , exceeds the death rate,  $d$ , i.e., when  $b/d > 1$ , and define the  $R_0$  this way (like above for the SIR model). Given this  $R_0$  of the resource the carrying capacity can be written as  $K = k(1 - 1/R_{0R})$  (see Chapter 3).

Similarly, the  $R_0$  of the consumer is its maximum birth rate,  $ca\bar{R}$ , times its expected life span,  $1/\delta$ , i.e.,  $R_{0N} = caK/\delta$ . Likewise, see that the maximum consumer birth rate,  $caK$ , should exceed its death rate,  $\delta$ , implying that  $R_{0N} = caK/\delta > 1$ . Hence, one can again derive the  $R_0$  parameters of this model in several ways. The  $R_0$  of the consumer can be used to simplify the expression for the non-trivial steady state of the resource, which is solved from  $dN/dt = 0$ , i.e.,  $\bar{R} = \frac{\delta}{ca}$ , and can now be expressed as  $\bar{R} = K/R_{0N}$ . This reveals the biological insight that the depletion of the resource population is proportional to the  $R_0$  of the consumer (like in the SIR model), which even means that one can estimate the  $R_0$  from an observed level of depletion.

We have also considered models where the birth rate of the consumer is a saturation function of its consumption, e.g.,

$$\frac{dR}{dt} = bR(1 - R/k) - dR - aRN \quad \text{and} \quad \frac{dN}{dt} = \frac{\beta RN}{h + R} - \delta N, \quad (6.16)$$

with the same equation,  $R_0$ , and carrying capacity of the resource. Now the  $R_0$  of the consumer can either be defined as  $R_0 = \beta/\delta$ , because  $\beta$  is a maximum birth rate of the consumer at infinite resource densities, or —more conventionally— as  $R_0 = \frac{\beta K}{\delta(h+K)}$ , which uses the consumer birth rate at carrying capacity of the resource for the maximum consumer birth rate. Since we aim for simplifying mathematical expressions, the simpler  $R_0 = \beta/\delta$  is typically the most useful definition. When  $h \ll K$  the two definitions of  $R_0$  approach one another. If not, an invasion criterion would correspond to the more complicated  $R_0$ , because consumers can only invade into a resource population at carrying capacity when  $\frac{\beta K}{h+K} > \delta$ . The simpler form of the consumer fitness,  $R_0 = \beta/\delta$ , instead allows us to simplify the expression for the steady state of the resource, which is again solved from  $dN/dt = 0$ , i.e.,  $\bar{R} = \frac{\delta h}{\beta - \delta} = \frac{h}{R_0 - 1}$ , revealing that the depletion of the prey still increases with the  $R_0$  of the predator, but that this is no longer proportional to either of the  $R_0$ s.

## 6.4 Summary

Epidemiological models typically take the form of SI, SIR, or SEIR models with an infection term that is either a mass-action,  $\beta SI$ , term, or one that is based upon the fraction of infected individuals in the populations,  $\beta SI/N$ . The  $R_0$  is an important concept that can be computed in a variety of ways: (1) by the survival method one computes the *per capita* arrival of new infected individuals over the infectious period, and multiplies this with survival fractions of all intermediate stages, (2) by the condition for the existence of a non-trivial endemic state, (3) by requiring that the largest eigenvalue of the uninfected steady state is positive, and (4) by the next generation method that we have not explained in this chapter. The largest eigenvalue of the uninfected steady state provides the initial expansion rate of the epidemic. In populations with a mass-action infection term,  $R_0$  predicts the depletion of the susceptibles, i.e.,  $\bar{S} = K/R_0$ . The parameter combination defining  $R_0$  often appears in steady state expressions, which enables us to simplify these expressions into more intuitive forms.

## 6.5 Exercises

### Question 6.1. SARS

Consider the appearance of a deadly infectious disease, e.g., SARS, and write the following model for the spread of the disease:

$$\frac{dI}{dt} = \beta I - \delta I,$$

where we assume that the availability of susceptibles is never limiting, and  $I$  is the number of human individuals infected with SARS,  $\beta$  is the number of new cases each infected individual causes per week, and  $1/\delta$  is the number of weeks an infected individual survives before he/she dies of SARS. Since an infected individual here is expected to live for  $1/\delta$  weeks, and is expected to cause  $\beta$  new cases per week, the  $R_0$  of this disease is  $\beta/\delta$ .

- It has been estimated that on average a SARS patient causes  $R_0 = 3$  new cases, during a typical disease period of two weeks (Lipsitch *et al.*, 2003). Most patients die at the end of these two weeks. How long does it take with these parameters to reach the point where  $3 \times 10^9$  individuals (i.e., half of the world population) are infected? Note that at this time point the healthy uninfected pool is less than half of the world population because many people will have died (i.e., your simple estimate is a worst case estimate).
- Do you think this is a realistic estimate? How would you extend the model to make it more realistic? Simulate your extended model to study how long it would take to reach the point where half of the world population is infected? You can use the R-script `sars.R`.

### Question 6.2. Evolution of virulence

The SI model can be described with two differential equations,

$$\frac{dS}{dt} = s - dS - \beta SI \quad \text{and} \quad \frac{dI}{dt} = \beta SI - (d + v)I,$$

where  $v$  is the virulence of the infection (i.e., the additional death experienced by infected individuals). The  $s$  parameter is the production of healthy individuals,  $d$  is their death rate, and  $\beta$  is a “mass-action” infection parameter. Because virulent pathogens typically spread better per encounter between two hosts, it is often assumed that the infection parameter,  $\beta$ , increases with the virulence parameter,  $v$ . The most simple assumption would be that  $\beta = cv$ , where  $c$  is a constant.

- What is the  $R_0$  of this infection when we take  $\beta$  as an independent parameter?
- What is the  $R_0$  of this infection when we assume that  $\beta = cv$ ?
- What do you expect for the evolution of virulence when several strains  $i = 1, 2, \dots, n$  that differ in their virulence,  $v_i$ , are circulating in the population, and all obey  $\beta_i = cv_i$ ? Hint: sketch  $R_0$  as a function of  $v$ . Which variant will dominate ultimately, and why? Thus, do pathogens become milder or more dangerous?
- Suppose now that the infection rate is a saturation function of the virulence, i.e., assume that  $\beta = \frac{cv}{h+v}$ . What is now the  $R_0$  of the infection?
- What do you expect now for the evolution of virulence: do pathogens become milder or more dangerous when  $\beta_i = \frac{cv_i}{h+v_i}$ ?

### Question 6.3. Sexually transmitted disease (STD)

Consider an incurable sexually transmitted disease (like AIDS) in the Netherlands. There is a constant source,  $a$ , of susceptibles,  $S$ , because youngsters become sexually active at a particular age, and we lose susceptibles at a rate  $d$  when they die, enter a monogamous relationship, or stop having sex. Susceptibles can become infected by having sex with infected individuals,  $I$ , in the Netherlands, or with a small probability,  $\epsilon$ , e.g. during holidays abroad. We therefore

extend the SI model with an additional small infection parameter,  $\epsilon$ , and write the following model

$$\frac{dS}{dt} = a - dS - \beta SI - \epsilon S \quad \text{and} \quad \frac{dI}{dt} = \beta SI + \epsilon S - \delta I .$$

Because STDs are expected to spread, i.e., have an  $R_0 > 1$ , in populations that are sufficiently promiscuous, we are interested in the effect of such an external source of infected individuals in a subpopulation where the  $R_0 < 1$ .

- What is the  $R_0$  of the epidemic when we ignore the foreign infections?
- Suppose **this**  $R_0 < 1$  in a particular subpopulation, do you expect the infection to disappear completely from this subpopulation in the presence of these rare external infections? Explain your answer shortly.
- Sketch nullclines of the full model with foreign infections, and discriminate between the situation that **this**  $R_0$  is larger or smaller than one. Sketch the vector field and determine the stability of the steady states.
- Interpret the two different cases, i.e.,  $R_0 > 1$  and  $R_0 < 1$ , in terms of the AIDS epidemic in the Netherlands.
- Can you derive this model from a more detailed model explicitly considering the people abroad?

#### Question 6.4. COVID-19 herd immunity in the Brazilian Amazon

Manaus in Brazil is a large city ( $2.2 \times 10^6$  inhabitants in 2020) that was hit hard by a first wave of the SARS CoV-2 pandemic, and also suffered badly from an even larger second wave of infection (Buss *et al.*, 2021; Sabino *et al.*, 2021). We have downloaded detailed data on the excess daily number of people dying from the disease over the period from 1 April 2020 to 1 April 2021, and provide that data on the website of the course in the file `data/excessDeaths.csv`.<sup>2</sup> We ask you to study whether this data can be described with classic SIR models of the form,

$$\frac{dS}{dt} = wR - \beta S \frac{I}{N}, \quad \frac{dI}{dt} = \beta S \frac{I}{N} - (d+r)I \quad \text{and} \quad \frac{dR}{dt} = rI - wR ,$$

with susceptible individuals,  $S$ , infected individuals,  $I$ , and recovered individuals,  $R$ . Here  $N = S + I + R$  is the total number of individuals,  $\beta$  the infection rate,  $r$  the recovery rate,  $d$  the death rate due to COVID-19, and  $w$  the rate at which immunity wanes. Buss *et al.* (2021) estimate that it takes about 10 days to recover, that about 0.2% of the infected people die, that  $R_0 = 2.5$ , and that the half life of the antibodies is about 106 days.

- Translate these estimates of Buss *et al.* (2021) into the parameters of the model. Since only a very small fraction of the infected people die, i.e.,  $d \ll r$ , it is save to assume that  $R_0 \simeq \beta/r$ . Hint the death rate  $d$  has to be estimated from the fraction of people dying, i.e., from  $f = \frac{d}{d+r} = 0.002$ .
- How would you define the daily number of excess deaths in this model?
- Use the script `manaus.R` to read the data from the `excessDeaths.csv` file, check for yourself that the model corresponds to the ODEs written above, check that the initial guesses for the parameter values correspond to the estimates of Buss *et al.* (2021), and that the `tweak` option adds a column with the excess deaths. Note that we have to guesstimate the number of infected individuals on 1 April 2020 (e.g., as  $I(0) = 10^4$ ).
- Define all 4 parameters and  $I(0)$  as free parameters, and fit the data from the first peak, i.e., the first 200 days, to the model (this may take a while because it is 200 data points, and we need to call the ‘Pseudo’ algorithm to carefully search the 5-dimensional parameter space). Do your parameter estimates agree with those of Buss *et al.* (2021)? Do you think  $w$  is a required and identifiable parameter? What is your estimated half life of the immunity?

<sup>2</sup>This data was compiled by Bruce Nelson from the Instituto Nacional de Pesquisas da Amazonia on [t.co/6g4HHEAuNY](https://t.co/6g4HHEAuNY). We here provide only the first 365 days of the excess deaths to speed up the fitting.

- e. Finding that  $R_0 = 2.48$  and that the loss rate from the infectious compartment,  $d+r \simeq 0.145 \text{ d}^{-1}$ , one can estimate the growth rate of the infection as  $\rho_0 = (R_0 - 1)(d+r) = 0.215 \text{ d}^{-1}$ . Since we estimated that  $I(0) = 15750$  on the first of April, can you now also estimate when the epidemic started with the first infected individual?
- f. Can the same model describe both peaks (i.e., all data)? If not, how would you extend the model?

### Extra questions

#### Question 6.5. SIR model

In Eq. (6.2) we define a frequency dependent SIR model where susceptible individuals meet an expected number of other individuals per day, and where the infection rate is proportional to the fraction of infected individuals.

- a. What is the  $R_0$  of this epidemic, and what is its initial growth rate,  $\rho_0$ ?
- b. What is the Jacobian of the uninfected steady state of this model (after leaving out the uninfluential recovered population)? What is the largest eigenvalue of this Jacobi matrix, and does it correspond to the  $\rho_0$  and the  $R_0$ ?
- c. Sketch the 2-dimensional nullclines of a frequency dependent SI version of this model (by setting  $R = 0$ ).
- d. Do these identify potential problems, and how would you repair them?

#### Question 6.6. Influenza virus infecting epithelial cells

Make the corresponding question in Chapter 14 and simplify your model into two ODEs by assuming that the time scales of the virus and the interferon are much faster than those of the epithelial cells. If you are interested in this system, use Grind to help you with sketching the nullclines. Analyze this QSSA model by phase plane analysis, i.e., sketch the nullclines, the vector field, and determine the stability of all steady states.

## Chapter 7

# Functional response

Most previous resource-consumer models were based upon a mass-action consumption term. Our analysis on Page 43 suggested that qualitatively different resource nullclines are expected when these consumption terms become saturated. In biology mass-action interaction terms are often a simplification that is valid only at low population densities. Mass-action terms can become very large when either of the involved populations becomes large, and, as a consequence, the *per capita* rate of one of the other population may become unrealistically fast. For example, the rate at which bacteria are infected by phages should not become extremely fast when the average number of phages surrounding a single bacterium becomes extremely large. Productive infection takes time because the phages have to attach, enter the cell, and interact with the intracellular machinery of the bacteria, and this “handling” time is not accounted for if infection is modeled with a mass-action infection term (unless every subprocess, such as the attachment and entry, are implemented as subsequent steps in the model).

Saturation functions provide a semi-mechanistic short-cut for limiting the interaction rate at high population densities, and in earlier chapters we have used Hill functions and exponential functions to allow for maximum birth rates at high resource densities. A famous paper by Holling in 1959 defined a number of such saturation functions. Holling employed his secretary, whom was picking up artificial “resource” items from a table, as an artificial consumer. These functions were coined “functional responses”, and Holling (1959) defined three non-linear responses:

$$f(R) = a \min\left(1, \frac{R}{2h}\right), \quad f(R) = a \frac{R}{h + R} \quad \text{and} \quad f(R) = a \frac{R^2}{h^2 + R^2}, \quad (7.1a,b,c)$$

which are called the Holling type-I, II, and III functions, respectively (see Fig. 7.1). All three functions approach a maximum,  $a$ , corresponding to the maximum amount of resource a consumer can catch and handle within a certain time unit (and when  $R = h$  they are half-maximal, i.e.,  $a/2$ ). Holling’s motivation for this maximum was the “handling time”: even at an infinite resource density the consumer cannot consume the resource infinitely fast because of the time required to handle, eat, and digest the resource (e.g., his blind-folded secretary had to find an item with her hands, pick it up, and store it). There is indeed a direct way to derive Eq. (7.1b). Let  $R$  be the number of prey items on the table, and  $n = atR$  be the number of prey items picked up by the secretary, with  $a$  her attack rate, and  $t$  for the amount of time available for searching, and  $R$  the number of prey-items on the table. The free time available for searching,  $t$ , is the total time of the experiment,  $T$ , minus the time spent on handling the items found,  $bn$ ,

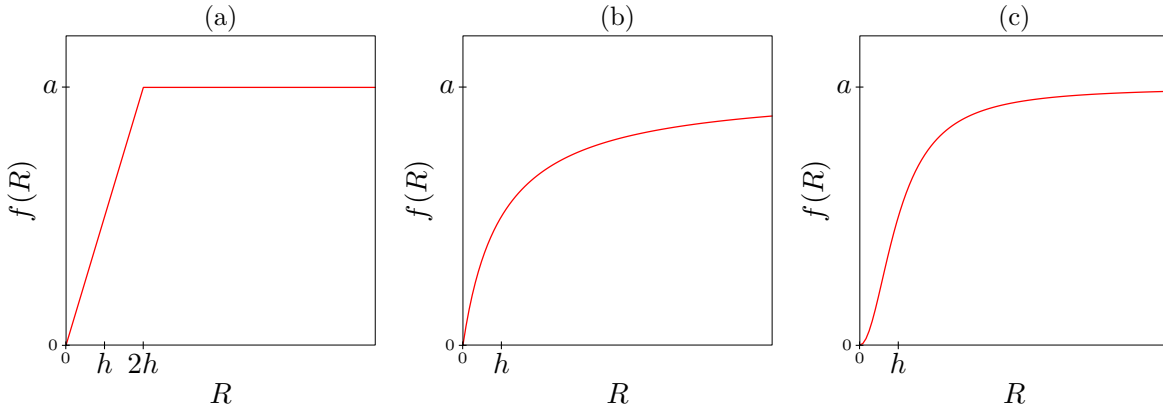


Figure 7.1: The functional responses defined by Eq. (7.1). The Holling type I functional response (a), the Monod (Holling type-II) functional response (b), and the sigmoid (Holling type-III) functional response (c). This figure was made with the file `functions.R`.

where  $b$  is the handling time per item. Substituting,  $t = T - bn$  into  $n = atR$  gives

$$n = a(T - bn)R \quad \text{or} \quad n = \frac{aTR}{1 + abR} = \frac{a'R}{h + R}, \quad (7.2)$$

where  $h = \frac{1}{ab}$  and  $a' = T/b$ . The parameter  $a'$  is dimensionless, and defines the maximum number of items collected when  $R \rightarrow \infty$ . The saturation constant,  $h$ , also is a dimensionless number of prey-items, and depends on both the attack rate and the handling time.

Eq. (7.1) shows that the Holling type-II and type III responses are conventional Hill functions. Thus, we know that  $a$  is the maximum consumption rate, and that  $h$  is the resource density at which the function consumption is half maximal. Synonyms of the type-II and III responses are the “Monod saturation” (Monod, 1949; Holling, 1959), and the “sigmoid” functional response, respectively. Both will be discussed at length in this chapter. The type-I response is linear until the *per capita* consumption rate equals the maximum of  $a$  per time unit.

## 7.1 Monod functional response

We start by considering a Monod saturated *per capita* killing rate of a logistically replicating resource,  $R$ , by a consumer,  $N$ ,

$$\frac{dR}{dt} = rR(1 - R/K) - \frac{aRN}{h + R} = rR(1 - R/K) - \frac{a'RN}{1 + R/h}, \quad (7.3)$$

where  $a$  is the maximum number of resource consumed (and/or killed) per consumer per unit of time,  $h$  is the resource density at the consumption rate is half-maximal, and  $a' = a/h$  is a mass-action killing rate. The latter form of the equation reveals that when the saturation constant,  $h$ , is large this model approaches the Lotka-Volterra model (here large would mean  $h \gg K$ ). The  $dR/dt = 0$  isocline can be found by setting Eq. (7.3) to zero, and solving

$$R = 0 \quad \text{and} \quad N = \frac{r}{a} (1 - R/K)(h + R), \quad (7.4)$$

where the latter is a parabola crossing  $N = 0$  at  $R = K$  and  $R = -h$ , and having its maximum value at  $R = (K - h)/2$ . In Fig. 7.2 this nullcline is depicted for positive population densities.

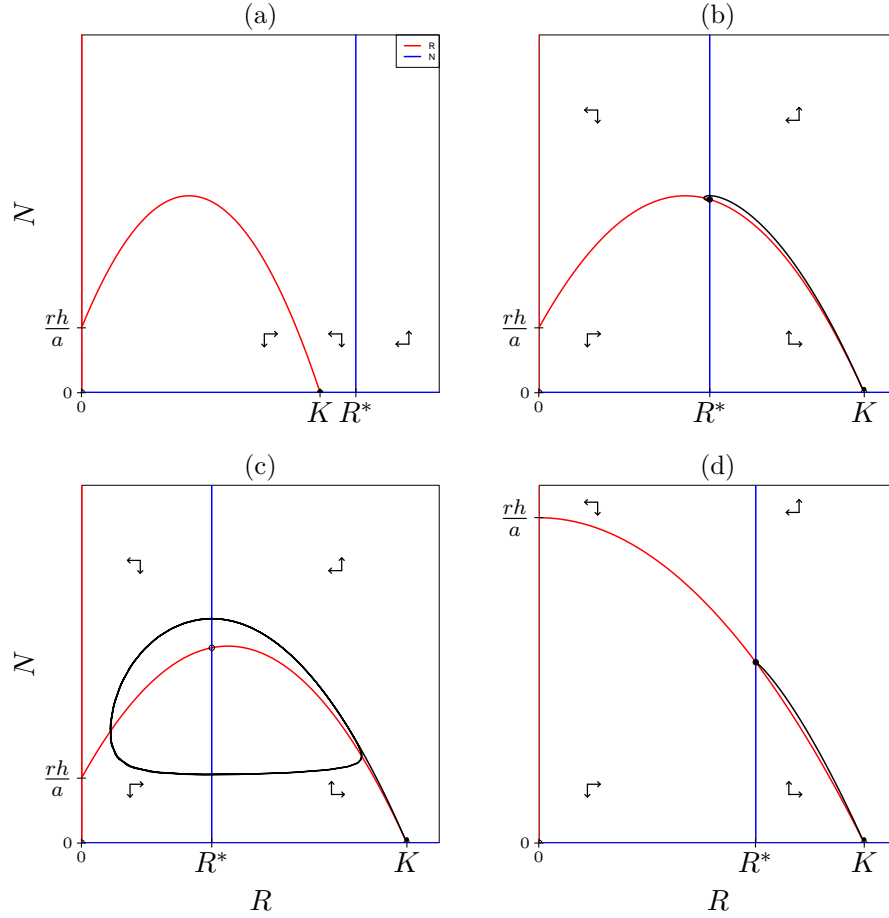


Figure 7.2: Qualitatively different phase spaces of the Monod saturated model of Eq. (7.3) and (7.5). The red parabola is the resource nullcline intersecting the horizontal axis at  $R = K$ , and the vertical axis at  $N = rh/a$ . The blue vertical consumer nullcline is located at  $R^* = h/(R_0 - 1)$ . Black lines are trajectories starting just above the carrying capacity of the resource. In Panels (a-c) we set  $h \ll K$  such that the maximum of the parabola, that is located at  $R = (K - h)/2$ , occurs approximately half-way the carrying capacity. In Panel (a)  $R^* > K$ , making the carrying capacity of the resource the only attractor. In Panel (b)  $R^* > (K - h)/2$ , making the non-trivial steady state stable. In Panel (c)  $R^* < (K - h)/2$ , making the non-trivial steady state unstable, and giving rise to a stable limit cycle, corresponding to periodic behavior. In Panel (d)  $h = K$ , which puts the top of the parabola at  $R = 0$  and makes the  $dR/dt = 0$  nullcline monotonically declining. This figure was made with the model `monodBM.R`.

When  $h < K$ , the resource nullcline in the positive quadrant is a parabola with an unstable part having vectors pointing away from it in the region where  $R < \frac{K-h}{2}$  (see Fig. 7.2a-c). When  $h \geq K$  the resource nullcline in the positive quadrant is a monotonically declining function resembling that of the (generalized) Lotka-Volterra model (see Fig. 7.2d). For the consumer it is typically assumed that the *per capita* birth rate is proportional to its *per capita* consumption,

$$\frac{dN}{dt} = \frac{caRN}{h + R} - \delta N, \quad (7.5)$$

which is identical to the consumer equation in Eq. (5.6), and therefore has the same  $R_0 = \frac{ca}{\delta}$  and nullcline at  $R = \frac{h}{R_0 - 1}$ . This nullcline again defines the resource density,  $R^*$ , that the consumers require to expand, i.e., at the right-hand side of the nullcline the vector-field points upwards.

In ecology this Monod-saturated model is sometimes referred to as the Rosenzweig-McArthur model. Depending on the parameter values, the model can have three steady states: two trivial states  $(\bar{R}, \bar{N}) = (0, 0)$  and  $(K, 0)$ , and a non-trivial co-existence state that is present when

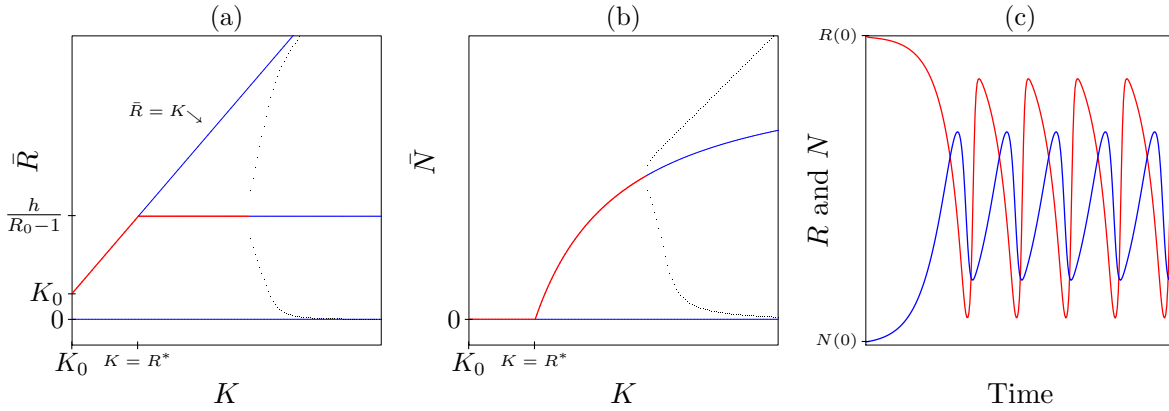


Figure 7.3: Bifurcation diagrams illustrating the effect of increasing the carrying capacity,  $K$  (starting at a  $K_0 > 0$ ). Heavy red lines represent stable steady states, light blue lines unstable steady states, and black points minima and maxima of a stable limit cycle. Panel (c) depicts the trajectory of Fig. 7.2c as a time plot ( $R$ : red and  $N$ : blue) starting at  $R(0) = K$  and a small value of  $N$ . This figure was made with the model `monodBM.R`.

$R^* < K$ . Fig. 7.2 depicts qualitatively different phase spaces of the model. In Fig. 7.2a the consumer cannot maintain itself because  $R^* > K$ , i.e., even the maximum resource density  $K$  is insufficient. As a consequence,  $(\bar{R}, \bar{N}) = (K, 0)$  is a stable steady state (see the vector field in Fig. 7.2a). Indeed systems containing too little nutrients are expected to have such a low carrying capacity of the resource that it is unable to sustain a consumer population.

Fig. 7.2b depicts the situation where the consumer nullcline is located at the right-hand side of the top of the parabolic resource nullcline, i.e., where  $(K - h)/2 < R^*$ . The local vector field is identical to that of the Lotka-Volterra model:

$$J = \begin{pmatrix} -\alpha & -\beta \\ \gamma & 0 \end{pmatrix} \quad \text{with} \quad \text{tr} = -\alpha < 0 \quad \text{and} \quad \det = \beta\gamma > 0. \quad (7.6)$$

Thus, the non-trivial steady state will be stable whenever the consumer nullcline intersects the resource nullcline at the right-hand side of the maximum of the parabola. The trajectory starting with few consumers in a resource population at carrying capacity reveals that for the parameters that were used to make Fig. 7.2b, the steady state is a stable spiral point. In Fig. 7.2c the nullclines intersect at the left-hand side of the maximum of the parabola. Here the resource nullcline is unstable, and from the local vector field one now reads from the graphical Jacobian

$$J = \begin{pmatrix} \alpha & -\beta \\ \gamma & 0 \end{pmatrix} \quad \text{that} \quad \text{tr} = \alpha > 0 \quad \text{and} \quad \det = \beta\gamma > 0. \quad (7.7)$$

The steady state is unstable because the local feedback of the resource on itself is positive: increasing the resource increases its growth rate. The reason for this positive feedback is the saturated functional response, as increasing the resource density will decrease the *per capita* killing rate,  $a/(h + R)$ , of the resource. The behavior of the model in this situation is a stable limit cycle (see Fig. 7.2c and Fig. 7.3c). One can indeed check that in Fig. 7.2c none of the trivial steady states, i.e.,  $(\bar{R}, \bar{N}) = (0, 0)$  or  $(K, 0)$ , is an attractor of the system. Therefore, the consumer cannot go extinct, and the stable limit cycle has to be the global attractor of the system. Fig. 7.2d just confirms that this model becomes similar to the Lotka-Volterra model when  $h \geq K$ .

## Paradox of enrichment

Models with the “humped” resource nullcline of Fig. 7.2 have been used for the famous Paradox of enrichment (Rosenzweig, 1971). Rosenzweig studied eutrophication (enrichment) of lakes with algae and zooplankton, and showed that increasing the carrying capacity of the algae failed to increase the density of the algae. The enrichment with nutrients for the algae rather increased the zooplankton density, lead to destabilization of the non-trivial steady state, and ultimately to stable limit cycles with such a wide amplitude that so closely approach the axes of the phase plane that species may go extinct (Rosenzweig, 1971). This ultimate loss of species richness was coined the “paradox of enrichment”. Because the amplitudes of limit-cycles of algae and zooplankton observed in the field tend to be much smaller than those in these models (Arditi & Ginzburg, 1989; Ginzburg & Akçakaya, 1992; McCauley *et al.*, 1999; Murdoch *et al.*, 2002; Scheffer & De Boer, 1995), it remains unclear whether or not the loss of species in aquatic ecosystems was due to enrichment only (i.e., due to the paradox of enrichment). Nevertheless, the bifurcation diagram in Fig. 7.3 reveals that increasing the carrying capacity,  $K$ , of this model:

1. first increases the density of the algae as long as there is no zooplankton,
2. subsequently leaves the density of the algae at  $R^* = h/(R_0 - 1)$  and increases the zooplankton density,
3. and finally destabilizes the system by a Hopf-bifurcation (see Chapter 12), leading to oscillations with larger and larger amplitudes.

Thus, enrichment of an oligotrophic system is expected to first increase the diversity of the system, i.e., when  $R^* \geq K$ , but could ultimately decrease the diversity by too large amplitude limit cycles (see Fig. 7.3b).

## Limit cycle behavior

The Hopf bifurcation that is leading to this oscillatory (or periodic) behavior can be illustrated by the phase plane of the Lotka-Volterra model with a horizontal resource and a vertical consumer nullcline, giving rise to a steady state with neutral stability, which is surrounded by infinitely many neutrally stable cycles (see Fig. 5.5b and the Jacobian of Eq. (5.21) having purely imaginary eigenvalues). The Hopf bifurcation depicted in Fig. 7.3 indeed occurs when the vertical consumer nullcline intersects the parabolic nullcline of the resource exactly at the top of this parabola (i.e., when  $R^* = \frac{K-h}{2}$ ). For this particular parameter condition the slope of the resource nullcline in the steady state is perfectly zero, which by the graphical Jacobian method indeed implies that both diagonal elements of the Jacobi matrix are zero, i.e.,

$$J = \begin{pmatrix} 0 & -\beta \\ \gamma & 0 \end{pmatrix} \quad \text{with} \quad \text{tr} = 0, \quad \det = \beta\gamma > 0 \quad \text{and} \quad \lambda_{\pm} = \pm i \sqrt{\beta\gamma}. \quad (7.8)$$

Hence the real part of the corresponding eigenvalues will be zero, meaning that when  $R^* = \frac{K-h}{2}$  the Monod-saturated predator-prey model undergoes a bifurcation where the non-trivial steady changes stability.

When the non-trivial steady state is unstable the model displays oscillatory behavior and approaches a stable limit cycle (Fig. 7.2c and Fig. 7.3c). On the limit cycle the consumer and resource densities oscillate in an “out of phase” manner because consumer densities increase only after the resource has increased. Oscillatory behavior is frequently observed in biological populations. A famous ecological example is the oscillatory behavior of lynx and hare populations in Canada, that were discovered in the records of the furs brought in by hunters in the last

century. Surprisingly, the hare and lynx cycles are not always out of phase, and ecologists are performing experiments to understand the precise mechanism underlying this famous oscillation (Stenseth *et al.*, 1999). Another ecological example of consumer resource oscillations are the cycles of algae and zooplankton in the spring (McCauley *et al.*, 1999; Fussmann *et al.*, 2000; Murdoch *et al.*, 2002; Yoshida *et al.*, 2003). Bacterial populations oscillate over several orders of magnitude because of their interaction with phages (Bohannan & Lenski, 1997, 1999), and due to their production of toxins (Cornejo *et al.*, 2009). Periodic behavior is easily obtained in mathematical models and is frequently observed in nature. Note that these oscillations are autonomous: there is no periodic forcing from outside driving this. The periodic behavior arose by the destabilization of the non-trivial steady state, i.e., at a Hopf bifurcation (see Fig. 7.3 and Chapter 12).

### Formal derivation of the Monod response by a QSSA

The Monod functional response can be derived in the same way as the conventional Michaelis-Menten enzyme expression was obtained. To this end one splits the consumers,  $N$ , into a subpopulation,  $C$ , that is actually handling the resource, and a free subpopulation,  $F$ , that is “free” to catch the resource,  $R$ . By conservation one knows that  $N = F + C$ . To describe the consumers catching and handling resource one could write

$$\frac{dC}{dt} = aRF - hC \quad \text{or} \quad \frac{dC}{dt} = aR(N - C) - hC, \quad (7.9)$$

where  $a$  is a rate at which the free consumers attack and catch resource, and  $1/h$  is the time they require to handle the resource. When the time scale of handling resource is much more rapid than the time scale at which the resource and consumers reproduce, one can make a quasi steady state assumption for the complex,  $dC/dt = 0$ , and obtain that

$$C = \frac{aNR}{h + aR} = \frac{NR}{h' + R}, \quad (7.10)$$

where  $h' = h/a$  is the resource density at which half of the consumers are expected to be handling resource. To see how this ends up in the resource population one could add  $dC/dt = aRF - hC = 0$  to an ODE for the resource, e.g.,  $dR/dt = rR(1 - R/K) - aRF$ , giving

$$\frac{dR}{dt} = rR(1 - R/K) - hC = rR(1 - R/K) - \frac{hNR}{h' + R}, \quad (7.11)$$

which is a normal Holling type-II functional response. For the consumers one could argue that the birth rate should be proportional to the number of consumers that are finished handling and consuming resource, and write that

$$\frac{dN}{dt} = chC - dN = \frac{chNR}{h' + R} - dN, \quad (7.12)$$

which together with Eq. (7.11) yields the Monod saturated consumer resource model.

One can also use this analysis to learn how to write ODEs for one consumer consuming several different resources. Let  $a_i$  be the attack rate of the consumer for resource  $i$ , and assume for simplicity that all resource species require the same handling time,  $1/h$ .<sup>1</sup> By the  $a_i$  parameter,

<sup>1</sup>This simplifying assumption is only for clarity and consistency with the above, we can also write  $dC_i/dt = a_i R_i F - h_i C_i = 0$  or  $a'_i R_i F = C_i$ , where  $a'_i = a_i/h_i$  and proceed as below.

the consumer can have different preferences for the different resource species. The conservation equation now becomes  $N = F + \sum_i C_i$ , and for each complex one writes

$$\frac{dC_i}{dt} = a_i R_i F - h C_i = 0 \quad \Leftrightarrow \quad a_i R_i \left( N - \sum_j C_j \right) = h C_i . \quad (7.13)$$

A trick to solve this, while having a sum term in the equation, is to sum the latter equation for all complexes, yielding,

$$\sum_i a_i R_i \left( N - \sum_j C_j \right) = h \sum_i C_i , \quad (7.14)$$

which can be rewritten into

$$\sum_i a_i R_i N = \sum_i a_i R_i \sum_j C_j + h \sum_j C_j = \sum_j C_j \left( \sum_i a_i R_i + h \right) . \quad (7.15)$$

Solving for  $\sum C_i$  gives

$$\sum_i C_i = \frac{N \sum_i a_i R_i}{h + \sum_j a_j R_j} \quad \text{and, hence,} \quad C_i = \frac{N a_i R_i}{h + \sum_j a_j R_j} . \quad (7.16)$$

For each resource,  $i$ , one can again add  $dC_i/dt = a_i R_i F - h C_i = 0$  to

$$\frac{dR_i}{dt} = r R_i (1 - R_i/K_i) - a_i R_i F \quad \text{giving} \quad \frac{dR_i}{dt} = r R_i (1 - R_i/K_i) - \frac{h N a_i R_i}{h + \sum_j a_j R_j} . \quad (7.17)$$

For the consumers one would argue that their reproduction is proportional to all consumer individuals finished with handling a complex,  $h C_i$ , and write that

$$\frac{dN}{dt} = c \sum_i h C_i - dN = \frac{c h N \sum_i a_i R_i}{h + \sum_j a_j R_j} - dN . \quad (7.18)$$

Although this all works out quite nicely, as we obtain high-dimensional Monod functions, this does not imply that saturated functional responses are truly due to the handling time derived here, or the one defined in Eq. (7.2). One could also argue that saturation is simply due to satiation of the consumers at high resource densities.

## Saturated birth rate

In Chapter 5 we studied the effect of a saturated birth rate of the consumer in the Lotka-Volterra model, and demonstrated that the consumer nullcline remains to be a straight line at the critical resource density,  $R^*$ . Since the consumption rate is now also a saturation function, we double-check how a birth rate that saturates as a function of the consumption would affect the equations now. Since the *per capita* consumption equals  $C = aR/(h + R)$ , one obtains for a saturated *per capita* birth rate of the consumer

$$g(C) = c \frac{C}{h + C} \quad \text{or} \quad g(R) = c \frac{\frac{aR}{h+R}}{H + \frac{aR}{h+R}} = \frac{caR}{H(h + R) + aR} = \frac{\beta R}{h' + R} , \quad (7.19)$$

which remains of the same form as the birth rate in Eq. (7.5), with a new birth rate,  $\beta = ca/(H + a)$ , and saturation constant,  $h' = hH/(H + a) < h$ . Note that  $h' < h$ , i.e., that the consumer birth rate is generally expected to saturate at lower resource densities than the consumer consumption rate. We conclude that a saturated consumer birth rate makes hardly any difference.

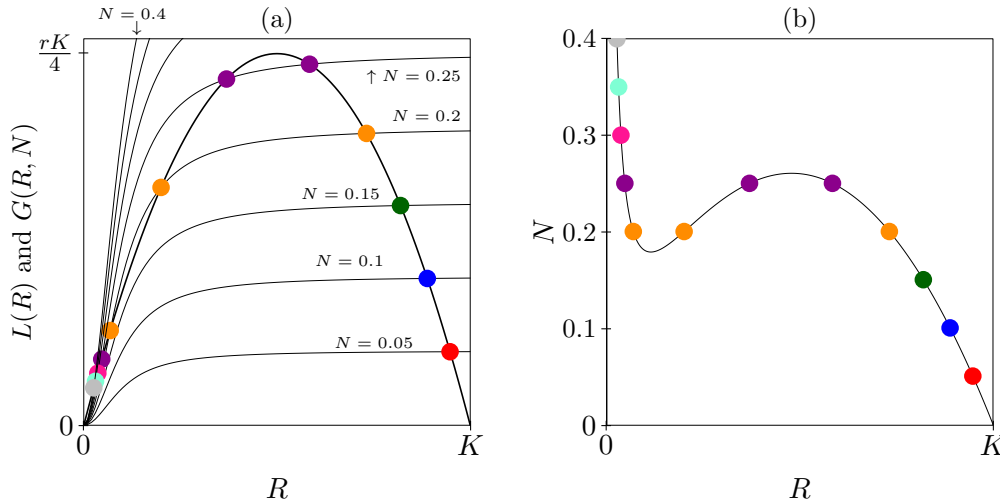


Figure 7.4: Graphical construction of the resource nullcline of a model with a sigmoid function response. Panel (a) depicts the positive and negative terms of Eq. (7.20a) separately in one graph. The positive term,  $L(R)$ , is a parabola intersecting the horizontal axis at  $R = 0$  and  $R = K$ . The negative sigmoid grazing term,  $G(R, N)$ , is depicted for  $N = 0.05, 0.1, 0.15, \dots, 0.35$  to  $N = 0.4$ . The location of the intersects in Panel (a) provide the points in the  $(R, N)$  phase plane where  $dR/dt = 0$  (see Panel (b)). Interpolation between these points yields the nullcline sketched in Panel (b). Parameters:  $r = K = a = 1$  and  $h = K/10$ . Figure made with the R-script `sigmoid0.R`.

## 7.2 Sigmoid functional response

For several types of prey one expects that they can hide efficiently in so-called “refugia” at low prey densities, which would lead to low consumption rates at low resource densities. For instance, prey species like zooplankton that are consumed by fish will hide in the vegetation when they sense the presence of fish. A mechanistic way to describe this would be a “shifted” Monod saturated functional response, i.e.,  $f(R) = (R - k)/(h + R - k)$ , where  $k$  is number of refugia, or the resource density at which consumption starts (you will sketch the nullclines resulting from this functional response with Grind in the exercises). Because this shifted Monod function is discontinuous, the same process is typically modeled with a more phenomenological sigmoid functional response, which indeed yields similar nullclines (see the same exercise). Another example of such a shifted or sigmoid functional response would be large herbivores that hardly spend time grazing when they know the vegetation cover is very poor. Sigmoid effects may also appear in the effect of the consumer on the resource (which will not be considered here). For example, tumor cells are quite resistant to the cytotoxic effect of killer cells in the immune system, and may require multiple contacts with such cytotoxic cells before they die. At low killer cell densities this leads to cooperative effects among the killers, when tumor cells are typically destroyed by interacting with multiple killer cells (Gadhamsetty *et al.*, 2017).

To model a sigmoid saturated functional response we replace the functional response,  $f(R)$ , of the previous model with a sigmoid Hill function, and obtain

$$\frac{dR}{dt} = rR(1 - R/K) - \frac{aR^2N}{h^2 + R^2} \quad \text{and} \quad \frac{dN}{dt} = \frac{caR^2N}{h^2 + R^2} - \delta N. \quad (7.20a,b)$$

The  $R_0$  of the consumer remains  $R_0 = ca/\delta$ , and the  $dN/dt = 0$  nullcline remains a straight line that is now located at  $R^* = h/\sqrt{R_0 - 1}$  (see Fig. 7.5). Sketching the nullcline of the resource is

more challenging. Setting  $dR/dt = 0$  and canceling the  $R = 0$  solution, one obtains

$$N = \frac{r}{a} \frac{h^2 + R^2}{R} \left(1 - \frac{R}{K}\right), \quad (7.21)$$

which has a vertical asymptote at  $R = 0$ , and is zero when  $R = K$ . One can take the derivative of this function with respect to  $R$  to find its minima and maxima. This reveals that the nullcline has a minimum and a maximum whenever  $h < K/5$ , and that for low  $h$  the minimum is located around  $R = h$  and the maximum around  $R = K/2$  (see Section 15.5 in the Appendix).

Complicated nullclines can also be sketched by separately plotting the positive and negative terms, and recording when these are equal, i.e., when they intersect (Noy-Meir, 1975).  $dR/dt$  has a positive logistic growth term,  $L(R) = rR(1 - R/K)$ , and a negative sigmoid consumption term,  $G(R, N) = \frac{aR^2N}{h^2 + R^2}$  ( $G$  for grazing). Both functions can be sketched as a function of the resource density  $R$ , the latter for various values of  $N$ , and the points where they intersect correspond to points of the  $dR/dt = 0$  nullcline (see Fig. 7.4a). The logistic function,  $L(R)$ , is a parabola intersecting the horizontal axis at  $R = 0$  and  $R = K$ . The consumption term,  $G(R, N)$ , is a sigmoid function with a maximum increasing with the consumer density,  $N$ . Sketching  $G(R, N)$  for various values of  $N$  we read in Fig. 7.4a at which  $R$  values  $G(R, N) = L(R)$ , and copy these  $R$  values with the corresponding value of  $N$  into a point of the nullcline into Fig. 7.4b (see the bullets).

To know where in Fig. 7.4a the curves intersect it is crucial to know their slopes around the origin, which is determined by their local derivative, i.e.,

$$\partial_R L(R) = r - 2rR/K, \quad \text{which for } R = 0 \text{ equals } r, \quad (7.22)$$

showing that the local slope of the parabola in the origin is  $r$ , and

$$\partial_R G(R, N) = \frac{2aRN}{h^2 + R^2} - \frac{2aR^3N}{(h^2 + R^2)^2}, \quad \text{which for } R = 0 \text{ yields } 0, \quad (7.23)$$

confirming that the sigmoid curves leave the origin with slope zero. The sigmoid curves therefore always start below the parabola, whatever the consumer density  $N$ . Because the maximum of the parabola is  $rK/4$ , and that of the grazing term is  $aN$ , the  $G(R, N)$  functions will exceed the top of the parabola at sufficiently high values of  $N$  (see Fig. 7.4a). When  $h \ll K$  this leads to the  $dR/dt = 0$  nullcline with a minimum and a maximum shown in Fig. 7.4b. When  $h > K/5$  the nullcline declines monotonically (see Fig. 7.5d and Section 15.5 in the Appendix).

When  $R^* < K$ , the model has three steady states: the trivial  $(0, 0)$  and  $(K, 0)$  saddle points, and a non-trivial steady state that in Fig. 7.5a and b is very similar to the monod-saturated model. When  $R^* > K/2$  the state is stable (Fig. 7.5a), and when the consumer nullcline is located in between the minimum and the maximum the steady state is unstable, such that the one and only attractor of the model is a stable limit cycle (Fig. 7.5b). There is a qualitatively new steady when the vertical consumer nullcline is located on the left-hand side of this minimum, and the graphical Jacobian of this new steady state is

$$J = \begin{pmatrix} -\alpha & -\beta \\ \gamma & 0 \end{pmatrix} \quad \text{with } \text{tr}J < 0 \quad \text{and} \quad \det J > 0, \quad (7.24)$$

which therefore is a stable point (Fig. 7.5c). As the non-trivial steady state will have neutral stability when the consumer nullcline is located such that it intersects the minimum or the maximum of the resource nullcline, this model can undergo two Hopf bifurcations (see below in Fig. 7.6e). When the saturation constant,  $h > K/5$ , the consumer nullcline declines monotonically, giving rise to a Lotka-Volterra-like phase plane, where the non-trivial steady state is always stable (Fig. 7.5d).

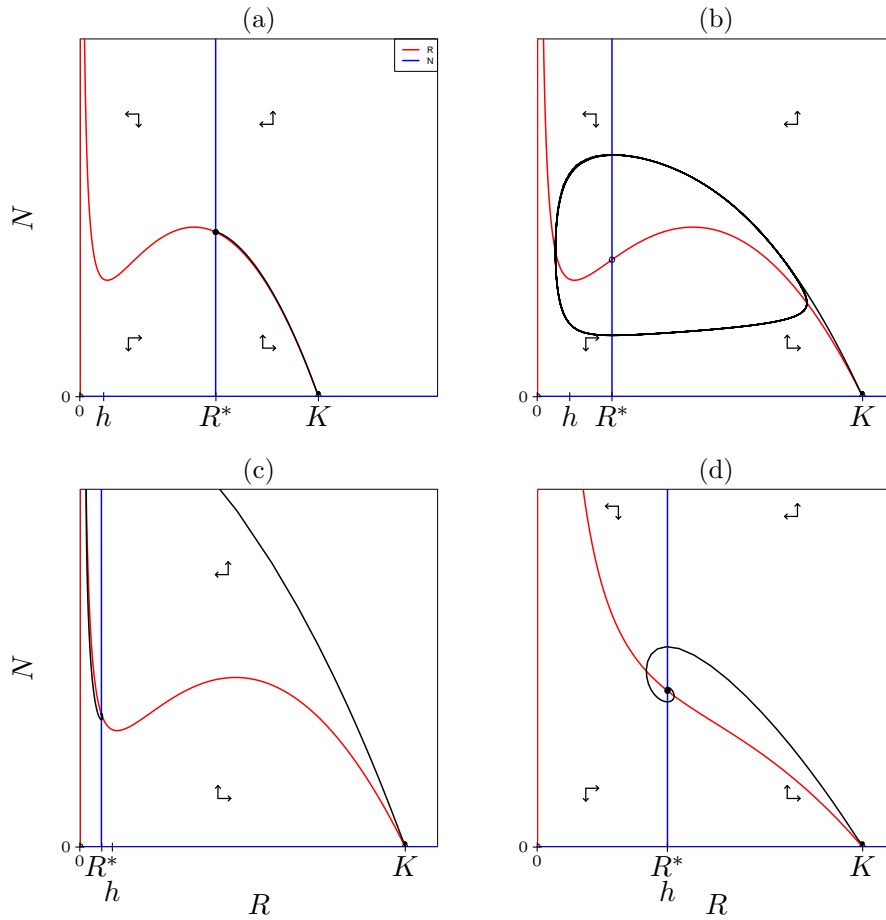


Figure 7.5: Qualitatively different phase spaces of the sigmoid saturated model of Eq. (7.20). The red line is the resource nullcline intersecting the horizontal axis at  $R = K$ . The blue vertical consumer nullcline is located at  $R^* = h/\sqrt{R_0 - 1}$ . Black lines are trajectories starting just above the carrying capacity of the resource. In Panels (a-c) we set  $h < K/5$  such that the resource nullcline has a minimum and a maximum, which are expected to be located around  $R = h$  and  $R = K/2$ , respectively (see Section 15.5). In Panel (a) we set  $R^* > K/2$ , making the non-trivial steady state stable. In Panel (b) we place  $R^*$  in between the minimum and the maximum of the resource nullcline (by setting  $h < R^* < K/2$ ), which makes the non-trivial steady state unstable, and gives rise to a stable limit cycle. In Panel (c) we place  $R^*$  below the minimum,  $R^* < h$ , which makes the non-trivial steady state stable again. In Panel (d) we set  $h > K/5$ , which makes the  $dR/dt = 0$  nullcline monotonically declining. This figure was made with the model `sigmoid.R`.

## Bifurcation diagrams

Enrichment, i.e., increasing  $K$ , can also cause a Hopf bifurcation in this model, giving rise to stable limit cycles that grow in amplitude with the distance to the Hopf bifurcation (Fig. 7.6a, b and d). However, because the resource nullcline keeps its asymptote approaching the vertical axis (Fig. 7.6c), the trajectory cannot approach this axis very closely, and resource and consumer densities do not become as small as in the Monod-saturated model. Enrichment still increases the consumer rather than the resource when both are present (Fig. 7.6a-c). Fig. 7.6c confirms that increasing  $K$  shifts the maximum of the resource nullcline up and to the right (because this maximum is located at  $R \simeq K/2$ ), and that the minimum hardly moves (because it is located at  $R \simeq h$ ). Hence a stable steady state with a consumer nullcline located at  $K/2 < R^* < K$  readily destabilizes when  $K$  is increased, but because the minimum is not moving along, such a state is not expected to become stable again at very large values of  $K$ . For the algae-zooplankton

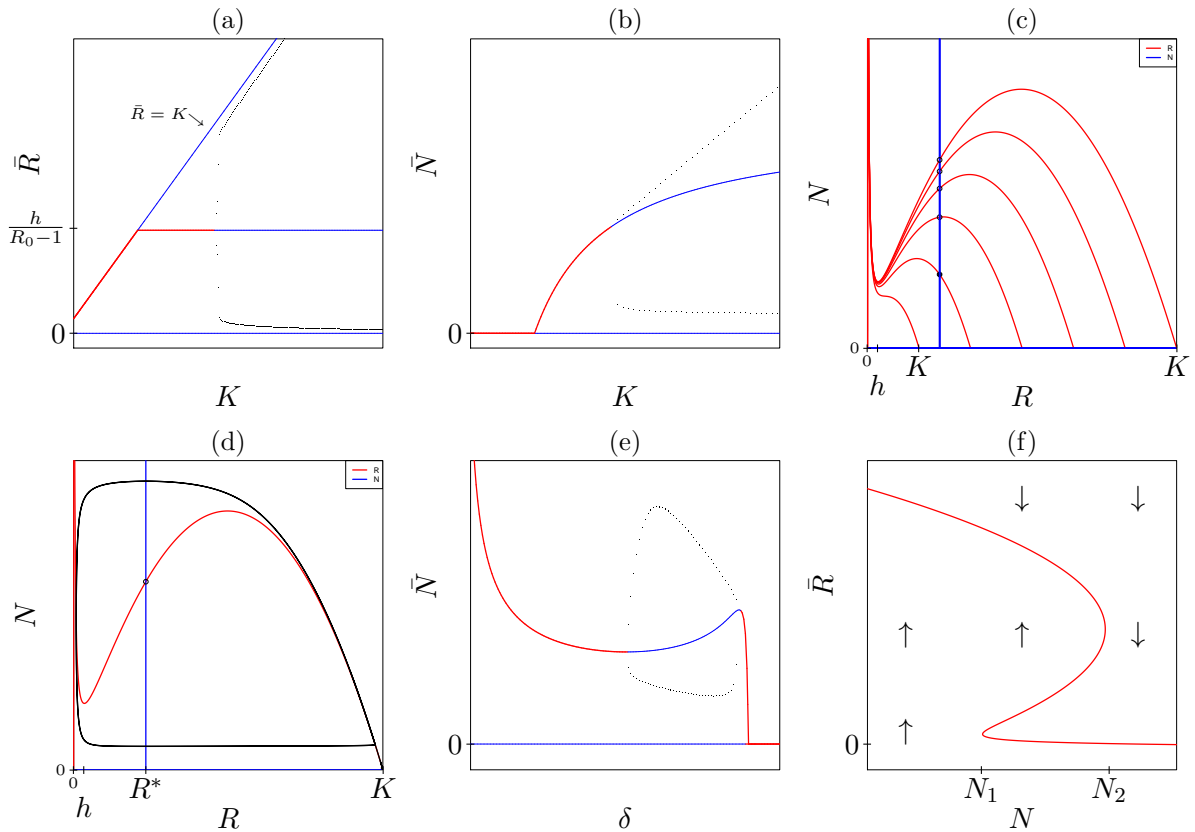


Figure 7.6: Bifurcation diagrams and phase planes of the sigmoid-saturated model. In the bifurcation diagrams heavy red lines represent stable steady states, light blue lines unstable steady states, and black points minima and maxima of a stable limit cycle. Panels (a–d) illustrate the effect of increasing the carrying capacity,  $K$ , as bifurcation diagram (a) and (b), a phase plane with nullclines for various values of  $K$  (c), and a phase plane with nullclines and trajectory for the largest value of  $K$  (d). Panel (e) depicts the effect of changing the death rate,  $\delta$ , of the consumer, where the black points indicate the minima and the maxima of the stable limit cycle that exists between the two Hopf bifurcations. Panel (f) is a bifurcation diagram made by showing the steady state of the resource taking the number of consumers as a “parameter”. This depicts the typical diagram with alternative steady states and hysteresis (see Chapter 12). This figure was made with the model `sigmoid.R`.

systems the reduced amplitude of the limit cycles is interesting because the oscillations that are observed in nature are much “milder” than those of the Monod-saturated model for realistic parameter values (Arditi & Ginzburg, 1989; Ginzburg & Akçakaya, 1992; McCauley *et al.*, 1999; Murdoch *et al.*, 2002; Scheffer & De Boer, 1995; Arditi & Ginzburg, 2012). Measurements of the functional response of zooplankton grazing on algae strongly support a Holling type-II response, however.

To illustrate the two Hopf bifurcations that this model may undergo we move the position of the consumer nullcline located at  $R = R^*$  by changing  $\delta$  (see Fig. 7.6e). When  $\delta$  is too large the consumer cannot be maintained (because  $R^* > K$ ), and  $(\bar{R}, \bar{N}) = (K, 0)$  is the one and only attractor (see Fig. 7.6e). Decreasing  $\delta$  somewhat allows the consumer to invade, its steady state value increases with decreasing  $\delta$ , and for a very narrow range of  $\delta$  the non-trivial steady state is stable. The value of  $\bar{N}$  is maximal at the Hopf bifurcation (because the consumer nullcline is located at the maximum of the resource nullcline). Here a stable limit cycle is born, the non-trivial steady state becomes unstable, and  $\bar{N}$  declines when  $\delta$  is further decreased. The second Hopf bifurcation occurs when the consumer nullcline is located at the minimum of the resource nullcline. The limit cycle dies, the steady state becomes stable again, and  $\bar{N}$  increases steeply

upon decreasing  $\delta$  further. First, note that the shape of  $\bar{N}$  in Fig. 7.6e) resembles the shape of the  $dR/dt = 0$  because we “travel” along that nullcline by changing  $\delta$ . Second, the steady state at high resource densities is only stable for a narrow range of consumer death rates,  $\delta$ , because the functional response loses its dependence of the resource at high resource densities, i.e.,  $G(R) = \frac{R^2}{h^2 + R^2} \simeq 1$  when  $R \gg h$ , and, as a consequence the ODE of the consumers simplifies to  $dN/dt \simeq (ca - \delta)N$ , which does not depend on  $R$ . Generically, the consumer nullcline is therefore expected to be located in regions where  $R \simeq h$ , and because we have to choose  $h \ll K$  to have a non-monotonic resource nullcline, this will typically be below  $K/2$ , i.e., below the maximum, like in Fig. 7.5c).

Finally, this model is famous because it allows for multiple steady states of the resource at particular values of the consumer. For instance, treating the consumer density as a “parameter”, which could represent the fixed rate at which the resource is being harvested, e.g., by a fixed stock of herbivores grazing vegetation, or a fixed fleet of fishermen, we only need to rotate the phase plane such that we plot the resource nullcline as a function of the consumer density,  $N$  (see Fig. 7.6f). The nullcline provides  $\bar{R}$  as a function of  $N$  because  $dR/dt = 0$  at this line. For intermediate values of  $N$  there are three alternative steady states for  $\bar{R}$ . The vector field taken from Fig. 7.5 demonstrates that the upper and lower states are stable, and that the middle one is unstable. At some high values of the consumers,  $N = N_2$ , the upper two states merge and disappear (this is a so-called saddle-node bifurcation), leaving the low  $\bar{R}$  state as the only attractor (corresponding to an over-exploited resource). At a much lower value of the consumers,  $N = N_1$ , the lower two states merge and disappear (another saddle-node bifurcation), leaving the upper  $\bar{R}$  state as the only attractor (corresponding to “healthy” harvested resource). If one were to start harvesting this resource, starting at  $N = 0$ , the resource would suddenly collapse at  $N = N_2$ . After the collapse it is difficult to restore the resource to “healthy” levels, because the harvesting rate has to be reduced to  $N = N_1 < N_2$ . This “memory” of the system is called hysteresis, and in one of the exercises we will study how such catastrophes can be predicted (Scheffer *et al.*, 2009; Veraart *et al.*, 2012; Scheffer *et al.*, 2012).

### 7.3 2-dimensional functional response functions

The functional responses considered hitherto depend on the resource density only, and can hence be written as 1-dimensional functions  $f(R)$ . If there is direct competition between consumers for catching resource one would have a situation where the *per capita* consumption efficiency declines with the consumer density, i.e., a 2-dimensional functional response  $f(R, N)$  for which  $\partial_N f() < 0$ . Predators that increase their feeding efficiency, e.g., by hunting in groups, also require a “predator-dependent functional response”, but with the property that  $\partial_N f() > 0$ . Additionally, arguing that predators are only expected to find prey located within their territory, Arditi and Ginzburg (1989; 1992) proposed a ratio-dependent functional response,  $f(R/N)$ , which is analyzed in the exercises.

In ecology Beddington (1975) and DeAngelis *et al.* (1975) independently proposed a 2-dimensional functional response by adding a term by which the consumers increase the saturation constant, e.g.,

$$f(R, N) = \frac{aR}{h + eN + R}, \quad (7.25)$$

which is intuitively appealing because increasing the consumer density just increases the resource density at which the consumption rate becomes half maximal, and because for  $e = 0$  this simplifies into the Monod saturated functional response (Abrams, 1994). The parameter  $e$

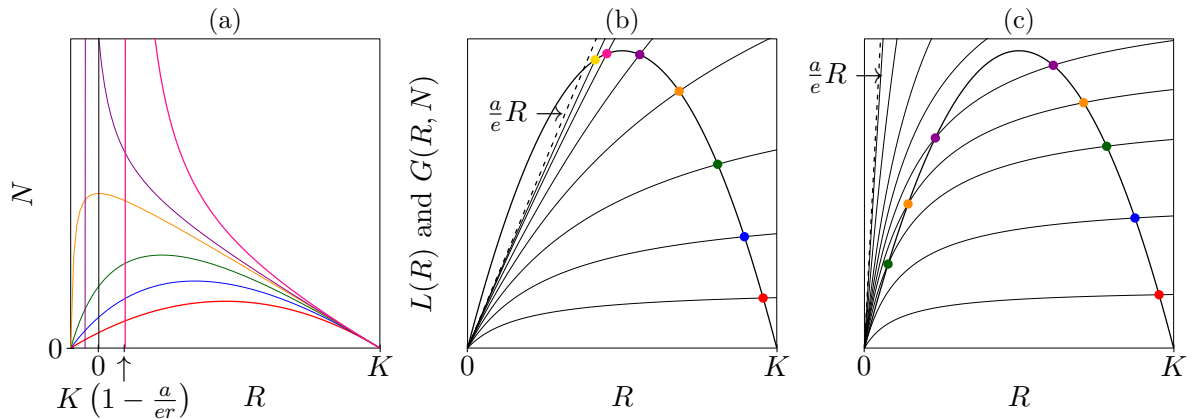


Figure 7.7: The two qualitatively different resource nullclines of the Beddington consumer-resource model. Panel (a) depicts Eq. (7.30) for various values of the intra-specific competition parameter:  $e = 0$  (red),  $e = 0.5$  (blue),  $e = 0.75$  (green),  $e = 0.9$  (orange),  $e = 0.95$  (purple), and  $e = 1.1$  (pink); for  $r = a = 1$  and  $h = K/10$ . The vertical lines depict asymptotes. Panel (b) and (c) depicts the positive and negative terms of Eq. (7.27) separately in one graph. The two parabolas depict the logistic function  $L(R) = rR(1 - R/K)$  as a function of  $R$ , and the saturation curves plot the grazing term  $G(R, N) = \frac{aRN}{h + eN + R}$  as a function of  $R$ , for various values of  $N$ . The colored intersects depict points where  $dR/dt = 0$ . The dashed lines depict the asymptote  $(a/e)R$ . In Panel (b) we have set  $a/e < r$  and in c we consider  $r < a/e$ . The resource nullclines that can be constructed from the intersects in Panels (b) and (c) are depicted in Fig. 7.8a and (b) and (c), respectively. This figure was made with the R-script `beddington0.R`.

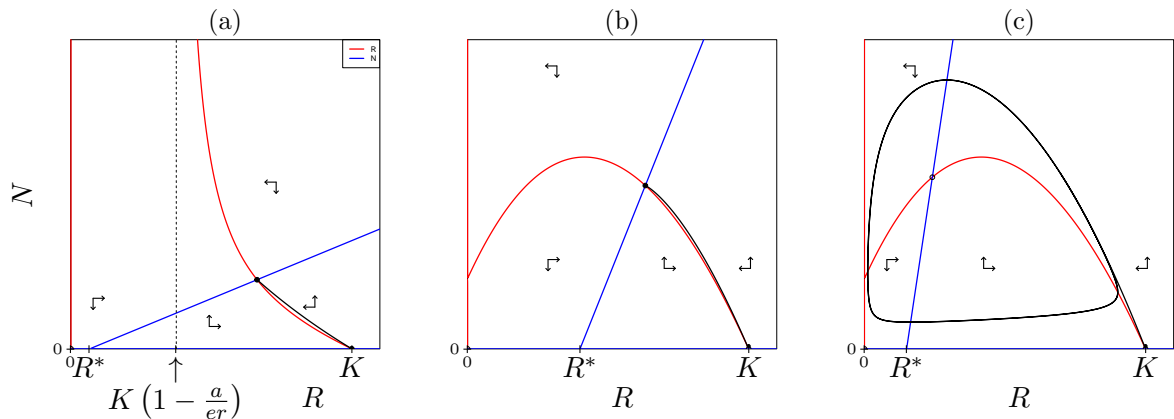


Figure 7.8: Three qualitatively different phase spaces of the Beddington consumer-resource model. The critical resource density for net consumer growth,  $R^* = \frac{h}{R_0 - 1}$ , defines the intersect with the horizontal axis. Panel (a) depicts a case where  $a/e < r$ . The steady state is a stable node. In Panel (b) and (c) we set  $a/e > r$ . The steady state is stable when the consumer nullclines intersects at the right-hand side of the maximum of the resource nullcline (Panel b). Otherwise it is unstable and the behavior is a stable limit cycle (Panel c). Figure was made with the R-script `beddington.R`.

defines the strength of the competition between the consumers. Setting  $e < 0$  would yield a function where consumers help each other. For a large resource population Eq. (7.25) approaches

$$\lim_{R \rightarrow \infty} \frac{aR}{h + eN + R} \leftrightarrow \lim_{R \rightarrow \infty} \frac{a}{h/R + eN/R + 1} = a, \quad (7.26)$$

showing that the interpretation of  $a$  remains the maximum amount of resource a consumer can handle per unit of time.

Because Eq. (7.25) appears to be quite general, we will study the nullclines of consumer-resource

models having this “Beddington” functional response,

$$\frac{dR}{dt} = rR(1 - R/K) - \frac{aRN}{h + eN + R} \quad (7.27)$$

$$\frac{dN}{dt} = \frac{caRN}{h + eN + R} - dN, \quad (7.28)$$

which remains to have an  $R_0 = ca/d$  of the consumer. The consumer nullcline is obtained by setting  $dN/dt = 0$  and finding the solutions

$$N = 0 \quad \text{and} \quad N = \frac{ca - d}{de} R - \frac{h}{e} = \frac{R_0 - 1}{e} R - \frac{h}{e}. \quad (7.29)$$

The last expression defines a line with slope  $(R_0 - 1)/e$  that intersects the horizontal axis at  $R = h/(R_0 - 1)$ . The consumer nullcline is therefore a slanted line with the same minimal resource density  $R^* = h/(R_0 - 1)$  as the Monod saturated model (see Fig. 7.8).

The resource nullcline is more difficult. One can solve  $N$  from Eq. (7.27),

$$N = \frac{r(1 - R/K)(h + R)}{a - er(1 - R/K)}, \quad (7.30)$$

which is identical the parabola of Eq. (7.4) when  $e = 0$ . Thus, for sufficiently small values of  $e$ , this resembles a parabola crossing the horizontal axis when  $R = -h$  and  $R = K$  (see the red line in Fig. 7.7a). Considering  $R < K$ , the denominator reveals that there can be a vertical asymptote at larger values of  $e$ , i.e., when  $er > a$ . Solving  $a - er(1 - R/K) = 0$  reveals that this asymptote is located at  $R = K(1 - \frac{a}{er})$ ; see the vertical lines in Fig. 7.7a, and note that these asymptotes are located at negative  $R$  values when  $a > er$ . Thus, depending on the parameters, the resource nullcline can adopt two qualitatively different forms, a parabola or a hyperbola, and this depends on the value of  $er/a$ .

These two shapes can also be revealed by a graphical construction method. The parabolas in Fig. 7.7b and c depict the positive term of Eq. (7.27), i.e., the logistic function  $L(R) = rR(1 - R/K)$ , having slope  $r$  in the origin. Plotting the total grazing term  $G(R, N) = \frac{aRN}{h + eN + R}$  for various values of  $N$  as a function of  $R$  defines a family of curves increasing with the consumer density  $N$  (see Fig. 7.7b and c). The slope of these functions in the origin is found by taking the derivative with respect to  $R$ :

$$\partial_R G(R, N) = \frac{aN}{h + eN + R} - \frac{aRN}{(h + eN + R)^2} \quad \text{which for } R = 0 \text{ yields } \frac{aN}{h + eN}. \quad (7.31)$$

The slope in the origin therefore increases with the consumer density until  $eN \gg h$ . Indeed, for large numbers of consumers we observe that the grazing term approaches

$$\lim_{N \rightarrow \infty} \frac{aRN}{h + eN + R} \leftrightarrow \lim_{N \rightarrow \infty} \frac{aR}{h/N + e + R/N} = \frac{a}{e} R, \quad (7.32)$$

showing that the grazing term,  $G(R, N)$ , approaches a slanted asymptote with slope  $a/e$ , when it is plotted as a function of  $R$  (see Fig. 7.7b and c).

This corresponds to the same two cases as defined above for different values of  $er/a$ . First, if  $a/e \ll r$  the predation functions intersect the logistic parabola only once, and one obtains a resource nullcline with a vertical asymptote (see Fig. 7.7b and Fig. 7.8a). Because  $a/e$  is relatively small, i.e., a low attack rate and high intraspecific competition, this first case is called “limited predation” (Arditi & Ginzburg, 1989; Ginzburg & Akçakaya, 1992). Second, when

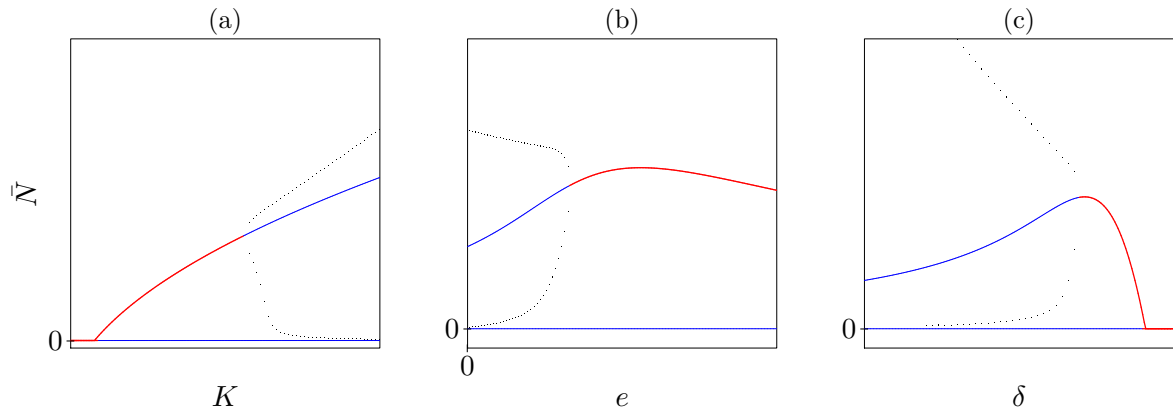


Figure 7.9: Bifurcation diagrams of the Beddington consumer-resource model. In Panel (a) we study the Paradox of enrichment by increasing the carrying capacity,  $K$ , of the resource starting with the stable steady state of Fig. 7.8b (where  $a/e > r$ ), and observe that enrichment results in a Hopf bifurcation, where a stable limit cycle is born which ultimately has a very wide amplitude. Panel (b) illustrates that increasing the consumer interference parameter,  $e$ , can take the unstable steady state of Fig. 7.8c through a Hopf bifurcation, where the stable limit cycle dies. Panel (c) depicts the effect of changing  $\delta$ . Figure was made with the model `beddington.R`.

$a/e \gg r$  there can be one intersection point at low consumer densities, two intersections at intermediate numbers, and no intersection points at high consumer numbers (see Fig. 7.7c). This yields a truncated “parabola” similar to that of the Monod-saturated model. Because the consumer nullcline can intersect either to the left side of the maximum, or to its right side, one obtains two qualitatively different phase spaces (see Fig. 7.8b & c). The non-trivial steady states of Fig. 7.8a and b are stable because the graphical Jacobian

$$J = \begin{pmatrix} - & - \\ + & - \end{pmatrix}, \quad (7.33)$$

has a negative trace and positive determinant. In Fig. 7.8c the consumer nullcline intersects the resource nullcline in its unstable part, and the Jacobian,

$$J = \begin{pmatrix} + & - \\ + & - \end{pmatrix}, \quad (7.34)$$

can have a positive trace when the local positive feedback of the resource onto itself exceeds the negative feedback of the consumer onto itself. The limit cycle that is approached by the trajectory shown in Fig. 7.8c confirms that the trace can become positive, and shows that this model can have very similar periodic behavior as the Monod and sigmoid-saturated models.

### Bifurcations of the Beddington model

Note that the monotonically declining “Beddington saturated” resource nullcline in the phase plane of Fig. 7.8a, that is obtained in the predation-limited case,  $a/e < r$ , is not very different from the “Monod saturated” nullcline in Fig. 7.2d, and the “sigmoid saturated” resource nullcline in Fig. 7.5d, which were both obtained by limiting the effect of the consumer by taking a high saturation constant  $h$  (e.g., setting  $h \simeq K$ ). In the first phase plane of the Beddington model, Fig. 7.8a, the *per capita* killing rate of the consumer is “limited” because it either attacks slowly, i.e., has a low  $a$ , or has strong interference, i.e., has a high  $e$ . The stable non-trivial steady state of the Beddington model in this limited situation will not undergo a Hopf bifurcation when

the carrying capacity,  $K$ , is increased simply because the  $a/e < r$  is independent of  $K$ , and hence there is no Paradox of enrichment (Huisman & De Boer, 1997). In the opposite case,  $a/e > r$ , with more vigorous consumption, the non-trivial steady state can be stable (Fig. 7.8b) or unstable (Fig. 7.8c), and the bifurcation diagram in Fig. 7.9a reveals the classic “enrichment” picture with Hopf bifurcation and a stable limit cycle growing in amplitude when  $K$  is increased. The effect of consumer interference,  $e$ , is shown in Fig. 7.9b, where starting in the unstable figuration of the Monod-saturated model,  $e = 0$ , we observe that the limit cycle shrinks and dies when  $e$  is increased. Increasing  $e$  decreases the steepness of the consumer nullcline, making it more likely to intersect in the stable part of the resource nullcline. Note that further increasing  $e$  will ultimately violate the condition,  $a/e > r$ . Thus, at some value of  $e$ , the consumer nullcline will change from its non-monotonic shape to a monotonically declining nullcline (like in Fig. 7.8a). Since this does not change the properties of the steady state, i.e., this is not a bifurcation, this change is not reflected in the bifurcation diagram of Fig. 7.9b. Finally, we study the effect of the consumer death rate,  $\delta$ , in Fig. 7.9c, and observe the same Hopf bifurcation, and that we now have a reasonable range of death rates where the non-trivial steady state is stable. Thus, slanting the consumer nullcline to the right by intra-specific competition allows for a wider range of parameters where the steady state is stable.

### The total quasi steady state assumption

The 2-dimensional functional response of Eq. (7.25) can be derived by an extension of the conventional Michaelis-Menten QSSA (Huisman & De Boer, 1997). Following the “total” QSSA of Borghans *et al.*(1996), we now split both the resource,  $R$ , and the consumers,  $N$ , into a subpopulation,  $C$ , when they form a complex, and a free subpopulation,  $R_F$  and  $N_F$ . Thus, we now write conservation equations for both the consumer and the resource,  $N = N_F + C$  and  $R = R_F + C$ . To describe the consumers catching and handling resource we again write

$$\frac{dC}{dt} = aR_F N_F - hC \quad \text{or} \quad \frac{dC}{dt} = a(R - C)(N - C) - hC, \quad (7.35)$$

where  $a$  is the attack rate with which the consumers catch free resource, and  $1/h$  is the time required to handle and kill the resource. By the QSSA  $dC/dt = 0$  we have to solve  $C$  from the quadratic equation

$$aC^2 - C(aR + aN + h) + aRN = C^2 - C(R + N + h') + RN = 0, \quad (7.36)$$

where  $h' = h/a$ , which for small  $C$  can be simplified into

$$C = \frac{RN}{h' + R + N}, \quad (7.37)$$

which indeed has a similar form as the consumption term in the Beddington model of Eq. (7.27).

This function has been used to describe various types of transient interactions between cells upon binding each other (De Boer & Perelson, 1995). One example is a paper successfully fitting Eq. (7.25) to experimental data on the rate at which neutrophils kill bacteria (Malika *et al.*, 2012). Finally, one can define a “continuum” between the Lotka-Volterra model and the Beddington model by writing

$$\frac{dR}{dt} = rR(1 - R/K) - \frac{aRN}{1 + R/k_R + N/k_N} \quad \text{and} \quad \frac{dN}{dt} = \frac{aRN}{1 + R/k_R + N/k_N} - dN, \quad (7.38)$$

which will have the mass-action interaction term of the Lotka-Volterra model when  $k_R \rightarrow \infty$  and  $k_N \rightarrow \infty$ . In one of the numerical exercises we will show that allowing for sufficiently

large values of  $k_R$  and  $k_N$  can dampen the oscillations of a model (see Page 151). Replacing a mass-action interaction term by this “double saturation” function, conveniently limits the rate of this interaction when one of the variables becomes large. When one of the variables is small the interaction term simplifies into a conventional saturation function, and when both variables are small, the interaction term simplifies into the original mass-action process,  $aRN$ .

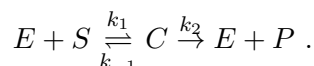
## 7.4 Summary

There are several generic saturation functions to model that “consumers” (e.g., predators, killer cells, or infectious hosts), cannot handle an infinite number of “resource” (e.g., prey, tumor cells, or susceptible hosts) per unit of time. The most well-known Holling type-II and III saturation functions correspond to the Hill functions explained in Chapter 15. Resource-consumer models based upon a saturated functional response tend to have a peaked resource nullcline, with stable and unstable parts (which was not possible in Lotka-Volterra like models). Because such saturation effects allow for a positive feedback within the resource population, by decreasing the *per capita* killing rate when resource densities increase, resource-consumer models with a saturated functional response can have a Hopf bifurcation where a stable limit cycle is born. Periodic behavior is therefore a very natural outcome in such models. In the steady states where the consumer is present, resource densities tend to be determined (largely) by the parameters of the consumer (which mimics results obtained with Lotka-Volterra like models). Because saturation functions can be derived mechanistically by quasi steady state assumptions, we know how to generalize them to high-dimensional situations with several resources and/or consumer species. An extension of the conventional Michaelis-Menten QSSA suggests a 2-dimensional functional response that depends on both resource and consumers. Models based upon this “Beddington” functional response have a slanted consumer nullcline, and either a peaked or a monotonically declining resource nullcline, and tend to have more dampened behavior.

## 7.5 Exercises

### Question 7.1. Michaelis-Menten

The famous Michaelis-Menten term is the result of a QSSA in enzymatic reactions. Since we have used similar QSSAs in the derivation of our functional responses, we here refresh our memory on the classic Michaelis-Menten derivation. Consider a chemical reaction for the formation of some product  $P$  from a substrate  $S$ , and let the enzyme  $E$  catalyzes the reaction, i.e.,



Because the enzyme is released when the complex dissociates, one writes a conservation equation,  $E + C = E_0$ .

- Write the differential equations for the product  $P$  and the complex  $C$ . Use the conservation equation!
- Assume that the formation of the complex is much faster than that of the product, i.e., make the QSSA  $dC/dt = 0$ .
- Write the new model for the product. Simplify by defining new parameters.
- Write an ODE for the substrate, and note that you can add  $dC/dt$  to simplify  $dS/dt$  because  $dC/dt = 0$ .
- Check that this resembles the derivation of Eqs. (7.11) and (7.12).

**Question 7.2. Parameters**

A simple resource consumer model based on a saturated functional response is:

$$\frac{dR}{dt} = a_1 R(1 - R/K) - b_1 N \frac{R}{c_1 + R}$$

$$\frac{dN}{dt} = -a_2 N + b_2 N \frac{R}{c_2 + R}$$

- Give a biological interpretation and the dimension of all parameters.
- Is it biologically reasonable to choose  $b_1 < b_2$ ?
- Give an interpretation for the following parameter choices  $c_1 = c_2$ ,  $c_1 > c_2$  and  $c_1 < c_2$ .

**Question 7.3. Type I functional response**

A consumer-resource model based upon Holling's type I functional response can be written as

$$\frac{dR}{dt} = rR(1 - R/K) - aN \min(R, L) \quad \text{with} \quad \frac{dN}{dt} = caN \min(R, L) - dN ,$$

where  $L$  (for limit) is the maximum amount of resource the consumer can handle per day. To sketch the nullclines of a model with a discontinuous function one basically makes two phase planes, one in which  $R < L$  and one in  $R > L$ . After that the phase planes are merged, taking the  $R < L$  picture at low  $R$  values, and the  $R > L$  diagram for large values of  $R$ . The intersection point of the two pictures in the merged phase plane defines the value of  $L$ .

- Analyze the model using phase plane analysis (i.e., sketch nullclines and vector field).
- Determine the stability of the steady states.
- Can the consumer nullcline be located at a resource density exceeding  $L$ ?
- Can the non-trivial steady state be unstable?

**Question 7.4. Luckinbill**

Fig. 7.10 depicts the data of Luckinbill (1973). The horizontal axis gives the time in either hours (Panel A) or days (Panels B & C). The vertical axis is population density in numbers per ml. The solid line depicts the resource *Paramecium* and the dotted line the consumer *Didinium*. Panel A: *Paramecium* and *Didinium* in normal medium. Panel B: *Paramecium* and *Didinium* in a medium with methyl-cellulose, which increases the viscosity of the medium. At day 17 *Didinium* dies out. Panel C: as Panel B after halving the concentration of food for the resource *Paramecium*. In Panels B and C the fat line at the top gives the density of *Paramecium* in the same medium in the absence of the consumer.

- Write a simple consumer resource model to explain these data.
- Identify the differences between the experiments with differences in parameter values of the model.
- Draw for each of the three situations the nullclines of the model, and a trajectory corresponding to the data.
- Does your model provide a good interpretation of the data?
- What are the most important differences between the model and the data?

**Question 7.5. Wolves**

Wolves hunt in packs and help each other catch resource (this is also true for several other consumer species, e.g., spoonbills).

- Devise a model for this situation using a functional response with  $\partial_N f(R, N) > 0$ .
- Study the model by phase plane analysis (depending on the functional response you have devised, you may require Grind).

**Question 7.6. Saturation in consumers**

Sometimes there is a maximum rate at which resource can be killed by the consumers. An

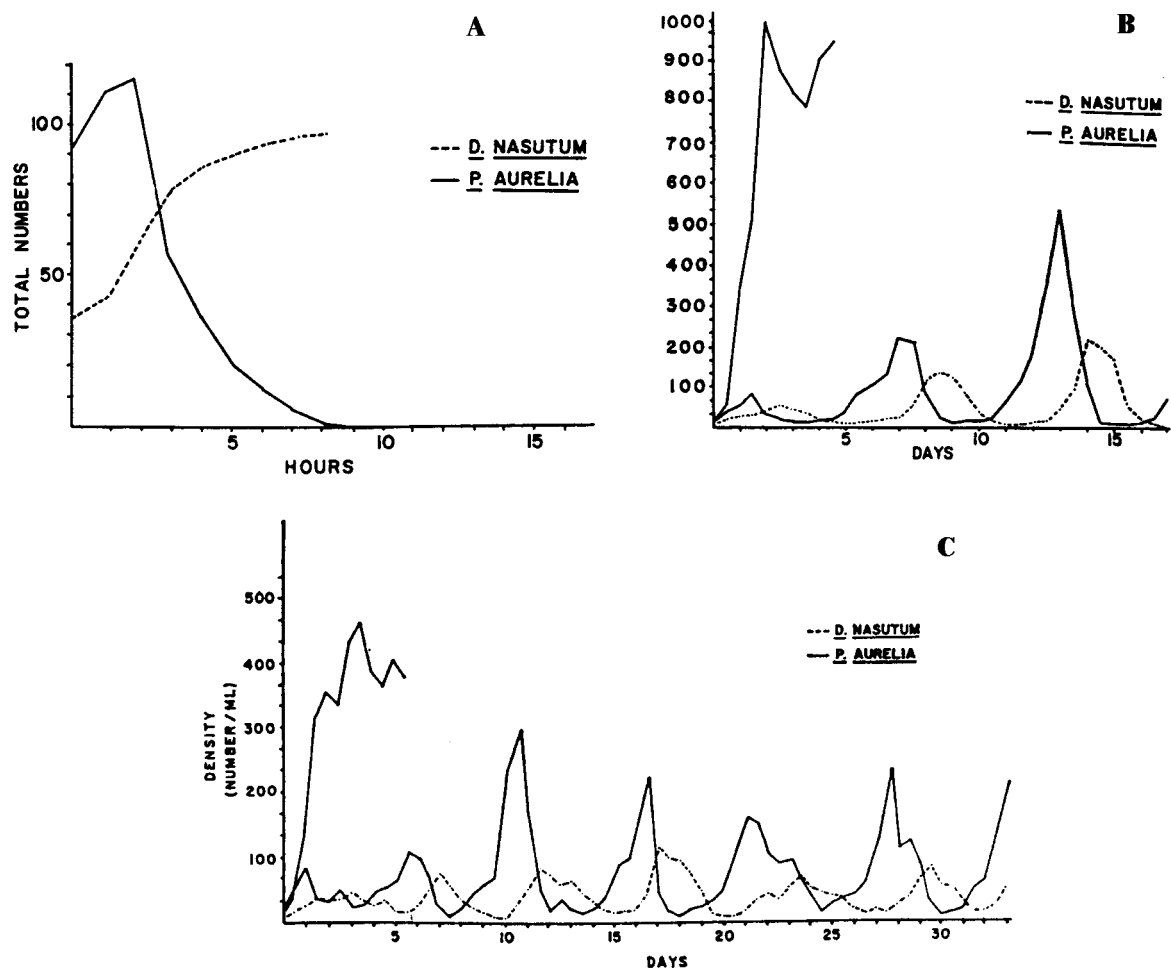


Figure 7.10: The data from Luckinbill (1973). The horizontal axis gives the time in either hours or days, and the vertical axis the population density in numbers per ml. The solid line is the resource *Paramecium* and the dotted line the consumer *Didinium*. Panel A: *Paramecium* and *Didinium* in normal medium. Panel B: *Paramecium* and *Didinium* in a medium with methyl-cellulose, which increases the viscosity of the medium, which decreases the food intake of *Didinium*. Panel C: as Panel B but with half the amount of food for *Paramecium*. In Panels B and C the fat line at the top represents the population density of *Paramecium* in the absence of the consumer.

example is susceptible hosts that are infected by infected individuals (see Chapter 6). One would then write something like

$$\frac{dR}{dt} = rR(1 - R/K) - aRf(N), \quad \frac{dN}{dt} = caRf(N) - dN \quad \text{where} \quad f(N) = \frac{N}{h + N}, \quad (7.39)$$

and where  $a$  is the maximum death rate of the resource  $R$  when there is an infinite consumer population.

- Analyze the model using phase plane analysis (i.e., sketch nullclines and vector field). Indicate intersection points of the nullclines with the axes. Be careful: there are two different possibilities.
- Determine the stability of the steady states.

### Question 7.7. Eutrophication

Consider an algae-zooplankton system based upon a sigmoid functional response (see Fig. 7.5). Since a perfectly vertical zooplankton nullcline need not be realistic (Arditi & Ginzburg, 1989;

Ginzburg & Akçakaya, 1992), we allow for some direct competition between zooplankton at high densities, and evaluate the model by studying the effect of eutrophication.

- Make a model of the system described above, and sketch the nullclines (by hand).
- What parameter best defines the nutrient availability in such an ecosystem, and how would you study the effect of eutrophication?
- What are the possible effects of eutrophication, given either a strong or a weak intra-specific competition for the zooplankton? Draw the qualitatively different nullcline situations.
- What do you learn from this about the usage of models to predict environmental effects?

## Extra questions

### Question 7.8. Ratio-dependent predation (Grind)

Arditi & Ginzburg (1989) and Ginzburg & Akçakaya (1992) criticized the consumer-resource models discussed in this chapter (see also their book (Arditi & Ginzburg, 2012) with an excellent review of many relevant data sets). One criticism is that these models “predict” that feeding the resource (i.e., increasing the carrying capacity) fails to increase the resource density at steady state. Another criticism is that when these models are used to describe algae-zooplankton systems, the models tend to oscillate with a too wide amplitude (Arditi & Ginzburg, 1989; Ginzburg & Akçakaya, 1992; McCauley *et al.*, 1999; Murdoch *et al.*, 2002; Scheffer & De Boer, 1995). Finally, they argue that a consumer will never interact with all individuals in the resource population, as it will typically only find resources present in its own neighborhood (e.g., territory). They proposed a modification of consumer-resource models by making the consumption dependent of the amount of resource per consumer,  $R/N$ , and called this “ratio-dependent predation”. When a consumer can only interact with the  $\hat{R} = R/N$  resources in its own environment, and we use a conventional functional response, one would write

$$f(\hat{R}) = \frac{a\hat{R}}{h + \hat{R}} \quad \text{or} \quad f(R, N) = \frac{aR/N}{h + R/N} = \frac{aR}{hN + R},$$

which then defines the ratio-dependent consumer resource model

$$\begin{aligned} \frac{dR}{dt} &= rR(1 - R/K) - \frac{aRN}{hN + R} \\ \frac{dN}{dt} &= \frac{caRN}{hN + R} - dN. \end{aligned}$$

To study the dimensions of the parameters one can test the functional response for a large resource population:

$$\lim_{R \rightarrow \infty} \frac{aR}{hN + R} = \lim_{R \rightarrow \infty} \frac{a}{hN/R + 1} = a,$$

which demonstrates that the parameter  $a$  has the simple interpretation of the maximum amount of resource consumed per consumer. One can therefore also define the fitness as  $R_0 = ca/d$ . This model is available on the website as the file `ratio.R`.

- Study the nullclines and trajectories. Hint: like in the Beddington model, there are two qualitatively different regimes.
- Can one destabilize the non-trivial steady state by eutrophication?
- What would be your major criticism on this model?

### Question 7.9. Nullcline construction

The resource nullcline of the sigmoid and the Beddington consumer-resource model was sketched using a graphical construction method based upon plotting the consumption curves and the

population growth curve as a function of the resource density. To develop some experience now use the same method to now sketch the mathematically fairly complicated resource nullcline depicted in Fig. 5.2a, which was based on the rather simple ODE  $dR/dt = s - wR - \frac{aRN}{h+R}$ , where  $R$  is the resource and  $N$  the consumer.

**Question 7.10. Exponential function response (Grind)**

Consumer-resource models with a saturated functional response are not always written with a Hill function. An equally simple saturation function is an exponential function that is scaled to be half-maximal at  $R = h$ , yielding a model like

$$\frac{dR}{dt} = rR(1 - R/K) - aN(1 - e^{-\ln[2]R/h}) \quad \text{with} \quad \frac{dN}{dt} = caN(1 - e^{-\ln[2]R/h}) - dN .$$

Indeed, solving  $1/2 = e^{-\ln[2]x/h}$  yields  $x = h$ .

- a. What is the meaning of the parameter  $a$ ?
- b. Check with Grind whether using an exponential functional response rather than a Monod function has a large impact on the phase space of this model (use the file `exp.R`).



## Chapter 8

# Modeling chains

The models considered hitherto were composed of maximally two ODEs, for a resource and its consumer, respectively. Here we begin by considering higher dimensional models by adding an ODE for the population controlling the “consumers”. This is the classic situation in ecological food webs that typically contain several “trophic” layers, where the consumers eating the first resource layer (e.g., algae,  $R$ ) are the resource of another consumer (e.g., zooplankton,  $N$ ), that may in turn be predated by a “top-predator” (e.g., fish,  $M$ ). It is typically not clear how many trophic levels one should implement in such a model, e.g., we could also start with nutrients as the first layer, and/or add predatory fish eating the former top-predator. Similar chain models appear when modeling viral infections in a host, because the intermediate population of infected cells,  $N$ , is responsible for removing susceptible target cells,  $R$ , by novel infections, and may also invoke an immune response,  $M$ , removing the infected cells. It is well known that the steady states of such chains strongly depend on the length of the chain (Arditi & Ginzburg, 1989; Abrams, 1994; Kaunzinger & Morin, 1998; De Boer, 2012), which is an worrisome result because we often make quite arbitrary choices on the number of levels to include in our models.

For instance, the immune response,  $M$ , could trigger a response of regulatory T cells. Or a lake with predatory fish controlling fish, that are controlling zooplankton, that are controlling algae, that are consuming nutrients, may (sometimes) be visited by birds catching the predatory fish. Unfortunately, adding another layer of control will radically change the properties of the state state. In most models, food chains with an even or odd number of layers have very different steady state properties (Arditi & Ginzburg, 1989; Abrams, 1994), and although this may seem strange, there is experimental data from 2-dimensional and 3-dimensional bacterial food chains confirming these “strange” predictions from the models (Kaunzinger & Morin, 1998). In this chapter we will first confirm this worrisome result, and then show it is at least partly a consequence of the mass action interaction terms of the models we typically write. Vitaly Ganusov (2016) argues that when modeling some biological phenomenon one should always develop multiple alternative models for the underlying processes to test whether or not results depend on the choices are being made. In this chapter confirm this, and learn that one should not only vary the underlying biological assumptions, but also the form of the mathematical terms.

## 8.1 A 3-dimensional Lotka-Volterra chain

Let us first consider models with mass-action interaction terms, i.e., Lotka-Volterra like models. Extending the Lotka-Volterra model with an additional layer,  $M$ , is straightforward, e.g.,

$$\frac{dR}{dt} = [r(1 - R/K) - bN]R, \quad \frac{dN}{dt} = [bR - d - cM]N \quad \text{and} \quad \frac{dM}{dt} = [cN - e]M, \quad (8.1a,b,c)$$

where  $M$  could be fish eating zooplankton,  $N$ , or an immune response of cells killing infected cells,  $N$ . This simple model has several steady states, and we will study what happens when the carrying capacity,  $K$ , of the resource,  $R$  (i.e., algae or target cells), is increased. In the ecological interpretation the carrying capacity reflects the amount of nutrients available for the algae in the ecosystem, and in the virological interpretation  $K$  is the number of target cells present in uninfected individuals, e.g., the size of the liver when we are considering a hepatitis virus. Assume for a moment that one can increase the size of the liver (e.g., by drinking too much alcohol). In the absence of the second population, the third one cannot be maintained, and when  $N = M = 0$ , one obtains the obvious  $\bar{R} = K$  from Eq. (8.1a), i.e., a resource at carrying capacity. Thus, increasing  $K$  likewise increases  $\bar{R}$  (see Fig. 8.1a). We have seen in the previous chapter that, in the absence of  $M$ , the consumer can only invade and be maintained when its  $R_0 > 1$ , which here means that  $bK/d > 1$ . Thus, at low values of the carrying capacity there is not enough resource,  $\bar{R} = K$ , in the system to maintain the consumer (i.e., as long as  $K < d/b$ ). If, after increasing  $K$ , the consumer has successfully invaded, the new steady state (still without  $M$ ) is

$$\bar{R} = \frac{d}{b} \quad \text{and} \quad \bar{N} = \frac{r}{b} \left(1 - \frac{d}{bK}\right) = \frac{r}{b} \left(1 - \frac{1}{R_0}\right). \quad (8.2a,b)$$

Note that the previous state  $(\bar{R}, \bar{N}, \bar{M}) = (K, 0, 0)$  still exists, but has become unstable because  $dN/dt > 0$  in the neighborhood of that state (see Fig. 8.1a). The nature of the steady state of the resource has changed radically because it is now completely determined, or “controlled”, by the parameters of the second population,  $b$  and  $d$ .

Similarly, the third population,  $M$ , can only invade when its  $R'_0 = c\bar{N}/e > 1$ . Because  $\bar{N}$  increases as a function of  $K$  (see Eq. (8.2b)), and would approach a maximum  $\bar{N} = r/b$  when  $K \rightarrow \infty$ , the fitness of the third population can be defined as  $R'_0 = \frac{cr}{be}$ . We see that the third population can only invade and be maintained when the carrying capacity,  $K$ , is sufficiently large, and  $cr > be$ . Considering the case when  $M$  is present we solve the steady state of the resource and consumer,

$$\bar{N} = \frac{e}{c}, \quad \bar{R} = K \left(1 - \frac{be}{cr}\right) \quad \text{and} \quad \bar{M} = \frac{b\bar{R} - d}{c}, \quad (8.3)$$

where we re-observe the parameter condition  $R'_0 = \frac{cr}{be} > 1$ . Since  $\bar{N}$  is solved from Eq. (8.1c),  $\bar{R}$  had to be solved from Eq. (8.1a), and the steady state  $\bar{M}$  had to be computed from Eq. (8.1b). The steady state of the resource is now again determined by its own parameters  $r, b$  and  $K$ , in combination with the two parameters of the third population,  $c$  and  $e$ .

If we were to add a fourth population,  $F$ , controlling the  $M$  population, e.g., predatory fish or regulatory T cells, one would write

$$\frac{dM}{dt} = [cN - e - fF]M \quad \text{and} \quad \frac{dF}{dt} = (fM - g)F, \quad (8.4a,b)$$

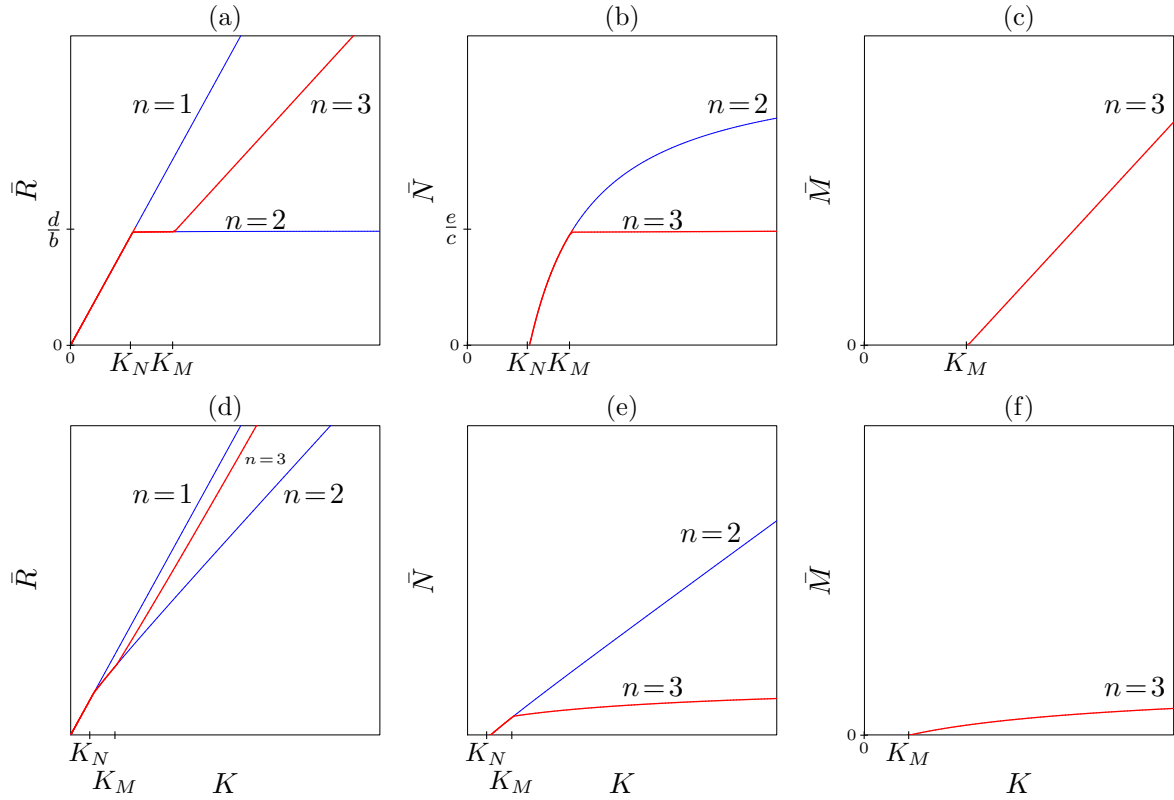


Figure 8.1: Bifurcation diagrams of the Lotka-Volterra food-chain of Eq. (8.1) in Panels (a-c), and of a similar food-chain based upon the Beddington functions of Eq. (8.7) in Panels (d-f). The second population,  $N$ , can invade at the transcritical bifurcation point where  $K = K_N$ , and the third population,  $M$ , can invade at the transcritical bifurcation point where  $K = K_M$ . The  $n = 1, 2$  and  $3$  texts denote the length of the chain, i.e., the dimension of the system. Note that no Hopf bifurcations are found in the bifurcation diagrams of Panels (d-f) because they were made for a “predation limited” parameter setting of Eq. (8.7). This figure was made with the model `chain.R`.

and one would have solve  $\bar{M} = g/f$  from Eq. (8.4b),  $\bar{R} = \frac{d+c\bar{M}}{b}$  from Eq. (8.1b),  $\bar{N}$  from Eq. (8.1a), and finally  $\bar{F} = \frac{c\bar{N}-e}{f}$  from Eq. (8.4a). Summarizing, we observe that the biological parameters determining the steady state of each population in this chain of populations controlling each other, depends on the length of the chain,  $n$ . When  $n = 1$  the steady state resource density,  $\bar{R} = K$ , when  $n = 2$  or  $n = 4$ ,  $\bar{R}$  is independent of  $K$ , and when  $n = 3$ ,  $\bar{R}$  is proportional to  $K$ . Which biological parameters determine the steady state of  $R$  therefore depends on the parity of  $n$ : for even length chains  $\bar{R}$  is determined by the parameters of its controller,  $N$ , and for odd length chains  $\bar{R}$  depends at least partly on its own parameters. Since it is typically unclear how many (trophic) layers one should incorporate in a model, this is a rather disturbing result pinpointing a lack of robustness of steady state expressions of these “chain of control” models (De Boer, 2012). In the exercises you will derive very similar results for a chain in which the resource is a non-replicating population, i.e.,  $dR/dt = s - rR - dRN$ , and the other populations remain the same.

## 8.2 Chains with saturating interacting terms

The results derived in the previous section have to do with the fact that most populations in these models are replicators, which means that their ODEs can be written as  $dx_i/dt = f_i(\mathbf{x})x_i$ ,

where  $\mathbf{x}$  is a vector representing the  $n$ -dimensional state of the system. Solving the non-trivial steady state therefore typically involves cancelling the  $x_i = 0$  solution from its own equation, and subsequently solving  $f_i(\mathbf{x}) = 0$ . Since the  $f_i(\mathbf{x})$  terms in Eq. (8.1) correspond to the terms within the square brackets, i.e.,

$$f_R(R, N) = r(1 - R/K) - bN, \quad f_N(R, M) = bR - d - cM \quad \text{and} \quad f_M(N) = cN - e, \quad (8.5)$$

we observe that only  $f_R$  depends on itself, i.e., on  $R$ . Because  $f_N$  and  $f_M$  are independent of  $N$  and  $M$ , respectively, their steady states are necessarily solved from another equation. For instance, for a 3-dimensional chain one solves  $\bar{N}$  from  $f_M = 0$ , then  $\bar{R}$  from  $f_R = 0$ , and finally  $\bar{M}$  from  $f_N = 0$ .

The fact that the steady state expression of  $x_i$  is independent of  $x_i$  is a consequence of the simplicity of the interaction terms, which are all mass action terms here. For instance, if we replace all mass action terms with conventional saturation terms, i.e.,

$$\begin{aligned} \frac{dR}{dt} &= \left[ r \left( 1 - \frac{R}{K} \right) - \frac{bN}{h_R + R} \right] R, & \frac{dN}{dt} &= \left[ \frac{bR}{h_R + R} - d - \frac{cM}{h_N + N} \right] N, \\ \text{and} \quad \frac{dM}{dt} &= \left[ \frac{cN}{h_N + N} - e \right] M, \end{aligned} \quad (8.6a,b,c)$$

we observe that  $f_N$  becomes dependent on  $N$  when  $M$  is present, but that  $f_M$  remains independent of  $M$ . All steady state expressions remain dependent on their own variable when we choose for a Beddington functional response, e.g.,

$$\begin{aligned} \frac{dR}{dt} &= \left[ r \left( 1 - \frac{R}{K} \right) - \frac{bN}{h_R + R + N} \right] R, & \frac{dN}{dt} &= \left[ \frac{bR}{h_R + R + N} - d - \frac{cM}{h_N + N + M} \right] N, \\ \text{and} \quad \frac{dM}{dt} &= \left[ \frac{cN}{h_N + N + M} - e \right] M \end{aligned} \quad (8.7a,b,c)$$

but unfortunately the steady state expressions of this model become so complicated that they are no longer insightful. Thus, the disturbing results derived in the previous section depend on the form of the interaction terms. One would therefore have to establish the functional form of these interactions before one knows whether or not these results are an artifact of our simplification, or a realistic feature of truly simple interaction terms.

Because solving the steady state of Eq. (8.7) is laborious, one can resort to studying the difference between these models numerically by bifurcation analysis. Fig. 8.1a-c depicts the steady states derived above for Eq. (8.1) that is based upon mass action interaction terms. The steady state of  $R$  is independent of the carrying capacity,  $K$ , when the chain is 2-dimensional, and increases with  $K$  when it is 1 or 3-dimensional.  $N$  and  $M$  can invade at transcritical bifurcations located at  $K = K_N$  and  $K = K_M$ , respectively. The steady state of  $N$  first increases as a function of  $K$ , but is independent of it when  $M$  is present (see Fig. 8.1a-c). For large values of the saturation constants,  $h_R$  and  $h_N$ , bifurcation diagrams of Eq. (8.7) will look very similar to Fig. 8.1a-c because the Beddington interaction terms approach a mass action term whenever  $h_R \gg R + N$  and  $h_N \gg N + M$ . (One can write the functions in Eq. (8.7) as  $\frac{b'N}{1+R/h_R+N/h_R}$  with  $b' = b/h_R$  to see that one can make  $h_R$  arbitrary large, and adjust  $b'$  to arrive at the same mass action term). The bifurcation diagrams in Fig. 8.1d-f reveal that all steady states increase with  $K$ , whatever the dimension,  $n$ , of the chain for reasonably small values of the saturation constants, i.e.,  $h_R \simeq h_M < K$ .

We conclude that the classic observation that steady states of ‘‘control’’ chains depend on a small subsets of the parameters only, and that this depends on the length of the chain (Arditi

& Ginzburg, 1989; Abrams, 1994; Kaunzinger & Morin, 1998; De Boer, 2012), is a consequence of the simple interaction terms of these chains. For more complicated interaction terms, like the Beddington functional response, it will depend on the parameters how strongly the nature of the steady state values changes when new populations are added to the chain. For instance, in Fig. 8.1d the dependence of  $\bar{R}$  of  $K$  hardly changes when  $N$  invades, but that of  $\bar{N}$  strongly depends on the presence of the third population,  $M$ . Finally, note that we have here chosen the carrying capacity,  $K$ , as a bifurcation parameter, basically to repeat the famous Paradox of enrichment result of Rosenzweig (1971), and that very similar results would have been obtained if other bifurcation parameters were chosen (you can test this by modifying the `chain.R` code).

### 8.3 Other famous chain models

The chain models discussed above have a form where a subsequent population “controls” the previous one, i.e., they have interaction terms between all populations of adjacent levels, like in an ecosystem where the next trophic level feeds upon the previous one. Fortunately, not all chains in biology are of this form, and hence need not suffer from the strong dependence on the chain length. For instance, the famous 4-dimensional chain of susceptible, exposed, infected and recovered (SEIR) model in epidemiology (see Chapter 6),

$$\frac{dS}{dt} = s - dS - \beta SI, \quad \frac{dE}{dt} = \beta SI - (d + \gamma)E, \quad \frac{dI}{dt} = \gamma E - (\delta + r)I \quad \text{and} \quad \frac{dR}{dt} = rI - dR,$$

has only one interaction term between the levels, i.e., the  $\beta SI$  term. The “resource” is here defined as susceptible hosts,  $S$ , that are infected at rate  $\beta$  by infected hosts,  $I$ , which first become exposed un-infectious hosts,  $E$ , then infectious hosts,  $I$ , that suffer from an additional death rate due to the virulence,  $\delta \geq d$ , and may recover into immune hosts,  $R$ . In the absence of infections  $\bar{S} = s/d$ . For an epidemic at steady state, we work from right to left to see that

$$\bar{R} = \frac{r}{d} \bar{I}, \quad \bar{I} = \frac{\gamma}{\delta + r} \bar{E}, \quad \bar{S} = \frac{(d + \gamma)(\delta + r)}{\gamma\beta}, \quad (8.8)$$

and hence that  $\bar{E} = \frac{s}{d + \gamma} - \frac{d(\delta + r)}{\gamma\beta}$  has to be solved from the first equation. This reveals that  $\bar{R}$  and  $\bar{I}$  are simply proportional to their previous level, and will always be present when  $\bar{E} > 0$ . The condition  $\bar{E} > 0$  defines the one and only transcritical bifurcation in this 4-dimensional chain, corresponding to the parameter condition where the infection can get established (i.e.,  $R_0 = \frac{s\gamma\beta}{d(d + \gamma)(\delta + r)} > 1$ ; see Fig. 8.2b and Chapter 6).

Another common chain to consider is the expansion of a population by a cascade of cell divisions,

$$\frac{dN_0}{dt} = s - (p + d)N_0, \quad \frac{dN_i}{dt} = 2pN_{i-1} - (p + d)N_i \quad \text{and} \quad \frac{dN_n}{dt} = 2pN_{n-1} - dN_n, \quad (8.9)$$

where  $s$  cells per day are entering a division cascade of  $n$  divisions, and the index  $i$  denotes the number of completed divisions. Here the cells stop after  $n$  cell-divisions, and this chain has no interaction terms between its levels. The proliferation rate,  $p$ , and the death rate,  $d$ , are independent of the number of divisions completed. These populations are not controlling each other, and the steady state can be derived by working from left to right, i.e.,

$$\bar{N}_0 = \frac{s}{p + d}, \quad \bar{N}_i = \frac{2p}{p + d} \bar{N}_{i-1} \quad \text{and} \quad \bar{N}_n = \frac{2p}{d} \bar{N}_{n-1}, \quad (8.10)$$

revealing that each level remains proportional to the previous one. Since the steady state of each sub-population,  $\bar{N}_i$ , is always positive there should always be a steady state. Furthermore, in

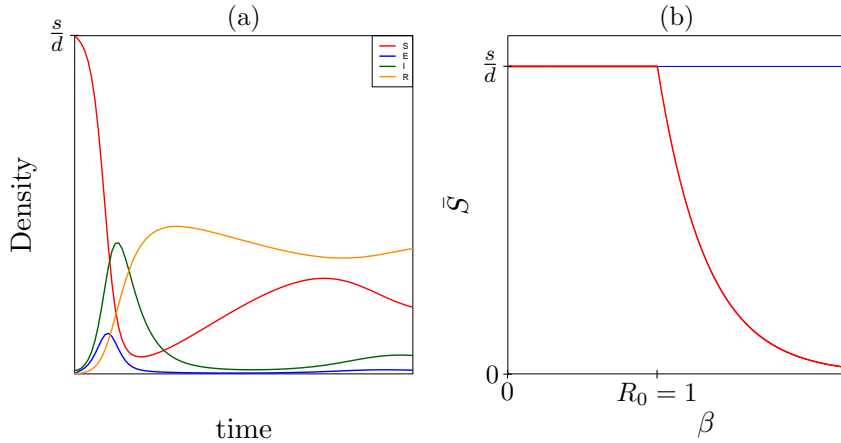


Figure 8.2: The behavior of the SEIR model. Panel (a) depicts the establishment of an epidemic in a population starting at the uninfected steady state. Panel (b) shows that the infection in Eq. (8.8) can invade at the transcritical bifurcation point where  $R_0 = 1$ . This figure was made with the R script `seir.R`.

the exercises you will see that the Jacobi matrix,  $J$ , of this system has a lower triangular form, i.e., all elements above the diagonal are zero. Since the eigenvalues of such matrices are solved from the characteristic equation, which here corresponds to a simplified determinant thanks to the fact that all off-diagonal elements are zero, i.e.,

$$(J_{00} - \lambda)(J_{11} - \lambda)(J_{22} - \lambda) \dots (J_{nn} - \lambda) = 0, \tag{8.11}$$

you will discover that this steady state is always stable, i.e.,  $\lambda_{\max} < 0$ . Intuitively, this is a natural result because in this chain each sub-population remains proportional to the previous one (see Eq. (8.10)), and the first sub-population approaches a steady state reflecting a balance between a source,  $s$ , and its loss rate,  $(p + d)$ . Eq. (8.10) can indeed be simplified into

$$\bar{N}_0 = \frac{s}{p + d}, \quad \bar{N}_i = \frac{2^i p^i s}{(p + d)^{i+1}} \quad \text{and} \quad \bar{N}_n = \frac{s}{d} \left( \frac{2p}{p + d} \right)^n, \tag{8.12a,b,c}$$

for  $i = 1, 2, \dots, n-1$ . Thus, the only effect of adding a level to this chain is that  $\bar{N}_n$  becomes  $\frac{2p}{p+d}$ -fold larger. Note that if we were to remove the factor two from these equations, this cascade would correspond to a chain of maturation steps, and that this would confirm that cells or individuals in such a chain would approach a stable “age” distribution. Finally, to model the source more explicitly, one could consider a population of quiescent cells,  $Q$ , that occasionally are triggered to enter a cascade of cell divisions. Then one would replace the source parameter,  $s$ , by the number of quiescent cells entering the cascade, e.g.,  $s = aQ$ , where  $a$  is a (potentially stochastic) activation rate, and add an ODE for the resting cells,

$$\frac{dQ}{dt} = -aQ - d_Q Q + d \sum f_i N_i, \quad \text{for } i = 1, 2, \dots, n, \tag{8.13}$$

which allows a fraction,  $0 \leq f_i \leq 1$ , of the cells that are lost from the cascade to revert to quiescence. Do you think this model with quiescent cells will also approach a steady state? <sup>1</sup>

<sup>1</sup>This is actually quite a challenging question since the steady state of the quiescent cells involves those of the activated cells,

$$\bar{Q} = \frac{d \sum f_i \bar{N}_i}{a + d_Q}, \quad \bar{N}_0 = \frac{a \bar{Q}}{p + d} \quad \text{and} \quad \bar{N}_i = \frac{2p}{p + d} \bar{N}_{i-1}.$$

But since this is a self-renewing population, of cells dividing and some eventually returning to the quiescent stage, where they will be activated into another division cascade, the existence of a non-trivial steady state would require negative density dependence. Otherwise the population either dies out, or explodes (just like an exponentially growing population).

## 8.4 Summary

Biological models can often be written as chains where each level controls the previous layer. In chains of populations controlling one another the nature of the steady state can strongly depend on the length of the chain, but this depends on the type of interaction function used to model the control that the populations exert on one another. Other classic chains that do not involve multiple levels of control, have steady states that depend much less on the length of the chain, but increasing the chain length may increase the sensitivity of the steady state to particular parameters, which becomes a “feature rather than a bug” in the Kinetic proofreading model of the last exercise. We have only discussed linear chains in this chapter because networks of populations controlling one another involve competition between populations, which is the subject of the next chapter.

## 8.5 Exercises

### Question 8.1. Food chain

Consider a variant of Eq. (8.1) where the resource is not replicating:

$$\frac{dR}{dt} = s - rR - bNR, \quad \frac{dN}{dt} = [bR - d - cM]N \quad \text{and} \quad \frac{dM}{dt} = [cN - e]M .$$

- Find all steady states.
- How does the steady state of the resource depend on the amount of resource flowing into the system, i.e., on  $s$ ? Does this depend on the length of the chain?

### Question 8.2. Triangular Jacobian

Write the Jacobian of Eq. (8.9) to discover that the matrix has a triangular form (i.e., here all elements above the diagonal are zero). Keep the matrix simple by not substituting the steady state expressions for  $\bar{N}_i$ . Because the product of all off-diagonal elements are zero, the determinant of a matrix in triangular form is given by the product of its diagonal elements. Because the determinant is equal to the product of all eigenvalues, this implies that the eigenvalues are equal to the diagonal elements. This confirms that solving the eigenvalues corresponds to solving Eq. (8.11). Note that the trace of this matrix is the sum of its diagonal elements, and that the determinant is the product of the diagonal elements.

### Question 8.3. Accumulating mutations (Grind)

Tumors like acute myeloid leukemia (AML) typically appear relatively late in life, and a recent paper by Abelson *et al.* (2018) demonstrates that the onset of AML is typically preceded by the slow accumulation of somatic mutations in the hematopoietic progenitor cells undergoing clonal expansion throughout life (to maintain the various types of cells circulating in the blood). People not developing AML also accumulate mutations in their peripheral blood cells (albeit to a somewhat lower extent), and the basic idea is that mutations accumulate with every division these progenitor cells perform. Thus, leukemias are expected to arise after cells have completed a large number of divisions. Since not all cells having completed many divisions will have accumulated the mutations required for becoming leukemic, we will argue that these cells become senescent and die, and write the following model,

$$\frac{dN_0}{dt} = s - (p + d)N_0, \quad \frac{dN_i}{dt} = 2pN_{i-1} - (p + d)N_i, \quad \text{for } i = 1, 2, \dots, n,$$

$$\frac{dS}{dt} = (1 - f)2pN_n - d_S S \quad \text{and} \quad \frac{dL}{dt} = f2pN_n + rL(1 - L/K) ,$$

where  $s$  is a source of progenitors from a stem cell compartment,  $p$  is a division rate,  $d$  is a death rate,  $S$  are senescent cells appearing after cells have completed  $n$  divisions, and  $L$  are leukemic cells that replicate autonomously at a rate  $r$ , and ultimately approach a potentially large and life threatening carrying capacity,  $K$ . Setting  $f$  to a small value would mean that most cells having completed  $n$  divisions do not become leukemic, and rather become senescent and die. This model is provided as the file `leukemia.R`.

- Do you think this is a reasonable model?
- In the numerical model the division rate of the progenitor cells is set to  $p = 1/365 \text{ d}^{-1}$ , to define a scenario where these cells on average divide once per year. Setting  $n = 50$  (which would correspond to a Hayflick (1988) limit) and  $f$  to a small value, one would expect leukemias to develop late and rarely. Do you agree with this expectation?
- Carefully read the model defined in the `leukemia.R` document to understand the notation by which the division cascade is implemented. Do you see leukemias develop late and rarely when you run this model?
- What goes wrong and how would you repair that?
- Would using the Smith-Martin (1973) model explained in Chapter 13 provide a solution?

#### Question 8.4. Chaos (Grind)

A simple system of a resource species,  $R$ , eaten by a consumer,  $N$ , that is eaten by a top-consumer,  $M$ , can have a chaotic attractor (Hogeweg & Hesper, 1978; Hastings & Powell, 1991); see Chapter 12. Consider the following system with two Holling type-II functional responses

$$\frac{dR}{dt} = R(1 - R) - c_1 N f(R) ,$$

$$\frac{dN}{dt} = -a_N N + c_1 N f(R) - c_2 M g(N) ,$$

$$\frac{dM}{dt} = -a_M M + c_2 M g(N) ,$$

where

$$f(R) = \frac{R}{1 + b_1 R} \quad \text{and} \quad g(N) = \frac{N}{1 + b_2 N} .$$

Hastings & Powell (1991) studied this system for the parameters  $2 \leq b_1 \leq 6.2$ ,  $c_1 = 5$ ,  $c_2 = 0.1$ ,  $b_2 = 2$ ,  $a_N = 0.4$ , en  $a_M = 0.01$ . For biological reasons the time scale of the interaction between  $N$  and  $M$  was made slower than that between  $R$  and  $N$ , i.e.,  $a_N \gg a_M$ . This model is available as the file `chaos.R`.

- Sketch with pencil and paper the phase space of  $R$  and  $N$ . Do you expect oscillations for their parameters in the absence of the top-consumer  $M$ ?
- Compute the expression of the  $dM/dt = 0$  nullcline, and sketch that line in the phase space of **a**. Do you expect  $M$  to invade?
- Sketch the nullclines with Grind and see how they match those sketched with pencil and paper.
- Vary the parameter  $b_1$  to observe how the model behavior changes (see the file `chaos.R`).
- Do this with and without noise on one of the parameters.

#### Extra questions

**Question 8.5. Detritus**

In a closed ecosystem nutrients should cycle through the food chain and become available again when resource, consumers, and top-consumers die and decompose. One could write a conservation equation,  $K = F + R + N + M$ , where the total amount of nutrients in the system,  $K$ , is the sum of the free nutrients,  $F$ , and that contained in all organisms. Assume that the growth of the  $R$ -population is proportional to the availability of free resources, and extend Eq. (8.1) to study how in this system with recycling nutrients the steady states change when the total amount of nutrients,  $K$ , is increased.

**Question 8.6. Maintenance and reproduction**

Make the corresponding question in Chapter 14 and simplify your model into two ODEs by assuming that the time scales of the eggs is much faster than that of adult *Daphnias*. Analyze this QSSA model by phase plane analysis, i.e., sketch the nullclines, the vector field, and determine the stability of all steady states.

**Question 8.7. Kinetic proofreading**

Read Section 15.9 in the Appendix to learn about an interesting example for theoretical predictions on how cells can use a chain of phosphorylation steps to discriminate between low and high affinity ligands. This prediction was much later confirmed by data. Try to derive Eq. (15.35) from Eq. (15.34). Hint write an ODE for the total amount of complexes and make a quasi steady assumption.



## Chapter 9

# Competition

Competition for resources like space, light, nutrients, food, growth factors, and/or susceptible hosts is ubiquitous in biology, and will occur whenever several populations are dependent on shared resources. An important concept in resource competition is the principle of “competitive exclusion”, stating that populations that are maintained by consuming the same shared resource have to exclude each other at steady state. A famous data set confirming this is the competition between two species of *Paramecium* by Gause (1934). Competitive exclusion is actually the basis of Darwin’s “Survival of the fittest” concept. We will show that the consumer depleting the shared resource most, will typically be the one and only survivor (Tilman, 1980, 1982), and that this need not be the species with the highest carrying capacity (or even the highest fitness,  $R_0$ ). Because the resource is depleted to a minimal density this is sometimes called the pessimization principle (Mylius & Diekmann, 1995).

We will first confirm the competitive exclusion principle with a few simple models, and then turn to the more complicated situation of a “network” in which several consumers are sharing several resources. Mathematical models for populations competing for resources can be derived mechanistically from the resource consumer models developed in the previous chapters by making a quasi steady state assumption (QSSA) for the resource densities. Removing the resource changes the indirect interaction between the consumers into a direct one, which hence provides a functional form for the resource competition process.

### 9.1 Competitive exclusion

To illustrate the concept in its most basic form, first consider a closed compartment with a fixed amount of resource,  $R$ , that is taken up by  $n$  consumer populations  $N_i$  (for  $i = 1, 2, \dots, n$ ), and is released when the organisms die. For  $n = 2$  this could reflect the two *Paramecium* species in the medium of Gause (1934) competing for a nutrient. Since the total amount of nutrient cannot change in this closed compartment, we write a conservation equation  $K = R + \sum_i^n e_i N_i$ , where  $K$  is the total amount of nutrient in the compartment,  $R$  represents the amount of free nutrient, and the  $e_i$  parameters specify the amount of nutrient contained in a single individual of consumer  $N_i$ . A first model, based upon mass-action terms would be

$$R = K - \sum_i^n e_i N_i, \quad \frac{dN_i}{dt} = N_i(b_i R - d_i), \quad \text{for } i = 1, 2, \dots, n, \quad (9.1)$$

where we would define  $R_{0_i} = b_i K / d_i$  for the fitness of each consumer. Since the steady state of each  $dN_i/dt = 0$  requires that  $\bar{R} = d_i/b_i = K/R_{0_i}$ , each consumer generically requires a unique nutrient availability, and hence they cannot co-exist. This proves the principle of competitive exclusion. (Note that the resource level at steady state does not depend to amount of resource,  $e_i$ , taken up by consumers). To study which consumer is expected to outcompete all others, let us order the consumers by their  $R_{0_i}$ , with  $N_1$  being the fittest consumer, and  $N_n$  having the lowest  $R_0$ . If the first species is present at its steady state (its carrying capacity), the nutrient density will be  $\bar{R} = d_1/b_1$ . Other species will not be able to invade into this state, because to invade their *per capita* growth rate should be larger than zero, i.e.,

$$b_i \bar{R} - d_i > 0 \quad \text{or} \quad b_i \frac{d_1}{b_1} - d_i > 0 \quad \text{or} \quad \frac{b_i}{d_i} \frac{d_1}{b_1} > 1 \quad \text{or} \quad \frac{b_i}{d_i} > \frac{b_1}{d_1}, \quad (9.2)$$

which is not true because of our ordering, i.e., by  $R_{0_1} > R_{0_i}$  we know that  $\frac{b_1}{d_1} > \frac{b_i}{d_i}$ . We conclude that the species with the highest fitness,  $R_{0_1} = b_1 K / d_1$ , outcompetes all others, and that this species depletes the resource to the lowest level  $\bar{R} = d_1/b_1 = K/R_{0_1}$  (the latter was also obtained in the earlier chapters). Finally, we compute the carrying capacity of the winning species from the conservation equation  $R = K - \sum_i^n e_i N_i$ , i.e., in the absence of the other species we obtain

$$\bar{R} = \frac{d_1}{b_1} = K - e_1 N_1 \quad \leftrightarrow \quad \bar{N}_1 = \frac{K - d_1/b_1}{e_1} = \frac{K(1 - 1/R_{0_1})}{e_1}, \quad (9.3)$$

which for large  $R_0$  would approach the quite natural  $\bar{N}_1 = K/e_1$  (i.e., total amount of resource divided by the content per individual). Because this carrying capacity depends on an additional parameter,  $e_1$ , which plays no role in the fitness or in steady state depletion of the resource, the species with the highest carrying capacity need not be the best competitor.

Considering the two species of *Paramecium* in the medium of Gause (1934) one can obtain the same result by examining the nullclines of Eq. (9.1) for  $n = 2$ . These form two parallel lines

$$N_2 = \frac{K - d_1/b_1}{e_2} - \frac{e_1}{e_2} N_1 = \frac{K(1 - 1/R_{0_1})}{e_2} - \frac{e_1}{e_2} N_1 \quad \text{and} \quad N_2 = \frac{K(1 - 1/R_{0_2})}{e_2} - \frac{e_1}{e_2} N_1, \quad (9.4)$$

for the first and second population, respectively, which have the same slope  $-\frac{e_1}{e_2} N_1$  when  $N_2$  is plotted on the vertical axis (see Fig. 9.1b). Since the species with the largest fitness,  $R_{0_i}$ , corresponds to the upper nullcline, we reconfirm that this species will outcompete the other from any initial condition (see Fig. 9.1b). Again, because the carrying capacity,  $\bar{N}_i$ , is inversely related to the nutrient content parameters,  $e_i$ , and the fitness,  $R_{0_i} = b_i K / d_i$ , is independent of the nutrient content parameter, the species winning the competition need not be the one with the high carrying capacity, i.e., one can parametrize the system such that  $R_{0_1} > R_{0_2}$  while  $K_1 < K_2$ , by choosing  $e_1 > e_2$ .

Importantly, the competitive exclusion result does not change when we make the birth rate a saturation function of the free resource density, i.e.,

$$R = K - \sum_i^n e_i N_i, \quad \frac{dN_i}{dt} = N_i \left( \frac{b_i R}{h_i + R} - d_i \right), \quad \text{for } i = 1, 2, \dots, n, \quad (9.5)$$

where we could define  $R_{0_i} = b_i/d_i$  for the fitness of each consumer. Solving the latter gives the now familiar  $\bar{R} = \frac{h_i}{R_{0_i} - 1}$ . Because these fitness values are only defined at infinite resource densities, one can now have a situation where the species with the largest fitness is outcompeted by the other species. The result that the species depleting the resource most, will outcompete the other ones remains valid, however. In this saturation model, the species with the lowest ratio

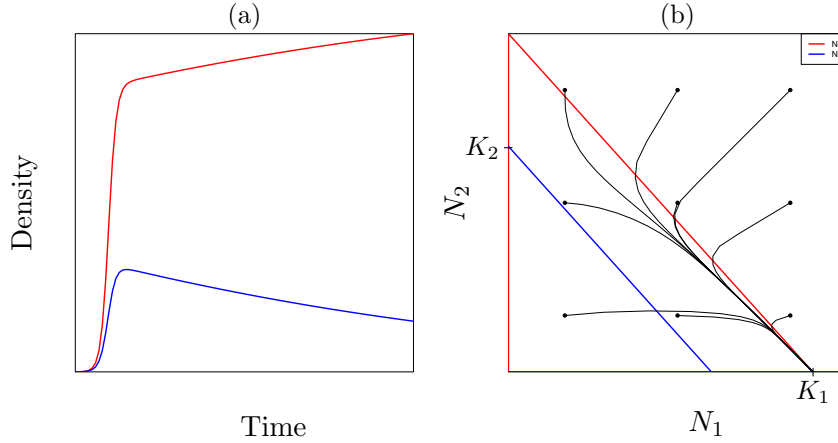


Figure 9.1: Competitive exclusion in the model of Eq. (9.1). Panel a depicts a time plot starting at low numbers, showing that both populations expand until the first species approaches densities at which it starts outcompeting the second species. Panel b depicts a phase plane with trajectories approaching the carrying capacity of the first species. This figure was made with the R-script `comp.R`.

of the saturation constant,  $h_i$ , over the “critical fitness”,  $R_{0_i} - 1$ , will deplete the resource to the lowest level. Thus, let us now order the species by their steady state resource level,  $\bar{R}_i = \frac{h_i}{R_{0_i} - 1}$ , with  $N_1$  having the lowest level  $\bar{R}_1$ . Because the minimum amount of resource required for the other species to invade is solved from

$$\frac{b_j \bar{R}_1}{h_j + \bar{R}_1} > d_j \quad \Leftrightarrow \quad \frac{R_{0_j} \bar{R}_1}{h_j + \bar{R}_1} > 1 \quad \Leftrightarrow \quad R_{0_j} \bar{R}_1 > h_j + \bar{R}_1 \quad \Leftrightarrow \quad \bar{R}_1 (R_{0_j} - 1) > h_j, \quad (9.6)$$

we obtain that

$$\bar{R}_1 = \frac{h_1}{R_{0_1} - 1} > \frac{h_j}{R_{0_j} - 1}, \quad (9.7)$$

which contradicts our ordering. Hence, we confirm that the species depleting the resource most, outcompetes the others. Species with a low saturation constant and a high  $R_0$  are therefore at an advantage. If one were to derive the nullclines for a 2-dimensional version of this system, one would again find that these are two parallel lines with slope  $-\frac{e_1}{e_2} N_1$  when  $N_2$  is plotted on the vertical axis (not shown). Finally, the carrying capacity of the winning population, i.e., the steady state of Eq. (9.5) with just one species, is solved from

$$R = \frac{h_1}{R_{0_1} - 1} = K - e_1 N_1 \quad \Leftrightarrow \quad \bar{N}_1 = \frac{K}{e_1} - \frac{h_1}{e_1 (R_{0_1} - 1)}, \quad (9.8)$$

which for high  $R_0$  and small  $h_1$  would also approach  $K/e_1$ .

## 9.2 Adding explicit resource dynamics

Since we learned in the previous chapter that the steady state of the resource is typically solved from the consumer equations, the results demonstrating competitive exclusion from the critical resource densities, are not expected to change when we “open” the system by replacing the conservation equation in Eq. (9.5) by a dynamic resource with its own kinetics. We have written resource equations with a source and loss term, or with a birth and death rate, and we have used mass-action and saturated functional responses to describe the consumption (e.g., see the

question on biotic and abiotic resources on page 49). Combining abiotic with biotic resources, and restricting ourselves to saturated consumer birth rates we could therefore write

$$\frac{dR}{dt} = s - dR - R \sum_{i=1}^n c_i N_i \quad \text{with} \quad \frac{dN_i}{dt} = N_i \left( \frac{b_i c_i R}{h_i + c_i R} - d_i \right) \quad \text{or} \quad (9.9)$$

$$\frac{dR}{dt} = s - dR - R \sum_{i=1}^n \frac{c_i N_i}{h_i + R} \quad \text{with} \quad \frac{dN_i}{dt} = N_i \left( \frac{b_i R}{h_i + R} - d_i \right) \quad \text{or} \quad (9.10)$$

$$\frac{dR}{dt} = rR(1 - R/K) - R \sum_{i=1}^n c_i N_i \quad \text{with} \quad \frac{dN_i}{dt} = N_i \left( \frac{b_i c_i R}{h_i + c_i R} - d_i \right) \quad \text{or} \quad (9.11)$$

$$\frac{dR}{dt} = rR(1 - R/K) - R \sum_{i=1}^n \frac{c_i N_i}{h_i + R} \quad \text{with} \quad \frac{dN_i}{dt} = N_i \left( \frac{b_i R}{h_i + R} - d_i \right), \quad (9.12)$$

for  $i = 1, 2, \dots, n$  consumers, and where the first two and the latter two ODEs represent a non-replicating (abiotic) and replicating (biotic) resource, respectively. Here  $c_i$  is the consumption rate of consumer  $i$ . In the two equations with mass-action consumption (Eqs. 9.9 and 9.11), we let the birth rate be a saturation function of the amount of resources consumed ( $c_i R$ ). The saturation constant,  $h_i$ , in Eqs. (9.9) and (9.11) here also plays a role in the conversion from resource to consumers (one could even simplify these terms by dividing the numerator and denominator by  $c_i$ , and defining a new saturation constant  $h'_i = h_i/c_i$ ).

For the two equations with a saturated consumption term, one could think of the situation where the amount of resource consumed is proportional to the growth rate of the consumers, i.e.,  $c_i = cb_i$ , where  $c$  is the amount of resource (e.g., nutrient) contained in a single consumer, as is typically done for bacterial growth (Monod, 1949). Alternatively, one could think of a conventional Monod-saturated predator-prey model, and assume that  $b_i = cc_i$ , where  $c$  is a conversion constant required for converting resource into consumers.

Because the critical resource density for each consumer in Eqs. (9.9–9.12) is defined as either

$$R_i^* = \frac{h_i/c_i}{R_{0i} - 1} \quad \text{or} \quad R_i^* = \frac{h_i}{R_{0i} - 1}, \quad \text{where} \quad R_{0i} = \frac{b_i}{d_i}, \quad (9.13)$$

all consumers require different resource densities at steady state, and hence cannot co-exist in equilibrium on a single resource, unless they have identical parameters  $h_i, c_i, b_i$  and  $d_i$  (i.e., unless they occupy exactly the same niche). If we rank the species by their critical  $R_i^*$  values, we see that at steady state the first species with the lowest critical resource density will outcompete all others because when

$$R = R_1^* \quad \text{one can see that} \quad \frac{dN_1}{dt} = 0 \quad \text{and} \quad \frac{dN_i}{dt} < 0 \quad \text{for} \quad i = 2, 3, \dots, n, \quad (9.14)$$

where  $n$  is the number of consumers. We conclude that competitive exclusion is a very general theoretical result and does not seem to depend on the form of the resource or consumer equations. This is quite paradoxical because in many systems one observes that many species competing for resources do co-exist, e.g., there can be a high diversity of plankton species in an aquatic ecosystem, of bacteria in a microbiome, of viruses in a quasi-species, and lymphocytes in the immune system of a single host.

Note that if we had written mass-action birth rates in Eqs. (9.9) and (9.11), i.e.,  $dN_i/dt = (b_i R - d_i)N_i$ , the critical resources densities would have been defined as  $R_i^* = \frac{d_i}{b_i} = \frac{K}{R_{0i}}$ , which again reveals that different consumers require different resource densities at steady state, and

that the species with the highest fitness,  $R_{0_i}$ , depletes the resources most, and outcompetes all other consumers. Finally, the steady state of the most competitive consumer, i.e., the one with the lowest  $R_i^*$ , need not be stable when the consumption is saturated (see Eqs. (9.10) and (9.12)). If this is the case one expects a stable limit cycle of  $R$  and this most competitive  $N_i$ , and the question becomes whether or not other consumers can invade at this limit cycle. In the exercises we will demonstrate that this is possible, which emphasizes that competitive exclusion is an equilibrium result only.

### Removing the resource by a quasi steady state assumption (QSSA)

To study how resource competition would shape the interaction between the two competitors, one can make a QSSA for the resource in Eqs. (9.9–9.12), and substitute that into the corresponding consumer equations. This is feasible only for Eqs. (9.9) and (9.11) with mass-action consumption terms. For the non-replication resource of Eq. (9.9) one obtains

$$\hat{R} = \frac{s}{d + \sum c_i N_i}, \quad (9.15)$$

revealing the intuitive result that a resource that turns over more rapidly (i.e., has a high  $d$ ) remains closer to its carrying capacity,  $s/d$ , than a resource with a slow turnover (i.e., with a low  $d$ ). Substitution of  $\hat{R}$  into the corresponding consumer equation gives

$$\frac{dN_i}{dt} = N_i \left( \frac{b_i s}{s + (h_i/c_i)(d + \sum c_j N_j)} - d_i \right) = N_i \left( \frac{\beta_i}{1 + \sum N_j/k_j} - d_i \right), \quad (9.16)$$

where  $\beta_i$  and  $k_j$  are complicated combinations of several parameters (i.e.,  $\beta_i = b_i c_i s / (c_i s + h_i d)$  and  $k_i = c_i h_i / (c_i s + h_i d)$ ). The simplified form in Eq. (9.16) reveals that this is an extension of one of the density dependent birth models in Chapter 3, with an inverse Hill function  $f(N) = 1/(1 + N/k)$  describing the effect of the population density on the *per capita* birth rate. The “carrying capacity”,  $K_i$ , of a consumer can be found by setting all other  $N_j = 0$  (i.e., all  $j \neq i$ ), and solving  $dN_i/dt = 0$  from Eq. (9.16)

$$K_i = \frac{s}{h_i} (R_{0_i} - 1) - \frac{d}{c_i} = \frac{s}{c_i R_i^*} - \frac{d}{c_i}, \quad (9.17)$$

where  $R_i^*$  is still defined by Eq. (9.13). Thus, the most competitive species having the lowest  $R_i^*$  tends to have the highest carrying capacity (although this depends on  $h_i$  and  $c_i$ ). For two species, the nullclines of this QSS model would again be two parallel lines (not shown; try in Grind).

For the replicating resource of Eq. (9.11) one obtains

$$\hat{R} = K \left( 1 - \frac{1}{r} \sum c_i N_i \right), \quad (9.18)$$

again confirming the intuition that a rapidly growing resource remains closer to its carrying capacity at steady state consumption. Substituting this into the consumer equation gives the quite complicated

$$\frac{dN_i}{dt} = N_i \left( \frac{b_i (r - \sum c_j N_j)}{(h_i/c_i)(r/K) + r - \sum c_j N_j} - d_i \right). \quad (9.19)$$

This model is different from the models we have considered in Chapter 3, and also differs from the classic Lotka-Volterra competition model that we will consider below (in Section 9.3).

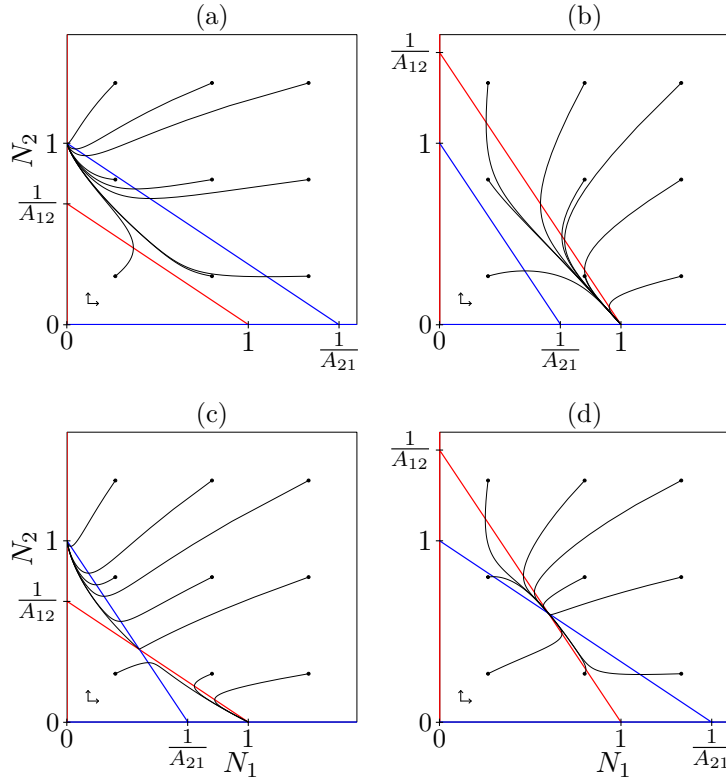


Figure 9.2: The four qualitatively different nullcline configurations of the Lotka-Volterra competition model given in Eq. (9.21). The red line and the blue lines depict the  $dN_1/dt = 0$  and  $dN_2/dt = 0$  nullclines, respectively, and the black lines are trajectories.  $N_1$  has a faster growth rate than  $N_2$ , i.e.,  $r_1 = 2r_2$ , which affects the trajectories but not the nullclines. This figure was made with the file `lotkaComp.R`.

One may recognize the mass-action terms of the Lotka-Volterra in the numerator of the birth term, implying that this may start to resemble the Lotka-Volterra competition model when  $(h_i/c_i)(r/K) + r \gg \sum c_j N_j$ . The “carrying capacity”,  $K_i$ , of a consumer can again be found by setting all other  $N_j = 0$  (for all  $j \neq i$ ), and solving  $dN_i/dt = 0$  from Eq. (9.19), i.e.,

$$\bar{N}_i = \frac{r}{c_i} \left( 1 - \frac{R_i^*}{K} \right),$$

where  $R_i^*$  is still defined by Eq. (9.13). For two species, the nullclines of this QSS model would again be two parallel lines (not shown; try in Grind).

Summarizing, we find competition equations with interaction terms that are more complicated than mass-action terms. Nevertheless, if we were to sketch the 2-dimensional nullclines of the QSS models of Eq. (9.16) and Eq. (9.19) we would find that these are linear, and resemble those of the Lotka-Volterra competition model.

### 9.3 The Lotka-Volterra competition model

The  $n$ -dimensional Lotka-Volterra competition model is typically written as

$$\frac{dN_i}{dt} = r_i N_i \left( 1 - \sum_{j=1}^n A_{ij} N_j \right), \quad (9.20)$$

where the interaction matrix,  $A_{ij}$ , collects the competition coefficients between the species (note that this model is very similar to Eq. (9.1)). The diagonal elements of this matrix define the carrying capacities, i.e.,  $K_i = 1/A_{ii}$ , because in the absence of interspecific competition Eq. (9.20) simplifies to logistic growth equation,  $dN_i/dt = r_i N_i(1 - A_{ii}N_i)$ . Thus, the Lotka-Volterra competition model basically extends the logistic growth model with additional mass-action competition terms.<sup>1</sup>

One can simplify the Lotka-Volterra competition model by scaling the carrying capacity of each species to one (by defining a non-dimensional population size  $n_i = N_i/K_i$ ). Thus, one can set all  $A_{ii} = 1$ , and recompute the other  $A_{ij}$  values by dividing them by  $K_j$  (see Section 15.4). The scaled version of the Lotka-Volterra competition model is very useful for depicting the famous four qualitatively different phase planes of two competing species. We sketch the nullclines of a 2-dimensional Lotka-Volterra competition model, by defining the horizontal axis by  $N_1$  and the vertical axis by  $N_2$ . Next solve  $N_2$  from  $dN_i/dt = 0$  in Eq. (9.20) for  $i = 1, 2$ , and set  $A_{11} = A_{22} = 1$ , to obtain

$$N_2 = \frac{1}{A_{12}} - \frac{A_{11}}{A_{12}} N_1 = \frac{1}{A_{12}} (1 - N_1) \quad \text{and} \quad N_2 = \frac{1}{A_{22}} - \frac{A_{21}}{A_{22}} N_1 = (1 - A_{21}N_1), \quad (9.21)$$

for  $dN_1/dt = 0$  and  $dN_2/dt = 0$ , respectively. The two simplified forms define the classic Lotka-Volterra nullclines running from  $N_i = 1$  on their own axis to  $1/A_{ij}$  on the opposite axis.

Choosing  $A_{ij}$  values that are either smaller or larger than one, one obtains the four classic diagrams shown in Fig. 9.2. When one of the  $A_{ij}$  parameters is smaller than one and the other is larger than one, the nullclines fail to intersect (see Fig. 9.2a and b), and the species with the smallest  $A_{ij}$  parameter outcompetes the other. When both  $A_{ij}$  parameters are larger than one, the interspecific competition exceeds the intraspecific competition for both species and the nullclines intersect in an unstable equilibrium (Fig. 9.2c). This is called the “founder controlled” situation because the species that initially has the highest abundance has the highest chance to exclude the other, and ultimately approach its carrying capacity. The steady state is stable (see Fig. 9.2d) when both  $A_{ij}$  parameters are smaller than one, i.e., when the intraspecific competition exceeds the interspecific competition for both species, which is the typical situation for resource competition because the niche overlap between two species should be smaller than the niche overlap among members of the same species.

Remember that the competition models we derived “mechanistically” above by a QSSA for the resource dynamics were quite different because of their non-mass-action interaction terms (O’Dwyer, 2018), but since these models in two dimensions also have straight nullclines, one would expect the same four situations as depicted in Fig. 9.2 (albeit for different parameter conditions). Moreover, we would have obtained the mass-action terms of the Lotka-Volterra model if the consumer model of Eq. (9.11) had been written with mass-action terms, e.g., as  $dN_i/dt = (b_i R - d_i)N_i$ , and we had substituted Eq. (9.18) or Eq. (9.1) for the resource. Finally, since the growth rates,  $r_i$ , can be cancelled when one considers the steady state of Eq. (9.20), the Lotka-Volterra competition model is sometimes defined as  $dN_i/dt = N_i(r_i - \sum_{j=1}^n A_{ij}N_j)$ , which is similar to more mechanistic models with explicit birth and death rates, e.g.,  $dN_i/dt = N_i(b_i[1 - \sum_{j=1}^n A_{ij}N_j] - d_i)$ . However, since a mass-action consumer model is not easily extendable into competition for several resources, as one would obtain a summation of several independent “birth rates”, e.g.,  $dN_i/dt = (\sum_{j=1}^n b_{ij}R_j - d_i)N_i$  when there are  $n$  different resources, we continue with saturated birth rates in the next sections.

<sup>1</sup>A Grind model with an arbitrary number of species,  $n$ , all having the same carrying capacity,  $K_i = 1$ , and having random off-diagonal  $A_{ij}$  elements is provided as the file `matrix.R`.

## 9.4 Several consumers on two resources

The previous sections demonstrated that several consumers on one resource are expected to exclude each other (at steady state). Two consumers living from two different resources should be able to co-exist whenever they specialize to have sufficiently different requirements for both resources, as this would again make the intraspecific competition larger than the interspecific competition. The most extreme example would be that each specializes on using just one of the two resources, implying that they do not compete and each approach a carrying capacity defined by the availability of their unique resource, their consumption and  $R_0$ . In the general 2-dimensional phase space of Fig. 9.2, such a situation would correspond to perpendicular nullclines intersecting in stable node (with a Jacobian having zero off-diagonal elements). Maintaining a steady state with more than two consumers using two resources should not be possible because the steady state expression of each consumer equation would have two unknown resource values, and one would have to solve more than two consumer equations with each two unknowns.

Next, we will go beyond Lotka-Volterra and write more mechanistic models for the situation where several consumers use several resources while allowing for an overlap in their diet. Studying consumers using several resources more mechanistically, one first has to decide whether or not these resources are “essential”, meaning that they cannot replace each other, or “substitutable”, meaning that they can be added up into a total intake (Tilman, 1980, 1982). First consider the situation of several consumers sharing several substitutable resources, by defining a birth rate depending on the summed resource intake, and generalize Eq. (9.9) into

$$\frac{dN_i}{dt} = \left( \beta_i \frac{\sum_j c_{ij} R_j}{h_i + \sum_j c_{ij} R_j} - \delta_i \right) N_i, \quad \frac{dR_j}{dt} = s_j - d_j R_j - \sum_i c_{ij} N_i R_j, \quad (9.22a,b)$$

where the consumption rates,  $c_{ij}$ , define the mass-action rates at which consumer  $i$  ingests resource  $j$ . Importantly,  $\beta_i$  is the birth rate that is approached when any of the resources is available at a high density. The saturation constants,  $h_i$ , define the density of consumed resources at which the birth rate is half-maximal. Since at low consumption rates the saturation functions approach  $\sum_j c_{ij} R_j / h_i$ , the saturation constants,  $h_i$ , also play the role of a trophic conversion factor from the resource to the consumer level. For simplicity we let each resource contribute equally to the birth rate of each consumer (this can be repaired by multiplying the  $c_{ij}$  terms in Eq. (9.22a) with a nutritious weight  $\alpha_{ij}$ ; see the online tutorial on [tbb.bio.uu.nl/rdb/bm/clips/tilman](http://tbb.bio.uu.nl/rdb/bm/clips/tilman)).

Since the *per capita* birth and death rates of the consumers in Eq. (9.22) only depend on the resource densities one can draw several  $dN_i/dt = 0$  nullclines in a space defined by the resources. For two resources such a picture is called a Tilman diagram (Tilman, 1980, 1982); see Fig. 9.3. Above, when we considered a single resource, we defined  $R_i^*$  as the critical resource density of consumer  $i$ . Now, for two resources the critical resource densities are defined by the consumer nullclines in the space spanned up by the resources, i.e., in Fig. 9.3 each consumer grows above its nullcline ( $dN_i/dt > 0$ ). If, and only if, two nullclines intersect, there is a combination of resource densities,  $(R_1, R_2)$ , at which  $dN_i/dt = dN_j/dt = 0$ , suggesting that there could be a steady state at which both species co-exist. To sketch the consumer nullclines in a 2-dimensional Tilman diagram we solve  $dN_i/dt = 0$  in Eq. (9.22) for  $R_2$ , to see that the nullclines all decline linearly as a function of  $R_1$ :

$$R_2 = \frac{h_i}{c_{i2}(R_{0_i} - 1)} - \frac{c_{i1}}{c_{i2}} R_1, \quad (9.23)$$

where  $R_{0_i} = \beta_i / \delta_i$ . Since the resources contribute additively, one can use  $dN_i/dt$  to define a

critical density,

$$R_{ij}^* = \frac{h_i}{c_{ij}(R_{0i} - 1)}, \quad (9.24)$$

for each resource  $j$  separately, and use this to simplify the nullcline of consumer  $i$  into  $R_2 = R_{i2}^* - \frac{c_{i1}}{c_{i2}} R_1$ . Two of these simplified nullclines can only intersect when their slopes are unequal, i.e., when  $\frac{c_{i1}}{c_{i2}} \neq \frac{c_{j1}}{c_{j2}}$ , and when their four intersects with the axes, i.e.,  $R_2 = R_{i2}^*$ ,  $R_1 = R_{i1}^*$ ,  $R_2 = R_{j2}^*$ , and  $R_1 = R_{j1}^*$ , also allow the nullclines to cross (see Fig. 9.3b). Note that when two species perfectly specialize on one resource, i.e.,  $c_{21} = c_{12} = 0$ , their Tilman diagram will have two intersecting perpendicular lines located at  $R_1 = R_{11}^*$  and  $R_2 = R_{22}^*$ .

When two consumers  $i$  and  $j$  have the same diet,  $c_{i1} = c_{j1}$  and  $c_{i2} = c_{j2}$ , their nullclines will be parallel lines, and the species will exclude each other (see Fig. 9.3a) where we plot the nullclines of three consumers differing in their saturation constants only, i.e.,  $h_3 > h_2 > h_1$ ). The fact that these lines are not intersecting means that there is no combination of resource densities,  $(R_1, R_2)$ , at which even two of the consumers can co-exist at steady state. Thus, the species with the lowest resource requirements,  $R_{ij}^*$ , i.e., the one with the lowest nullcline in the Tilman diagram of Fig. 9.3a will outcompete the others. Requiring low amounts of consumed resources, i.e., having a low  $h_i$  parameter, consuming a lot, i.e., having high  $c_{ij}$  parameters, and having a high  $R_0$ , all contribute to having low  $R_{ij}^*$ s, and becoming the superior competitor (see Fig. 9.3a). Since a 2-dimensional Tilman diagram can contain any number of consumer nullclines, it is not limited to a maximum of three consumers, and can be used to establish the superior competitor(s) in a large set of consumers.

When the consumers have different diets their nullclines in the Tilman diagram may intersect, and in Fig. 9.3b we made a situation with three pairwise intersections by letting  $N_1$  specialize on  $R_1$  (by setting  $c_{11} > c_{12}$ ),  $N_2$  specialize on  $R_2$  (by setting  $c_{22} > c_{21}$ ), and making  $N_3$  a generalist (by setting  $c_{31} \simeq c_{32}$ ). Since the three nullclines do not intersect in one point, one can safely conclude that there is no combination of resource densities where all three  $dN_i/dt = 0$ , and hence that these three consumers cannot co-exist on just two resources (confirming the general competitive exclusion principle). Because the slopes of these nullclines depend on the ratio of the consumption rates,  $c_{i1}/c_{i2}$ , their heights on the saturation constant,  $h_i$ , and the fitness,  $R_{0i}$  of each consumer (see Eq. (9.23)), it is generically not expected to have an intersection point of more than two nullclines (see the exercises for a non-generic counterexample (Posfai *et al.*, 2017)). However, depending on the parameters, any pair of consumer nullclines may intersect, and this intersection point would correspond to a steady state provided that for these resource densities there is also a steady state density of the two consumers such that  $dR_1/dt = dR_2/dt = 0$ . Thus, an intersection between two consumer nullclines need not be a steady state of the full system, i.e., of Eq. (9.22). Using `newton()` in Grind we have marked all steady states with two consumers with bullets (stable) and circles (unstable) in Fig. 9.3b. This illustrates that only two of the pairwise intersections correspond to a steady state. The intersection point in the middle, where  $dN_1/dt = dN_2/dt = 0$ , is a stable steady state because it is located below the  $dN_3/dt = 0$  nullcline, implying that  $N_3$  will decline at these resource densities (i.e.,  $N_3$  cannot invade). The left-most intersection point, where  $dN_1/dt = dN_3/dt = 0$ , is an unstable steady state because it is located above the  $dN_2/dt = 0$  nullcline, implying that  $N_2$  would successfully invade if introduced into this equilibrium of  $N_1$  and  $N_3$  with the two resources. For reasons that are not readily obvious from the Tilman diagram in Fig. 9.3b, the right-most intersection point, where  $dN_2/dt = dN_3/dt = 0$ , is not a steady state (see the online tutorial). Importantly, such a Tilman diagram can be made for any set of consumers, and this analysis tells us (1) that the consumers depleting the resources the most are expected to be the superior competitors, and (2) at steady state no more than two consumers are expected to be maintained by two resources. Again the consumer depleting resources to a minimal density tends to win the competition.

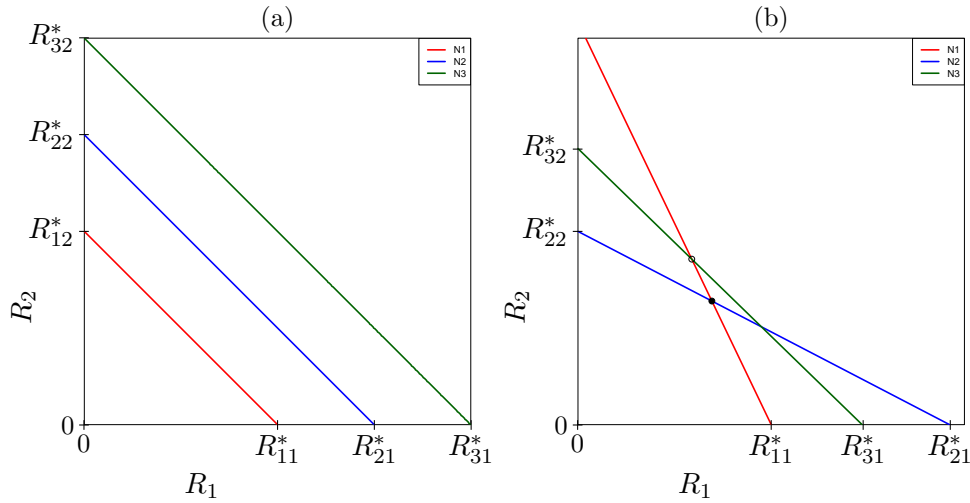


Figure 9.3: Three consumers on two substitutable resources. The nullclines of the consumers are defined by Eq. (9.22a) and because they then obey Eq. (9.23), they form straight lines with slope  $c_{i1}/c_{i2}$ . In Panel (a) the consumers have the same diet which corresponds to parallel nullclines. Thus, when the consumers have the same (or a too similar) diet the nullclines fail to intersect, which implies that there is no combination of resource densities,  $(R_1, R_2)$ , at which at least two of the consumers can co-exist at steady state. Giving  $N_1$  an advantage over the other two consumers by setting  $h_1 < h_2 < h_3$ , the  $dN_1/dt = 0$  nullcline is located at the lowest resource densities, and  $N_1$  will outcompete the other two consumers. In Panel b we let  $N_1$  specialize on  $R_1$  by setting  $c_{11} > c_{12}$ ,  $N_2$  specialize on  $R_2$  by setting  $c_{22} > c_{21}$ , and make  $N_3$  a generalist by setting  $c_{31} \simeq c_{32}$ . Thus,  $N_1$  has the steepest nullcline,  $N_2$  the flattest, and  $N_3$  has a slope close to  $-1$ . Because we have given the consumers similar total consumption rates,  $c_{i1} + c_{i2}$ , and identical saturation constants,  $h_i$ , the nullclines tend to intersect in pairs. Only the middle intersection point where  $dN_1/dt = dN_2/dt = 0$  can be a stable steady state because this is below the  $dN_3/dt = 0$  nullcline, meaning that  $N_3$  cannot invade at these low resource densities. The upper intersection point where  $dN_1/dt = dN_3/dt = 0$  is a steady state, but because it is above the  $dN_2/dt = 0$  nullcline it has to be unstable. The lower intersection point where  $dN_2/dt = dN_3/dt = 0$  is not a steady state, and solving the system in the absence of  $N_1$  would lead to trajectories approaching  $N_2 = K_2$ . The bullet and the circle were obtained numerically by solving the system for all pairwise combinations of consumers. This figure was made with the model `additive.R`, where we have chosen a steady state of the resources in the absence of the consumers,  $(\bar{R}_1, \bar{R}_2) = (s_1/d_1, s_2/d_2)$ , that is located above the three nullclines and falling outside of the Tilman diagram.

Because one cannot easily tell from a Tilman diagram whether or not an intersection point corresponds to a steady state, these diagrams are most informative for establishing which intersections are absent, which truly indicates the absence of a steady state (see Fig. 9.3), and to establish which pairwise intersection point is located at the lowest resource densities, which predicts which pair of consumers forms the superior set of competitors. It is tempting to use an invasion criterion to establish whether or not a steady state is stable, i.e., to conclude that the steady state located at the lowest combination of resource densities should be stable because the other consumers necessarily decline at these resource densities. However, in a Tilman diagram this could be invalid because the lowest intersection point (1) also needs to be a 4-dimensional steady state where  $dR_1/dt = dR_2/dt = dN_1/dt = dN_2/dt = 0$ , and (2) even if it is a steady state, it could still be unstable (see the online tutorial).

## 9.5 Essential Resources

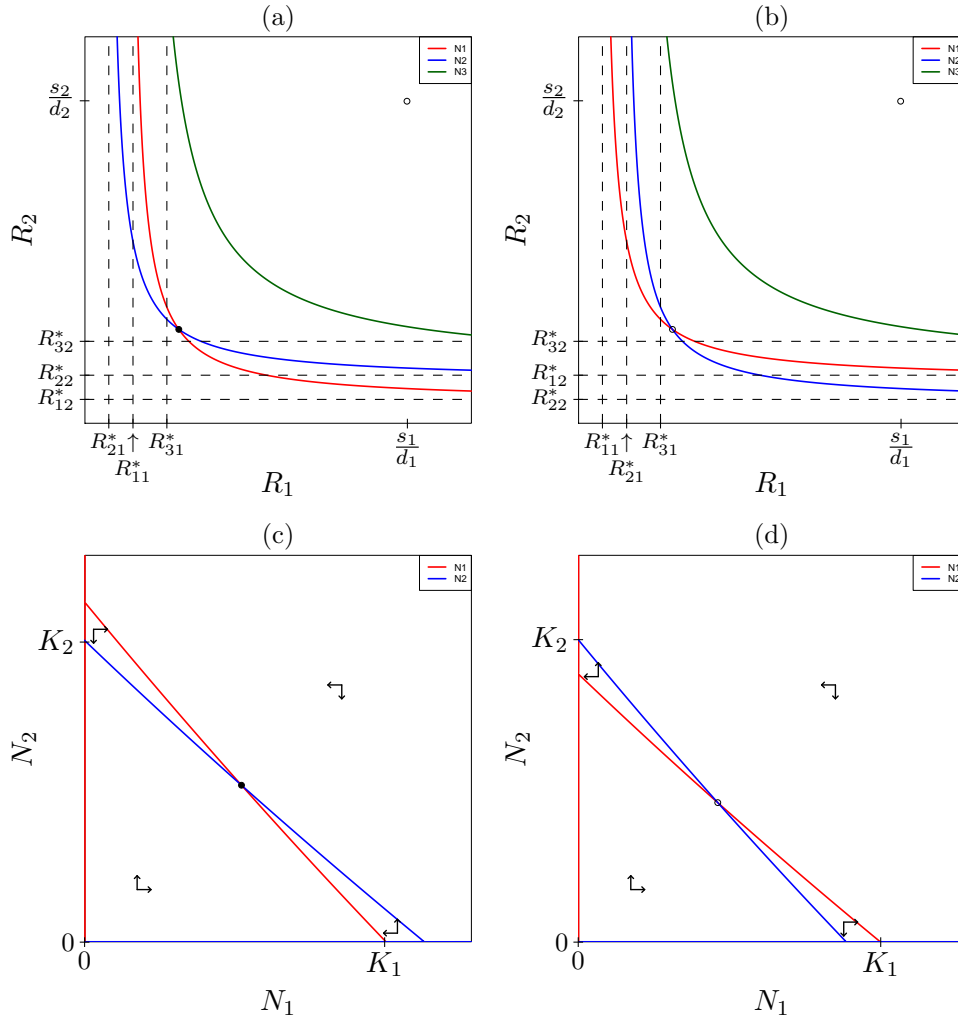


Figure 9.4: Consumer nullclines for a situation with two essential resources for a stable steady state (Panels (a) and (c)) and for an unstable steady state (Panels (b) and (d)). The panels at the top depict the nullclines of Eqs. (9.26) and (9.27) as function of the resource densities (these are Tilman diagrams). The dashed lines are the asymptotes of the nullclines. The circle in the upper corners depicts the (unstable) steady state of the resources in the absence of consumers. The other bullets and circles reflects a stability of steady state with consumers. The panels at the bottom provide the nullclines of Eqs. (9.26) and (9.27) after making a QSSA for the two resources defined by Eq. (9.25). This figure was made with the model `essential.R`.

To mechanistically model “essential” resources one could change Eq. (9.22) into

$$\frac{dN_i}{dt} = \left( \beta_i \prod_j \frac{c_{ij}R_j}{h_{ij} + c_{ij}R_j} - \delta_i \right) N_i, \quad \frac{dR_j}{dt} = s_j - d_j R_j - \sum_i c_{ij} N_i R_j, \quad (9.25a,b)$$

where by the multiplication of saturation functions we require that all resources should be consumed in sufficient amounts. Note again that this can be simplified by dividing the numerator and denominator in each saturation function by  $c_{ij}$ , and define  $h'_{ij} = h_{ij}/c_{ij}$ . An alternative is to define a birth rate that is completely determined by resource that is limiting most, which is called “Liebig’s law of the minimum”, and use a minimum function instead of a product (see the exercises). Since the nullclines of Eq. (9.25a) only depend on the resource densities, one can

again plot many  $dN_i/dt = 0$  in a single Tilman diagram spanned up by two resources. For two consumers on two resources Eq. (9.25a) translates into

$$\frac{dN_1}{dt} = \left( \beta_1 \frac{c_{11}R_1}{h_{11} + c_{11}R_1} \frac{c_{12}R_2}{h_{12} + c_{12}R_2} - \delta_1 \right) N_1, \quad (9.26)$$

$$\frac{dN_2}{dt} = \left( \beta_2 \frac{c_{21}R_1}{h_{21} + c_{21}R_1} \frac{c_{22}R_2}{h_{22} + c_{22}R_2} - \delta_2 \right) N_2, \quad (9.27)$$

and Fig. 9.4(a) and (b) depicts two Tilman diagrams for this model. The consumer nullclines in a phase spanned up by the two resources are hyperbolic functions with asymptotes defining the minimal resource densities these consumers require. These asymptotes can be found by setting  $dN_i/dt = 0$  for  $R_1 \rightarrow \infty$  or  $R_2 \rightarrow \infty$ , i.e.,  $R_1 = R_{i1}^*$  and  $R_2 = R_{i2}^*$  for  $i = 1, 2, \dots, n$ , respectively, where the  $R_{ij}^*$ s are still defined by Eq. (9.24). Whether or not the nullclines will intersect therefore depends on the  $R^*$ s, and the species with the lowest requirements,  $h_{ij}$ , the highest consumption rates,  $c_{ij}$ , and highest  $R_0$  will have the lowest nullcline, and be the winner whenever the nullclines fail to intersect (see Fig. 9.4a and b).

In all panels of Fig. 9.4 we have again set  $c_{11} > c_{12}$ ,  $c_{22} > c_{21}$  and  $c_{31} \simeq c_{32}$ , i.e., consumer one specializes on resource one, consumer two on resource two, and consumer three is a generalist, and in Fig. 9.4(c) and (d) we have used non-replicating resources defined by Eq. (9.25b). In the stable situation of Fig. 9.4a and c we accordingly set  $h_{11} > h_{12}$ ,  $h_{22} > h_{21}$  and  $h_{31} = h_{32}$ , to let each species require most of the resource it eats most (which would be “optimal” in an evolutionary sense (see the chapter by Tilman in (McLean & May, 2007))). We have made the unstable situation of Fig. 9.4(b) and (d) by setting  $h_{11} = h_{12} = h_{21} = h_{22} < h_{31} = h_{32}$ , which means that on  $R_2$  the first consumer competes more strongly with the second consumer than with itself because the second consumer eats more of resource two than the first consumer, whereas they both require the same amount. This leads to an unstable steady state between them, and a situation where only one of the consumers survives. The initial condition will determine who persists, and hence this is called a “founder controlled” situation.<sup>2</sup>

## 9.6 Summary

The competitive exclusion principle stating that at steady  $n$  resources can maximally maintain  $n$  different consumers is a very general theoretical result that nevertheless seems to be contradicted by various biological systems maintaining a diverse community of consumers on a very limited variety of resources. Mechanistic models for resource competition require a distinction between essential and substitutable resources. One can study systems with many consumers using two (or three) resources in Tilman diagrams, and this reveals that the species depleting the resources most, tend to be the superior competitors (because they can survive on the lowest resource densities). The lowest resource density,  $R^*$ , required by a consumer to expand is therefore the most informative measure defining the most superior competitors, and species will only co-exist at equilibrium when their niches are sufficiently different. Replicating and non-replicating resources yield similar results for the outcome of the competition. The classic Lotka-Volterra competition equations turn out to be bold simplifications generalizing over any number of essential and substitutable resources, and are not readily obtained from QSS assumptions in more mechanistic consumer-resource models. The Lotka-Volterra competition

<sup>2</sup>The online tutorial on [tbb.bio.uu.nl/rdb/bm/clips/tilman](http://tbb.bio.uu.nl/rdb/bm/clips/tilman) explains Tilman’s quite complicated procedure to address the stability of steady states for simpler models based upon mass-action interaction terms (and Section 15.10 in the Appendix applies this approach to the two more complicated models discussed here).

equations nevertheless allow one to summarize the four qualitatively different phase diagrams that one may expect for two competing populations.

## 9.7 Exercises

### Question 9.1. Migration

Extend the scaled Lotka-Volterra competition model of Eq. (9.20) with a small constant immigration of individuals.

- Write the new differential equations for a 2-dimensional system.
- Analyze the model using nullclines. Hint: first sketch the well-known qualitatively different phase spaces without this migration term, and then reason how the nullclines change if you add a *small* immigration parameter.
- Determine the stability of all the steady states.
- Discuss competitive exclusion in this model.

### Question 9.2. Equilibrium co-existence

Throughout this chapter we have concluded that two competitors cannot be maintained together in steady state when they are competing for a single resource. To study a potential counterexample we here borrow the metapopulation model proposed by Tilman *et al.* (1994), in which they define competition by ordering their species by competitive strength, i.e., the first species can overgrow patches occupied by all other species, the second all but the first one, and so on. One could think of an area where trees can overgrow land occupied by grass, or a petri dish seeded with bacterial species that can overgrow each other according to some ranking. For simplicity we consider two species, and a total amount of resource,  $T$ , where  $T$  could be total available area (that one could scale to one). For the two species one would write

$$\frac{dN_1}{dt} = b_1 N_1 (T - N_1) - d_1 N_1 \quad \text{and} \quad \frac{dN_2}{dt} = b_2 N_2 (T - N_1 - N_2) - d_2 N_2 - b_1 N_1 N_2, \quad (9.28a,b)$$

with birth rates  $b_i$  and death rates  $d_i$ . Assuming that grass cannot grow under trees, and that trees can seed themselves into areas occupied by grass, one could model the competition between grass and trees with Eq. (9.28) by defining  $N_1$  and  $N_2$  as the densities of trees and grass, respectively.

- Explain why the grass density is absent from Eq. (9.28a), and why the birth rate of the trees appears in Eq. (9.28b).
- Sketch the nullclines of this system.
- Can the two species co-exist in steady state? If so, what is the condition for co-existence in terms of the parameters?
- Is this a counterexample for the so general result on competitive exclusion derived in this chapter? If so, how can this be?

### Question 9.3. Non-equilibrium co-existence (Grind)

We have seen in this chapter that two species competing for the same resource cannot co-exist in a steady state. A fine example of non-equilibrium co-existence of two consumers using the same resource was devised by Yodzis (1989). By making a smart choice of the functional response functions, one can make a system where one consumer grows faster than the other at low prey densities, while the other does better at high prey densities. If the prey population oscillates between densities where the two consumers differ in performance, they need not exclude each other. Note that the two consumer nullclines remain parallel planes in the phase space, precluding the existence of a 3-dimensional steady state, and hence this remains in agreement with the equilibrium analyses in this chapter. To find parameters corresponding to this behavior

one should design an oscillatory predator-prey system like we did in Chapter 7, and use invasion criteria allowing each of the predators to invade at the average prey density in the attractor set by the other predators. An example of a model allowing for the non-equilibrium co-existence is

$$\begin{aligned}\frac{dR}{dt} &= rR(1 - R/K) - \frac{a_1RN_1}{h + R} - a_2RN_2, \\ \frac{dN_1}{dt} &= \frac{a_1RN_1}{h + R} - d_1N_1, \\ \frac{dN_2}{dt} &= a_2RN_2 - d_2N_2,\end{aligned}\tag{9.29}$$

where the first consumer has a saturated Holling type-II response, and the second one has a linear functional response.

- Sketch the nullclines of  $R$  with  $N_1$  and  $R$  with  $N_2$  by hand.
- Use pencil and paper to find parameters giving functional responses that intersect each other.
- Use the latter in Grind to find parameter values for which the consumers co-exist. Check the invasion of each of the predators in the attractor of the other.
- Can one obtain the same result when both predators have a saturated functional response?

#### Question 9.4. Larvae and adults

- Write a simple model for an insect population with an early larval stage, and a late adult stage. Assume that larvae only compete among themselves, and make sure that the insect population as a whole has a carrying capacity.
- Let there be two “predators”, one feeding on the larvae and the other on the adults, e.g., a wasp laying eggs in the larvae and birds eating the adults. Since these predators are foraging on the same species they seem to occupy the same niche. Can these two predators nevertheless co-exist?

#### Question 9.5. Gradients with sharp borders

In vegetations one sometimes observes sharp borderlines between the areas covered by different species in situations where one does not expect an underlying sharp transition in the environmental conditions. An example is the sharp zonation in different vegetations along a smooth environmental gradient, like a salt gradient or an altitude gradient. Consider a plant species competing for a stylized resource like space,  $R$ , and having an additional death rate,  $d_S$ , influenced by some environmental condition, e.g., the concentration of salt,

$$\frac{dN_1}{dt} = N_1(b_1R - d_1 - d_S),$$

where  $R = 1 - N_1$  is the scaled availability of free space, and  $d_S$  reflects the death rate due to the salt. Suppose we study vegetation plots taken along a salt gradient, and that the vegetation is in steady state.

- What is the carrying capacity, and how does it depend on the concentration salt?
- Sketch the carrying capacity along the gradient, i.e., as a function of  $d_S$ .
- Next we add a second species that is tolerant to salt, and due to a trade-off has a somewhat lower fitness, i.e., now define  $R = 1 - N_1 - N_2$  and  $dN_2/dt = N_2(b_2R - d_2)$ , where  $b_2/d_2 < b_1/d_1$ . Sketch the nullclines for a situation with such a low concentration of salt that  $d_S = 0$ , and provide a biological interpretation. What happens to these nullclines along the salt gradient?
- Now sketch the steady state of both  $N_1$  and  $N_2$  along the gradient, and interpret your result.

#### Question 9.6. Density dependent birth rate

In this chapter we used mass-action consumption terms, but made the birth rate of the consumer a saturation function of the amount of resources consumed. Since this seems realistic we will

investigate what kind of density dependence this yields for the consumers. To keep things simple start with a scaled resource equation for a replicating resource,

$$\frac{dR}{dt} = R(1 - R) - aRN \quad \text{and} \quad \frac{dN}{dt} = \left[ b \frac{aR}{h + aR} - d \right] N,$$

where  $N$  is the consumer with a maximum birth rate  $b$ . We proceed as normal: make a QSS assumption for the resource and substitute this into the consumer equations.

- What is the  $R_0$  of the consumer?
- Perform the QSSA and write the complete ODE for a single consumer. Combine parameters to have it in its simplest form.
- What is now the  $R_0$  of the consumer?
- Sketch the *per capita* birth rate of the consumer as a function of the consumer density.
- Which of the growth models of Chapter 3 describes this best?
- We considered a replicating resource in this question. If you have time you can also sketch the *per capita* birth rate of the consumer for a non-replicating resource, e.g.,  $dR/dt = 1 - R - aRN$ , where source and death have been scaled.

### Extra questions

#### Question 9.7. Fitting Lotka-Volterra competition to the Gause data from 1934

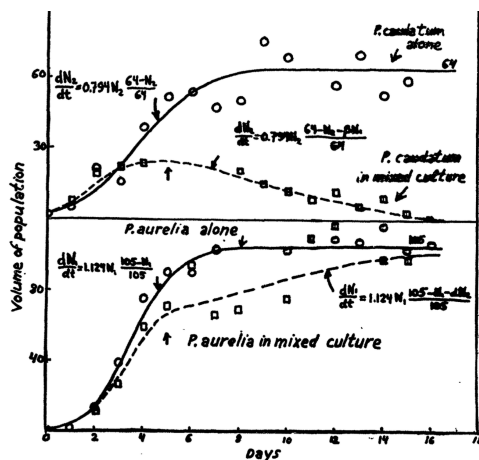


Figure 1 from Gause (1934).

The classic experiments of Gause (1934) demonstrated that two species cannot coexist on a single resource. In his experiments he was growing several species *Paramecium* either in isolation, or in combination. Gause showed that the growth curve of *P. aurelia* and *P. caudatum* on their own (circles) can reasonably be described by a logistic growth equation (solid lines), and the competition data (squares) were well described with a Lotka-Volterra competition model (dashed lines). In Chapter 3 we have fitted the logistic growth of both species in Chapter 3, let us now fit the two competition experiments with Eq. (9.20).

- The data is available in the directory [tbb.bio.uu.nl/rdb/bm/models/data](http://tbb.bio.uu.nl/rdb/bm/models/data), in the files `aurelia1.txt` and `caudatum1.txt` for the solitary experiments, and in the files `aurelia2.txt` and `caudatum2.txt` for the combined experiment. The file `gause2.R` allows you to read these files and fit the data. We follow Gause's notation and rewrite Eq. (9.20) into  $dA/dt = r_A A(1 - (A + \alpha C)/k_A)$  and  $dC/dt = r_C(1 - (C + \beta A)/k_C)$  for the `model()` in this file. Check for yourself that this is the same as Gause's handwritten model. Next, copy/paste the estimated growth rates and carrying capacities from the exercise in Chapter 3 into the parameter vector:

```
pA <- c(rA=1.11, kA=104.73)
pC <- c(rC=0.916, kC=60.277)
```

```
p <- c(pA,pC,alpha=0,beta=0)
```

and confirm by setting  $\alpha = \beta = 0$  that these indeed describe the solidarity data well

```
s <- c(A=A0[1], C=C0[2])
```

```
run(18,legend=FALSE)
```

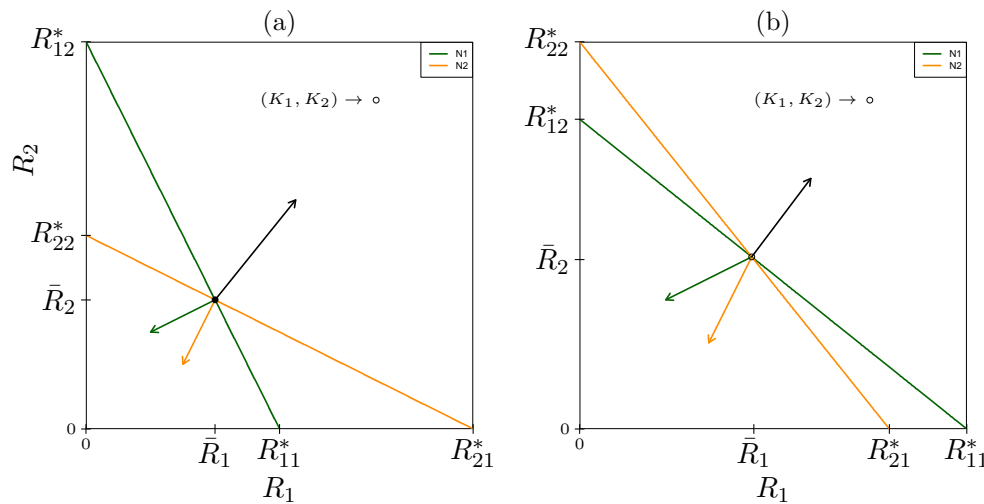


Figure 9.5: Two Tilman diagrams from the online tutorial on [tbb.bio.uu.nl/rdb/bm/clips/tilman/script.pdf](http://tbb.bio.uu.nl/rdb/bm/clips/tilman/script.pdf) are based upon Eq. (9.30) with  $\alpha_{11} = \alpha_{12} = \alpha_{21} = \alpha_{22} = 1$  in Panel (a), and  $\alpha_{11} = \alpha_{22} < \alpha_{12} = \alpha_{21}$  in Panel (b). In both panels  $N_1$  consumes most of  $R_1$  and  $N_2$  most of  $R_2$ . The intersection point in Panel (a) corresponds to a stable steady state, whereas the one in Panel (b) is a saddle point.

```
timePlot(aurelia1,draw=points,add=TRUE,legend=FALSE)
timePlot(caudatum1,draw=points,add=TRUE,colMap=2,legend=FALSE)
```

- Next estimate the two inter-specific competition parameters  $\alpha$  and  $\beta$ . Which species suffers most from its competitor? Would you have expected that?
- Sketch the nullclines for the estimated parameters.
- Since *P. aurelia*'s competition parameter is larger than one, *P. aurelia*'s appears to suffer more from its competitor than from its conspecifics. Can this be explained by resource competition? Is  $\alpha$  truly larger than one?
- Fitting the data in two separate steps need not yield the best possible combination of parameter estimates. Therefore, we also fit all parameters (except the initial conditions) to the four data sets simultaneously. Note that we need to fix the initial condition in each experiment to model the two solitary experiments. Do you find similar results?
- Finally, one can bootstrap the data to obtain confidence intervals on the parameter estimates (this may take a while!). Are the two competition parameters  $\alpha$  and  $\beta$  sufficiently different to indeed conclude that  $\alpha > \beta$ ?
- What is your summary of these results?

### Question 9.8. Tilman's competition model (Grind)

In this chapter we have used Tilman diagrams to study the competition for substitutable and essential resources using saturation functions of the total consumption. David Tilman in his original papers used a large variety of models (Tilman, 1980, 1982), and we here ask you to first study the most simple model in which the consumption is a mass-action term (like in the Lotka-Volterra model), and the birth rate of the consumers is just proportional to their consumption of the two resources,

$$\begin{aligned} \frac{dN_1}{dt} &= [\alpha_{11}c_{11}R_1 + \alpha_{12}c_{12}R_2 - \delta_1]N_1, \\ \frac{dN_2}{dt} &= [\alpha_{21}c_{21}R_1 + \alpha_{22}c_{22}R_2 - \delta_2]N_2. \end{aligned} \quad (9.30)$$

The online tutorial on [tbb.bio.uu.nl/rdb/bm/clips/tilman/script.pdf](http://tbb.bio.uu.nl/rdb/bm/clips/tilman/script.pdf) analyses this model in

depth, by considering cases where  $N_1$  consumes most of  $R_1$  and  $N_2$  most of  $R_2$  (which being an arbitrary choice keeps the model generic). These Tilman diagrams in Fig. 9.5 are explained in the tutorial and are sketched for resources that equally nutritious, i.e.,  $\alpha_{11} = \alpha_{12} = \alpha_{21} = \alpha_{22} = 1$ , and for a situation where the resource that each species eats most is the least nutritious, i.e.,  $\alpha_{11} = \alpha_{22} < \alpha_{12} = \alpha_{21}$ .

- Define the critical resource densities,  $R^*$ , in terms of the parameters in Eq. (9.30).
- Define the qualitative difference between the two panels in Fig. 9.5 in terms of the  $R^*$  parameters.

A simple model for two consumers using two essential resources can be made from Eq. (9.30) by using minimum functions in the birth rates (Tilman, 1980, 1982; McLean & May, 2007),

$$\begin{aligned}\frac{dN_1}{dt} &= [\min(\alpha_{11}c_{11}R_1, \alpha_{12}c_{12}R_2) - \delta_1]N_1, \\ \frac{dN_2}{dt} &= [\min(\alpha_{21}c_{21}R_1, \alpha_{22}c_{22}R_2) - \delta_2]N_2.\end{aligned}\tag{9.31}$$

The minimum function makes the resources both “essential”, i.e., both have to be consumed in sufficient amount, and the actual birth rate is limited by the resource that is most needed.

- Explain that this indeed corresponds to a model for two essential resources.
- Sketch Tilman diagrams of this model for  $\alpha_{11} = \alpha_{12} = \alpha_{21} = \alpha_{22} = 1$  and  $\alpha_{11} = \alpha_{22} < \alpha_{12} = \alpha_{21}$  (you can help yourself by using the `tilmanMin.R` model). Note, that Grind model calls `newton()` to compute the 4-D Jacobian.
- What is now the condition on having stable co-existence, and can you explain that?
- Like in the online tutorial one can define two non-replicating resources, which we here simplify by scaling the resource densities, and the time, by setting  $s_i = d_i = 1$ , i.e.,  $dR_i/dt = 1 - R_i - c_{1i}N_1R_i - c_{2i}N_2R_i$  for  $i = 1, 2$ , such that we can write the quasi steady state resource densities as

$$R_1 = \frac{1}{1 + c_{11}N_1 + c_{21}N_2} \quad \text{and} \quad R_2 = \frac{1}{1 + c_{12}N_1 + c_{22}N_2}.$$

Use the QSSA model in `tilmanMin.R` to study the phase space of the two consumers, and confirm what you found above.

### Question 9.9. Co-existence by trade-offs?

Posfai *et al.* (2017) study the “Paradox of the plankton” by modeling resource competition between a large number of consumers. Their major idea is that consumers are expected to specialize on a subset of the resources, and therefore they introduce trade-offs among the consumption rates when parametrizing their model. Surprisingly, they find that an unlimited number of species can coexist, and that their model reproduces several features of natural ecosystems, including keystone species and population dynamics characteristic of neutral theory. The consumer equation of their model takes the following form:

$$\frac{dN_i}{dt} = \left( \sum_j \frac{\beta_{ij}c_{ij}R_j}{h_{ij} + c_{ij}R_j} - \delta_i \right) N_i,$$

where each additional resource increases the maximum birth rate,  $\beta_i = \sum_j \beta_{ij}$ , that is approached when all resources are available at large densities, i.e., when  $R_j \gg h_{ij}$  for all  $j$  (which would be the natural situation when all consumer densities are low).

- This is different from Eq. (9.22a): is this a proper model for substitutable resources?
- This is also different from Eq. (9.25a): is this a proper model for essential resources?
- When you choose this as a project, you could use Grind to study the idea of a trade-off in our own models for competition between substitutable or essential resources. Do we find similar results, and —if so— what is actually required to repeat these results? What do you think of this paper: is this indeed resolving the Paradox of the plankton?

**Question 9.10. Fitness (challenging)**

In this book we typically used the fitness  $R_0 = b/d$  to clean up the equations, and in Eq. (9.13)b we have seen that the critical resource requirement,  $R_i^* = h_i/(R_{0_i} - 1)$ , where  $R_{0_i} = b_i/d_i$  defines which species is the best competitor. This  $R_0$  is based upon an infinite resource density, however. We could also have used the carrying capacity of the resource to define the  $R_0$ , and would then have arrived at a complicated expression for the fitness, i.e.,

$$\hat{R}_{0_i} = \frac{b_i}{d_i} \frac{\bar{R}}{h_i + \bar{R}},$$

where  $\bar{R} = s/d$ . Since this contains all parameters defining  $R_i^*$ , and one could think that the species having the highest fitness,  $\hat{R}_{0_i}$ , should also be the best competitor, i.e., have the lowest  $R_i^*$ . Due to the fact that the birth rates are saturation functions of the amount of resources consumed, one can already see that this need not always be true, as a consumer that is best at high resource densities, need not be the best one at low resource densities, i.e., around  $R^*$ .

- a. Can you formalize this and show that the species with the lowest fitness,  $\hat{R}_{0_i}$ , can be the best competitor?
- b. A related challenge is to make a phase plane where a typical  $r$ -selected species, with rapid birth and death rates and a low carrying capacity, outcompetes a typical  $K$ -selected species.

## Chapter 10

# Co-existence in large communities

The scaled Lotka-Volterra competition model of Eq. (9.20) has been used in many different theoretical studies of competition in ecosystems. Thanks to its simplicity it has few parameters, and this has allowed theoretical ecologists to define “understandable” models for communities composed of many competing species. We here discuss a few classic examples. The first considers competition along a resource axis, and has the “natural” restriction discussed in Chapter 9 that all intra-specific competition parameters are smaller than the inter-specific parameters. We proceed by discussing classic work based upon the Jacobi matrix of large random dynamical systems. We investigate this further by returning to high-dimensional Lotka-Volterra models, and saturated consumer-resource models, by assigning randomly chosen parameters to the species of these communities. We close by discussing “neutral” models that ignore ecological interactions, and focus completely on random immigration and death, and with models for cross-feeding in microbial communities.

### 10.1 Niche space models

There is an interesting classic modeling formalism for resource competition that is based on a resource axis along which species are distributed (see Fig. 10.1) (MacArthur, 1972; May, 1974; Scheffer & Van Nes, 2006). Think of several species of Darwin finches that each have a preferred seed size because they evolved different beak sizes. The preference of each species can be modeled with a Gaussian function of the seed size  $x$ , i.e.,  $f(\hat{x}) = \exp[-(x - \hat{x})^2/(2\sigma^2)]$  that is centered around the preferred seed size  $\hat{x}_i$  of species  $i$  (see Fig. 10.1). One can interpret this function as the probability of using a seed of size  $x$ , where seeds of the preferred size are consumed with probability one. For simplicity, one assumes that the species are evenly distributed over the niche space (one would expect evolution to select for such a maximal niche separation). This simplifies the whole problem of niche overlap to just two parameters:  $\sigma$  for the standard deviation of the Gaussian functions, and  $d$  for the distance between the preferred seed sizes of neighboring species. One can define the niche overlap between two consumers separated at a distance  $d$  on the resource axis as the probability of both species eating seeds of the same size, i.e., as the product of their Gaussian preference functions at all seed sizes. To properly scale

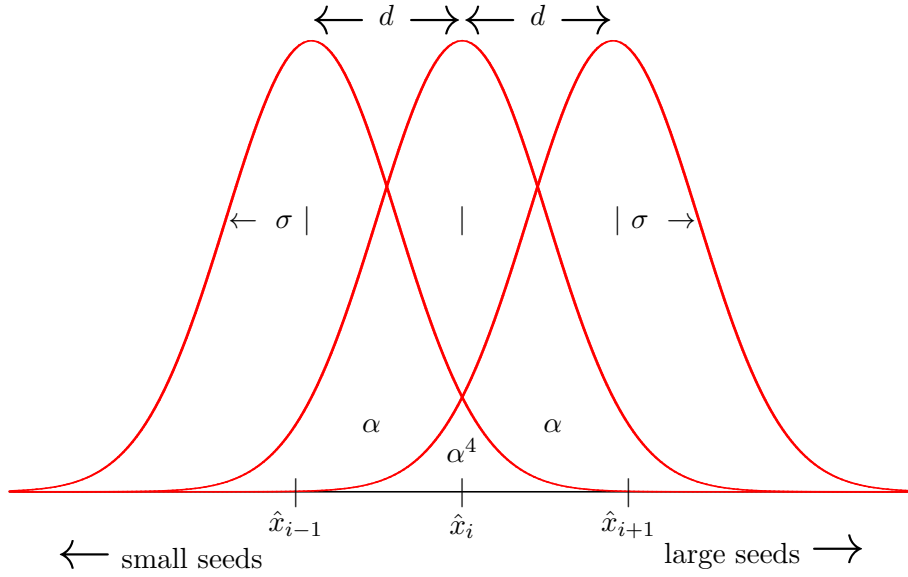


Figure 10.1: Resource usage of three “finch species” consuming seeds of different sizes. The distance between the preferred seed size of neighboring species is  $d$ , and  $\sigma$  is the standard deviation of the Gaussian seed-size preference functions. The niche overlap between neighboring species at distance  $d$  is called  $\alpha$ , and hence the overlap between species at distance  $2d$  is  $\alpha^4$  (see Eq. (10.2)).

this, we normalize with the overlap that a species has with itself,

$$\alpha = \frac{\int_{-\infty}^{\infty} e^{-\frac{x^2}{2\sigma^2}} \times e^{-\frac{|x-d|^2}{2\sigma^2}} dx}{\int_{-\infty}^{\infty} e^{-\frac{x^2}{2\sigma^2}} \times e^{-\frac{x^2}{2\sigma^2}} dx} = e^{-\left(\frac{d}{2\sigma}\right)^2}, \quad (10.1)$$

which is maximally one, i.e.,  $\alpha \leq 1$ . With  $\alpha = e^{-\left(\frac{d}{2\sigma}\right)^2}$ , the niche overlap only depends on the distance  $d$  weighted by the standard deviation  $\sigma$ , and the overlap of a species with itself is indeed one (because at a distance zero,  $\alpha = e^0 = 1$ ). The overlap between the first and the last species in Fig. 10.1 is determined substituting by their distance  $2d$  into Eq. (10.1), i.e.,

$$e^{-\left(\frac{2d}{2\sigma}\right)^2} = e^{-4\left(\frac{d}{2\sigma}\right)^2} = \alpha^4. \quad (10.2)$$

Likewise, one can see that the niche overlap between species at distance  $3d$  will be  $\alpha^9$ .

An ecosystem of  $n$  competing species that are equally distributed at distances  $d$  on a resource axis can therefore be described with the Lotka-Volterra competition model of Eq. (9.20),

$$\frac{dN_i}{dt} = rN_i \left(1 - \sum_{j=1}^n A_{ij}N_j\right), \quad (10.3)$$

where we now know all the elements of the interaction matrix,

$$A = \begin{pmatrix} 1 & \alpha & \alpha^4 & \alpha^9 & \alpha^{16} & \dots \\ \alpha & 1 & \alpha & \alpha^4 & \alpha^9 & \dots \\ \alpha^4 & \alpha & 1 & \alpha & \alpha^4 & \dots \\ \alpha^9 & \alpha^4 & \alpha & 1 & \alpha & \alpha^4 \dots \\ \dots & \dots & \dots & \dots & \dots & \dots \end{pmatrix} \quad (10.4)$$

and where we have given all species the same natural rate of increase,  $r$  (because a different  $r_i$  in Eq. (9.20) play no role in the competitive strength of the species at steady state).

One can analyse this model by increasing its diversity,  $n$ , one by one. A system of two species obeys

$$\frac{dN_1}{dt} = rN_1(1 - N_1 - \alpha N_2) \quad \text{and} \quad \frac{dN_2}{dt} = rN_2(1 - N_2 - \alpha N_1). \quad (10.5)$$

We have learned in Fig. 9.2d that this 2-dimensional ecosystem will have a stable non-trivial steady state whenever  $\alpha < 1$ . Thanks to our definition of the maximal niche overlap one would conclude that two species can be located infinitely close on the resource axis and co-exist. Thus, the critical niche overlap of a 2-dimensional system is  $\alpha = 1$  (or  $d/\sigma \rightarrow 0$ ). Note that this is an “artifact” of using the scaled version of the competition model, i.e., Eq. (9.20). If two species have different birth rates, consumption rates, death rates, and carrying capacities, they will not co-exist when the niche overlap for their limiting resource is very small.

Next consider three species. What would be the maximal niche overlap, or the minimal distance  $d$ , required for co-existence of all three species? This can be analyzed by considering Fig. 10.1 and numbering the species from left to right as  $N_1$ ,  $N_2$ , and  $N_3$ . This is a symmetric system, i.e., the ODEs of  $N_1$  and  $N_3$  should have the same form, and  $dN_2/dt$  should have the strongest competition because it has two direct neighbors, i.e.,

$$\begin{aligned} \frac{dN_1}{dt} &= rN_1(1 - N_1 - \alpha N_2 - \alpha^4 N_3), \\ \frac{dN_2}{dt} &= rN_2(1 - N_2 - \alpha[N_1 + N_3]), \\ \frac{dN_3}{dt} &= rN_3(1 - N_3 - \alpha N_2 - \alpha^4 N_1). \end{aligned} \quad (10.6)$$

The existence and stability of the 3-dimensional steady state can be investigated by testing the invasion of the species in the middle,  $N_2$ , in the steady state of those at the ends. For this invasion criterion one first sets  $N_2 = 0$  to compute the steady state of the 2-dimensional system. Employing the symmetry of the system one sets  $N_1 = N_3$ , and obtains their steady state by solving  $\bar{N} = 1/(1 + \alpha^4)$  from  $1 - N - \alpha^4 N = 0$ . When  $N_2 \rightarrow 0$  the invasion of  $N_2$  is described by  $dN_2/dt \simeq rN_2(1 - 2\alpha\bar{N})$ . This means that co-existence is guaranteed whenever

$$1 - \frac{2\alpha}{1 + \alpha^4} > 0 \quad \text{or} \quad 1 + \alpha^4 - 2\alpha > 0. \quad (10.7)$$

This fourth order equation can be solved numerically as  $\alpha < 0.54$  (or  $d/\sigma > 1.54$ ), which means that the maximal niche overlap of a 3-dimensional system is  $\alpha \simeq 0.54$ .

Since all species approach their carrying capacity,  $\bar{N}_i = 1$ , when  $\alpha = 0$ , one can generalize this approach by considering an  $n$ -dimensional system and gradually increasing  $\alpha$  from zero to one, until some of the species start going extinct. In the script `niche.R` this is performed for a range of values of  $n$ . Because the steady state values of the first and the last species,  $\bar{N}_1$  and  $\bar{N}_n$ , are the largest, as they suffer from only half of the competitive interactions, it is typically the second,  $N_2$ , and the one-but-last,  $N_{n-1}$ , species that go extinct first (see Fig. 10.2a). The results of such an analysis are summarized in Fig. 10.2b, which depicts the lowest niche overlap at which at least one species goes extinct, as a function of the diversity  $n$  of the system. The figure reveals a fast convergence to  $\alpha \simeq 0.63$  (i.e., to  $d/\sigma \simeq 1.3$ ). This niche overlap that is ultimately approached is called the “limiting similarity”, which means that species cannot be too similar. Otherwise they start excluding each other.<sup>1</sup> The value of  $\alpha$  where  $N_2$  and  $N_{n-1}$  go

<sup>1</sup>Remember this when we discuss the neutral model of Hubbell (1979, 2001) below.

extinct actually corresponds to a transcritical bifurcation (see Chapter 12). So instead of tracing at which value of  $\alpha$  a population becomes zero (as we do in the script `niche.R`), one could also trace the largest eigenvalue to test at what value of  $\alpha$  the largest eigenvalue,  $\lambda_{\max} = 0$ .

Finally, one can obtain some intuition why this limiting similarity corresponds to  $\alpha = 0.63$ . Consider the steady state of an infinite version of Eq. (10.3) where all species are the same, i.e.,

$$\frac{dN}{dt} = N(1 - \sum_j A_{ij}N) = N(1 - N \sum_j A_{ij}) \quad (10.8)$$

which has the steady state

$$\bar{N} = \frac{1}{\sum A_{ij}} = \frac{1}{1 + 2\alpha + 2\alpha^4 + 2\alpha^9 + \dots} \simeq \frac{1}{1 + 2\alpha}, \quad (10.9)$$

where in the latter we have ignored all higher order terms of  $\alpha$  for  $k \geq 4$ . Thus, in a large system all species in the middle should therefore approach  $\bar{N} \simeq 1/(1 + 2\alpha)$ . Using this approximation one can write for the first 3 species at the left boundary

$$\begin{aligned} \frac{dN_1}{dt} &= N_1(1 - N_1 - \alpha N_2), \\ \frac{dN_2}{dt} &= N_2(1 - \alpha N_1 - N_2 - \alpha N_3), \\ \frac{dN_3}{dt} &= N_3(1 - \alpha N_2 - N_3 - \alpha N_4) \simeq N_3(1 - \alpha N_2 - N_3 - \alpha \bar{N}), \end{aligned} \quad (10.10)$$

where  $\bar{N}$  in the last equation is given by Eq. (10.9). The steady state of these 3 species at the boundary is defined by 3 linear equations that can be solved (e.g., by Mathematica). Subsequently, solving at which value of  $\alpha$  the second species goes extinct, i.e., solving when

$$\bar{N}_2 = \frac{3\alpha^2 - 1}{(1 + 2\alpha)(2\alpha^2 - 1)} = 0 \quad \text{or} \quad \alpha^3 = \frac{1}{3}, \quad (10.11)$$

gives  $\alpha = 1/\sqrt[3]{3} \simeq 0.58$ . Despite the simplifications this resembles the critical  $\alpha = 0.63$ .

## Infinite resource axis

The original analysis of this model by May (1974) addressed the relationship between the niche overlap and the diversity of the system by also considering an infinite resource axis along which infinitely many species were distributed at distance  $d$ . An infinite system has the mathematical advantage that the effects of the edges disappear, which means that all equations become identical (see Eq. (10.8)). Thanks to this simplification, May (1974) was able to compute the Jacobian of the infinite system, and he could compute the largest eigenvalue of the Jacobian as a function of the niche overlap  $\alpha$ . Because all equations were identical by the assumption of an infinite system, no single species could ever go extinct, and the largest eigenvalue was approaching zero when the niche overlap  $\alpha$  was approaching our limiting similarity of  $\alpha \simeq 0.63$ . In our analysis we were breaking the symmetry of the system by distinguishing the species in the middle from those at the borders, and were obtaining (transcritical) bifurcation points when increasing  $\alpha$ . Because the symmetry could not break in the original infinite system, the largest eigenvalue was just approaching zero. May (1974) therefore had to define variation in the abiotic circumstances that required the value of the largest eigenvalue to remain below some critical negative level. Doing so he obtained a limiting similarity that is very similar to the one derived numerically in Fig. 10.2b. The mathematical analysis of May (1974) is addressed further in one of the extra exercises.

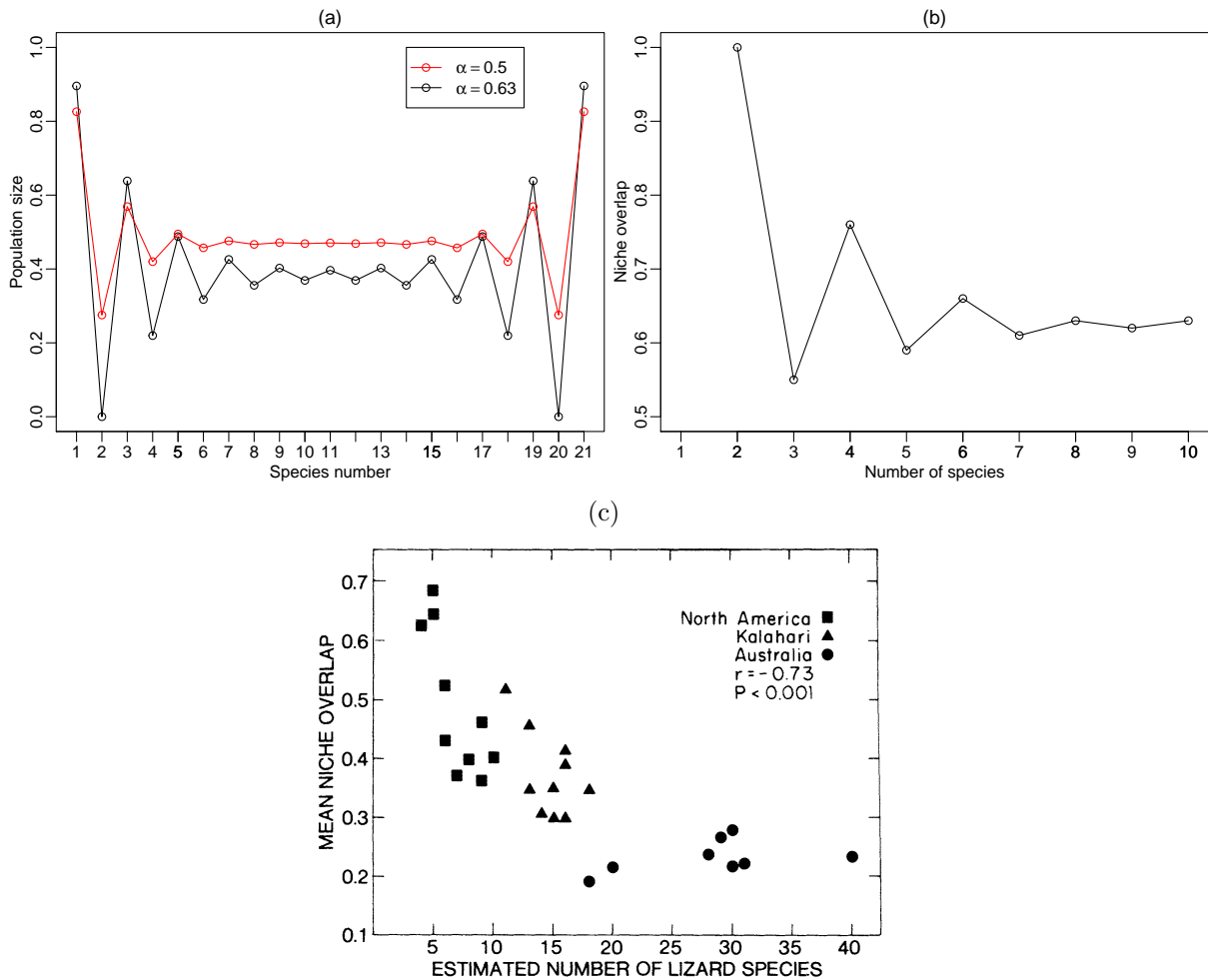


Figure 10.2: Properties of the niche model of Eq. (10.3). Panel (a) depicts the steady state population sizes,  $\bar{N}_i$ , for  $n = 21$  species at the critical niche overlap  $\alpha = 0.63$ , and at a lower niche overlap  $\alpha = 0.5$ . Note that  $\bar{N}_2 = \bar{N}_{20} \rightarrow 0$  when  $\alpha = 0.63$ . Panel (b) depicts the limiting overlap as a function of the diversity,  $n$ , computed numerically with the script `niche.R`. Panel (c) depicts the results of Pianka (1974).

## Lizard man

Pianka (1974) measured the niche overlaps between several species of lizards in various desert habitats from all over the world. He distinguished three niche dimensions: (1) food, as determined from the contents of their stomachs, (2) habitat, and (3) the time of the day at which they were active. These observations were translated into a single measure of the niche overlap by considering both additive and multiplicative measures for defining the total niche overlap. Pianka confirmed that the niche overlap decreased to a limiting value when the diversity of the ecosystem increased (see Fig. 10.2c). This occurred at about 20 species in the data, and around about 10 species in the model (compare Fig. 10.2b with c). A natural solution for this difference was proposed by Rappoldt & Hogeweg (1980) who extended the model into a 2-dimensional niche space, where the Gaussian curves become circular and are tiled in a hexagonal lattice. In such a 2-dimensional lattice there are many more species at the borders of the niche space, and hence it takes a higher diversity for the effects of the borders to peter out.

## 10.2 Stability and Persistence

The relationship between the complexity of a biological system and its stability has been debated over decades. Based on fairly romantic considerations ecologists have liked to think that the more diverse and complex an ecosystem, the higher its degree of stability. However, one could also turn this around by arguing that stable ecosystems have had more evolutionary time to become diverse. Additionally, it remains unclear what one means with the stability of an ecosystem. This could vary from a local neighborhood stability defined by the largest eigenvalue, (i.e., a robustness against minor perturbations around the steady state), to having large basins of attraction (i.e., robustness to macroscopic perturbations), to a mere persistence over time. It is rather obvious that most biological systems are not persisting as stable steady states, because they are all driven by diurnal rhythms, seasonal fluctuations, and/or “random” temporal disturbances. Finally, robustness to invasion by new species can also be considered to be a form of stability. Unfortunately, we have no well-defined modeling approach to study what properties of an ecosystem would make it resilient to perturbations like the removal or introduction of a species.

Classic studies of the properties of random matrices that were used as a model for the Jacobi matrix of a steady state of a random complex system, have facilitated our thinking about the relationship between stability and complexity (Gardner & Ashby, 1970; May, 1972, 1974). Consider an arbitrary steady state of an arbitrary (eco)system, and address the question whether or not this steady state is expected to be stable. To do so, one can write a random Jacobian  $J$ , of a system with  $n$  species. To keep the analysis manageable they posed the following requirements:

1. Let every population have a carrying capacity and the same return time to this carrying capacity. For the Jacobian matrix this means that all elements on the diagonal are scaled to  $J_{ii} = -1$ .
2. The off-diagonal elements of the matrix are set with a probability  $P$ . Thus,  $P$  determines the likelihood that two species are involved in an interaction. Hence  $P$  determines the connectivity of the system, i.e., each species is expected to have  $P(n - 1)$  interactions with other species.
3. The interaction elements that are set are drawn from a normal distribution with mean  $\mu = 0$  and standard deviation  $\sigma$ .

Summarizing, one draws a random matrix with dimension  $n \times n$  of the following form

$$J = \begin{pmatrix} -1 & 0 & 0 & a & 0 & 0 & b & 0 & \dots \\ 0 & -1 & 0 & 0 & 0 & c & \dots & & \\ 0 & 0 & -1 & 0 & \dots & & & & \\ d & \dots & & -1 & \dots & & & & \end{pmatrix}, \quad (10.12)$$

where  $a, b, \dots, d$  are randomly chosen values from a standard normal distribution centered at zero. This matrix is interpreted as the Jacobian of a steady state of an (eco)system. Having drawn such a random Jacobian matrix, the question is how its stability depends on the parameters  $n$ ,  $P$ , and  $\sigma$ . One can use the theory on the largest eigenvalue of large random matrices to prove that the probability that the largest eigenvalue is negative, i.e.,  $\lambda_{\max} < 0$ , is described by

$$\sigma\sqrt{nP} < 1. \quad (10.13)$$

The biological interpretation of this rather abstract analysis is that increasing the number of interactions per species,  $(n - 1)P$ , and/or increasing the absolute interactions strengths,  $\sigma$ , decreases the chance that the steady state is stable. This suggests that complex systems cannot *a priori* be expected to be stable (Gardner & Ashby, 1970; May, 1972, 1974). In the exercises we will suggest that the critical interaction strength scales as function of  $\sqrt{nP}$  because the standard

deviation of the sum of the  $nP$  random variates in each row in the matrix<sup>2</sup> is proportional to  $\sqrt{nP}$ , and that the  $< 1$  in Eq. (10.13) hinges upon the diagonal elements being  $-1$ .

The result of Eq. (10.13) seems to contradict the co-existence of many species in the niche-space model (MacArthur, 1972; May, 1974). However, in the niche-space model the average interaction strength decreases when the diversity increases (see Eq. (10.4)). Increasing the diversity  $n$  therefore implicitly decreases the interaction strength  $\sigma$  in Eq. (10.13). This may also be true for natural systems: when the number of species  $n$  increases, the number of connections per species,  $nP$ , need not increase, and the strength of their connections,  $\sigma$ , may decrease. Another criticism on this analysis is that it only considers one steady state of the system, and that complex systems may have very many steady states, of which only a few need to be stable to guarantee its persistence as a high-dimensional system. Additionally, communities need not be stable and can persist by periodic or non-periodic behavior.

Despite these criticisms, this classic work did change the historical view of “diversity entails stability” into questions like “how do complex systems persist over long periods of time?” and “why are complex systems relatively resistant to macroscopic perturbations?”. Addressing these questions has indeed led to novel results showing that the non-random architecture of natural food webs makes a difference. The fact that most ecosystems have a pyramid structure, having much more biomass at the bottom than at the top, makes that loops within the network tend to have a low weight (Neutel *et al.*, 2002). Weak interactions indeed tend to have a stabilizing effect (McCann *et al.*, 1998; Cui *et al.*, 2021; Gellner *et al.*, 2023), and it was shown for several soil communities that feedback loops caused by omnivory tend to remain weak because of this pyramidal shape (Neutel *et al.*, 2007).

### 10.3 Random assembly

For several decades theoretical ecologists have tried to create complex artificial ecosystems by drawing randomly chosen parameters for new species, and studying which of these species can together form a persistent community (Pimm, 1980; Post & Pimm, 1983; Law & Blackford, 1992; Yodzis, 1989; Roberts, 1974; McCann *et al.*, 1998; Huisman *et al.*, 2001; Rodriguez-Sanchez *et al.*, 2020). Typically most of the randomly assigned species will go extinct, as they could be unviable ( $R_0 < 1$ ), unable to invade into the current state of the system, or become excluded later when other species invade. However, since these studies can allow for a large initial set of random species, the ultimate diversity of such an artificial system could still be large. A major advantage of this approach is that species may persist because the system develops periodic or chaotic behavior, which may circumvent the expected competitive exclusion in equilibrium situations (Law & Blackford, 1992). Investigators have added space, with migration between different areas, and have created systems that become diverse because of spatial heterogeneity, i.e., with different species persisting in different areas (Yodzis, 1989). Tilman diagrams have been studied in high dimensions to study the relationship with productivity and diversity in plant ecosystems (Tilman *et al.*, 1997). We here review a small subset of these randomly parametrized and/or high-dimensional studies to become familiar with the most common approaches, and the results that are typically obtained.

<sup>2</sup>Remember that the linear system  $x' = Jx$  involves sum of random  $J_{ij}$  values as  $x'_i = \sum J_{ij}x_j$ .

## Random Lotka-Volterra models

Roberts (1974) criticized the work on the stability of random Jacobi matrices (Gardner & Ashby, 1970; May, 1972, 1974), arguing that these matrices may include “unfeasible” systems having negative population sizes. Although this criticism is ill-defined, as there are no explicit population sizes in random Jacobi matrices, he illustrated his point by numerically analyzing the stability and the feasibility of a random Lotka-Volterra model,

$$\frac{dN_i}{dt} = N_i \left( r_i - \sum_j^n A_{ij} N_j \right), \quad (10.14)$$

where  $r_i = 1$  for all  $n$  species, the diagonal elements of the interaction matrix were all set to  $A_{ii} = 1$ , and the off-diagonal elements were set randomly to  $A_{ij} = \pm z$ , with equal probability for a positive and negative elements, and a fixed value of  $z$ . Roberts (1974) computed the steady state of Eq. (10.14) by solving the corresponding  $n$ -dimensional algebraic system of linear equations, i.e.,  $\vec{r} - A\vec{N} = 0$ . After computing the inverse of the matrix,  $A^{-1}$ , this solution was given by  $\vec{N} = A^{-1}\vec{r}$  (see the accompanying Ebook (Panfilov *et al.*, 2025) and `roberts.R` for a script). Solving such a linear system indeed does not guarantee that the vector  $\vec{N}$  is strictly positive, and he found that the fraction of feasible (i.e., all  $\bar{N}_i$  positive) steady states decreases with  $z$  and  $n$ .

Nowadays we have fast computers and one can just numerically integrate such a model (see the script `roberts.R`). Doing so one finds that a subset of the species can go extinct, but that the remainder tend to persist in a stable steady state.<sup>3</sup> Thus, although it is unlikely that a complete  $n$ -dimensional system has a stable equilibrium where all species are present, it appears to be quite likely that a subset of the species can coexist in a stable steady state. Moreover, we suggest in the exercises that the likelihood of stability indeed obeys Eq. (10.13). Unfortunately, like the random Jacobi matrix analyses, this analysis remains fairly abstract because it is difficult to envision biological populations corresponding to this model with a random sign-structure of the interaction matrix.

Especially, the assumption that  $A_{ii} = -1$  for all species is open to debate. In the earlier chapters we have seen that consumers need not have any intra-specific competition, i.e., consumers tend to have  $A_{ii} = 0$ . Instead, in the Roberts (1974) model each of the species has a carrying capacity that will be approached when they have weak interactions with the other species (i.e., when all off-diagonal elements  $A_{ij} \rightarrow 0$ ). Thus all species apparently are consumers relying on some limiting resource(s), which enables them to establish a population at carrying capacity. Nevertheless, they also have positive and negative interactions with the other consumers, which one would have to interpret as symbiotic ( $A_{ij} = A_{ji} = +z$ , 25% of the cases), competitive ( $A_{ij} = A_{ji} = -z$ , 25%), or parasitic ( $A_{ij} = +z$  with  $A_{ji} = -z$ ), 50% of the cases). In the exercises you will be challenged to modernize this model by drawing random positive and negative interaction values, and to study a random Lotka-Volterra competition model by restricting the interaction matrix to competitive interactions (i.e., by keeping  $A_{11} = 1$  and drawing all off-diagonal elements  $A_{ij} = A_{ji} \geq 0$ ). Additionally, one can also assign negative  $r_i$  values to a subset of the species to define consumers with a death rate  $r_i$  (Gellner *et al.*, 2023).

<sup>3</sup>When all species survive this steady state has to be identical to the one solved from the linear algebraic system.

## Random pre-defined food chains

Several decades ago, when the first computers became generally available for basic research, theoretical ecologists already created multi-layered food webs by randomly assigning interaction parameters (Pimm, 1980; Post & Pimm, 1983). One early approach was based upon a high-dimensional Lotka-Volterra model like the one provided in Eq. (10.14). They started with a random layer of 6 non-competing resources, by setting all off-diagonal elements to zero, i.e., all  $A_{ij} = 0$ , and setting the diagonal elements,  $0 < A_{ii} < 1$ , and all growth rates,  $0 < r_i < 1$ , to random values drawn from a uniform distribution, for the first six species. Subsequently random consumers, and later consumers of these consumers were added by choosing an  $r_i$  randomly from the interval  $(-0.1, 0)$  to allow for a density-independent death rate, by setting their  $A_{ii} = 0$  to not allow for intra-specific competition among consumers, and by assigning a fraction of the off-diagonal elements,  $A_{ij}$ , to random values representing consumption of an existing species, or being consumed by an existing species. These mass-action consumption parameters,  $A_{ij}$ , were sampled from uniform distributions, with the constraint that the positive  $A_{ij}$  parameter of a predator  $i$  eating prey species  $j$  was on average 10-fold lower than the corresponding consumption rate  $A_{ji}$  (to model the typical 10% trophic conversion). Novel species were only allowed to enter the system after testing whether they were able to invade ( $R_0 > 1$ ), and after testing that the new species would not form a loop, like A eats B eats C eats A (Post & Pimm, 1983). Each successful invasion adds a row and a column to the interaction matrix,  $A_{ij}$ . At the time this was quite a heroic attempt. For instance, it was not feasible to numerically solve high-dimensional systems of ODEs. Rather Post & Pimm (1983) also solved the steady states by computing the inverse of  $A$  to solve the linear algebraic system  $r_i - \sum A_{ij}N_j = 0$ , and disregarding solutions having negative population densities.

Their major findings were that (1) the number of species grows over time (but  $n$  remained fairly small), (2) the larger the number of resident species, the more difficult it is to invade, (3) that the return time,  $T_R$ , of the full system at steady state decreases when the diversity increases, and (4) that invaders that eat little, but grow well, and die slowly, do best. Thus, the system becomes more resistant to invaders over time, which is a form of robustness, but approaches a lower degree of stability as measured by the largest eigenvalue. The former was recently confirmed in microbial communities that indeed are more resistant to invading species when the diversity is high (Spragge *et al.*, 2023).

Later it was realized that communities of primary resources, consumers, and consumers of consumers, need not persist in a stable equilibrium, as species can co-exist indefinitely on a limit cycle or a chaotic attractor (Law & Blackford, 1992; McCann *et al.*, 1998). In these two papers the network of interactions in the community was predefined, e.g., as a linear food chain, a branched food chain with two competing consumers at the same level, or a chain with consumers eating from various levels (i.e., omnivores), and the interactions strengths were drawn randomly. It was indeed found that for a large fraction of the parameter realizations the full community was persisting by periodic or aperiodic behavior in the absence of an  $n$ -dimensional stable equilibrium (Law & Blackford, 1992). Interestingly, it was shown that adding weak interactions to such networks facilitated the persistence of the full community (McCann *et al.*, 1998; Marsland *et al.*, 2020; Cui *et al.*, 2021).

## Random high-dimensional resource-consumer models

Several authors have studied the general Tilman model for  $n$  cellular consumers competing for  $m$  essential resources in a chemostat (Tilman, 1982),

$$\begin{aligned} \frac{dN_i}{dt} &= N_i(b_i f_i(R_1, \dots, R_m) - d_i), \quad \text{for } i = 1, \dots, n \\ \frac{dR_j}{dt} &= D(S_j - R_j) - \sum_i^n c_{ij} b_i f_i(R_1, \dots, R_m) N_i, \quad \text{for } j = 1, \dots, m \\ \text{with } f_i() &= \min\left(\frac{R_1}{h_{i1} + R_1}, \dots, \frac{R_m}{h_{im} + R_1}\right), \end{aligned} \quad (10.15)$$

where  $f_i()$  takes the minimum of all Monod saturation functions for each consumer to define its actual birth rate  $b_i f_i()$ . The resource is consumed proportional to this birth rate multiplied with the amount of resource,  $c_{ij}$ , contained in each cell of species  $i$ . The model would therefore apply well for algae or bacterial growing in a chemostat (or bacteria in the gut microbiome). The concentration of resources in the inflow is defined by the  $S_j$  parameters,  $D$  is their turnover rate (with  $1/D$  the residence time), and if the consumers are largely lost by being washed out from the chemostat, one would set  $d_i = D$  (Huisman & Weissing, 1999; Huisman *et al.*, 2001). Drawing random values for the saturation constants,  $h_{ij}$ , and the amount of resource contained in each cell,  $c_{ij}$ , one can study how many consumers can coexist on a limited number of resources,  $m$ . One ‘‘realistic’’ scenario considered by Huisman *et al.* (2001) was that species containing a large amount of a particular resource also need a high concentration of this resource to achieve a half-maximal birth rate, i.e., that  $h_{ij}$  and  $c_{ij}$  are positively correlated.

Huisman & Weissing (1999) studied this model in parameter regime where the populations fluctuate (periodically or chaotically), to show that in such non-equilibrium situations many consumers can be maintained on a limited number of resources, i.e., they proposed that the ‘‘Paradox of the plankton’’ (Hutchinson, 1961) can be solved in non-equilibrium situations. Remember that we have seen in Eq. (5.6) that the non-trivial steady state of a 2-dimensional Monod-saturated consumer-resource model with a non-replicating resource tends to be stable. Huisman & Weissing (1999) therefore enabled the high-dimensional system to oscillate by defining cyclic dependencies between the consumers, e.g., when species succeed each other by being the better competitor for a unique resource, while they are limited more by another resource, that the next species is the better competitor for (Huisman & Weissing, 1999). Because such a cyclic topology need not be realistic (Huisman *et al.*, 2001), we have an exercise where you can study the same competitive system with a more random network of interactions in the exercises, e.g., by drawing random values for the saturation constants,  $h_{ji}$ , and assuming the  $c_{jis}$  to be proportional (which is scenario 3 in Huisman *et al.* (2001)).

Rodriguez-Sanchez *et al.* (2020) study a somewhat similar system with replicating resources to study under what parameter regimes chaos or periodic behavior is to be expected. They define a high-dimensional form of the Monod-saturated consumer-resource model that is parameterized on freshwater plankton systems. They consider additive resources, i.e.,

$$\begin{aligned} \frac{dN_i}{dt} &= \frac{egN_i \sum_j^m S_{ij} R_j}{h + \sum_j^m S_{ij} R_j} - dN_i, \\ \frac{dR_j}{dt} &= r_j R_j \left(1 - \sum_i^m A_{ij} R_i / K\right) - gR_j \sum_i^n \frac{S_{ij} N_i}{h + \sum_k^m S_{ik} R_k}, \end{aligned} \quad (10.16)$$

for  $i = 1, \dots, n$  consumers and  $j = 1, \dots, m$  resources, respectively. Note that we have derived a similar  $n$ -dimensional functional response in Eq. (7.18), and that this function allows for a

“kill-the-winner” effect (Winter *et al.*, 2010), because a heavy consumption of one particular resource, i.e., a large  $S_{ij}R_j$  element, reduces the consumption of the other resources. Here  $r_i$  is the maximal growth rate of the resource,  $K$  is a carrying capacity,  $g$  is a grazing rate,  $e$  is a conversion factor,  $h$  is the saturation constant of the saturation function,  $d$  is the death rate of consumers,  $A$  the  $m \times m$  competition matrix between resources, and  $S$  the  $n \times m$  consumer-preference matrix (Rodriguez-Sanchez *et al.*, 2020). They vary the total number of resources and consumers, but initialize the system with more resources than consumers, i.e.,  $n : m = 2 : 3$  (Rodriguez-Sanchez *et al.*, 2020). The competition coefficients,  $A_{ij}$ , were drawn randomly from different uniform distributions centered below, around and above one (keeping  $A_{ii} = 1, \forall i$ ).

They run simulations with strong interspecific competition ( $A_{ij} > A_{ii}$ ), with near-neutral systems ( $A_{ij} \simeq A_{ii}$ ), and with systems where the intra-specific competition ( $A_{ij} < A_{ii}$ ) dominates. Since not all resource species survive in these simulations, they may find non-equilibrium situations where the number of persisting consumers outnumbers the number of surviving resource (despite starting with  $n : m = 2 : 3$ ). The major result is that this system is most likely to be chaotic or periodic, when the competition coefficients are very similar (i.e., in the near-neutral  $A_{ij} \simeq 1$  regime). This establishes a connection between explaining high diversity with non-equilibrium behavior (Huisman & Weissing, 1999), and with neutral competition (Hubbell, 1979, 2001). In the exercises you can study this system to see whether or not the number of persisting consumers is likely to outnumber the number of surviving resources in this parameter regime.

### Founder effects in space

Yodzis (1978) studied a spatial model where consumers obeying a Lotka-Volterra competition model migrate between several areas (all having identical environmental parameters). He was interested in parameter regimes where for most pairs of species the competitive interaction would be strong and hence define founder-controlled relationships (i.e., the unstable steady state of Fig. 9.2c). Distributing  $n$  consumers over  $m$  areas, using the general Lotka-Volterra competition model to define the competitive interactions in each area, and diffusive flux between the areas, one ends up with a model ecosystem of  $n \times m$  equations,

$$\frac{dN_{a_i}}{dt} = r_i N_{a_i} \left( 1 - \sum_{j=1}^n A_{ij} N_{a_j} \right) + \sum_{b=1}^m D_{ab} (N_{b_i} - N_{a_i}), \quad (10.17)$$

for  $a = 1, \dots, m$  and  $i = 1, \dots, n$ . Here  $N_{a_i}$  defines the population size of species  $i$  in habitat  $a$ . The flux of individuals of species  $i$  between habitats  $a$  and  $b$  is described by a symmetric “dispersal” matrix  $D$ , where  $D_{ab} = D_{ba}$  is inversely related the distance between habitat  $a$  to  $b$ . The net flux of individuals between two habitats is then given by  $D_{ab}(N_{b_i} - N_{a_i})$ , which is like a diffusion term where the net flux is proportional to the difference in the concentrations. All species have the same intra-specific competition by setting  $A_{ii} = 1, \forall i$ , and the natural rates of increase were all scaled to  $r_i = 1$ . The off-diagonal competition coefficients,  $A_{ij}$ , and the dispersal rates,  $D_{ab}$ , were drawn randomly. The system was initialized by distributing the species at low densities sparsely over the areas. The interaction strengths were drawn randomly from various distributions centered around a relatively high mean, such that typically most of the off-diagonal,  $A_{ij}$  elements were larger than one (i.e., larger than the intra-specific competition,  $A_{ii} = 1$ ). The fraction of off-diagonal elements larger than one was counted and expressed as  $C = P(A_{ij} > 1)$ . Yodzis (1978) performed many simulations starting with different numbers of species,  $3 \leq n \leq 80$ , and for different values of the average competition strength, i.e., for

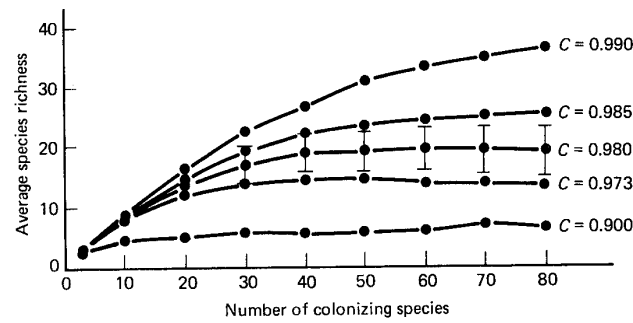


Figure 10.3: Figure 5.5 in Yodzis (1989) page 144: the steady state diversity as a function of the initial number of species, for various intensities of the competition  $C = P(A_{ij} > 1)$ .

$0.9 \leq C \leq 0.99$ . The average number of species persisting in these simulations is depicted in Fig. 10.3.

Increasing the competition strength increased the total diversity of the communities distributed over all areas (Fig. 10.3). One readily achieves quite diverse ecosystems, e.g., almost 40 of the  $n = 80$  species persist when  $C = 0.99$ . This seems unexpected (Gardner & Ashby, 1970; May, 1972, 1974; Grime, 1997; Hanksi, 1997; McCann *et al.*, 1998), but the reason why the diversity increases with competition strength in these simulations is the spatial embedding, i.e., in each habitat one initially finds only a small subset of the species. Having many founder controlled situations the species that settle initially in a habitat tend to win the competition. Basically the model is a “resident always wins” system, where the final diversity is largely determined by the number of species that are distributed initially over the habitats. Diversity does not come about by stable coexistence but by the spatial distribution of the species over the habitats.

## 10.4 Neutral coexistence

A null-model for explaining the high diversity of ecosystems and of microbial communities is the neutral model proposed by Hubbell (Hubbell, 1979, 2001). In its most simple form one considers a community of individuals of several species, and at each time point one randomly picks an individual to die, and replaces the empty spot by an offspring of a randomly selected individual from the local community (and/or from a large community elsewhere). In case the newborns are sampled from the local community only, one needs to add a “mutation” rate whereby new species are being formed, i.e., with some small probability the newborn is a new species (otherwise species will go extinct). If the model is completely neutral, meaning that all death rates and birth rates are equal, there will be no competitive exclusion because all species have the same fitness. This model readily accounts for highly diverse communities. Several properties of this stochastic model can be captured by analytically derived equations (Etienne, 2007). Surprisingly, this simple neutral model lacking any form of ecology, tends to be in good agreement with experimental data. Most importantly, neutral theory very reasonably describes the measured abundances of species in several ecological and microbial communities (Caswell, 1976; Hubbell, 1979; Etienne, 2007; Woodcock *et al.*, 2007). This has spurred a lot of debate because biologists tend to think that –besides migration– these species are involved in various types of ecological interactions (like depletion of resources by consumption, competition, mutualism, and cross-feeding).

This neutral model where a species going extinct in a local community can be re-introduced by

individuals from elsewhere, resembles the 1-dimensional metapopulation model of Levins (1969) and Levins & Culver (1971) that we analyzed in one of the exercises in Chapter 3. Variants of this metapopulation model has been used as a paradigm system for the “Single Large Or Several Small” (SLOSS) discussion on the optimal design of fragmented ecosystems (Hanski, 1998). These metapopulation models in turn are built upon the famous Island theory (MacArthur & Wilson, 1967) for the species richness on islands receiving immigration of individuals from a large continent. Island theory also ignores the abundances of the species, and only keeps track of the species richness,  $n$ , on an island,

$$\frac{dn}{dt} = i(N - n) - en , \quad (10.18)$$

where  $n$  is the number of species on an island,  $N$  is the total number of species on the continent, and  $i$  and  $e$  are the immigration and extinction rates. Because the steady state richness of Eq. (10.18) is defined by a balance of the immigration and extinction rates, i.e.,  $\bar{n} = iN/(i + e) < N$ , small islands (high extinction) that are far from the continent (low immigration) are expected to have the lowest diversity. Hubbell’s neutral models do describe the abundance of each species (Hubbell, 1979, 2001).

## 10.5 Cross-feeding

Microbial communities, like the microbiome in our gut or bacterial ecosystems in the soil, are famous examples of highly diverse and complex communities also exhibiting the paradox of the plankton (Hutchinson, 1961). An important new factor in microbial systems is the secretion of novel resources by the consumers, which is called “cross-feeding” (Goldford *et al.*, 2018; Dal Bello *et al.*, 2021). These novel resources are typically metabolic byproducts produced by the microbiota after consuming a primary resource. Since the consumption of these byproducts by other microbes can lead to the production of yet other metabolic byproducts, one obtains networks where consumers create novel niches that may be exploited by other consumers, which in a recursive manner can again create novel niches. Although novel niches should become more “narrow” (smaller) because somehow energy needs to be conserved, cross-feeding should be able account for high diversity of a community at steady state, since by even maintaining just a single species within each niche, creating novel niches allows for a higher diversity.

Models for cross-feeding tend to consider chemostat equations, and tend to use mass-action consumption terms (Goldford *et al.*, 2018; Dal Bello *et al.*, 2021). In two recent papers, the formation of novel metabolic byproducts has been chosen randomly (Goldford *et al.*, 2018), or has been based upon the stoichiometry of the metabolites (Dal Bello *et al.*, 2021). In both papers the biomass, or energy content, of metabolites is conserved by defining fractions summing up to one (Goldford *et al.*, 2018; Dal Bello *et al.*, 2021).

Dal Bello *et al.* (2021) define a stoichiometric matrix based upon known metabolic pathways, and consider a chemostat where every consumer,  $N_i$ , feeds upon a single resource,  $R_i$ ,

$$\begin{aligned} \frac{dN_i}{dt} &= (1 - \alpha_i)b_iR_iN_i - wN_i , \\ \frac{dR_i}{dt} &= w(\hat{R}_i - R_i) - b_iR_iN_i + \sum_j S_{ij}\alpha_jb_jR_jN_j , \end{aligned} \quad (10.19)$$

where  $b_i$  is a mass-action consumption rate (also defining the birth rate of the consumer), and  $\alpha_i$  defines a fractional “leakage” parameter. The  $N_i$  concentration is therefore scaled by the energy

content its resource.  $\hat{R}_i$  is the concentration of resource  $i$  in the supply (which is zero for all novel metabolic byproducts). The stoichiometric matrix  $S$  defines whether the  $i$ th metabolite is produced when metabolite  $j$  is consumed (Dal Bello *et al.*, 2021). The chemostat starts with  $n$  consumers specifically feeding upon the  $n$  resources in the supply, which will lead to additional resources being formed, allowing additional consumers to invade (invasion is not represented in Eq. (10.19)). In their paper, the properties of large microbial communities formed by the model were compared with experimental measurements (Dal Bello *et al.*, 2021). In the exercises you will be asked to simplify this model for a situation with one resource in the source and one metabolic byproduct, to better understand the mechanisms underlying Eq. (10.19).

Goldford *et al.* (2018) define a somewhat more complicated model because they allow each resource to be consumed by several bacterial species. They also extend standard mass-action resource-consumer models with the formation of novel resources, i.e.,

$$\begin{aligned}\frac{dN_i}{dt} &= N_i \left( \sum_j C_{ij} A_{ij} R_j - w \right), \\ \frac{dR_j}{dt} &= w(\hat{R}_j - R_j) - \sum_i A_{ij} N_i R_j + \sum_i \sum_k S_{i,jk} A_{ik} N_i R_k,\end{aligned}\quad (10.20)$$

where  $C$  is a matrix defining the conversion rates from resource  $j$  into species  $i$ ,  $S_i$  is a species-specific stoichiometric matrix, with  $S_{i,jk}$  defining the number of molecules of resource  $j$  secreted by species  $i$  per molecule of resource  $k$  it has taken up. The interaction matrix  $A$  collects the mass-action consumption rates of species  $i$  on resources  $j$ .  $\hat{R}_i$  is the concentration of resource  $i$  in the supply, which is zero for all novel metabolic byproducts, and  $w$  is the dilution rate of the chemostat. The energy (or biomass) of the resource is conserved because the conversion rates,  $C_{ij}$ , are scaled by the secretion rates, i.e.,  $C_{ij} = c_j - \sum_k S_{i,jk} c_k$ , where  $c_j$  is the maximum energy (or biomass) supplied by resource  $j$  (Goldford *et al.*, 2018). The co-existence of several bacterial species was studied in chemostats where bacteria are feeding on various carbon sources, like glucose, citrate and/or leucine. It was shown that several species can co-exist on a single resource because novel metabolic by-products are secreted into the solution (Goldford *et al.*, 2018). These matrixes were defined by drawing random parameters for hundreds of species, and it was demonstrate that a model like this can account for data where many species co-existed in equilibrium with just a limited number of resources in the supply, and species form functional groups specialized on particular resources (Goldford *et al.*, 2018). In the exercises you will confirm that Eq. (10.20) and Eq. (10.19) become identical in a situation with one resource in the source and one metabolic byproduct.

Both models consider additive resources and mass-action consumption rates. For the resources studied in these experiments (Goldford *et al.*, 2018; Dal Bello *et al.*, 2021), where species can grow on single compounds, the resources should indeed be substitutable. Moreover, bacteria have evolved mechanisms like the lac-operon, to readily switch between different resources (Jacob & Monod, 1961). However, bacterial consumption is typically best explained by a Monod-saturation (Monod, 1949), and not by mass-action. Liao *et al.* (2020) define models for a variety of cross-feeding scenarios using Monod-saturated feeding functions resembling Eq. (10.15).

## 10.6 Summary

The simplicity of the scaled Lotka-Volterra competition model has allowed one to formulate interesting and understandable models for large communities. When a sufficient number of species

is packed along a (long) resource axis their degree of competition approaches a fixed niche overlap corresponding to a limiting similarity. Large communities of randomly interacting species have been studied by analyzing the properties of random matrices that were interpreted to represent the Jacobi matrix of such communities, by solving the steady state of randomly parametrized systems of ODEs, and/or by numerical integration of such systems. Communities can persist by approaching a stable equilibrium, a limit cycle, or a chaotic attractor. Such aperiodic behavior can allow for the persistence of multiple consumers on fewer resources. One typically finds that only a small subset of a randomly constructed system persists. Spatial heterogeneity is an important factor allowing for diversity over a combination of different communities, species that invade or evolve may be quite similar to resident species allowing for neutral competition, and consumers can modify the environment thus creating novel niches (e.g., by cross-feeding). Thus, although complex random communities are unlikely to have a stable steady state, answering the question on the relationship between system complexity and its persistence, requires more than just neighborhood stability. We at least need to consider non-equilibrium persistence, robustness to invasion by novel species, spatial heterogeneity, near-neutral competition, and the emergence of novel niches by resident species.

## 10.7 Exercises

### Question 10.1. Invasion criterion

Consider a species immigrating into an area in which two other species are present that do not compete with each other. Each of these two species therefore has a density equal to their carrying capacity, and we let the new species compete equally with the other two species. Consider the case where the carrying capacities are the same for all three species (which could be achieved by scaling).

- Consider a situation where competition takes place in a one dimensional resource space like the one depicted in Fig. 10.1. Redraw this figure for the system where the established species do not compete, and where the new species competes with both.
- Make an ODE model of three equations.
- Determine the parameter conditions for successful invasion of the third species in the steady state of the other two, and give a biological interpretation in terms of competition strengths.

### Question 10.2. Random Jacobian (R-script)

On the website we provide an R-script `gardner.R` that fills a random fraction,  $P$ , of the off-diagonal elements of a matrix with random numbers drawn from a normal distribution with an average  $\mu = 0$  and a standard deviation  $\sigma$ . All diagonal elements are set to  $-1$ , and the largest eigenvalue,  $\lambda$ , is calculated. Interpreting this random matrix as the Jacobian of some dynamical system you can use this script to numerically repeat the analysis of Gardner & Ashby (1970) and May (1972, 1974).

- What is the largest eigenvalue when the connectivity,  $P$ , is very low?
- Can you confirm their result that  $\lambda < 0$  when Eq. (10.13) holds?
- The consumers in the models we have discussed typically do not have  $J_{ii} = -1$  diagonal elements when we derived the Jacobian of their steady states. How do results depend to the value of the diagonal elements? How do the results change when the diagonal elements have different values?
- The second half of this script provides a model of a paper reporting opposite results (Cui *et al.*, 2021). In a similar analysis they conserve the total interaction strength per species when the connectivity of the matrix is increased. It would be an interesting project to understand their analysis and discuss whether or not it contradicts Eq. (10.13). Then note that the same

group also studied simplified large scale models for microbial diversity (Marsland *et al.*, 2020).

**Question 10.3. Roberts' random Lotka-Volterra model (R-script)**

In this chapter we shortly reviewed the work of Roberts (1974), who argued that the work of Gardner & Ashby (1970) and May (1972, 1974) incorrectly allowed for negative population sizes, i.e., for unfeasible systems. To better understand his criticism on their results obtained with random Jacobi matrices we ask you to repeat his work using the script `roberts.R`. The script modernizes the model somewhat by redefining  $z$  as an average, i.e., by drawing the off-diagonal  $A_{ij}$  elements from a normal distribution with an average of  $+z$  or  $-z$ . This prevents undesired symmetries due to species having identical interactions, and with a small standard deviation should not have a major impact. Moreover, it could be interesting how results change when one allows for a larger standard deviation.

- Study how the diversity of the system, and the likelihood that a system is stable and/or feasible, depends on the interaction strength,  $z$ , and the maximum diversity  $n$ . Hint, remember that Eq. (10.13) suggested that stronger interactions decrease the likelihood of finding a stable steady state, and that this scales with  $\sqrt{n}$  in a fully connected system.
- Do the results change when the species have different growth rates,  $r_i$ ? Hint `r<-rnorm(n,1,0.1)` draws  $n$  growth rates for a normal distribution with mean 1 and standard deviation 0.1.
- Do the results change when the diagonal elements are not all equal to one?

**Question 10.4. Random Lotka-Volterra competition models (R-script)**

We also concluded that the work of Roberts (1974) remains somewhat abstract because the model defines consumers experiencing resource-independent symbiotic interactions, interference competition, or parasitic interactions with all other species. We therefore ask you to repeat the analysis with a well-defined random Lotka-Volterra competition model. A good start would be a model for resource competition where all off-diagonal elements are positive and smaller than one,  $0 < A_{ij} < 1$ , and where interactions are symmetric,  $A_{ij} = A_{ji}$ , and where species could have different birth and death rates, e.g.,  $dN_i/dt = b_i N_i (1 - \sum_j^n A_{ij} N_j) - d_i N_i$ , for  $i = 1, 2, \dots, n$ .

- Define such a model in R, and/or make use of the `randomCompetition.R` script.
- Setting  $b_i = 1$  and  $d_i = 0$  for all  $i$ , makes the model identical to that of Roberts. Study how having competitive interactions only changes the relationship between diversity of the system and the average interaction strength and the maximum number of species  $n$ .
- Do the results change when the birth rates are not identical? Do they change when the death rates are not identical?
- Compare the properties of the species that survive with those that are excluded.
- You can also write expressions for the average population sizes,  $\bar{N}$ , and the average total interaction strength,  $\bar{F}$ , for a system where are species survive.

**Question 10.5. Control by parasites**

Many species of birds in their natural environment are infected with parasites and viruses. Consider a population of birds with a birth rate that declines linearly with the population size, and with a death rate that is independent of the population density. Let the individuals be susceptible to an infection with a parasite that increases the death rate somewhat, but hardly affects the birth rate. Assume that transmission of parasites occurs upon contacts between infected and susceptible individuals, and obeys mass action kinetics. Let there be no vertical transmission, i.e., the parasite is not transmitted to eggs.

- Write a natural model.
- What is the  $R_0$  and the carrying capacity of the population in the absence of the parasite?
- What is the  $R_0$  of the infection?
- What is the population density of the susceptibles when the parasite is endemic?
- Suppose this bird species competes with related bird species that occupies the same niche, but has a somewhat shorter life span, and is not susceptible to the parasite. Write a natural

model for the 3-dimensional system.

- f. Do you expect the resistant bird species to be present?
- g. What would you expect for a large community of bird species, all sharing the same resource, but each being susceptible to a host specific parasite species?

### Question 10.6. Cross-feeding

The model of Eq. (10.19) considered several bacterial species in a chemostat each feeding upon a unique resource, with the potential of leaking metabolic byproducts that form novel resources for other bacteria.

- a. Construct a specific example of this model for the situation with a single resource in the source, e.g., saccharose (table sugar), which is bi-saccharide composed of glucose and fructose, and a bacterial species using half of this sugar (i.e., glucose) for this own growth, while leaking the other (i.e., fructose) into the environment. Define a second bacterial species fully using fructose for its growth. In the original model the contribution of compounds within a resource was scaled by their energy content, which had to be conserved, i.e.,  $\alpha_i < 1$ . Here we can assume that the two components are equally nutritious, i.e.,  $\alpha_1 = 0.5$ . Define the new model by writing out all equations and removing the sum term.
- b. What is steady state of the model? Can you use this to define parameter conditions for presence of both bacteria?
- c. Formulate the same situation in the model of Eq. (10.20). Are both cross-feeding models defined in the Chapter identical for this bi-saccharide in the source?

### Question 10.7. Neutral theory of biodiversity

Does the fact that Hubbell's neutral model can account for measured species-abundance distribution in several ecological and microbial communities demonstrate that the abundances of these species are hardly affected by ecological interactions (like competition, cross-feeding, and consumption)? If not, how would you disprove such a seemingly perfect agreement?

## Extra questions

### Question 10.8. Huisman (R-script)

To facilitate the comparison of the R-script `huisman.R` with the model defined in their paper, we here first repeat Eq. (10.15) in the original notation of the Huisman & Weissing (1999) paper:

$$\begin{aligned} \frac{dN_i}{dt} &= N_i(\mu_i(R_1, \dots, R_m) - D), \quad \text{for } i = 1, \dots, n \\ \frac{dR_j}{dt} &= D(S_j - R_j) - \sum_i^n c_{ij} \mu_i(R_1, \dots, R_m) N_i, \quad \text{for } j = 1, \dots, m \\ \text{with } \mu_i() &= r_i \min \left( \frac{R_1}{K_{i1} + R_1}, \dots, \frac{R_m}{K_{im} + R_1} \right), \end{aligned}$$

In the R-script `huisman.R` we allow for `nr` different resources, i.e.,  $m = nr$ , and we define a potentially endless list of consumers, i.e.,  $n = 1, 2, \dots, \infty$ , each having a birth rate  $r_i$ , a vector of  $m$  randomly chosen saturation constants,  $K_{ij}$ , and a vector of  $m$  resource contents,  $c_{ij}$ . The birth rates of all consumers are collected in the vector `r`, the vectors of saturation constants in the list `Ks`, and the vectors of resource contents in the list `Cs`. To not allow for consumers with low saturation constants for all resources the average of the  $m$  saturation constants is scaled to 0.5 for every invader, i.e., `Ki <- runif(nr, 0, 1); Ki <- 0.5*Ki/mean(Ki)`, and by default the resource constants correlate with the saturation constants, i.e., `Cs[[i]] <- 0.05*Ki*rnorm(nr, 1, 0.01)` (Huisman *et al.*, 2001). A total of `Ninvaders` consumers is introduced sequentially. If a new consumer cannot invade into the current state of the system, new

parameters are drawn until a successful colonist is found (this may take many trials after the community has filled up). Typically only a small subset of them can co-exist on  $m$  resources. This is reported at the end by the variable `Npresent`.

- Does this procedure of letting random consumers sequentially invade lead to the aperiodicity that is required for having more consumers than resources?
- Is this more easy when starting with more resources, i.e., after increasing  $m$  in the R-script?
- What kind of consumers is this procedure selecting for? Why is the script not report the average  $h_{ij}$ ?

#### Question 10.9. Scheffer (R-script)

The R-script `scheffer.R` implements Eq. (10.16) using a pre-defined  $m \times m$  competition matrix,  $A$ , between the resources, and a  $m \times n$  interaction matrix,  $S$ , defining the consumption rates. In the script `nr` defines  $m$ , the number of resources, and `nn` defines  $n$ , the initial diversity of consumers. Both resources and consumers start at a small random initial density. The off-diagonal elements of the competition matrix are drawn from a uniform distribution centered at  $1 + \text{eps}$ , with a given width  $w$ , i.e., `runif(nr*nr, 1+eps-w, 1+eps+w)`. The diagonal terms are equal to 1. When the parameter `eps` is negative the off-diagonal  $A_{ij}$  elements tend to be smaller than the diagonal  $A_{ii} = 1$  elements, when `eps` is positive the interspecific competition tends to be stronger than the intra-specific competition, and they call the `eps=0` case “near-neutral” competition (Rodriguez-Sanchez *et al.*, 2020). They vary `eps` between -0.8 and 0.8 and set the width to `w=0.1`. Have a look at the (short) paper to see what behavior they find over this range from weak to strong inter-specific competition.

- Is there a range of `eps`-values with attractors having more consumers than resources?
- Does this depend on the initial diversity of resources and consumers?
- What kind of consumers is this procedure selecting for?

#### Question 10.10. Monopolization

In the scaled Lotka-Volterra model of Eq. (9.20) we have seen that the natural rate of increase of a species,  $r_i$ , has no effect on the competitive ability of a species. We know this is a consequence of the scaling because we also know that it is the species with the lowest resource requirements,  $R_i^*$ , that is the best competitor, and that  $R_i^*$  depends on several parameters, including the birth and death rates, and hence the natural rate of increase  $r_i = b_i - d_i$ . In the model of Yodzis (1989) the natural rates of increase were also removed, see Eq. (10.17).

- Do you expect that if species were to have different growth rates, that those with fast growth rates would be expected to survive better in the simulations?
- Would this make a difference for the general conclusion that the diversity increases with the intensity of the competition?

#### Question 10.11. Symbiosis

This book has a strong emphasis on the competition between populations. This seems a rather negative view on biology because many populations are also involved in symbiotic interactions. In ecology one distinguishes two basic forms: obligatory symbionts cannot grow in the absence of each other, and facultative symbionts help each other but do not strictly require each other.

- Write a model for two symbiotic populations that strictly require each other, and study your model by phase plane analysis (a model is available as the file `symbiosis.R`).
- Change the previous model in an asymmetric symbiotic interaction. Let the first species be dependent on the second, and let the second be ignorant of the first. An example would be saprophytes.
- Write a model for a facultative symbiosis.
- Can you change the latter model into a model of obligatory symbionts by just changing the parameters?

#### Question 10.12. Infinite niche space (Challenging)

In an infinite implementation the niche model we have seen in Eq. (10.9) that all species have

the same steady state

$$\bar{N} = \frac{1}{\sum A_{ij}} = \frac{1}{1 + 2\alpha + 2\alpha^4 + 2\alpha^9 + \dots} .$$

- a. What is the Jacobian corresponding to this steady state? Hint: do not substitute the expression for the equilibrium density, but write  $\bar{N}$ , and observe that the elements on the diagonal can be written as  $1 - \bar{N} - \sum A_{ij}\bar{N}$ .
- b. Can one obtain the stability of the system directly from the interaction matrix  $A$ , or should one first compute the Jacobian?



# Chapter 11

## Maps

The models considered hitherto have neglected externally driven oscillations, i.e., periodic forcing, and have mostly been formulated in autonomous ordinary differential equations. Ecological models sometimes implement seasonal variation by means of sine or cosine function influencing a few of the parameters of the model (we have an exercise on a seasonal algae-zooplankton model proposed by Scheffer *et al.* (1997)). Insect populations are also strongly influenced by the season, and many of the insect species in the temperate climate zones have a relatively short season in which they are active, and a long period around winter during which they survive as larvae. Because the growth season is short, insect populations are often modeled with maps, or difference equations, that describe the population size in the next year as a function of the population size in the current year. Since the behavioral properties of maps differ significantly from those of ODEs we will first cover some theory on maps, and then derive the Beverton-Holt model ourselves from a seasonally reproducing insect population.

### 11.1 Stability

First consider one-dimensional maps for the growth of a single population, i.e.,

$$N_{t+1} = f(N_t) , \quad (11.1)$$

where  $f()$  is an arbitrary function mapping the population size at time  $t$  to a new population size at time  $t + 1$ . Between times  $t$  and  $t + 1$  the population size is undefined, and can be interpreted as the hibernation stage during a winter season. Typical examples of maps used in ecology are

$$f(N) = rN(1 - N/k) \quad \text{and} \quad f(N) = \frac{rN}{1 + N/k} , \quad (11.2)$$

which are called the “logistic map” and the “Beverton-Holt” model, respectively. Because we have used similar functions to describe the birth rate in ODEs, we are already familiar with the shape of these two functions. The logistic map is a parabola, which by being non-monotonic assumes that the maximum population size in the next year is attained from an intermediate population size in the current year. Importantly, by intraspecific competition, large populations tend to be mapped into small populations in the next year. The second model is a monotonically increasing Hill function assuming the population size in the next year is a saturation function of the population size in the current year. Below we will derive the Beverton & Holt (1957) model

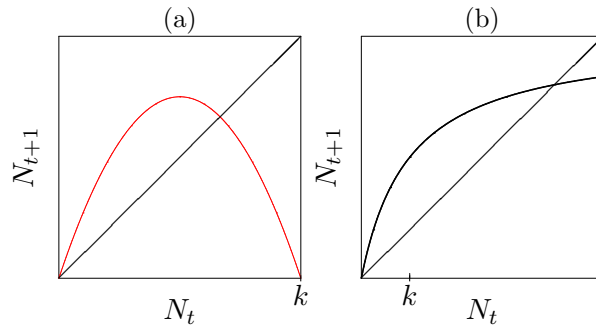


Figure 11.1: Stability of maps. Panel (a) depicts the logistic map, which is a parabola, and Panel (b) shows the saturation function underlying the map of Eq. (11.2)b. The diagonal line is the line at which  $N_{t+1} = N_t$ . Steady states therefore correspond to the intersections of the map with the diagonal line.

ourselves. The same equation has also been proposed by Maynard Smith & Slatkin (1973) and later by Hassell (1975).

The steady states and the stability properties of maps differ from those of ODEs. To compute the steady state of a map one should not set  $f(N)$  to zero, but compute the population size,  $\bar{N}$ , for which  $N_{t+1} = N_t$ . To see how one computes the stability of a steady state of a map, one should redo the linearization, i.e.,

$$N_{t+1} = f(N_t) \simeq f(\bar{N}) + \partial_N f(\bar{N})(N_t - \bar{N}) = \bar{N} + \lambda h_t, \quad (11.3)$$

where we have defined  $\lambda = \partial_N f(\bar{N})$  and the distance to the steady state,  $h_t = N_t - \bar{N}$ . Subtracting  $\bar{N}$  from the left hand side and the right hand side one obtains

$$h_{t+1} \simeq \lambda h_t, \quad (11.4)$$

because  $h_{t+1} = N_{t+1} - \bar{N}$ . Thus, like in 1-dimensional ODEs,  $\lambda$  remains to be the derivative of the population growth function at the steady state value,  $\bar{N}$ . The difference with ODEs is that the steady state is not stable when  $\lambda < 0$ , but when the next size of the perturbation,  $h_{t+1}$ , is smaller than the current,  $h_t$ . In maps this is the case when  $-1 < \lambda < 1$  (general these  $\lambda$ s are called Floquet multipliers). For  $-1 < \lambda < 0$  the sign of  $h_t$  is alternating in time, which corresponds to a dampened oscillation approaching  $h_t = 0$ . Since  $\lambda$  is the slope of the map at the steady state, one immediately sees an important difference between the two maps in Eq. (11.2). Since the function of Eq. (11.2)b is monotonically increasing,  $\lambda$  is always larger than zero, and the behavior of the map will never be oscillatory. Conversely, the logistic map has a positive slope when  $N < k/2$ , and a negative slope when  $N > k/2$ , and should therefore be capable of oscillatory behavior when the steady state is located above  $N > k/2$ .

A graphic method for finding steady states of maps is to sketch the map, and the diagonal  $N_{t+1} = N_t$  in one graph (see Fig. 11.1). The points at which the two lines intersect are steady states. We have learned above that the slope of the map at these intersection points determines the stability of the steady state. For example, let us determine the stability of the steady state of the logistic map, and solve the steady state from

$$N = rN(1 - N/k) \quad \text{or} \quad \bar{N} = \frac{r-1}{r} k. \quad (11.5)$$

Because  $\partial_N f(N) = r - 2rN/k$ , one obtains by substitution of the steady state value that  $\lambda = 2 - r$ . Since the steady state is stable when  $-1 < \lambda < 1$ , i.e., when  $-1 < 2 - r < 1$ , the condition for stability is that  $2 - r < 1$  and  $-1 < 2 - r$ , i.e., that  $1 < r < 3$ . The requirement

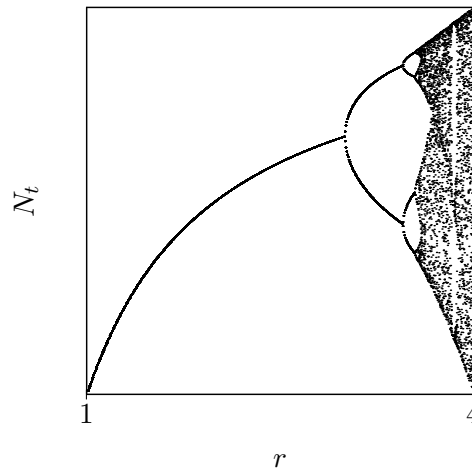


Figure 11.2: The behavior of the logistic map as a function of its natural rate of increase  $r$ . For each value of  $r$  the map is run for a long time until the attractor is approached. Subsequently the map is run for twenty time steps, and each value of  $N_t$  is depicted as a point. For  $r < 3$  all points collapse onto the steady state value  $\bar{N} = k(r - 1)/r$ , for  $3 < r < 3.45$   $N_t$  oscillates between two values, for  $3.45 < r < 3.55$   $N_t$  oscillates between four values, and so on. Note the window of  $r$  values where the logistic map has a three point cycle. This led to the famous paper by Li & Yorke (1975) with the title “Period three implies chaos”.

that  $r > 1$  is trivial because the population cannot maintain itself when the next population size is always smaller than the current one. The instability at  $r = 3$  leads to oscillatory behavior: when  $r \rightarrow 3$  the slope  $\lambda = 2 - r \rightarrow -1$ , and the steady state is approached by a dampened oscillation. For  $r > 3$  the oscillation is no longer dampened but approaches a stable limit cycle. For  $3 < r < 4$  this limit cycle undergoes a period doubling cascade (see Chapter 12), giving rise to the famous chaotic behavior of the logistic map (see Fig. 11.2).

The stability of the steady state of the second example in Eq. (11.2) is computed similarly. The steady state is derived from

$$\bar{N} = \frac{rN}{1 + N/k}, \quad \text{i.e.,} \quad \bar{N} = k(r - 1), \quad (11.6)$$

and because

$$\partial_N f = \frac{r}{1 + N/k} - \frac{rN/k}{(1 + N/k)^2}, \quad (11.7)$$

one obtains for the slope at the steady state  $\bar{N}$  that

$$\lambda = \frac{r}{r} - \frac{r(r - 1)}{r^2} = \frac{r - (r - 1)}{r} = \frac{1}{r}. \quad (11.8)$$

Thus, whenever the population can maintain itself, i.e., whenever  $r > 1$ , the steady state will always be stable.

Oscillatory behavior is therefore not necessarily expected for populations described by maps. This is important because the insect populations that one typically models with maps often have a very large natural rate of increase  $r$ , i.e., an insect can lay thousands of eggs. The logistic map has  $r = 4$  as the maximum rate of increase; for larger  $r$  the population size becomes negative. Finally, note that the second example in Eq. (11.2) generalizes to the Maynard Smith & Slatkin (1973) model

$$N_{t+1} = \frac{rN}{1 + (N/k)^n}, \quad (11.9)$$

where the density dependence is a simple inverse Hill function. For  $n = 1$  this provides the Beverton-Holt model considered above. Whenever the exponent,  $n$ , of the Hill function becomes larger than one, the function will no longer be monotonic (see Chapter 15), and chaos and oscillations will be possible (Hassell *et al.*, 1976).

## 11.2 Deriving a map mechanistically

The two examples of maps of Eq. (11.2) have frequently been used for describing seasonal population growth. However, the logistic map is typically used for convenience, and not because one really has data supporting the so crucial humped shape of the map. The chaotic behavior that theoretical ecologists generally attribute to seasonally growing populations could therefore well be an artifact of too easily adopting humped or logistic equations. To develop an opinion of what type of maps would be appropriate we develop the model ourselves (by essentially following the derivation proposed by Beverton & Holt (1957)).

The biology that is typically neglected when populations are described with maps is that seasonal populations do have a season in which they are active, and which could be modeled with a conventional ODE. Think of insects that lay their eggs at the end of the season shortly before they die, and where the new generation hatches from the eggs at the start of the next season. During the season the insects do not reproduce, as all growth is determined by the number of eggs deposited at the end of the season. Density dependent regulation of the population most likely takes place during the season, as the eggs probably have a density independent chance to survive the winter season. It could therefore be that most of the population regulation takes place during a normal continuous part of the year. What we will do next is to derive a map for the seasonal insect population sketched in this paragraph.

Let the population size during the season be described by  $n(t)$ , where  $t$  is the time (e.g., in days) since the start of the season. Let  $N_j$  be the population size at the end of the season, where  $j$  measures times in years, i.e.,  $j = 0, 1, 2, \dots$ . For a season length of  $\tau$  days, one should have in year  $j$  that  $N_j = n(\tau)$ . Assuming that at the end of the season each individual lays  $g$  eggs that are expected to survive the winter season, one obtains that at the start of the season  $n(0) = gN_{j-1}$  (see Fig. 11.3a).

The main challenge is to write a natural model for the population during the active season. Since there is no reproduction one could assume a straightforward density dependent death model like

$$\frac{dn}{dt} = -dn(1 + n/k) \quad \text{with the solution} \quad n(t) = \frac{kn(0)}{ke^{dt} + n(0)[e^{dt} - 1]}, \quad (11.10)$$

where  $d$  is a normal density independent death rate, e.g., due to predation by birds, and the parameter  $k$  determines the density dependent death rate (i.e., at  $n(t) = k$  the death rate has doubled).<sup>1</sup> For a season of a fixed length of  $\tau$  days, and a starting number of  $n(0) = gN_{j-1}$  the solution becomes

$$N_j = n(\tau) = \frac{kgN_{j-1}}{ke^{d\tau} + gN_{j-1}[e^{d\tau} - 1]}, \quad (11.11)$$

and because  $e^{d\tau}$  is just a certain value (for which we happen to know that  $e^{d\tau} - 1 > 0$ ), this can be rewritten into

$$N_{j+1} = \frac{rN_j}{1 + N_j/c} \quad \text{where} \quad r = ge^{-d\tau} \quad \text{and} \quad c = \frac{k}{g(1 - e^{-d\tau})}. \quad (11.12)$$

<sup>1</sup>This solution is known as Eq. (11.10) is a Logistic growth model with opposite signs of the parameters.

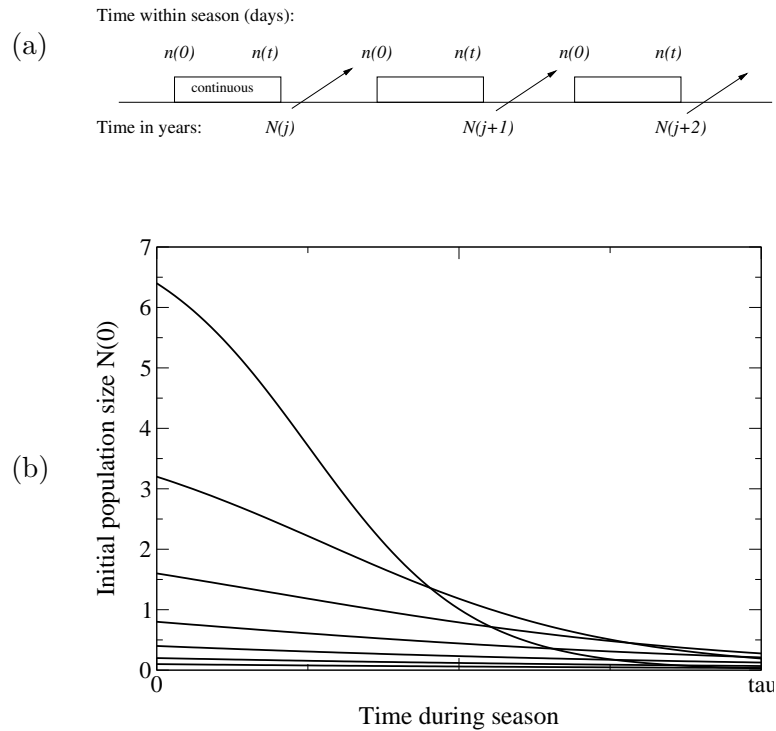


Figure 11.3: Discrete and continuous seasons in an population of insects (a). To obtain a humped relationship between the initial and the final population size trajectories have to cross (b).

This has the form of the Beverton-Holt model that we have studied above, which implies that we expect our seasonal insect population to approach a stable state value over the years, and never be oscillatory or chaotic (see Eq. (11.8)). This does not mean that we predict that insect populations should typically approach a steady state, but demonstrates that we need not expect that seasonal populations readily become chaotic.

An even simpler alternative of Eq. (11.10) is to ignore the density independent death and write

$$\frac{dn}{dt} = -dn^2 \quad \text{with the solution} \quad n(t) = \frac{n(0)}{1 + dt n(0)}, \quad (11.13)$$

which for a fixed length of the season also assumes the form of the Beverton-Holt model.

The fact that we fail to obtain periodic behavior with a single ODE describing density dependent death during the season seems quite general. We learned that oscillatory behavior can be obtained only when the map has a maximum, and hence has a region where its slope  $\lambda < 0$ . This can only come about when there is a range of large  $n(0)$  values for which the number of individuals,  $n(\tau)$ , at the end of the season is smaller than what would have survived at intermediate  $n(0)$  values. This cannot happen in the one-dimensional phase space of an ODE, because at some point in time the trajectory with a large starting number should cross the one with an intermediate starting number. At this point in time the two trajectories should obey the same derivative, and cannot end differently (see Fig. 11.3b).

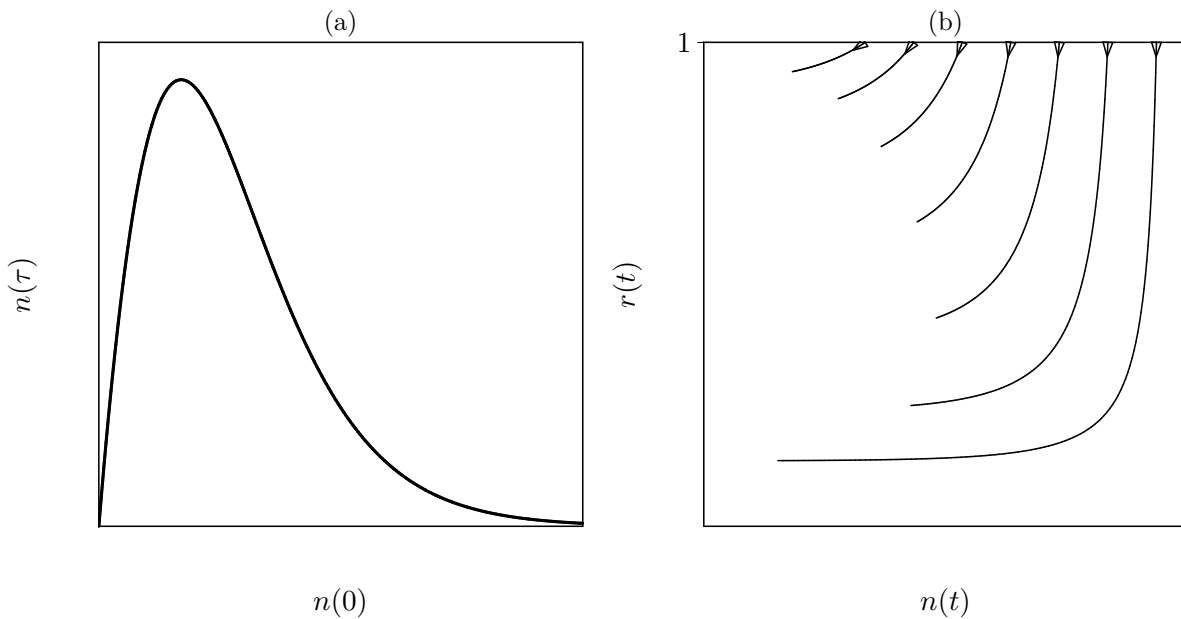


Figure 11.4: The solution of Eq. (11.15) (a) and various simulations of the model of Eq. (11.14) for one season of  $\tau = 10$  days, and  $c = d = 0.1$  per day, starting at a scaled food density of  $r(0) = 1$ .

### How to obtain oscillations?

As simple one-dimensional death models fail to do the job, we apparently have to do some work to allow for oscillations in biologically realistic maps. One could argue that if a large initial population depletes most of the available food during the early days of the season, that many will die by starvation during the later half of the season. Intuitively, it seems that too large populations could be at a disadvantage, and end up with less survivors than populations of an intermediate size. Since we know this requires a 2-dimensional model one could propose

$$\frac{dr}{dt} = -crn \quad \text{and} \quad \frac{dn}{dt} = -dn/r, \quad (11.14)$$

where  $r$  is the amount of resource,  $c$  is the feeding rate of the insects on the resource, and  $d/r$  is the *per capita* death rate of the insects. It is somewhat disturbing to divide by the resource density  $r$  in  $dn/dt$ , but because  $r$  will always remain larger than zero, and because we need a model that can be solved analytically, this seems allowable here. One can scale the initial food availability to  $r(0) = 1$ , such that  $d$  is a normal *per capita* death rate when food is abundant, which increases rapidly when the amount of food declines. Because we have deliberately kept the model simple one can still obtain the solution

$$n(t) = f[n(0)] = \frac{cn(0) + d}{c + de^{t[cn(0)+d]/n(0)}}. \quad (11.15)$$

Plotting the population size at the end of the season, i.e.,  $n(\tau)$ , as a function of the initial population size,  $n(0)$ , one obtains a humped shape for  $f[n(0)]$  because Eq. (11.15) is an increasing function when  $n(0)$  is small, while it approaches zero when  $n(0)$  is large, i.e.,

$$\lim_{n(0) \rightarrow 0} f[n(0)] = e^{-d\tau} n(0) \quad \text{and} \quad \lim_{n(0) \rightarrow \infty} f[n(0)] = 0. \quad (11.16)$$

Substituting parameter values indeed reveals a humped relationship (see Fig. 11.4a), and simulations of the 2-dimensional model confirm that large population have fewer survivors because they deplete the resource faster (see Fig. 11.4b).

### 11.3 Eggs produced during the season

Geritz & Kisdi (2004) also derived maps from populations competing within a continuous season. Working with models where eggs are produced during the season there were able to provide a mechanistic underpinning of various different maps, such as the logistic map, the Beverton-Holt model, and the Ricker model. Their basic model was a single ODE for the number of eggs produced over the season. The number of eggs at the end of the season depended on the total number of adults and the availability of resource during the season, and they easily obtain a non-monotonic relation between the initial number of adults and the final number of eggs. Starting with few adults few eggs are produced. Starting with too many adults the resource availability is low, and again few eggs are produced. The maximum number of eggs is produced when the season starts with an intermediate number of adults. Eggs also “die” during the season.

One example of their models has a resource growing logistically:

$$\frac{dR}{dt} = rR(1 - R) - bRA \quad \text{and} \quad \frac{dE}{dt} = cbRA - dE, \quad (11.17)$$

where  $R$  is the resource,  $E$  is the egg density, and  $A$  is the fixed number of adults the season starts with, e.g., for a season of length  $\tau$  one would write  $A_j = \alpha E(\tau)_{j-1}$ . Assuming that the dynamics of the resource is fast compared to that of the eggs, Geritz & Kisdi (2004) simplified by writing the quasi state of the resource,  $R = 1 - bA/r$ , obtaining for the eggs

$$\frac{dE}{dt} = cb(1 - bA/r)A - dE. \quad (11.18)$$

Since  $cb(1 - bA/r)A$  does not depend on time,  $t$ , this is a source/death model similar to those solved in Chapter 2, i.e.,

$$E(t) = \frac{cb(1 - bA/r)A}{d} (1 - e^{-dt}). \quad (11.19)$$

For a fixed length of the season of  $\tau$  days  $E(\tau)$  is therefore completely defined by the parameters and the number of adults  $A$ . Defining a map for the number of adults  $A_{j+1}$  in year  $j + 1$  as a function of those in year  $j$ , one obtains

$$A_{j+1} = \alpha E(\tau)_j = \rho A_j [1 - A_j/K], \quad (11.20)$$

where  $\rho = \alpha cb[1 - e^{-d\tau}]/d$  and  $K = r/b$ , which is the conventional logistic map. Taking non-logistic growth functions of the resource other maps were obtained (Geritz & Kisdi, 2004); see the exercises.

The within season models studied by Geritz & Kisdi (2004) provide a non-monotonic map with just one ODE, whereas we needed at least two ODEs to obtain this with the density dependent death model of Eq. (11.10). How can this be? The simple reason is that in the model of Eq. (11.10) the information transferred between the years is an *initial* condition, i.e.,  $n(0)$  is the number of adults hatching from the eggs produced the year before. In the models of Geritz & Kisdi (2004) the number of adults in the current year is a *parameter* set by the within season dynamics of the previous year. The problem that trajectories cannot cross if just the initial condition is different (see Fig. 11.3) therefore never arises: if the continuous dynamics in a season are parameterized by the previous year it is perfectly possible to have a humped relation between the initial population size and the final population size. An interesting question now is if we can identify populations where the information transfer between the years goes via an initial condition (e.g., the number of eggs) or via a parameter (e.g., a fixed number of adults). It is again somewhat disturbing that such a technical difference seems so important for the expected behavior of the population.

## 11.4 Summary

Oscillations and chaos are by no means the expected behavior of seasonally reproducing populations. Periodic behavior or chaos is not difficult to obtain, but we had to do work to obtain this when the information transfer between the years was just an initial condition. Finding chaos or oscillations by modeling populations with an arbitrary humped map could well be artificial, and one basically needs evidence, or a good argument, to use a humped survival function.

## 11.5 Exercises

### Question 11.1. Geritz & Kisdi (2004)

Follow the procedure of Geritz & Kisdi (2004) explained in this Chapter to show that the Gompertz equation for population growth, i.e.,  $dR/dt = rR(1 - \ln[R]) - bRA$ , delivers the Ricker map,  $N_{t+1} = aN_t e^{-bN_t}$ .

### Question 11.2. Insect population

In the model of Eq. (11.14) the death rate of the insects will go to infinity when the amount of resource approaches zero. This was done to keep the model simple, such that it remained feasible to obtain a solution.

- Write a more realistic version of Eq. (11.14).
- Study the model numerically to see if the humped relationship between  $n(\tau)$  at the end of the season and  $n(0)$  at the start of the season remains a possibility. Begin with studying one season with various initial values of  $n(0)$  (and keep  $r(0) = 1$ ).
- On the website you will find a file `discreteSeason.R` as an example of the seasonal population of Eq. (11.14). Try to obtain oscillations and/or chaos in your extension of this model.

### Question 11.3. Periodic forcing

Scheffer *et al.* (1997) have extended the Monod saturated algae zooplankton model of Chapter 7 with a seasonal variation of the birth rates to model the bloom of algae in the spring. As a consequence the model became capable of chaotic behavior. In R code one would write something like:

```
b <- b0 + e*(sin(2*3.1416*(t-Delta)/365))
dA <- b*A*(1-A/k) - d*A ....
```

where the parameter `Delta` can be used to shift the peak of the seasonal variation to the appropriate time of the year, and the parameter `e` defines the amplitude of the variation around the average value `b0` (see the file `season.R`).

## Chapter 12

# Bifurcation analysis

In several chapters of this course we have encountered examples where a property of a steady state changes at some critical parameter value. A good example is the steady state of the Monod saturated consumer-resource model, which changes stability precisely when the vertical consumer nullcline intersects the top of the parabolic resource nullcline. We have seen that at this “Hopf bifurcation point” the stability of the steady state is carried over to a stable limit cycle (or *vice versa*). In the same model there was another bifurcation point when the consumer nullcline crosses the carrying capacity of the resource. This is a so-called “transcritical bifurcation” at which the presence of the consumer is determined. In ODE models there are only four different types of bifurcations that can happen when one is changing a single parameter. This chapter illustrates all four of them and explains each of them in phase plane pictures.

Bifurcation diagrams depict what occurs when one changes a parameter, and therefore provide a powerful graphical representation of the different behaviors a model may exhibit for different values of its parameters. Bifurcation diagrams are typically made with special purpose software tools (like MatCont by Yuri Kuznetsov or the `deBif` R-package by Andre de Roos). Grind has a fairly primitive algorithm for continuing steady states (`continue`). In the exercises you will be challenged to sketch a bifurcation diagram with pencil and paper.

Several other bifurcations may occur when one is changing two parameters at the same time. These can be summarized in 2-dimensional bifurcation diagrams, which can provide an even better overview of the possible behaviors of a model. Such 2-dimensional bifurcations will not be discussed here, and we refer you to books or courses on bifurcation analysis.

### 12.1 Hopf bifurcation

At a Hopf bifurcation a limit cycle is born from a spiral point that is switching stability. This was already discussed at length in Chapter 7 for models with a saturated functional response. Fig. 12.1 depicts the nullclines of a consumer-resource model with a sigmoid functional response for several different values of the death rate,  $d$ , of the consumer  $N$ . In Chapter 7 we already calculated for the model

$$\frac{dR}{dt} = rR(1 - R/K) - \frac{bR^2N}{h^2 + R^2} \quad \text{and} \quad \frac{dN}{dt} = \frac{cbNR^2}{h^2 + R^2} - dN, \quad (12.1)$$

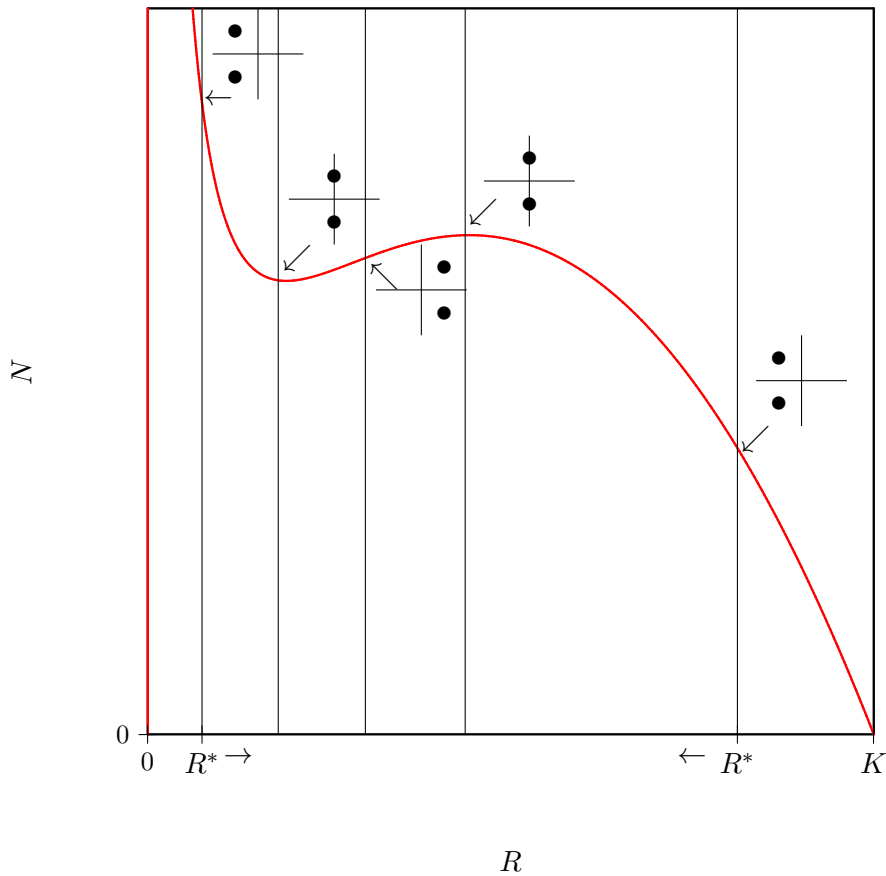


Figure 12.1: Two Hopf bifurcations in the sigmoid consumer-resource model. The vertical lines depict the  $dN/dt = 0$  nullcline for various values of  $R^* = \frac{h}{\sqrt{R_0 - 1}}$ . The “Argand diagrams” depict the eigenvalues by plotting the real part on the horizontal, and the imaginary part on the vertical axis (see also Fig. 15.6). Hopf bifurcations corresponds to a complex pair moving through the imaginary axis.

that the non-trivial consumer nullcline is a vertical line located at the resource density  $R^* = h/\sqrt{R_0 - 1}$  where  $R_0 = cb/d$ . Thus by changing the consumer death rate  $d$  one actually moves the consumer nullcline, and because the consumer death rate is not part of the ODE of the resource, the resource nullcline remains identical.

First consider values of the death rate  $d$  in Fig. 12.1 for which the consumer nullcline is located at the right side of the top of the humped resource nullcline. The graphical Jacobian is

$$A = \begin{pmatrix} -a & -b \\ c & 0 \end{pmatrix} \quad \text{such that} \quad \text{tr} = -a < 0 \quad \text{and} \quad \det = bc > 0. \quad (12.2)$$

Close to the top of the resource nullcline the discriminant of this matrix,  $D = a^2 - 4bc$ , will become negative, and the steady state is a stable spiral point with eigenvalues  $\lambda_{\pm} = -a \pm ib$ . (Below we will see that the same steady state will be a stable node when the nullcline intersects in the neighborhood of the carrying capacity.) Decreasing the parameter  $d$  the consumer nullcline is shifted to the left, and will cross through the top of the resource nullcline. When located left of this top the graphical Jacobian is

$$A = \begin{pmatrix} a & -b \\ c & 0 \end{pmatrix} \quad \text{such that} \quad \text{tr} = a > 0 \quad \text{and} \quad \det = bc > 0. \quad (12.3)$$

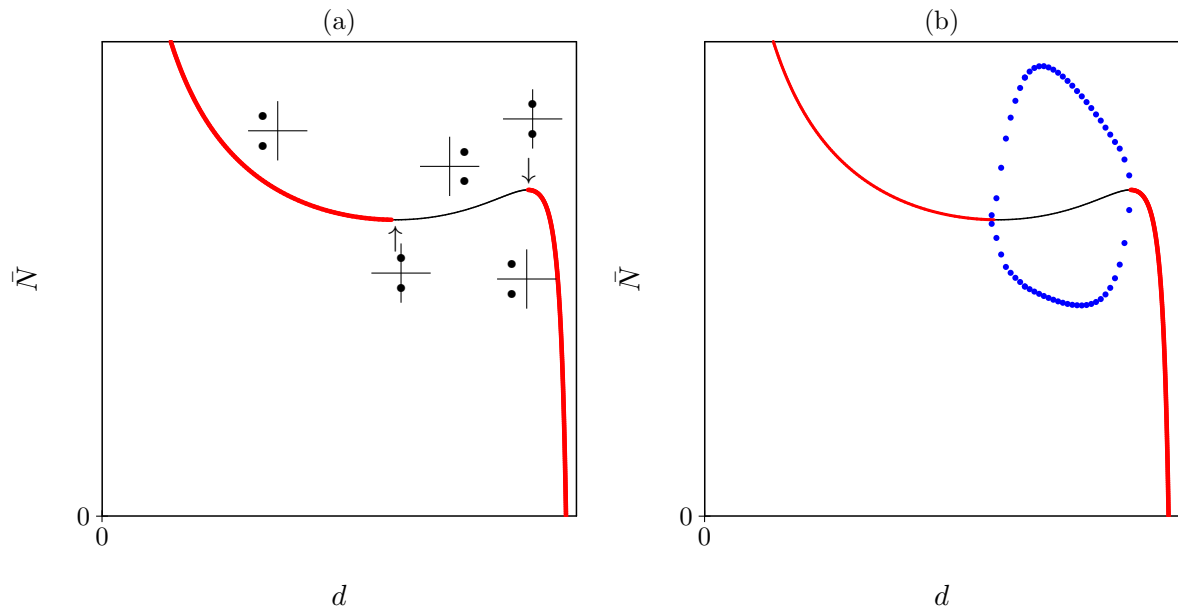


Figure 12.2: A bifurcation diagram with the two Hopf bifurcations of Fig. 12.1. The circles in panel (b) depict the stable limit cycle that exist between the two Hopf bifurcations for many different values of the parameter  $d$ .

Close to the top the discriminant,  $D = a^2 - 4bc = \text{tr}^2 - 4\det$ , will remain to be negative, and the steady state is an unstable spiral point.

For the critical value of  $d$  where the consumer nullcline is located at the top, i.e., at  $R^* = (K - h)/2$  (see Chapter 7), the local slope of the parabolic nullcline in the space of  $N$  versus  $R$  is perfectly horizontal, and as a consequence the graphical Jacobian is

$$A = \begin{pmatrix} 0 & -b \\ c & 0 \end{pmatrix} \quad \text{such that} \quad \text{tr} = 0 \quad \text{and} \quad \det = bc > 0. \quad (12.4)$$

The imaginary eigenvalues  $\lambda_{\pm} = \pm i\sqrt{bc}$  have no real part and correspond to the structurally unstable equilibrium point of the Lotka-Volterra model lacking a carrying capacity of the resource (see Eq. (5.20)). Summarizing, at a Hopf bifurcation a complex pair of eigenvalues moves through the imaginary axis. At the bifurcation point the steady state has a neutral stability, and a limit cycle is born.

Fig. 12.1 has little diagrams displaying the nature of the eigenvalues. These so-called “Argand diagrams” depict complex numbers as a vector representing the real part of an eigenvalue on the horizontal axis, and the imaginary part on the vertical axis (see Fig. 15.6). In these diagrams a complex pair of eigenvalues,  $\lambda_{\pm} = a \pm ib$ , is located at one specific  $x$ -value ( $a$ ), with two opposite imaginary parts ( $+b$  and  $-b$ ). A real eigenvalue will be a point on the horizontal axis. The Hopf bifurcation can neatly be summarized as a complex pair moving horizontally through the vertical imaginary axis (see Fig. 12.1).

This is summarized in the bifurcation diagram of Fig. 12.2 which depicts the steady state value of the consumer as a function of its death rate  $d$ . Here stable steady states are drawn as heavy red lines, and unstable steady states as light blue lines. We have chosen to have the consumer on the vertical axis to facilitate the comparison with the phase portrait of Fig. 12.1, which also has the consumer on the vertical axis (note that if we had chosen the resource on the vertical axis the steady state would be a line at  $\bar{R} = h/\sqrt{R_0 - 1}$ ). Sometimes one depicts the “norm”, i.e.,

$N^2 + R^2$ , on the vertical axis. It is not so important what is exactly plotted on the vertical axis as long as it provides a measure of the location of the steady state. The bifurcation diagram displays another Hopf bifurcation that occurs when the consumer nullcline goes through the minimum of the resource nullcline. Between these critical values of  $d$  there exists a stable limit cycle, of which we depict the amplitude by the bullets in Fig. 12.2b. Decreasing  $d$  the limit cycle is born at the top and it dies at the bottom of the resource nullcline. Increasing  $d$  this would just be the other way around. Fig. 12.2 does provide a good summary of the behavior of the model as a function of the death rate  $d$ .

In Fig. 12.2b the amplitude of limit cycle is depicted by the bullets. Conventionally closed circles are used to depict stable limit cycles, and open circles are used for unstable limit cycles (that we have not discussed explicitly in this book; but there is one in on the front page of this book). Grind plots the minima and maxima of the limit cycle for each value of the bifurcation parameter. To depict and study limit cycles one can also plot the consumer value when the limit cycles crosses through a particular resource value. Such a value is called a Poincaré section, and on this Poincaré plane one can define the limit cycle as a map, mapping one point on the section to the next crossing by the limit cycle. The stability of the limit cycle is then determined from the “Floquet multipliers” of this map (see Chapter 11).

## 12.2 Transcritical bifurcation

If one starts with a consumer nullcline located at the right hand side of the top of the parabolic resource nullcline, i.e., at  $(K - h)/2 < R^* < K$ , and increases the death rate  $d$  in the same model, the consumer nullcline moves further to the right. As long as this nullcline remains left of the carrying capacity the non-trivial steady state will remain stable. However, at one specific value of  $d$  it will change from a stable spiral into a stable node. In the Argand diagram this means that the complex pair collapses into a single point on the horizontal axis, after which the eigenvalues drift apart on the horizontal (real) axis (see Fig. 12.3b). When the consumer nullcline is about to hit the carrying capacity, one can be sure the steady state has become a stable node, i.e., it will have two real eigenvalues smaller than zero.

Increasing  $d$  further leads to a transcritical bifurcation at  $K = h/\sqrt{R_0 - 1}$ . Here the stable node collapses with the saddle point  $(\bar{N}, \bar{R}) = (K, 0)$ . After increasing  $d$  further the saddle point becomes a stable node, and the non-trivial steady state becomes a saddle point located at a negative consumer density. At the bifurcation point one of the eigenvalues goes through zero (see the arrow in Fig. 12.3d), which again corresponds to the structurally unstable neutral stability. Transcritical bifurcations typically take place in a situation where the steady state value of one of the variables becomes zero, i.e., correspond to situations where one of the trivial steady states changes stability. Because in biological models a population size of zero often corresponds to an equilibrium, transcritical bifurcations are very common in biological models.

## 12.3 Saddle node bifurcation

The saddle-node bifurcations that occur in the sigmoid consumer-resource model of Eq. (12.1) are famous because of their interpretation of catastrophic switches between rich and poor steady states that may occur in arid habitats like the Sahel zone (Noy-Meir, 1975; May, 1977; Rietkerk & Van de Koppel, 1997; Scheffer *et al.*, 2001; Scheffer, 2009; Hirota *et al.*, 2011; Veraart *et al.*, 2012).

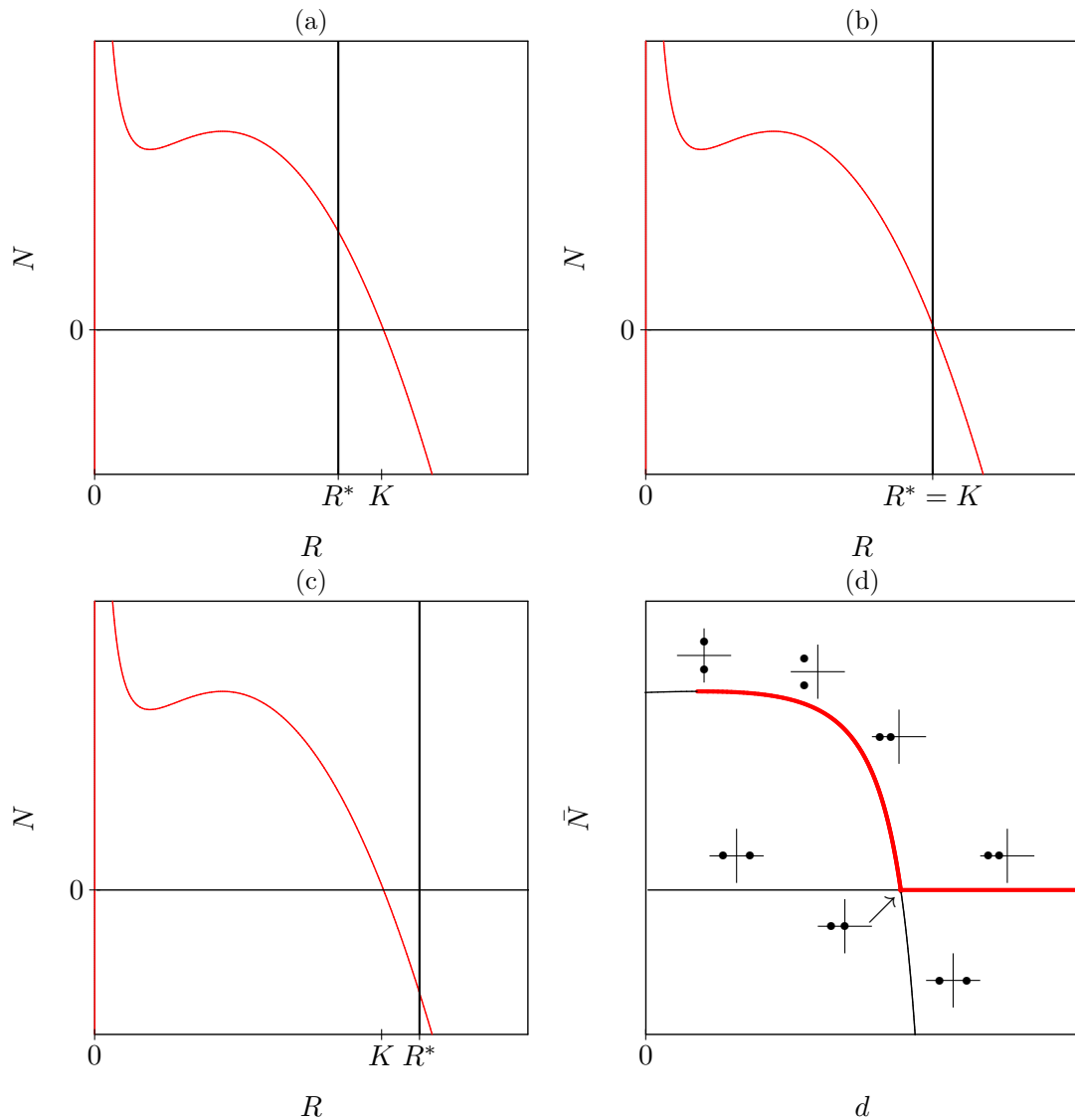


Figure 12.3: Panels (a–c) depict the phase space for three values of  $d$  around a transcritical bifurcation, that is occurring in Panel (b). Panel (d) depicts the corresponding bifurcation diagram of a transcritical bifurcation with  $d$  as the bifurcation parameter on the horizontal axis.

To illustrate this bifurcation one can treat the consumer density as a parameter, representing the number of cattle (herbivores) that people let graze in a certain habitat. This reduces the model of Eq. (12.1) to the  $dR/dt$  equation. The steady states of this 1-dimensional model are depicted in Fig. 12.4a with the number of herbivores,  $N$ , as a bifurcation parameter plotted on the horizontal axis. Because this parameter is identical to the consumer variable plotted on the vertical axis of the phase spaces considered before, these steady states correspond to the  $dR/dt = 0$  nullcline. The bifurcation diagram shows two saddle-node bifurcations (see Fig. 12.4a). At some critical value of the herbivore density on the upper branch, corresponding to a rich vegetation, disappears. At intermediate herbivore densities the vegetation can be in one of two alternative steady states, that are separated by an unstable branch (see Fig. 12.4a). This bifurcation diagram has the famous hysteresis where, after a catastrophic collapse of the vegetation, one has to sell a lot of cattle before the vegetation recovers (Noy-Meir, 1975; May, 1977; Rietkerk & Van de Koppel, 1997; Scheffer *et al.*, 2001; Scheffer, 2009).

To show a more complicated bifurcation diagram with a Hopf bifurcation, and two different

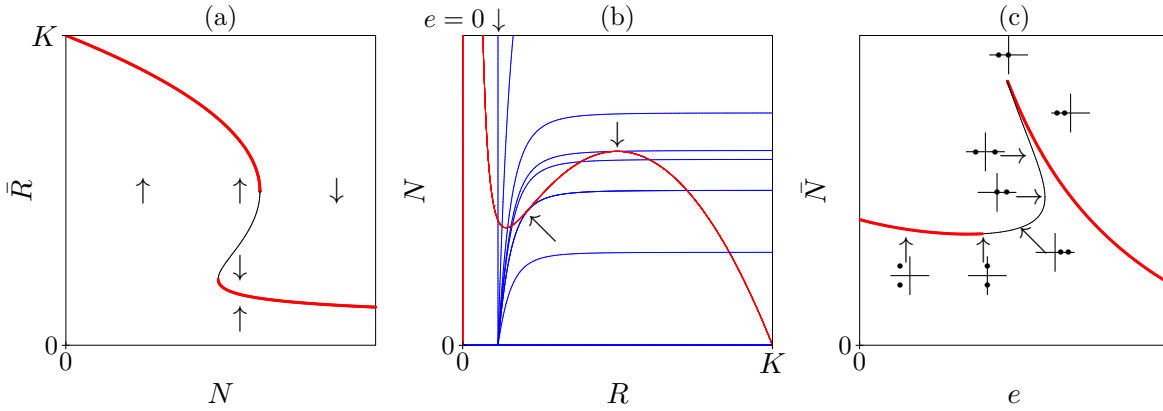


Figure 12.4: The bifurcation diagram of the saddle node bifurcations in Eq. (12.1a) with a fixed number of consumers  $N$  as a bifurcation parameter, and the phase space (b) and bifurcation diagram (c) of the full model of Eq. (12.5) with the density dependent death rate  $e$  as a bifurcation parameter. The phase space in (b) is drawn for several values of  $e$ , and the arrows denote the two saddle-node bifurcations.

saddle-node bifurcations in the same consumer-resource model, we extend Eq. (12.1) with direct interference competition between the consumers, i.e.,

$$\frac{dN}{dt} = \frac{cbNR^2}{h^2 + R^2} - dN - eN^2 . \quad (12.5)$$

To illustrate the saddle node bifurcations we will study the model as a function of the competition parameter  $e$ , and will sketch a bifurcation diagram with  $e$  on the horizontal axis (see Fig. 12.4c).

First, choose a value of the death rate,  $d$ , such that the consumer nullcline intersects at the left of the valley in the resource nullcline (see Fig. 12.4a). For  $e = 0$  there is a single stable steady state. Increasing  $e$  the consumer nullcline will bend because the consumer nullcline can be written as the sigmoid function

$$N = \frac{(cb/e)R^2}{h^2 + R^2} - d/e , \quad (12.6)$$

intersecting the horizontal axis at the now familiar  $R^* = h/\sqrt{R_0 - 1}$ . The resource nullcline remains the same because it does not depend on the  $e$  parameter. By increasing the curvature with  $e$ , this low steady state first undergoes a Hopf bifurcation in the valley of the resource nullcline (see Fig. 12.4b & c). Then the consumer nullcline will hit the resource nullcline close to its top (see the highest arrow), which creates two new steady states at a completely different location in phase space. Increasing  $e$  a little further leads to the formation of two steady states around this first intersection point (see the lowest arrow). One is a saddle point and the other a unstable node (see Fig. 12.4c). A “saddle node” bifurcation is a catastrophic bifurcation because it creates (or annihilates) a completely new configuration of steady states located just somewhere else in phase space.

## 12.4 Pitchfork bifurcation

Thus far we have discussed three bifurcations, i.e., the Hopf, transcritical, and saddle node bifurcation, and we could all let them occur in a conventional consumer-resource model. The

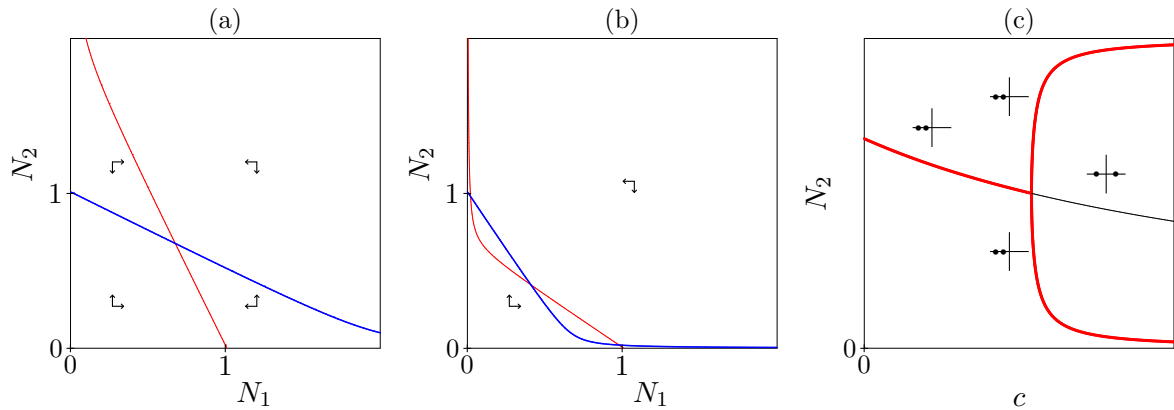


Figure 12.5: The Pitchfork bifurcation of the Lotka-Volterra competition model. Panel (a) and (b) show the phase spaces for  $c < 1$  and  $c > 1$ , and Panel (c) shows the bifurcation diagram.

fourth, and final, bifurcation is called the pitchfork bifurcation, and can be demonstrated from the scaled competition model of Eq. (9.20), when extended with a small immigration term:

$$\frac{dN_1}{dt} = i + rN_1(1 - N_1 - cN_2) \quad \text{and} \quad \frac{dN_2}{dt} = i + rN_2(1 - N_2 - cN_1). \quad (12.7)$$

Whenever the competition parameter  $c$  is smaller than one, the species are hampered more by intraspecific competition than by interspecific competition, and they will co-exist in a stable node (see Fig. 12.5a), and there will be one stable steady state. Increasing  $c$  above one will change this node into the saddle point corresponding to the unstable founder controlled competition (see Fig. 12.5b). In between these two cases there is a bifurcation point of  $c$ , where one real eigenvalue goes through zero (see Fig. 12.5c). Because of the hyperbolic nature of the nullclines, one can see that when the non-trivial steady state becomes a saddle, the nullclines form new steady states around the two carrying capacities. These new states are stable nodes (see Fig. 12.5b & c). In the bifurcation diagram this is depicted as three branches, one for the stable node becoming a saddle point, and two for the stable nodes born at the bifurcation point. Because of the shape of the solutions in this bifurcation diagram this is called a pitchfork bifurcation.

Both the pitchfork bifurcation and the Hopf bifurcation have mirror images. At a so-called subcritical Hopf bifurcation point an unstable limit cycle is born from an unstable spiral point becoming stable. In a subcritical pitchfork bifurcation, an unstable branch of two outward steady states encloses a stable branch in the middle. Both will not further be discussed here.

## 12.5 Period doubling cascade leading to chaos

Having covered all possible bifurcations of steady states in ODE models we will illustrate the period doubling bifurcation that limit cycles may undergo when one parameter is changed (because this occurs in a large variety of ODE models (and in maps; see Fig. 11.2). The period doubling bifurcation is interesting because a cascade of period doubling bifurcations is a route to chaotic behavior approaching a “strange” attractor. Thus in ODE models one can have three types of attractors: (1) stable steady states, (2) stable limit cycles, and (3) chaotic (or strange) attractors.

Since chaos can only occur in ODE models having at least three variables, the bifurcation will be explained by means of an 3-dimensional ODE model taken from Yodzis (1989). It is a simplified

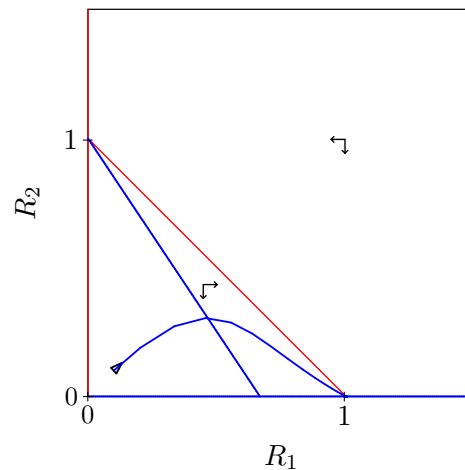


Figure 12.6: The nullclines of the two resource species of Eq. (12.8) in the absence of the consumer. The curved line is a trajectory.

model with two resource species that are eaten by a single consumer

$$\begin{aligned}
 \frac{dR_1}{dt} &= R_1(1 - R_1 - \alpha_{12}R_2) - a_1R_1N, \\
 \frac{dR_2}{dt} &= R_2(1 - R_2 - \alpha_{21}R_1) - a_2R_2N, \\
 \frac{dN}{dt} &= N(ca_1R_1 + ca_2R_2 - 1),
 \end{aligned} \tag{12.8}$$

with mass-action predation terms. Time is scaled by setting the growth rates of the two resource species and the death rate of the consumer to one. Additionally, both carrying capacities have been scaled to one. Setting the parameters  $\alpha_{12} = 1$  and  $\alpha_{21} = 1.5$  the resource species exclude each other in the absence of the consumer (see Fig. 12.6). The behavior of the model is studied by varying the predation pressure,  $a_1$ , on the winning species. By setting  $a_2 = 1$  and  $c = 0.5$ , i.e.,  $ca_2 = 0.5$ , the model is designed such that the consumer cannot survive on  $R_2$  alone. For  $3.4 \leq a_1 \leq 5.5$  one obtains a stable steady state where all three species co-exist. Around  $a_1 = 5.5$  this steady state undergoes a Hopf bifurcation, and a stable limit cycle is born. (Note that at  $a_1 = 2$  a transcritical bifurcation occurs when the consumer can invade, and that at  $a_1 = 3.4$  a second transcritical bifurcation allows the second resource to invade (because the first one now suffers sufficiently from the predation)).

Fig. 12.7 shows what happens if  $a_1$  is increased further. For  $a_1 = 6$  there is a simple stable limit cycle that was born at the Hopf bifurcation (see Fig. 12.7a). At  $a_1 = 8$  this limit cycle makes two rounds before returning to its starting point: the period has approximately doubled at a period doubling bifurcation somewhere between  $6 < a_1 < 8$ . This repeats itself several times, and at  $a_1 = 10$  the system is already chaotic (see Fig. 12.8).

Chaotic behavior is defined by two important properties:

1. An extreme sensitivity for the initial conditions. An arbitrary small deviation from a chaotic trajectory will after sufficient time expand into a macroscopic distance. This is the famous “butterfly” effect where the disturbance in the air flow caused by a butterfly in Africa flying to the next flower causes a rainstorm in Europe after some time.
2. A fractal structure: a strange attractor has a layered structure that will appear layered again when one zooms in (e.g., see Fig. 12.8).

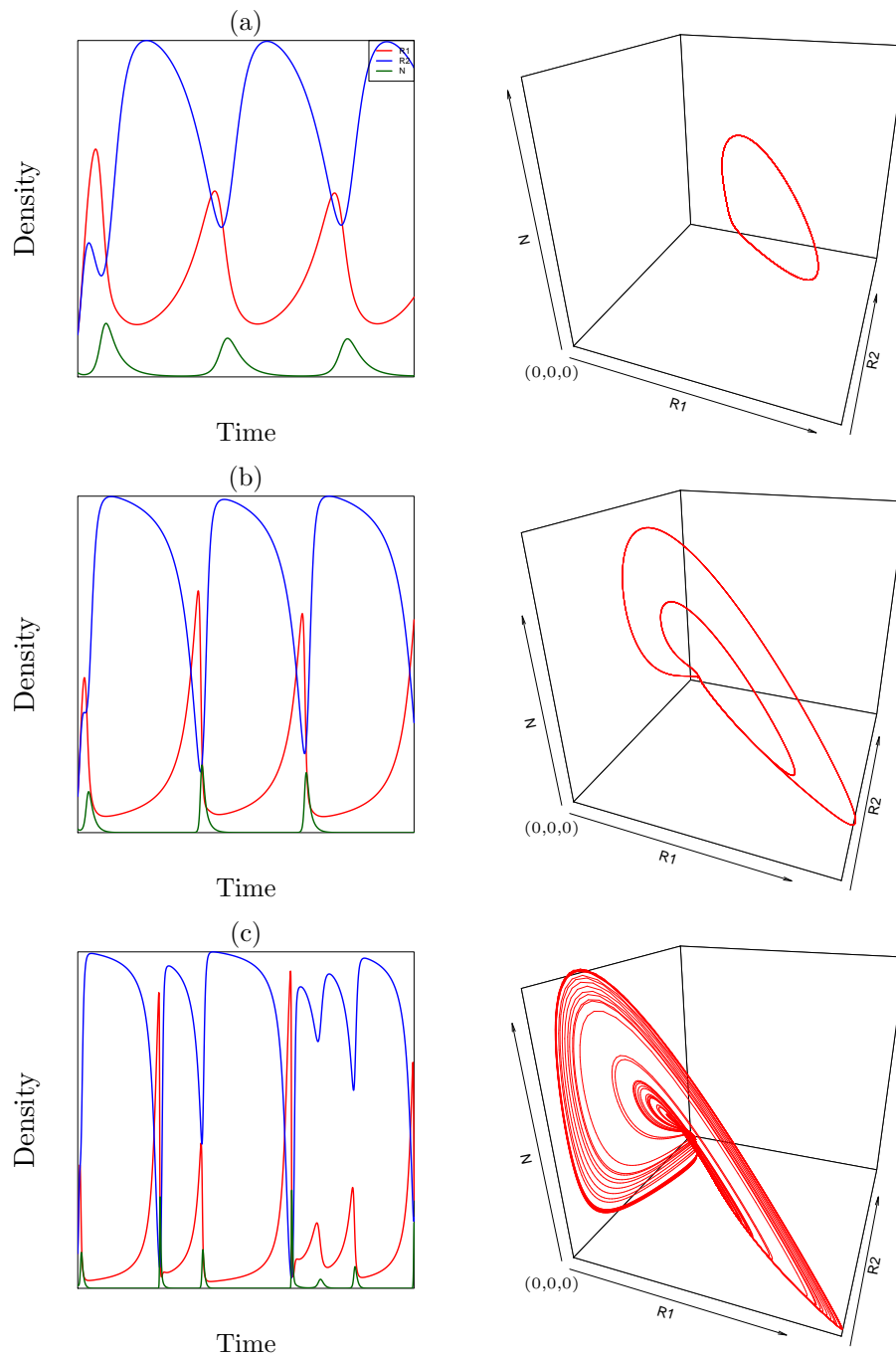


Figure 12.7: Period doubling cascade of the limit cycle of Eq. (12.8). In Panel (a) we set  $a_1 = 6$  and the model behavior is a simple limit cycle, in Panel (b) we set  $a_1 = 8$  and the limit cycle makes two loops before returning to the same point, and in Panel (c) we set  $a_1 = 10$  and find a chaotic attractor. This figure was made with the file `rrn.R`.

The first property is obviously important for the predictability of biological models, as this suggests that we will never be able to predict the precise future behavior of several ecosystems (like we will never be able to predict the weather on June 17 in the next year). This sensitivity comes about from the “folding” and “stretching” regions in strange attractors where many trajectories almost coincide and are torn apart again.

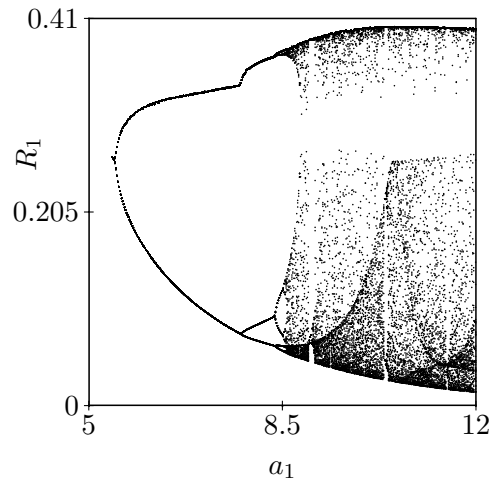


Figure 12.8: Period doubling cascade of the limit cycle of Eq. (12.8) illustrated by plotting 200 values of  $R_1$  obtained for many different values of  $a_1$ . The values of  $R_1$  are recorded when the trajectory crosses a Poincaré plane located around  $R_2 = 0.8$ . Note how similar this is to the famous bifurcation diagram of the Logistic map.

## 12.6 Summary

Varying a single parameter of an ODE model a steady state may undergo one of four different bifurcations: a Hopf, transcritical, saddle-node, or a pitch-fork bifurcation. A saddle-node bifurcation is called catastrophic because it involves a large jump in phase space. Bifurcation diagrams provide an excellent summary of the possible behaviors of a model. We have discussed chaotic behavior to demonstrate that it is strange but expected behavior of simple ecological models having at least three variables. Thus, despite being strange it is normal.

## 12.7 Exercises

### Question 12.1. Biomanipulation

Lakes often look green because of eutrophication. Such lakes have a high density of algae and fish, and little zoo-plankton. Experiments show that catching sufficient fish can make the water clear again. Scheffer (1991) proposed the following model:

$$\frac{dA}{dt} = A(1 - A/k) - pZ \frac{A}{1 + A},$$

$$\frac{dZ}{dt} = -mZ + pZ \frac{A}{1 + A} - F \frac{Z^2}{h^2 + Z^2},$$

where  $A$  represents algae and  $Z$  zoo-plankton. Basically, this is the same Holling type II model as considered above, extended with predation by a fixed density of the fish,  $F$ , having a sigmoid functional response. Study the model for the parameters:  $h = 1, m = 0.4, p = 0.5, 5 \leq k \leq 15$ , and  $0 \leq F \leq 1$ ; see the model `fish.R`.

- Choose different values for the parameters indicated by the ranges, and draw nullclines with Grind.
- Is it possible to have a permanent effect by temporarily (e.g., once) removing a large fraction of the fish?

- c. Sketch the bifurcation diagram of the model with the carrying capacity  $k$  on the horizontal axis, and  $\bar{Z}$  on the vertical axis. Identify all the bifurcations.

### Question 12.2. Early warning signals

The notion that we might be able to observe “early warning” signals in time series data of systems that are about to collapse is receiving a lot of attention recently (Scheffer *et al.*, 2009; Veraart *et al.*, 2012; Scheffer *et al.*, 2012). This theory is based upon the fact that when a system approaches a catastrophic bifurcation (like a saddle-node bifurcation) the dominant eigenvalue is approaching zero, implying that the return time of the system to its steady state is becoming very long. Thus, an increasing return time of a system under slowly changing environmental conditions could provide a warning signal for an upcoming catastrophe. It would be extremely important if one could indeed detect such early warning signals in the time series of any particular system, because one could change the environmental conditions to prevent a future disaster. Long return times should be associated with more variation in the data, and hence to a better correlation between subsequent data points. The review paper by Scheffer *et al.* (2009) provide interesting examples of early warning signals in biological data, and clearly explain the underlying theory in several boxes. Read this paper before you embark on this exercise. On the website we provide a Grind model (`warning.R`) based upon the ODE,  $dX/dt = X(1 - X/K) - \frac{cX^2}{1+X^2}$ , that they use in the legend of their first figure, where they set  $K = 10$  and vary the consumption rate  $c$ . In the Grind model we make  $c$  a function of time such that we can slowly change the consumption rate, by writing  $c(t) = c + \epsilon t$ .

- Plot the steady state of  $X$  as a function of the consumption parameter  $c$  (using the `continue()` function and set  $\epsilon = 0$ ).
- Add noise to the system by adding and removing individuals using the option `after` in your call to `run()`. It is wise to prevent negative values of  $x$  by calling `abs()` within `after` (see the file `warning.R`). Check for different—but fixed—values of  $c$  how the system responds to the noise (i.e., keep  $\epsilon = 0$  and vary  $c$ ). Plot  $X_{t+1}$  as a function of  $X_t$  and compute the (auto)correlation between the two. Note that you plot autocorrelations by saving the data provided by model simulations, e.g., `data <- run(1000, ..., table=TRUE)`, and then plot the value of  $X$  as a function of a previous value of  $X$ , e.g., `plot(data$X[1:999], data$X[2:1000], pch=".")`. Finally note that you can calculate correlations with the R-function `cor()`.
- Study the behavior of the model for a slowly changing  $c$  by setting  $\epsilon$  to a small positive or negative value (with and without noise). Check beforehand how  $c(t)$  changes over time for your settings of  $c$ ,  $\epsilon$ , and the run time.
- Another form of stochasticity is to allow for noise on a parameter, i.e., on  $K$ . Test how the system responds to noise on one of its parameters.
- Do you think you would be able to predict a catastrophic bifurcation, and what would be the best approach to detect this?

You have seen that early warning signals are not always present, and one of the reasons for this is discussed in a paper by Boerlijst *et al.* (2013). Boettiger and Hastings also discuss the predictability of critical transitions (Boettiger & Hastings, 2012, 2013; Boettiger *et al.*, 2016).



# Chapter 13

## Numerical exercises

### 13.1 Grind

Most phase portraits in this book were made with a computer script called Grind, for Great integrator differential equations. Grind is an R-script called `grind.R`,<sup>1</sup> and is based upon the R-packages `deSolve`, `FME`, and `rootSolve` developed by Karline Soetaert and colleagues (Soetaert & Herman, 2009; Soetaert *et al.*, 2010; Soetaert, 2009; Soetaert & Petzoldt, 2010). Grind uses a function in R for plotting contour lines to make phase planes. Grind simplifies the interface to these libraries by having five easy-to-use functions:

- `run()` integrates a model numerically and provides a time plot, or a trajectory in the phase plane,
- `plane()` draws nullclines and can provide a vector field or phase portrait,
- `newton()` finds steady states (using the Newton-Raphson method) and can provide the Jacobian with its eigenvalues and eigenvectors.
- `continue()` performs parameter continuation of a steady state, providing a bifurcation diagram,
- `fit()` fits a model to time-course data by estimating its parameters, and depicts the result in a timeplot.

The best way to get started is to try a few tutorials provided on the Grind homepage, [tbb.bio.uu.nl/rdb/grind.html](http://tbb.bio.uu.nl/rdb/grind.html). These were made in the RStudio environment (watch the video [tbb.bio.uu.nl/rdb/bm/clips/grind](http://tbb.bio.uu.nl/rdb/bm/clips/grind) if you are not used to RStudio). Start with the main tutorial on “phaseplane” analysis and parameter continuation. The “running” tutorial provides examples on add noise to simulations. Read the “fitting” tutorial on parameter estimation before fitting any data.

Download the `grind.R` and the `lotka.R` files via the two links on the Grind homepage (or save them directly from the Grind directory [tbb.bio.uu.nl/rdb/grindR/](http://tbb.bio.uu.nl/rdb/grindR/)). Store both R-scripts in a local directory, and open them via the **File** menu. Both will become tabs in the code window. Set the working directory to the folder where your R-codes are stored (**Set working directory** in the **Session** menu of RStudio). Files will then be opened and saved in that directory.

First “source” the `grind.R` file (button in right hand top corner) to define the five functions.

---

<sup>1</sup>Previous versions were coded in C or Fortran: Grind has a very long history that started in 1983!

(In case you get an error message like “Error in library(deSolve): there is no package called deSolve”, the three Soetaert libraries have to be installed by using `Install Packages` in the `Tools` menu of RStudio). When `grind.R` is successfully “sourced”, it is time to “run” the model with its parameter and state definitions from the `lotka.R` script. In the R-console below the `lotka.R` panel, one can then type the function calls given in the example session below. Once you have a picture that you like, you may copy the lines creating that figure into the `lotka.R` window for later usage. (Use “Run” or “Control Enter” to execute lines from the `lotka.R` panel into the console).

## 13.2 Numerical exercises

### Question 13.1. Cell division takes time

A simple model for a population of proliferating cells is  $dN/dt = (p - d)N$ , which defines cells that are dividing at a rate  $p$  and dying at a rate  $d$ . Both rates are density independent. Like all ODEs, this model assumes that cellular division and death times are exponentially distributed, which actually means that most cells divide and die instantaneously. Since the process of cell division is composed of various “time consuming” phases, i.e., DNA has to be synthesized, and chromosomes have to properly align, cell division cannot occur instantaneously, and takes a minimal amount of time. The quite famous Smith-Martin model (Smith & Martin, 1973) accounts for this by implementing a fixed time delay between an exponentially distributed “trigger” to initiate division, and the time at which the cell actually divides. This model successfully described the growth of tumor cells *in vitro*. Smith & Martin (1973) wrote: “Some time after mitosis all cells enter a state (A) in which their activity is not directed towards replication. A cell may remain in the A-state for any length of time, throughout which its probability of leaving A-state remains constant. On leaving A-state, cells enter B-phase in which their activities are deterministic, and directed towards replication.” To introduce the model we first ignore the death rate and write the delay-differential equation (DDE):

$$\frac{dA(t)}{dt} = 2pA_{t-\Delta} - pA(t) \quad \text{and} \quad \frac{dB(t)}{dt} = pA(t) - pA_{t-\Delta}, \quad (13.1)$$

defining that cells in the A-state move to the B-phase at rate  $p$ , and that the same cells disappear from the B-phase after a delay,  $\Delta$ , and at the same time re-appear in the A-state as two daughter cells. Note that  $dA/dt$  is independent of  $B$ , and that the equation for the B-phase is just required for bookkeeping the total cell number. Adding an exponentially distributed death rate,  $d$ , which in the most simple form is not different between the A-state and B-phase, we need to allow for the fraction of cells surviving the time period,  $\Delta$ , in the B-phase. Since the exponential decay of a single cell over a time window  $\Delta$  is defined as its survival probability,  $e^{-d\Delta}$ , we arrive at the Smith-Martin model

$$\frac{dA(t)}{dt} = 2pA_{t-\Delta}e^{-d\Delta} - (p + d)A(t) \quad \text{and} \quad \frac{dB(t)}{dt} = pA(t) - dB(t) - pA_{t-\Delta}e^{-d\Delta}, \quad (13.2)$$

where  $e^{-d\Delta}$  is the fraction of cells surviving the B-phase. The total number of cells at time  $t$  is defined as  $N(t) = A(t) + B(t)$ , and starting with a quiescent population  $N(0) = A(0)$  it will take at least  $\Delta$  time units before the first new cells are born. Ganusov *et al.* (2005) have analyzed the Smith-Martin model, and derive that after an initial phase the total number of cells,  $N(t)$ , approaches a growth rate,  $r$ , that can be solved from the equation

$$2pe^{-(d+r)\Delta} - (r + p + d) = 0, \quad (13.3)$$

which for  $\Delta = 0$  indeed yields  $r = p - d$ . The Smith-Martin model, with a function call solving Eq. (13.3) numerically is available as the file `sm.R`.

Because DDEs are difficult to solve numerically, and because fixed time delays need not be realistic, it can sometimes be better to replace the time delay by defining a large number,  $n$ , of “dummy” intermediate populations,  $B_i$ , with a transition rate,  $\frac{n}{\Delta}$ , such that the expected length of the delay remains  $\Delta$  time steps, irrespective of  $n$ . For large  $n$  this model approaches a “smooth” time delay of  $\Delta$  time steps (smooth here means without a discontinuity). An alternative formulation of the Smith-Martin model would therefore be

$$\frac{dA}{dt} = 2 \frac{n}{\Delta} B_n - (p+d)A, \quad \frac{dB_1}{dt} = pA - \left(d + \frac{n}{\Delta}\right) B_1 \quad \text{and} \quad \frac{dB_i}{dt} = \frac{n}{\Delta} (B_{i-1} - B_i) - dB_i, \quad (13.4)$$

for  $i = 2, 3, \dots, n$ . This model is available as the function `er1()` (for Erlang distribution) in the file `sm.R`. Here the total number of cells is defined as  $A + \sum_i^n B_i$ .

- What is the ODE for total number of cells in the Smith-Martin model at early time points, i.e., for  $t < \Delta$ ? Would that be different in the model with a flexible delay?
- What is  $dA/dt$  in the Smith-Martin model at early time points, i.e., for  $t < \Delta$ , when we start with a quiescent population, i.e.,  $N(0) = A(0)$ ? Verify your answer by running the Smith-Martin model and the `er1()` model for a short period of time.
- What is the expected time between divisions in the  $dN/dt = (p' - d)N$  ODE model, and how is this division time defined in the Smith-Martin model? How would you redefine  $p'$  in the ODE model to have an equivalent interdivision time in both models?
- Would the cells grow equally fast if after defining this equivalent interdivision time in the ODE model?
- What is the asymptotic behavior of the Smith-Martin model? How different is it from the  $dN/dt = (p' - d)N$  model, and how does this depend on the relative length of the A-stage ( $1/p$ ) and the B-phase ( $\Delta$ )?

### Question 13.2. Sexual reproduction

All population models considered thus far fail to distinguish between the two sexes. Basically these models only consider the females in a population, and ignore the males. Extend the Lotka-Volterra competition model with sexual reproduction, using a Hill function for the probability that a female finds a male, and see how this effects its possible phase spaces, and their biological interpretation. A Grind model is provided in the file `sexual.R`.

### Question 13.3. Paradox of Enrichment

Repeat the Rosenzweig (1971) analysis with the Holling type II consumer resource model:

$$\frac{dR}{dt} = bR(1 - R/k) - d_1R - \frac{eNR}{h + R} \quad \text{and} \quad \frac{dN}{dt} = -d_2N + \frac{ceNR}{h + R},$$

which is provided on the website [tbb.bio.uu.nl/rdb/bm/models](http://tbb.bio.uu.nl/rdb/bm/models) as `rosenzweig.R`.

- Think about scaled and/or reasonable parameter values. Use pencil and paper during your computer exercises: make sure that populations can grow, i.e., have an  $R_0 > 1$ .
- Draw nullclines, check the various possibilities, and run trajectories for each case.
- Study the effect of eutrophication by increasing the carrying capacity.
- Continue the non-trivial steady state as a function of  $k$  (with the `continue()` command).
- Do the same for a model having a functional response with “predator interference”.
- Replace the  $f = R/(h + R)$  functional response by one with a refugium with a size of  $r$  prey individuals, i.e., define  $\hat{R} = \max[0, R - r]$  and  $f = \hat{R}/(h + \hat{R})$ ; see Page 68. You may want to use the R-file `refugium.R` where the parallel `pmax()` function is called to achieve this.

### Question 13.4. Dampened oscillations

Because simplification is so important when we make models for complex biological systems we also tend to use mass-action terms for most of the interactions between the various populations in a model. Although mass-action terms provide a natural starting point, they come with several drawbacks. First, mass-action terms tend to give rise to models resembling the Lotka-Volterra equations, in which one can often cancel each variable from its own ODE when computing steady states. This leads to the strange result that the length of the food chain determines which variables respond to a change of parameters (Arditi & Ginzburg, 1989; Abrams, 1994; Kaunzinger & Morin, 1998; De Boer, 2012). Second, mass-action terms can give rise to “wild” dynamics because they involve the multiplication of two population densities that may both be small and both be large. One area where this is causing problems is the standard model for HIV infection, with target cells,  $T$ , infected cells,  $I$ , and an immune response  $E$ , which typically only approaches its steady state after dampened oscillations that are not found in data. This can be solved by using interaction terms based upon the Beddington functional response (Gadhamsetty *et al.*, 2016).

On the website we provide a simplified example of this in the Grind script `dampen.R`, which implements two models, i.e., a scaled Lotka-Volterra model that is based upon a mass-action killing rate  $a_1$ , and a scaled Beddington model based upon Eq. (7.38) with a mass-action killing rate  $a_2$ , and a saturation constant  $h = k_R = k_N$ . Both models with trivially be identical whenever  $h$  is large. We also make both models “equivalent” for low values of  $h$ , by requiring that they have the same steady state. This can be achieved by computing both non-trivial steady states, and solving for which value of  $a_2$  they are identical, which leads to

$$a_2 = a_1 + \frac{1+d}{h} - \frac{d}{a_1 h},$$

where  $d$  is the death rate (see the Mathematica notebook `dampen.nb` for the fairly complicated derivation of this expression for  $a_2$ ). Note that we indeed obtain that  $a_2 \rightarrow a_1$  when  $h$  is large.

- Which parameters in the model were removed by the scaling?
- Study the dynamics of both models for various values of  $h$ . Confirm that the behavior of the Beddington version is similar when the saturation constants are set to high values, and that lowering the saturation constant dampens the oscillations.
- Can you provide a biological argument why using these “Beddington” interaction terms does make some sense?
- Study the eigenvalues of the non-trivial steady state. Is the Return time a function of  $h$ ? How come that the Beddington functional response is dampening the oscillations?

### Question 13.5. Stem cell renewal

Many tissues and populations of cells are maintained by a subpopulation of stem cells. Classic examples are the formation of several populations of circulating cells in the blood by a relatively small population of haematopoietic stem cells (HSCs) in the bone marrow, and the stem cells located deep in the crypts of the epithelial layer lining the gut. Stem cells are self-renewing cells that (at least sometimes) divide into two different daughter cells, which is called an asymmetric division. When a sufficient fraction of their daughter cells remains as a stem cell, the stem cell population can maintain itself, and provide progeny to the populations of differentiated cells that depend on it. It is unclear how stem cells regulate the fraction of asymmetric divisions, as at least half of their cell divisions should give a daughter with stem cell properties. Otherwise the stem cell population declines. The first question of this exercise is to write a model for the simplest situation where on average half of the daughter cells remains a stem cell while the other half differentiates. You will see that to compensate for the death of stem cells, this fraction should be more than one half, and hence that it is unclear how the fraction of asymmetric divisions is regulated.

Lander *et al.* (2009) developed an interesting model for this problem by arguing that the fraction of renewal divisions providing a daughter with stem cell properties should depend on the density of the population. This could either be the total density, i.e., stem cells plus differentiated cells, the density of differentiated cells, or the density of stem cells. This is interesting because this entails the population with at least two density dependent mechanisms, one regulating the fraction of self-renewal divisions, and another regulating the rate of cell division. They develop a chain of equations where at every level cells may divide asymmetrically. Lander *et al.* (2009) show that the parameters of that system determine which population in the chain will function as stem cells for the entire chain. Here we simplify their model by considering just two populations: stem cells,  $S$ , and differentiated cells,  $D$ . In the questions below we ask you to devise a model where both the fraction of asymmetric divisions,  $0 < f(D) \leq 1$ , and the division rate of the stem cells,  $g(D)$  for growth, depends on the density of differentiated cells. Following Lander *et al.* (2009) suggestions it would be natural to allow for a larger fraction of asymmetric divisions, and a higher division rate, when the population is small and the tissue should be regenerated. Such a model can be studied numerically by taking the file `lander.R` as a template.

- Write a model for a population of stem cells,  $S$ , and differentiated cells,  $D$ , with a fixed division rate of the stem cells, and where on average half of the stem cell divisions are asymmetric.
- Expand your model to account for the situation where the fraction of asymmetric divisions,  $0 < f(D) \leq 1$ , is regulated by the density of differentiated cells.
- Expand the previous model to allow for a density dependent division rate of the stem cells.
- Differentiated cells may also divide, and this rate could also depend on the density. How would that change the model, and do you expect qualitatively different dynamical regimes?
- Finally, remember that we made a spatial model where the stem cells are localized on a substrate allowing a maximum of  $K$  cells to bind in Chapter 3. Does that model properly regulate the fraction of self-renewal divisions?

### Question 13.6. Lymphocyte migration

Naive T cells in the immune system circulate via the blood between various lymphoid organs, such as the spleen and many different lymph nodes. The residence time in the blood is short, and under normal conditions only a small percentage of the naive T cells reside in the blood. In the spleen the residence time is about 6 hours and a typical residence time for a peripheral lymph node is about 13.5 hours (Textor *et al.*, 2014). A model considering the number,  $N$ , of naive T cells specific for a particular antigen (e.g., a peptide derived from a virus) would be

$$B = N - S - L, \quad \frac{dS}{dt} = i_S B - e_S S \quad \text{and} \quad \frac{dL}{dt} = n i_L B - e_L L, \quad (13.5)$$

where  $B$  is the number of cognate naive T cells in the blood,  $S$  is the number of cells in the spleen,  $L$  is the total number of cells in all  $n$  lymph nodes, and the  $i$  and  $e$  parameters are influx rates and efflux rates into the lymphoid organs. Textor *et al.* (2014) estimate that  $i_S = 1\text{h}^{-1}$  and that  $n i_L = 1.5\text{h}^{-1}$ , i.e., most cells leave the blood by entering a lymph node, but the spleen is the organ receiving the vast majority of naive T cells from the blood. Estimating  $n$  is difficult because lymph nodes have different volumes, and there are many small “nodes” like Peyers patches in the gut. Textor *et al.* (2014) estimate that in a mouse there are about  $n = 39$  major lymph nodes.

When an organism is challenged by a pathogen in one of its tissues, proteins from the pathogen are transported to the lymph node(s) draining this tissue, and this triggers an immune response by the cognate naive T cells that are present in this lymph node(s). Since there are so many lymph nodes, only a small fraction, i.e., about  $1/n$ , of the naive T cells is expected to be present in the draining lymph node. However, various experiments have demonstrated that during a localized infection almost all cognate naive T cells are recruited into the immune response on a

time scale of a few days. Since cognate naive T cells are trapped in the draining lymph node when they find their antigen there, one would predict that they will slowly accumulate there. This accumulation is expected to be too slow because naive T cells exiting from another lymph node have only a  $1/n$  probability to arrive in the draining lymph node, and therefore probably end up in another node, where they are expected to spend another 13.5 hours (Textor *et al.*, 2014). In one of the questions below you will study how long this would take. The real solution for recruiting most naive T cells is to enlarge the influx into the draining lymph node, and it is quite spectacular how inflamed lymph nodes can increase their blood supply by angiogenesis. To study this we extend the model by assigning one of the lymph nodes as the draining lymph node, and provide this one lymph node with parameters  $f_i$  and  $f_e$  to modify its influx and efflux upon infection,

$$\frac{dS}{dt} = i_S B - e_S S, \quad \frac{dL}{dt} = (n-1)i_L B - e_L L \quad \text{and} \quad \frac{dD}{dt} = f_i i_L B - f_e e_L D, \quad (13.6)$$

where  $B = N - S - L - D$  and  $f_i = f_e = 1$  when there is no infection. This model is available as the file `circulation.R`

- a. Why can this model be written without a differential equation the number of cells in the blood? What would  $dB/dt$  be if one were to write it? Would that be an identical model?
- b. Find the steady state of Eq. (13.6) by running the model in the absence of an infection for a cognate naive T cell population of a 100 cells (which for most antigens in mice is a realistic number). How many cognate naive T cells are there in any particular lymph node?
- c. The steady state of Eq. (13.5) is

$$\bar{S} = \frac{e_L i_S N}{e_L e_S + e_L i_S + e_S n i_L} \quad \text{and} \quad \bar{L} = \frac{e_S n i_L N}{e_L e_S + e_L i_S + e_S n i_L},$$

(see the Mathematica notebook `circulation.nb`). How many cells do you expect to be present in the blood at steady state? Do you understand why the number of cells in the spleen,  $\bar{S}$ , increases with the efflux,  $e_L$ , of cells from the lymph nodes?

- d. If cognate naive T cells fail to egress from the draining lymph node containing their antigen, how long would it take to accumulate 50% of the cells? Hint: run the model.
- e. Textor *et al.* (2014) cite papers showing that the rate of influx in a draining lymph node can increase 9-fold within a few days. How long would it take to accumulate 50% of the cells in the draining lymph node if the influx is increased 9-fold from the start? Hint: do this numerically with Grind.
- f. How would you modify Eq. (13.6) to increase the influx into the draining lymph node more gradually?

# Chapter 14

## Make a model

The ultimate aim of this course is that you learn to devise a natural mathematical model describing the particular biological system you are interested in. In several of the exercises in the previous chapters you have been challenged to translate a biological story into ODEs, and subsequently analyze the steady states and the behavior of that model to test its validity, and then explore what the model tells us about this particular biological system. Our procedure for developing models was to write a mathematical term for each individual biological process, to define natural concepts like “empty space” and the “concentration of EPO”, and to sketch simple graphs for how each process depends on these concepts, and/or directly on the variables of the model. In this chapter we focus just on this procedure for devising natural models for biological populations. To avoid any distraction, these novel models will not be analyzed (this will be done in some of the exercises in the other chapters). Here we will only need to explain the choices we make, and discuss possible alternatives, to arrive at a reasonable model. Complex biological systems can be translated into many different mathematical models, but only few of them will be relevant and natural when our aim is to better understand the biological system.

### 14.1 Exercises

#### **Question 14.1. Seedlings over-shadowed by adult plants**

Consider a field in which the seeds of one particular plant species are sprouting from a large slow seed bank. The seeds in the seed bank are so long lived that the production of novel seeds by the current population hardly matters. On a daily basis a few seeds sprout from the soil to form small seedlings that either die or mature to become an adult plant (we ignore seasonality). Adult plants die (and produce seeds), and have to be replaced by novel seedlings that successfully mature. Since adult plants are larger than the small seedlings, seedlings growing under the cover of adult plants will receive less sunlight, and hence mature slower than those that directly exposed to the sun. Make a natural model for the number of seedlings and adult plants in the field.

#### **Question 14.2. Whales**

Develop a simple model for a population of whales in the oceans. The special thing about whales is that at low population densities the females face difficulties finding a male. Therefore include the likelihood of finding a mate in your model. Also make sure that the population has

a carrying capacity.

### Question 14.3. Kingfishers

Consider a lake that is visited by members from a population of Common Kingfishers (a colorful bird diving into the water when spotting a fish fitting its beak). The kingfishers have no suitable nesting places at this particular lake, and fly in depending on the availability of fish in the lake, and out after they have caught a fish. Since the kingfishers also forage in other lakes in the area, we assume that their density in the area is independent of their consumption in this particular lake. The fish in the lake grow logistically and have these kingfishers as their major predator. Write a natural model for the total fish density and the density of kingfishers present at this lake.

### Question 14.4. Influenza virus infecting epithelial cells

Epithelial cells in the lungs form a two-dimensional tissue, filling in voids through cell division. Healthy cells have a life expectancy of a few weeks. During a flu infection, the influenza virus spreads across this tissue by infecting epithelial cells. Infected cells have a life expectancy of a few days and produce new viruses. In addition, infected cells produce a protein (interferon) that rapidly spreads through the tissue, and protects uninfected cells against new infections. Assume that the virus and the interferon spread so rapidly through the tissue that it is reasonable to ignore spatial effects, and make a natural model in terms of ODEs for the uninfected epithelial cells, the infected cells, the virus, and for the interferon.

### Question 14.5. DNA circles

T cells are lymphocytes that play an important role in the immune response to viruses. During their development in the thymus they rearrange the DNA coding for the protein with which they recognize viral fragments (and other peptides). As a consequence of this rearrangement, a small piece of DNA is excised, which forms a plasmid-like circle that persists in the cytoplasm. Mature T cells leave the thymus and enter the circulation to check the body for viruses. They now-and-again divide, and because the DNA circle is not replicated during cell division, only one of the two daughter cells inherits the circle. Using a PCR based method one can measure the *fraction* of T cells containing such a circle, and this fraction has been used as a proxy for the contribution of the thymus to the maintenance of the population (Hazenberg *et al.*, 2000; Den Braber *et al.*, 2012). Indeed one can view such a DNA circle as a marker for a cell that was born in the thymus. Write a natural model for the number of cells and the fraction of circles they contain.

### Question 14.6. Maintenance and reproduction

Zooplankton species like *Daphnia* eat algae and need this resource both for their own maintenance (i.e., in order to survive), and to reproduce (e.g., the production of eggs). Both processes depend on the amount of algae that they consume and when they consume too little, no (or virtually no) eggs are produced because they need all they can eat for their maintenance. Sketch simple curves for the survival rate, and the rate at which eggs are produced, as a function of the *per capita* consumption, and write a natural model for the zooplankton, their eggs, and algae in an aquarium.

## Chapter 15

# Appendix: mathematical prerequisites

### 15.1 Phase plane analysis

Most mathematical models in biology have non-linearities and can therefore not be solved explicitly. One can nevertheless obtain insight into the behavior of the model by numerical (computer) analysis, by sketching nullclines, and by solving for steady states. One determines the stability of these steady states can be determined by linearization around the steady state, or from the vector field. Two simple examples for sketching nullclines and finding steady states are given in our online tutorial [tbb.bio.uu.nl/rdb/bm/clips/nullclines](http://tbb.bio.uu.nl/rdb/bm/clips/nullclines). The remainder of this paragraph provides some background information.

The long-term behavior of a model typically approaches a stable steady state, a stable limit cycle, or a chaotic attractor. Phase plane analysis is a graphical method to analyze a model to investigate these behavioral properties. Considering a model of two variables  $x$  and  $y$ ,

$$\frac{dx}{dt} = f(x, y) \quad \text{and} \quad \frac{dy}{dt} = g(x, y) , \quad (15.1)$$

one can define a “phase space” or “state space” with  $x$  on the horizontal axis and  $y$  on the vertical axis, where each point in this space is one particular “state” of the model. To obtain further insight in the model one sketches the “nullclines”  $f(x, y) = 0$  and  $g(x, y) = 0$ . This is useful because at the  $x$ -nullcline  $dx/dt$  switches sign, and at the  $y$ -nullcline  $dy/dt$  switches sign. Two simple nullclines therefore typically define regions in the state space with qualitatively different signs of the ODEs. Nullclines enable one to localize all steady states of the model because these correspond to the intersections of their (i.e.,  $f(x, y) = g(x, y) = 0$ ). This is very useful because models may have multiple steady states that could be difficult to find analytically.

For each steady state one has to determine whether it is an attractor, i.e., a stable steady state, or a repeller, i.e., an unstable equilibrium. The local vector field around a steady state in a phase space with nullclines often provides sufficient information to see whether the steady state is stable or unstable. In 2-dimensional phase spaces there are three classes of steady states: nodes, saddles, and spirals. Nodes and spirals are either stable or unstable, and a saddle point is always unstable because it has a stable and an unstable direction. The two nullclines intersecting at the equilibrium point define four local regions of phase space around the steady state, each

with its unique local vector field. These four local vector fields define the nature of the steady state.

A simple example is a “stable node”, for which all four vector fields point towards the steady state (see Fig. 15.1a). A stable node is therefore approached by trajectories from all four directions (Fig. 15.1b). When the vector fields point outward in all four regions the equilibrium is an “unstable node” (Fig. 15.1c), and trajectories are repelled in all four directions (Fig. 15.1d). The local vector fields in Fig. 15.1e define a “saddle point”, which has a stable and an unstable direction (Fig. 15.1f). The stable direction of a saddle point defines a “separatrix” because all trajectories starting at either side of this line end up in another attractor (i.e., a separatrix defines different basins of attractions).

The local vector field can also suggest rotation (see Fig. 15.2), suggesting (!) that the steady state is a spiral point. This need not be true, however. Fig. 15.2e illustrates an example of a stable node surrounded by rotating vector field. A rotating local vector field provides little information for determining the stability of a steady state, and one typically needs to resort to linearization and determine the Jacobi matrix (see the accompanying Ebook (Panfilov *et al.*, 2025)). There is a simple trick that can provide an indication on the stability of a steady state surrounded by a rotating vector field. First, such a steady state cannot be a saddle point because the local vector field has no stable and unstable direction, i.e., the determinant of the Jacobi matrix will be positive. Thus, it would be sufficient to know the sign of the trace of the Jacobian. Second, we can graphically determine the sign of the two elements of the diagonal of the Jacobian by studying the local feedback of the populations onto themselves. For instance, in Fig. 15.2c, one can see that increasing  $y$  from its steady state value makes  $dy/dt > 0$ , which corresponds to a positive local feedback allowing  $y$  to increase further when  $y$  increases. This is definitely destabilizing, and establishes that  $\partial_y dy/dt > 0$ , allowing the trace to be positive. Fig. 15.2d confirms that this is an “unstable spiral” point. Conversely, the spiral point in Fig. 15.2a is stable, and locally has negative feedback for both  $x$  and  $y$ , i.e., increasing  $x$  makes  $dx/dt < 0$  and increasing  $y$  makes  $dy/dt < 0$ . This has a stabilizing influence, and establishes that  $\partial_x dx/dt < 0$  and  $\partial_y dy/dt < 0$ , which defines the trace to be negative. Thus, if neither of the two variables has a positive local feedback onto itself, one may expect a steady state surrounded by a rotating vector field to be stable.

This trick of determining the local feedback from the vector field can be generalized, as one can determine all signs of the Jacobi matrix from the local vector field around the steady state (again see the accompanying Ebook (Panfilov *et al.*, 2025)). Consider the vector field around the steady state of some system  $dx/dt = f(x, y)$  and  $dy/dt = g(x, y)$ . Around the steady state  $(\bar{x}, \bar{y})$  in the phase space  $(x, y)$  the sign of  $dx/dt$  is given by the horizontal arrows, i.e., the horizontal component of the vector field. The sign of  $\partial_x f$  can therefore be determined by making a small step to the right, i.e., in the  $x$  direction, and reading the sign of  $dx/dt$  from the vector field. Similarly, a small step upwards gives the effect of  $y$  on  $dx/dt$ , i.e., gives  $\partial_y f$ , and the sign can be read from the vertical arrow of the vector field. Trying this for the non-trivial steady states in Fig. 15.2, one finds in Fig. 15.2a and e the graphical Jacobian,

$$J = \begin{pmatrix} -\alpha & -\beta \\ \gamma & -\delta \end{pmatrix}, \quad (15.2)$$

and because  $\text{tr}(J) = -\alpha - \delta < 0$  and  $\det(J) = \alpha\delta + \beta\gamma > 0$  this firmly establishes that the equilibrium is stable. Conversely, the Jacobian of the non-trivial steady state in Fig. 15.2c,

$$J = \begin{pmatrix} -\alpha & -\beta \\ \gamma & \delta \end{pmatrix}, \quad (15.3)$$

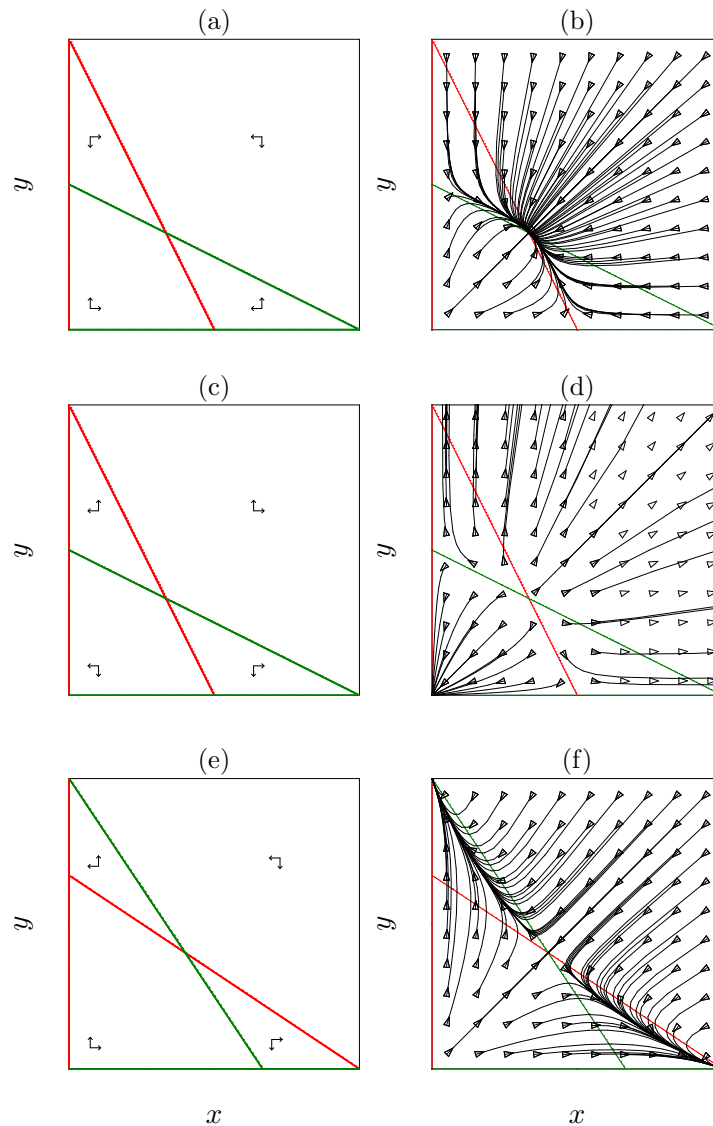


Figure 15.1: Qualitatively different steady states are determined by the local vector field in the four regions defined by the nullclines. Stable node (a,b): the vector field points inwards in all four sections. Unstable node (c,d): the vector field points outwards in all four sections. Saddle point (e,f): the vector field points inwards in two sections, and outwards in the other two regions. A saddle point is an unstable steady state with a stable and an unstable direction.

has  $\text{tr}(J) = -\alpha + \delta$  and  $\det(J) = -\alpha\delta + \beta\gamma$ , which both have an unknown sign, confirming that the steady state need not be stable. This graphical method is also explained in the book of Hastings (1997).

## 15.2 Linearization

Complicated non-linear functions,  $f(x)$ , can be approximated by a local linearization around any particular value of  $x$  (see the accompanying Ebook (Panfilov *et al.*, 2025)). Fig. 15.3 shows that the local tangent at some point linearizes the function so that nearby function values can be estimated. This derivative can be used to approximate the curved  $f(x)$  around a particular

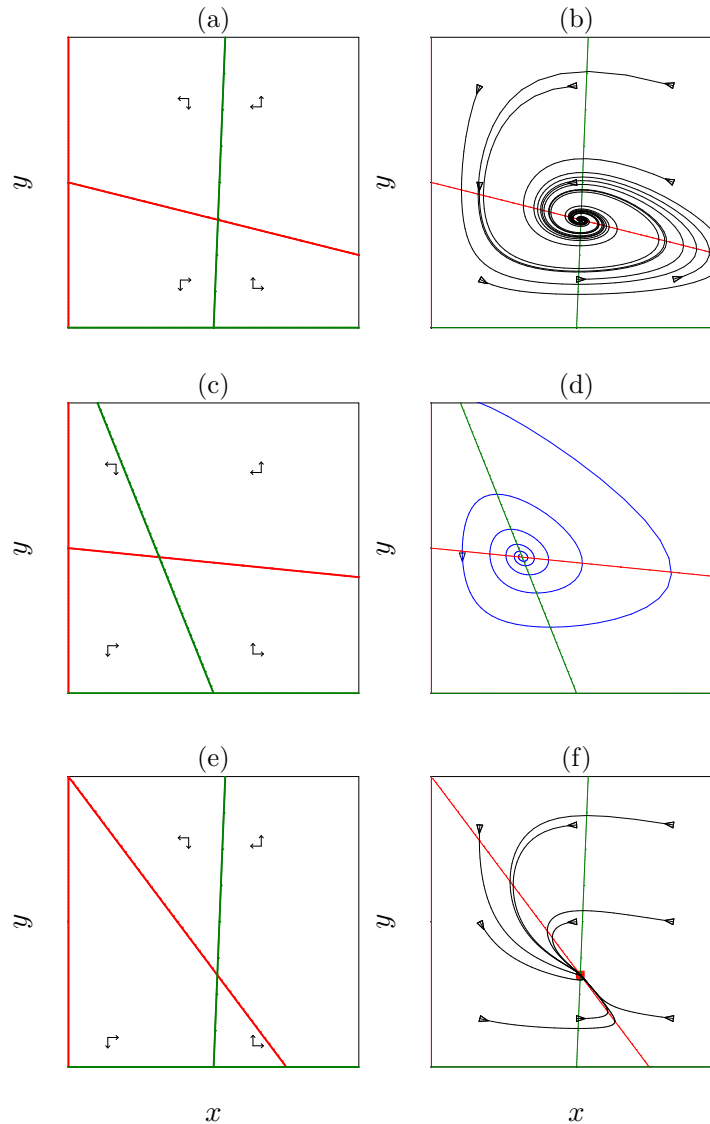


Figure 15.2: Stability of steady states surrounded by a rotating vector field. In all Panels the vector field rotates anti-clock wise, but the phase portraits show that the steady state can be a stable spiral point (a-b), an unstable spiral point (c-d), or a stable node (e-f). The stability in Panels (a) and (e) can be guessed because increasing  $x$  at the steady states makes  $dx/dt < 0$ , and increasing  $y$  at the steady states makes  $dy/dt < 0$  (which is both stabilizing). The unstable spiral in Panel (c) can be guessed because increasing  $y$  at the steady states makes  $dy/dt > 0$  (which is destabilizing). Panels (e & f) reveal that one cannot tell from the local field whether or not a steady state is a spiral point or a node.

value  $\bar{x}$ , and from Fig. 15.3 we can read that

$$f(x) \simeq f(\bar{x}) + \partial_x f(\bar{x})(x - \bar{x}) ,$$

where  $h = x - \bar{x}$  is a small step in the  $x$ -direction that we multiply with the local slope,  $\partial_x f(\bar{x})$ , to approximate the required change in the vertical direction. Basically, one estimates the vertical displacement by multiplying the local slope with the horizontal displacement. A simple example would be the function  $f(x) = 3\sqrt{x}$  (with derivative  $f' = 3/[2\sqrt{x}]$ ). The true function values for  $x = 4$  and  $x = 5$  are  $f(4) = 6$  and  $f(5) = 6.71$ , respectively. We can approximate the latter by

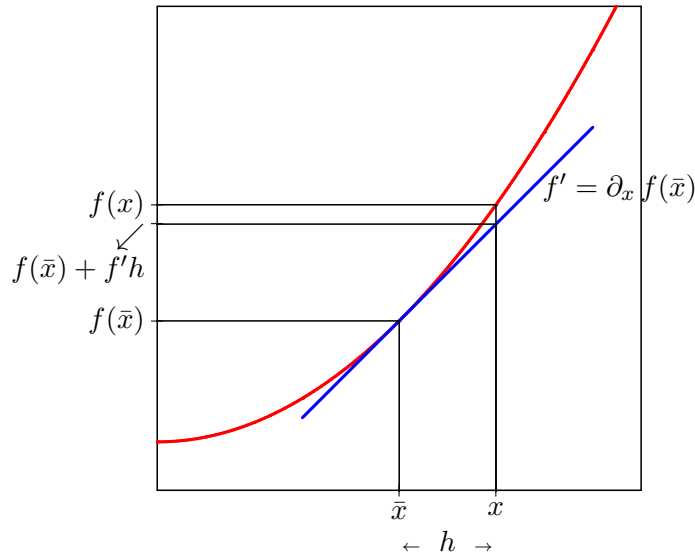


Figure 15.3: Linearization of a non-linear function:  $f(x) \simeq f(\bar{x}) + \partial_x f(\bar{x})(x - \bar{x}) = f(\bar{x}) + f'h$ . The heavy line is the local tangent  $f' = \partial_x f(\bar{x})$  at  $x = \bar{x}$ .

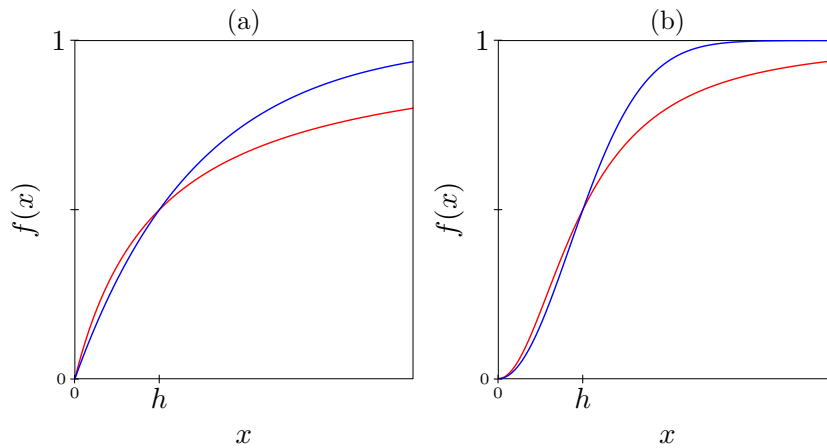


Figure 15.4: Increasing saturation functions defined by Eqs. (15.7) and (15.11). Panel (a) depicts  $f(x) = x/(h + x)$  (red) and  $f(x) = 1 - e^{-\ln[2]x/h}$  (blue), which both have the convenient property that  $0 \leq f(x) < 1$  and  $f(x) = 0.5$  when  $x = h$ . In Panel (b) we draw their corresponding sigmoid variants  $f(x) = x^2/(h^2 + x^2)$  (red) and  $f(x) = 1 - e^{-\ln[2](x/h)^2}$  (blue). Figure made with `hillFunctions.R`.

writing

$$f(5) \simeq f(4) + \frac{3}{2\sqrt{4}} \times 1 = 6 + 3/4 = 6.75 , \tag{15.4}$$

which is indeed close to  $f(5) = 6.71$ . The same can be done for 2-dimensional functions, i.e.,

$$f(x, y) \simeq f(\bar{x}, \bar{y}) + \partial_x f(\bar{x}, \bar{y})(x - \bar{x}) + \partial_y f(\bar{x}, \bar{y})(y - \bar{y}) . \tag{15.5}$$

### 15.3 Convenient functions

Once we have a sketch of how some process should depend on a variable of the model, we need to translate this graph into a mathematical function. We therefore need simple and preferably non-dimensional functions. For instance, a simple and convenient non-dimensional function is

$$f(x) = 1 - (x/k)^n, \quad (15.6)$$

which declines from one to zero over the interval  $x = 0$  to  $x = k$ . When  $n = 1$  the decline is linear, when  $n > 1$  the function is concave, and when  $n < 1$  it is convex. A drawback of this function is that it becomes negative when  $x > k$ , which we repair in Eq. (3.12) by adding a maximum function, i.e.,  $f(x) = \max[0, 1 - (x/k)^n]$ . Obviously, the same power term,  $(x/k)^n$ , can also be used to define increasing non-dimensional functions, e.g.,  $f(x) = (x/k)^n$ .

Another convenient family of non-dimensional functions are the Hill-functions and exponential functions, which are frequently used to formulate positive and negative effects of populations onto each other. Because these functions are dimensionless and remain bounded between zero and one, i.e.,  $0 \leq f(x) \leq 1$ , one can easily multiply any term in a model (corresponding to some biological process) with such a function. We here define families of functions,  $f(x)$ , that increase with  $x$ , are zero when  $x = 0$ , and approach a maximum  $f(x) = 1$  when  $x \rightarrow \infty$ . Whenever one would need a different maximum in the model, one could simply multiply  $f(x)$  with some parameter. Having increasing functions  $0 \leq f(x) \leq 1$ , one can easily define decreasing functions by considering  $g(x) = 1 - f(x)$ .

Hill functions define a very conventional and convenient family of saturation functions:

$$f(x) = \frac{x^n}{h^n + x^n} \quad \text{and} \quad g(x) = 1 - f(x) = \frac{1}{1 + (x/h)^n}, \quad (15.7)$$

in which you may recognize the classic Michaelis-Menten saturation function for  $n = 1$  (see Fig. 15.4a). The ‘‘saturation constant’’  $h$  is the value of  $x$  where  $f(x)$  or  $g(x)$  attains half of its maximal value. The exponent  $n$  determines the steepness of the function: whenever  $n > 1$  the function is sigmoid (see Fig. 15.4b). For  $n \rightarrow \infty$  both  $f(x)$  and  $g(x)$  become step functions switching between zero and one at  $x = h$ . The slope of  $f(x)$  in the origin is determined from its derivative, which for  $n = 1$  equals

$$\partial_x f(x) = \frac{1}{h+x} - \frac{x}{(h+x)^2}, \quad (15.8)$$

which gives a slope of  $1/h$  for  $x = 0$ . For  $n > 1$  the derivative is

$$\partial_x f(x) = \frac{nx^{n-1}}{h^n + x^n} - \frac{nx^{2n-1}}{(h^n + x^n)^2}, \quad (15.9)$$

which means that for  $x = 0$  the slope is zero. An advantage of using Hill functions in mathematical models is that solving steady states corresponds to solving polynomial functions.

The declining power function of Eq. (15.6) and the declining Hill function of Eq. (15.7) differ in the interpretation of their parameters  $k$  and  $h$ , because  $k$  is the density at which  $f(x) = 0$  in Eq. (15.6), and  $h$  is the density at which  $g(x) = 0.5$  in Eq. (15.7). Obviously, we can re-define  $k$  in Eq. (15.6) into an  $h$  parameter corresponding to the  $x$ -value where  $f(x) = 0.5$ . To do so we define  $f(x) = 1 - (x/(\alpha k))^n$ , set  $x = k$ , and solve  $\alpha$  from  $0.5 = 1 - (1/\alpha)^n$ , which gives  $\alpha = \sqrt[n]{2}$  as a scaling factor. Thus, renaming  $k$  into  $h$ , and defining

$$f(x) = 1 - \left( \frac{x}{\sqrt[n]{2}h} \right)^n, \quad (15.10)$$

we have simple linear, convex, or concave declining function that is half-maximal at  $x = h$ .

The following exponential functions,

$$f(x) = 1 - e^{-\ln[2]x/h} \quad \text{and} \quad g(x) = e^{-\ln[2]x/h}, \quad (15.11)$$

are similar to Hill functions, because by adding the  $\ln[2]$  correction we have again scaled  $h$  such that  $f(x) = g(x) = 0.5$  when  $x = h$  ( $e^{-\ln[2]} = 0.5$ ). Like Hill functions we have  $f(0) = 0$ , and the slope in the origin is determined from the derivative  $\partial_x[1 - e^{-\ln[2]x/h}] = (\ln[2]/h)e^{-\ln[2]x/h}$ , which for  $x = 0$  gives a slope of  $\ln[2]/h$ . The sigmoid form of the exponential function is known as the Gaussian distribution

$$f(x) = 1 - e^{-\ln[2](x/h)^2}, \quad \text{and} \quad g(x) = e^{-\ln[2](x/h)^2}. \quad (15.12)$$

Thanks to the same scaling with  $\ln[2]$  these sigmoid functions are also half maximal when  $x = h$  (and  $x = -h$ ); see Fig. 15.4b. Exponential functions may be more convenient for finding solutions of equations, but they are more cumbersome when it comes to finding steady states.

Finally, we have seen that discontinuous saturation functions can easily be written with minimum and maximum functions. For instance,  $f(x) = \min[1, x/(2h)]$  has its half-maximal value  $f(x) = 0.5$  when  $x = h$ , and has a discontinuity at  $x = 2h$  where  $f(x) = 1$ . Summarizing, we have a variety of simple non-dimensional functions at hand to define various sorts of density dependent relationships in our models.

## 15.4 Scaling

Models can be simplified by scaling variables and time to reduce the number of parameters. Such scaled variables are typically dimensionless. Reducing the number of parameters of a model can be very helpful to completely understand its behavior, e.g., there will be fewer parameters that need to be studied by bifurcation analysis. The technique is explained here by making a dimensionless logistic growth model. In the exercises you will be asked to make a non-dimensional Lotka-Volterra model.

Write the logistic equation as

$$\frac{dN}{dT} = rN[1 - N/k], \quad (15.13)$$

where  $r$  is the *per capita* maximum rate of increase, and  $k$  is the carrying capacity. The parameter  $r$  is a rate, with dimension  $1/T$ , and the parameter  $k$  has the dimension “biomass” or “number of individuals”. First scale the biomass such that the carrying capacity becomes one. We introduce a new variable  $n$  with the property  $n = N/k$  such that  $n = 1$  when  $N = k$ . Now substitute  $N = kn$  in Eq. (15.13), i.e.,

$$\frac{dkn}{dT} = k \frac{dn}{dT} = rkn[1 - kn/k], \quad (15.14)$$

which simplifies into

$$\frac{dn}{dT} = rn[1 - n], \quad (15.15)$$

which indeed has a carrying capacity  $\bar{n} = 1$ .

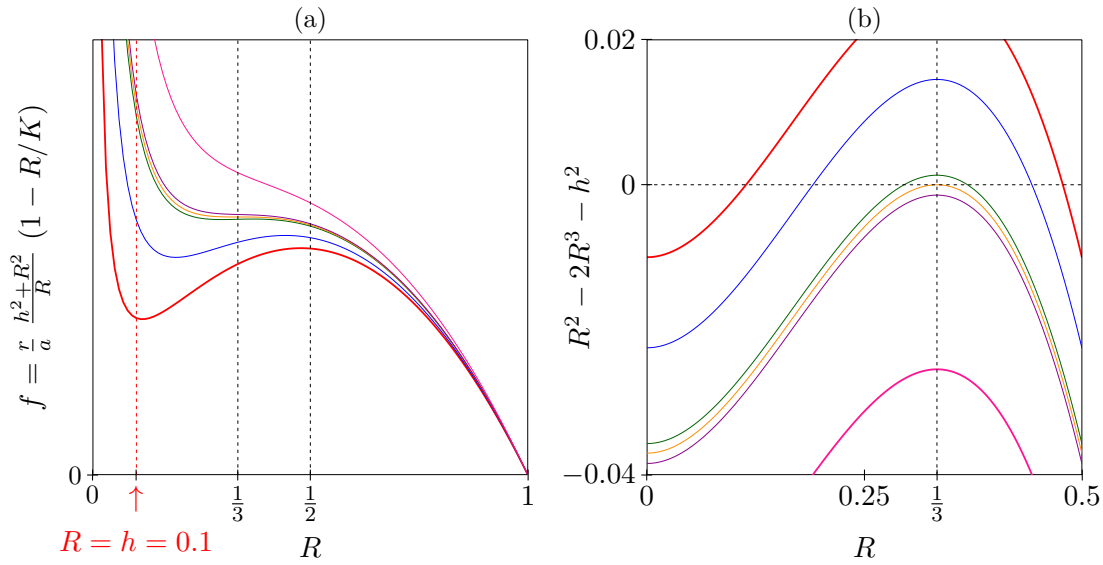


Figure 15.5: Finding the saturation constant,  $h$ , at which the resource nullcline of a model with a sigmoid functional response has its characteristic non-monotonic shape. Panel (a) plots Eq. (15.18) for  $r/a = K = 1$  and  $h = 0.1$  (red),  $h = 0.15$  (blue),  $h = 1/\sqrt{28} \simeq 0.189$  (green),  $h = 1/\sqrt{27} \simeq 0.192$  (orange),  $h = 1/\sqrt{26} \simeq 0.196$  (purple), and  $h = 0.25$  (pink), respectively. Panel (b) plots the simplified numerator,  $R^2 - 2R^3/K - h^2$ , of Eq. (15.19) for  $K = 1$  and the same six values of  $h$  (using the same colors), which shows that  $R^2 - 2R^3 - h^2 = 0$  only has two positive solutions when  $h$  is sufficiently small (i.e., only the red, blue and green lines intersect the dashed horizontal line at 0 twice). The orange line depicts the critical value,  $h = 1/\sqrt{27} \simeq 0.2$  touching the horizontal axis at  $R = 1/3$ . This figure was made with the script `sigmoid0.R`.

Having lost one parameter one can scale time,  $t = rT$ , such that the parameter  $r$  disappears, i.e.,

$$\frac{dn}{dT} = \frac{dn}{(1/r)dt} = r \frac{dn}{dt} = rn[1 - n]. \quad (15.16)$$

This defines a new time scale for which

$$\frac{dn}{dt} = n[1 - n]. \quad (15.17)$$

This non-dimensional form of the logistic growth equation proves that its solution is always the same sigmoid function. Thus, the only effect of choosing different parameter values of  $r$  and  $k$  while plotting  $N(T)$  as a function of time, is a scaling of the horizontal and vertical axis.

## 15.5 The resource nullcline with a sigmoid functional response

In Section 7.2 we wrote the resource nullcline of a model with a sigmoid functional response as the following function

$$f = \frac{r}{a} \frac{h^2 + R^2}{R} \left(1 - \frac{R}{K}\right), \quad (15.18)$$

which has a vertical asymptote at  $R = 0$ , is zero when  $R = K$  (see Fig. 15.5a), and is scaled vertically by a constant  $r/a$ . This function will have minima and/or maxima when its derivative,  $\partial_R f = 0$ , i.e., when

$$\partial_R f = \frac{r}{a} \frac{R^2 - 2R^3/K - h^2}{R} = 0. \quad (15.19)$$

After scaling  $R$  and  $h$  by setting  $K = 1$  this simplifies to solving when the numerator equals zero, i.e., to solving when  $R^2 - 2R^3 - h^2 = 0$ . Since this expression has only one (scaled) parameter,  $h$ , we plot it as a function of  $R$  for various values of  $h$  in Fig. 15.5b. This reveals that this equation has no positive solutions when  $h^2 > 1/27$ , and has two positive solutions when  $h^2 < 1/27$  (see the red, blue and green lines in Fig. 15.5b). Thus, the critical value for having a minimum and maximum is  $h < 1/\sqrt{27} \simeq 1/5$ . The value of  $R$  at this critical value of  $h$  can be solved from  $R^2 - 2R^3 - 1/27 = 0$ , yielding  $R = 1/3$  (see the vertical dashed line in Fig. 15.5b). The minimum and the maximum are therefore located below and above  $R = 1/3$ . Since we scaled  $K = 1$  this generalizes to  $h < K/5$  and  $R_{\min} < K/3 < R_{\max}$ .

The location of the minimum,  $R_{\min}$ , can be estimated by considering that it is located at small values of  $R$ , i.e., by assuming that  $2R^3/K \simeq 0$ , after which one obtains  $R_{\min} \simeq h$  from solving the numerator  $R^2 - h^2 = 0$ , which is independent of the carrying capacity  $K$ . Conversely, for large values of  $R$  (i.e., when  $R \rightarrow K$ ) and small values of  $h$  (since  $h < K/5$  anyway), the location of the maximum can be solved from  $R^2 - 2R^3/K = 0$  yielding  $R_{\max} \simeq K/2$ . The heavy red nullcline in Fig. 15.5a, where  $K = 1$  and  $h = 0.1$ , confirms these estimates (see the vertical dashed lines). Note that the location of the maximum can also be estimated by considering  $h \simeq 0$  in Eq. (15.18), which then approaches  $f = (r/a)R(1 - R/K)$ , which is a parabola having its maximum at  $R = K/2$ .

## 15.6 A few useful mathematical formulas

The website [tbb.bio.uu.nl/rdb/bm/clips/algebra](http://tbb.bio.uu.nl/rdb/bm/clips/algebra) provides a tutorial summarizing some basic algebra. Here we just provide a few standard formulas

$$\ln 1 = 0, \quad \ln xy = \ln x + \ln y, \quad \ln x/y = \ln x - \ln y, \quad e^{ix} = \cos x + i \sin x, \quad (15.20)$$

and the two roots of the quadratic equation

$$ax^2 + bx + c = 0 \quad \text{are} \quad x_{\pm} = \frac{-b \pm \sqrt{b^2 - 4ac}}{2a}. \quad (15.21)$$

The standard rules of differentiation are

$$[cx]' = c, \quad [cx^n]' = ncx^{n-1}, \quad [f(x) + g(x)]' = f'(x) + g'(x), \quad (15.22)$$

where the  $'$  means  $\partial_x$ , and

$$[f(x)g(x)]' = f'(x)g(x) + f(x)g'(x), \quad \left[ \frac{f(x)}{g(x)} \right]' = \frac{f'(x)}{g(x)} - \frac{f(x)g'(x)}{g(x)^2}, \quad (15.23)$$

and the famous chain rule

$$f[g(x)]' = f'(g) g'(x) \quad , \text{ e.g., } \quad \sqrt{1+ax}' = \left[ \frac{1}{2}(1+ax)^{-\frac{1}{2}} \right] a = \frac{a}{2\sqrt{1+ax}}. \quad (15.24)$$

### Trace and determinant

In the accompanying Ebook (Panfilov *et al.*, 2025) we explain that the eigenvalues of an arbitrary matrix

$$A = \begin{pmatrix} a & b \\ c & d \end{pmatrix} \quad (15.25)$$

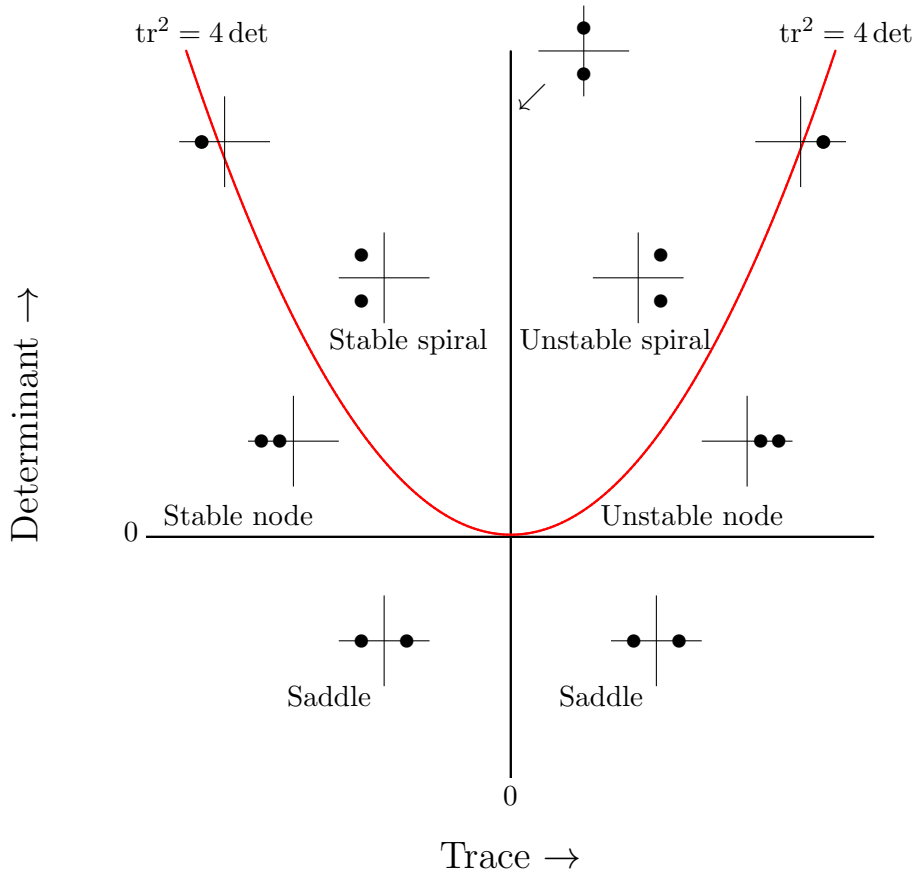


Figure 15.6: The stability of a steady state as a function of the trace and determinant of a 2-dimensional Jacobi-matrix. The bullets depict the real and imaginary parts of the eigenvalues in so-called Argand diagrams (where the horizontal axis reflects the real part, and the vertical axis the imaginary part of the eigenvalue).

are the solutions of the characteristic equation

$$(a - \lambda)(d - \lambda) - bc = \lambda^2 - \lambda(a + d) + (ad - bc) = 0 . \tag{15.26}$$

Defining the “trace” of the matrix as  $tr = a + d$  and the “determinant” as  $\det = ad - bc$ , the characteristic equation simplifies into

$$\lambda^2 - tr\lambda + \det = 0 \tag{15.27}$$

with solutions

$$\lambda_{\pm} = \frac{tr \pm \sqrt{tr^2 - 4 \det}}{2} = \frac{tr \pm \sqrt{D}}{2} , \tag{15.28}$$

where  $D \equiv tr^2 - 4 \det$  is the “discriminant” of the matrix. If  $D < 0$  the  $\sqrt{D}$  yields imaginary solutions that correspond with oscillations ( $e^{ix} = \cos[x] + i \sin[x]$ ).

Summing the two eigenvalues  $\lambda_{\pm}$  yields

$$\frac{tr + \sqrt{tr^2 - 4 \det}}{2} + \frac{tr - \sqrt{tr^2 - 4 \det}}{2} = tr , \tag{15.29}$$

and the product gives

$$\frac{tr + \sqrt{tr^2 - 4 \det}}{2} \times \frac{tr - \sqrt{tr^2 - 4 \det}}{2} = \det . \tag{15.30}$$

If this matrix was the Jacobian of a steady state, we now observe that to check for stability, i.e.,  $\lambda_+ < 0$  and  $\lambda_- < 0$ , it is therefore in many cases sufficient to know the values of the trace and the determinant. When  $\det > 0$  one knows that either both eigenvalues are negative or that they are both positive. Having  $\det > 0$  and  $\text{tr} < 0$  one knows that they cannot be positive, and therefore that they are both negative and the steady state has to be stable. Summarizing an easy test for stability is  $\text{tr}[J] < 0$  and  $\det[J] > 0$  (see Fig. 15.6).

Although we do not prove this here, this result for the trace and determinant are also true for high-dimensional matrices, i.e.,  $\sum \lambda_i = \text{tr}(A)$  and  $\prod \lambda_i = \det(A)$ . The latter also tells you that the eigenvalues of a matrix in a triangular form, i.e., a matrix whose elements above or below the main diagonal are all zero, can be solved from the characteristic equation  $(A_{11} - \lambda)(A_{22} - \lambda) \dots (A_{nn} - \lambda) = 0$ .

## 15.7 Parameter estimation

The interpretation of data comprised of longitudinal measurements of population densities can be improved by describing the data points with an appropriate mathematical model. The parameters of a mechanistic model that reasonably “fits” the data provide quantitative information on the biological processes implemented in the model, which together apparently suffice to explain the data. Thus, it can be very useful to identify the models and parameters that can account for the population dynamics described by data. The main problem with most interesting models in biology is that they have complicated non-linear terms, and several parameters, which makes it difficult to find the “optimal” set of parameters by simple statistical procedures (such as linear regression).

There are several numerical techniques to fit complex models to data, and most of these are based upon clever gradient descent methods, where one makes an initial guess on the parameter values, and the algorithm subsequently makes small changes to all “free” parameters until it finds a direction in parameter space bringing the prediction of the model closer to the data. This process of taking small steps through parameter space is repeated until a minimum is found where small changes no longer improve the quality of the fit. Although this may sound like a straightforward approach, it is difficult to know whether or not this minimum corresponds to the true optimum, i.e., to the global minimum. Additionally, whether or not these methods find the optimum can crucially depend on the initial values of the free parameters, which are usually based upon a wild guess. Complex models typically have several local optima and gradient descent methods easily get stuck in a local minimum. It is therefore essential (1) to have an informed initial guess, (2) to limit the number of free parameters, and (3) to try a variety of initial guesses.

Non-linear parameter fitting procedures attempt to reduce the distance between the model prediction and the data, and this distance is typically defined as the summed squared residuals (SSR). For instance, consider a data set of population densities,  $N(t)$ , measured at various points in time,  $t$ . Since we may have several measurements at each time point we will call them  $N(t_i)_i$ , where  $i$  is the index of the data point, and  $t_i$  the time point at which the data point was measured. Having a mathematical model with a vector of parameters,  $p$ , and an initial condition,  $S(0)$  (for state), we can predict the state of this model,  $S(t)$  for all time points,  $t_i$ , in the data, by numerically solving the model. The distance between the data,  $N(t_i)_i$ , and the

model prediction,  $S(t)$ , for parameters,  $p$ , can then be defined as

$$\text{SSR} = \sum_i^n [N(t_i)_i - S(t_i)]^2, \quad (15.31)$$

where we have  $n$  data points, and we sum the squared differences between each observed population density and the corresponding predicted density. Minimizing the SSR by an algorithm searching better parameter values is called a “least-squares” approach. Note that an appropriate model may require more variables than are available in the data, i.e., not all variables need to be observed, and we then have to match a subset of the variable(s) of the model to the corresponding observable(s) in the data. Once a gradient descent method has minimized the SSR and halts, the SSR is a measure for the quality of the fit of the model to the data.

One major problem with non-linear parameter fitting procedures is that there may be several local minima, and that not all parameters need to be “identifiable” (James *et al.*, 2014; Castro & De Boer, 2020). The methods will nevertheless halt and report an SSR with an associated set of “optimal” parameter values. For instance, if one were to fit the birth-death model,  $dN/dt = (b - d)N$ , to the densities of a population that is growing exponentially by equivalent birth and death events, the values of  $b$  and  $d$  are nevertheless not identifiable because the observed time series of population densities only contains information on the net replication rate  $r = b - d$ . Thus, the only identifiable parameters would be  $r$  and the initial condition  $N(0)$ . The estimates for  $b$  and  $d$  can take any value depending on their initial guesses, and these values will be correlated because  $b = r + d$ . This is a trivial example, but in complex models it can be very difficult to determine which parameters are identifiable.

It is therefore essential to quantify the potential variation of parameter estimates, and to check for such correlations. An excellent approach to obtain such “confidence intervals” on the parameter estimates is “bootstrapping” (James *et al.*, 2014), which basically means that new data sets are created by sampling the original data (with replacement). Fitting the model to many of these different “new” data sets provides a variety of values for every free parameter. Sorting these, one can exclude the outliers (that apparently are due to outliers in the data), and report the range of parameter values that is typically obtained, e.g., a 95% confidence interval for a parameter corresponds to the range of its values observed in 95% of the fits to the bootstrapped data. Since bootstrapping provides a variety of estimates for each parameter, one can also check for pairwise correlations between parameters by plotting their individual estimates as a function of each other (R provides the `pairs()` function for this).

Full textbooks have been written on this important topic, and this section is nothing more than a short introduction. We end by saying that Eq. (15.31) may (or should) involve normalization of the data, e.g., by taking the logarithm of the data and the prediction, and that it may (or should) be weighted by the variance of the data. The latter is typically done in “maximum likelihood” methods (that are favored by statisticians). Fortunately, as long one is fitting a single data set, least-square and maximum likelihood methods are expected to give identical results (provided the errors in the data are distributed normally). A more recent development is to use Bayesian inference methods, and for this the <https://mc-stan.org/> platform is gaining popularity. In this course we use the least-square methods implemented in FME (Soetaert & Petzoldt, 2010), which you can easily call by the `fit()` function in Grind. The parameter `bootstrap` in `fit()` allows you to bootstrap the data (setting `bootstrap=500` will make 500 re-sampled data sets, and will probably take a while).

## 15.8 Gillespie algorithm

Differential equations describe the rate of change of populations, and although biological populations are composed of discrete individuals, cells, or molecules, in ODEs these changes typically correspond to non-integer values (i.e., to real values). As a consequence the population densities allow for fractions of individuals, and this will become unrealistic whenever population densities are low (e.g., during an oscillation). This is sometimes referred to as the “atto fox” problem (atto stands for  $10^{-18}$ ), coming from models where tiny fractions of foxes were able to invade into new territories. Whenever population numbers are low one should account for stochasticity and only allow for integer numbers of individuals.

A solution to this problem is the Gillespie algorithm (Gillespie, 1977, 2007), in which the terms of a model are interpreted as probabilities (or propensities), for the likelihood that particular events, like a bi-molecular interaction, a birth, or a death, will occur within a short time interval, given the current state of the system. Upon the completion of the randomly chosen event, the population sizes are changed accordingly by a discrete number of individuals (which keeps all population sizes an integer number of individuals). Thus, the Gillespie algorithm is a stochastic simulation of a system of differential equations, and in linear (or linearized) systems it can be demonstrated that the average of many of these simulations corresponds to the solution of the system of ODEs (Gillespie, 1977, 2007).

For example, consider a Lotka-Volterra model with explicit birth and death rates, for prey,  $R$ , and predators,  $N$ ,

$$\frac{dR}{dt} = bR(1 - R/k) - dR - aRN \quad \text{and} \quad \frac{dN}{dt} = aRN - \delta N . \quad (15.32)$$

This model describes four potential events: birth of a prey individual (at a rate  $p_1 = bR(1 - R/k)$ ), normal death of prey individual (at a rate  $p_2 = dR$ ), killing of a prey resulting in the birth of a predator individual (at a rate  $p_3 = aRN$ ), and death of predator individual (at a rate  $p_4 = \delta N$ ). Knowing the current state of the system at time  $t$ , i.e.,  $(R(t), N(t))$ , one can compute these four rates at this point in time, and hence one would know the relative probabilities with which they are expected to occur in a next very small step,  $\tau$ , i.e., within the time interval  $[t, t + \tau]$ . According to the Gillespie algorithm, one draws a random number to select which of the four events is going to happen, where the likelihood that a particular event is chosen is proportional to its relative rate, i.e., to  $p_i / \sum p_i$ . For example, one can draw a random variable,  $0 < u < 1$ , from a uniform distribution (e.g., by calling `runif(1)` in R), define the cumulative sum of the rates,  $\hat{p}_i = \sum_1^i p_j$ , and find the smallest index  $i$  satisfying  $\hat{p}_i > u \sum_j p_j$ . After choosing the event, the state of the system is updated accordingly (here by adding or removing one prey and/or predator individual).

Since in ODEs the time span between two events is exponentially distributed, and is inversely proportional to the rate, one sums the rates to define an expected time  $\bar{\tau} = 1 / \sum p_i$  to the next event. Next the actual time interval is determined stochastically by drawing from exponentially distributed random numbers (`rexp()` in R). This random number is multiplied with the expected time,  $\tau = \bar{\tau} \times \text{rexp}()$ , and times is advanced by this time step, i.e.,  $t \leftarrow t + \tau$ . Time therefore progresses in small intervals,  $\tau$ , when there are many likely events, e.g., when populations are large, and with larger steps,  $\tau$ , when the system is slow, i.e., when the rates are small. Summarizing, at each time step we need to determine the rates,  $p_i$ , a random number to draw which of the events will happen, and a random number to compute the time step (Gillespie, 1977, 2007).

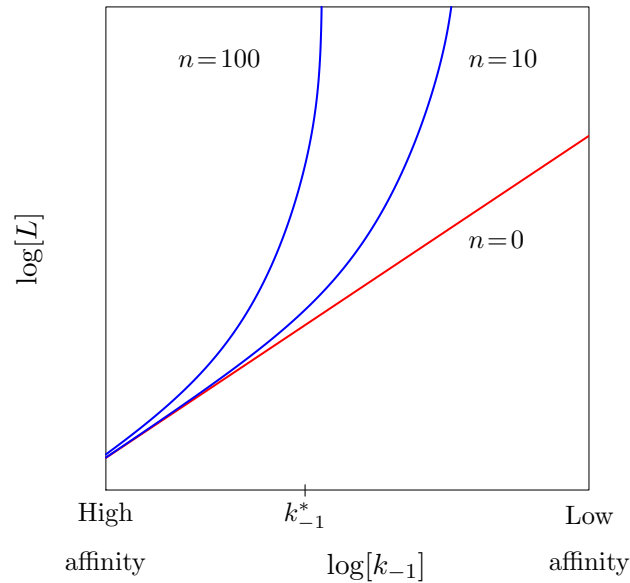


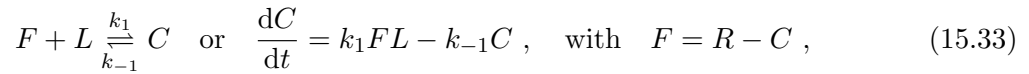
Figure 15.7: The Kinetic proofreading model. The figure shows the contour lines where  $C$  (red,  $n = 0$  line) or  $C_n$  (blue,  $n = 10$  or  $n = 100$  curved lines) exceeds a certain threshold,  $\theta$ . This was done for the Michaelis Menten model of Eq. (15.33) and the Kinetic proofreading model of Eq. (15.34), respectively, where the cells will get activated above the line, i.e., when the off-rate is sufficiently low and/or the ligand concentration is sufficiently large. For  $n = 100$  the  $C_n = \theta$ -cline approaches a vertical asymptote corresponding to the critical off-rate above which signaling never starts, whatever the ligand concentration,  $L$ . This figure was made with `proof.R`.

The R-script `gillespie.R` provides an example where a Grind model for Eq. (15.32) is also simulated with the Gillespie algorithm. The four rates are collected in the vector `rates`, the cumulative rates in the vector `summed`, and the associated changes of the state in the list `updates`. Note that the R function `which.max()` here returns the index of the first ‘true’ element in a vector (e.g., `which.max(c(F,F,T,T))` returns a 3). The script runs several simulations of Eq. (15.32) starting with  $R = 90$  and  $N = 10$  individuals, until the time exceeds a 100 time units (or until the system has died, i.e.,  $R = N = 0$ , making the sum of the rates zero). These trajectories typically approach the steady state of Eq. (15.32), and fluctuate around it. After running the simulations, the system of ODEs is integrated numerically, which illustrates that most simulations hover around the expected trajectory.

## 15.9 Kinetic proofreading

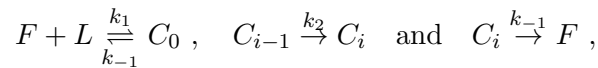
A famous chain of equations is the “Kinetic proofreading” chain, that was first proposed to improve the accuracy of transcription and translation (Hopfield, 1974; Ninio, 1975), and later to allow for the discrimination between ligands of low and high affinity during the activation of T cells (McKeithan, 1995). Quite recently experimental data confirmed that T cells indeed employ kinetic proofreading to respond, or not respond, to antigens (Voisinne *et al.*, 2022; Britain *et al.*, 2022); which is a fine example where theoretical predictions precede experimental confirmation by several decades (which is common in Theoretical Physics and apparently also happens in Theoretical Biology). We here shortly address kinetic proofreading in T cells by modeling the chain of phosphorylation events that receptors may undergo after binding their cognate ligand. Consider a population of  $R$  receptors on a cell with an on-rate,  $k_1$ , and an off-rate,  $k_{-1}$ , for a

particular ligand with a certain concentration  $L$ , and assume that the cell will become activated when sufficient receptors are ligated into a receptor-ligand complex  $C$ . The classic scheme for this is the Michaelis Menten reaction,



where the density of free receptors,  $F$ , is given by the conservation equation  $R = F + C$ . After making the QSSA  $dC/dt = 0$  one obtains the classic  $C = \frac{RL}{K_m + L}$ , where the Michaelis Menten constant,  $K_m = k_{-1}/k_1$ , is the inverse of the affinity. Since the number of complexes increases with the ligand concentration,  $L$ , until all receptors are ligated ( $\bar{C} = R$ ), high concentrations of low affinity ligands will ultimately activate the cell. Ligands can therefore not be discriminated on the basis of affinity, as a high concentration of a low affinity ligand can provide the same activation signal,  $C$ , as a low concentration of a high affinity ligand (see the red straight line in Fig. 15.7).

Kinetic proofreading does allow cells to discriminate between ligands, and the only requirement for that was the (realistic) extension of this scheme with a chain of modification steps of the complex, like phosphorylation events, that only occur when the receptor is binding the ligand. If the complex can become phosphorylated at a rate  $k_2$ , the scheme becomes



where  $F$  is again the concentration of free receptors, and the index  $i$  tracks the number of phosphorylation steps. For receptors having  $n$  different phosphorylation sites, this translates into the following chain

$$\frac{dC_0}{dt} = k_1FL - (k_{-1} + k_2)C_0, \quad \frac{dC_i}{dt} = k_2C_{i-1} - (k_{-1} + k_2)C_i, \quad \text{and} \quad \frac{dC_n}{dt} = k_2C_{n-1} - k_{-1}C_n \quad (15.34)$$

for  $i = 1, 2, \dots, n-1$ , and with the conservation equation  $F = R - \sum_i^n C_i$ . Upon dissociation of the ligand the receptor is assumed to de-phosphorylate rapidly (McKeithan, 1995). At steady state, the concentration of the fully phosphorylated complex can be written as

$$\bar{C}_n = \frac{RL}{K_m + L} \left( \frac{k_2}{k_{-1} + k_2} \right)^n, \quad (15.35)$$

where the first term is the same Michaelis Menten function, and the second term resembling Eq. (8.12c) introduces a novel dependence on the off-rate,  $k_{-1}$ , which becomes steep for sufficiently large  $k_{-1}$  and  $n$  (McKeithan, 1995). High concentrations of low-affinity ligands (with a fast off-rate) will therefore no longer lead to high concentrations of  $C_n$  on the cell surface (see Fig. 15.7). This allows cells to discriminate between high and low affinity ligands when their signaling is initiated after several phosphorylation steps only. In one of the exercises in Chapter 8 you were challenged to derive Eq. (15.35).

## 15.10 Tilman diagrams: the 4-dimensional Jacobian

In our online tutorial on Tilman diagrams [tbb.bio.uu.nl/rdb/bm/clips/tilman](http://tbb.bio.uu.nl/rdb/bm/clips/tilman) we explain that one can study the stability of the steady state of simple resource-consumer models by the Jacobian of the 4-dimensional system. The models used in Chapter 9 are somewhat more complicated because they use saturation functions for the amount of resources consumed for

defining the birth rate of the consumers. As a consequence, the Jacobi matrices are somewhat more complicated, but the interpretation remains very similar. For instance, the Jacobian of a  $2 \times 2$  model with substitutable resources, i.e., Eq. (9.22) for two consumers and two resources, can be written as

$$J = \begin{pmatrix} \partial_{R_1} R'_1 & \dots & \partial_{N_2} R'_1 \\ \vdots & \ddots & \\ \partial_{R_1} N'_2 & \dots & \partial_{N_2} N'_2 \end{pmatrix} = \begin{pmatrix} -d_1 - c_{11}\bar{N}_1 - c_{21}\bar{N}_2 & 0 & -c_{11}\bar{R}_1 & -c_{21}\bar{R}_1 \\ 0 & -d_2 - c_{12}\bar{N}_1 - c_{22}\bar{N}_2 & -c_{12}\bar{R}_2 & -c_{22}\bar{R}_2 \\ \Phi_1 c_{11} & \Phi_1 c_{12} & 0 & 0 \\ \Phi_2 c_{21} & \Phi_2 c_{22} & 0 & 0 \end{pmatrix} \quad (15.36)$$

where

$$\Phi_1 = \frac{\beta_1 h_1 \bar{N}_1}{(h_1 + c_{11}\bar{R}_1 + c_{12}\bar{R}_2)^2} \quad \text{and} \quad \Phi_2 = \frac{\beta_2 h_2 \bar{N}_2}{(h_2 + c_{21}\bar{R}_1 + c_{22}\bar{R}_2)^2}.$$

Fortunately, this more complicated matrix can be simplified into the same Jacobian used in the tutorial, i.e.,

$$J = \begin{pmatrix} -\rho_1 & 0 & -\gamma_{11} & -\gamma_{21} \\ 0 & -\rho_2 & -\gamma_{12} & -\gamma_{22} \\ \phi_{11} & \phi_{12} & 0 & 0 \\ \phi_{21} & \phi_{22} & 0 & 0 \end{pmatrix}. \quad (15.37)$$

In the tutorial we explain that the four eigenvalues defined by the characteristic equation of this Jacobi matrix will all be negative when the Routh-Horwitz criterion,

$$(\gamma_{11}\gamma_{22} - \gamma_{12}\gamma_{21})(\phi_{11}\phi_{22} - \phi_{12}\phi_{21}) > 0, \quad (15.38)$$

if fulfilled.

For substitutable resources, we know that the steady state can only exist if the two consumers have a sufficiently different diet (see Fig. 9.3a). Therefore consider a case where consumer one specializes on resource one, and consumer two on resource two, i.e.,  $c_{11} > c_{12}$  and  $c_{22} > c_{21}$  (see Fig. 9.3b). Checking the first term of Eq. (15.38) we see that in this case

$$(\gamma_{11}\gamma_{22} - \gamma_{12}\gamma_{21}) = (c_{11}\bar{R}_1 c_{22}\bar{R}_2 - c_{12}\bar{R}_2 c_{21}\bar{R}_1) > 0,$$

because  $c_{11}c_{22} > c_{12}c_{21}$ . For the second term of the  $a_0$  equation we observe in Eq. (15.36) that  $\phi_{11} > \phi_{12}$  when  $c_{11} > c_{12}$  and that  $\phi_{22} > \phi_{21}$  when  $c_{22} > c_{21}$ . As a consequence

$$\phi_{11}\phi_{22} - \phi_{12}\phi_{21} > 0 \quad \text{and, hence} \quad a_0 > 0,$$

which fulfills this Routh-Horwitz criterion, allowing the steady state to be stable. We conclude that if two consumers using two substitutable resources can co-exist, this steady state is expected to be stable (see Fig. 9.3b). Note that in the tutorial a similar steady state can also be unstable, which is not possible here because both resources are equally nutritious, i.e., they are weighted equally in the sum term of Eq. (9.22a).

**Essential resources.** Can the Routh-Horwitz criteria also tell the difference between the stable and unstable situation in Fig. 9.4? Using a  $2 \times 2$  version of Eq. (9.25) for two consumers using two “essential” resources, we obtain a Jacobian that is quite similar to that of Eq. (15.36) because only the four  $\partial_R N'$  elements change:

$$\begin{pmatrix} \partial_{R_1} N'_1 & \partial_{R_2} N'_1 \\ \partial_{R_1} N'_2 & \partial_{R_2} N'_2 \end{pmatrix} = \begin{pmatrix} \Phi_1 \frac{\bar{R}_2}{1 + \bar{R}_1/H_{11}} & \Phi_1 \frac{\bar{R}_1}{1 + \bar{R}_2/H_{12}} \\ \Phi_2 \frac{\bar{R}_2}{1 + \bar{R}_1/H_{21}} & \Phi_2 \frac{\bar{R}_1}{1 + \bar{R}_2/H_{22}} \end{pmatrix} = \begin{pmatrix} \phi_{11} & \phi_{12} \\ \phi_{21} & \phi_{22} \end{pmatrix} \quad (15.39)$$

where  $H_{ij} = h_{ij}/c_{ij}$  and

$$\Phi_1 = \frac{\beta_1 \bar{N}_1}{(H_{11} + \bar{R}_1)(H_{12} + \bar{R}_2)} \quad \text{and} \quad \Phi_2 = \frac{\beta_2 \bar{N}_2}{(H_{21} + \bar{R}_1)(H_{22} + \bar{R}_2)}.$$

The full Jacobian therefore has the same signs and zeros as the matrix in Eq. (15.36), which means that the same  $a_0 > 0$  criterion remains a condition for stability.

Again consider a case where consumer one specializes on resource one, and consumer two on resource two, i.e.,  $c_{11} > c_{12}$  and  $c_{22} > c_{21}$ . Like above, the first term of the  $a_0 > 0$  criterion,  $\gamma_{11}\gamma_{22} > \gamma_{12}\gamma_{21}$ , remains satisfied. However, the second term,  $\phi_{11}\phi_{22} > \phi_{12}\phi_{21}$ , need not be satisfied because the relative values of  $\phi_{ij}$  elements are no longer determined by the corresponding consumption rates,  $c_{ij}$ . For instance, if species one, which consumes most of resource one, would require more of resource two, i.e., if  $h_{11} < h_{12}$  (see Fig. 9.4b), the positive contribution of the first resource may become smaller than that of the second, and one can obtain that  $\phi_{11} < \phi_{12}$ . Setting the same “non-optimal” requirements for the second consumer one would also obtain that  $\phi_{22} < \phi_{21}$  (see Fig. 9.4b). Whenever  $(\phi_{11}\phi_{22} - \phi_{12}\phi_{21}) < 0$  and  $(\gamma_{11}\gamma_{22} - \gamma_{12}\gamma_{21}) > 0$ , the Routh-Horwitz criterion  $a_0 > 0$  fails, and the steady state is expected to be unstable (see Fig. 9.4d).

Like in the tutorial, we see that both consumers need to be restricted most by the resource they eat most. When consumers strongly require a resource that is more strongly depleted by another consumer than by themselves, they suffer more competition from the other consumer than from themselves. This destabilizes the steady state and leads to the “founder controlled” phase space of Fig. 9.4(d), where the initial condition determines which of the consumers survives.

## 15.11 Exercises

### Question 15.1. Sketch a few functions

In this course we sketch nullclines from models with free parameters. It is important therefore to know how to sketch arbitrary functions with free parameters (see the tutorial [tbb.bio.uu.nl/rdb/bm/clips/sketch](http://tbb.bio.uu.nl/rdb/bm/clips/sketch)):

- Sketch  $y = \frac{h}{h+x}$ .
- Sketch  $y = \frac{x}{h+x}$ .
- Sketch  $aA - bLA - cL = 0$  plotting  $L$  as a function of  $A$ , and plotting  $A$  as a function of  $L$ .
- Sketch  $0 = aY(1 - Y) - \frac{bYX}{c+Y}$ . Hint: think beforehand which variable can best be expressed as a function of the other variable.
- Sketch  $y = a \frac{k-x}{q+k-x} - d$  assuming that  $a > d$ .

### Question 15.2. Linearization

Consider the function  $f(x) = x^2$ .

- What is the derivative  $\partial_x f(x)$ ?
- Use linearization around  $x = 3$  to estimate the function value at  $x = 3.1$ . What is the true value at  $x = 3.1$ ?

### Question 15.3. Linear models

Study the linear system

$$\frac{dx}{dt} = ax + by \quad \text{and} \quad \frac{dy}{dt} = cx + dy .$$

What is the steady state of this system? Derive the Jacobi matrix for this system and use your knowledge of the eigenvalues of this matrix to choose values of  $a, b, c$ , and  $d$  such that you obtain a stable node, a spiral, and a saddle point. The model is provided as the file `linear.R`.



# Bibliography

- ABELSON, S., COLLORD, G., NG, S. W. K., WEISSBROD, O., MENDELSON COHEN, N., NIEMEYER, E., BARDA, N., ZUZARTE, P. C., HEISLER, L., SUNDARAVADANAM, Y., LUBEN, R., HAYAT, S., WANG, T. T., ZHAO, Z., CIRLAN, I., PUGH, T. J., SOAVE, D., NG, K., LATIMER, C., HARDY, C., RAINE, K., JONES, D., HOULT, D., BRITTEN, A., MCPHERSON, J. D., JOHANSSON, M., MBABAALI, F., EAGLES, J., MILLER, J. K., PASTERNAK, D., TIMMS, L., KRZYZANOWSKI, P., AWADALLA, P., COSTA, R., SEGAL, E., BRATMAN, S. V., BEER, P., BEHJATI, S., MARTINCORENA, I., WANG, J. C. Y., BOWLES, K. M., QUIROS, J. R., KARAKATSANI, A., LA VECCHIA, C., TRICHOPOULOU, A., SALAMANCA-FERNANDEZ, E., HUERTA, J. M., BARRICARTE, A., TRAVIS, R. C., TUMINO, R., MASALA, G., BOEING, H., PANICO, S., KAAKS, R., KRAMER, A., SIERI, S., RIBOLI, E., VINEIS, P., FOLL, M., MCKAY, J., POLIDORO, S., SALA, N., KHAW, K. T., VERMEULEN, R., CAMPBELL, P. J., PAPAEMMANUIL, E., MINDEN, M. D., TANAY, A., BALICER, R. D., WAREHAM, N. J., GERSTUNG, M., DICK, J. E., BRENNAN, P., VASSILIOU, G. S. & SHLUSH, L. I. (2018). Prediction of acute myeloid leukaemia risk in healthy individuals. *Nature* **559**, 400–404.
- ABRAMS, P. A. (1994). The fallacies of “ratio-dependent” predation. *Ecology* **75**, 1842–1850.
- ADLER, F. R. (1997). *Modeling the Dynamics of Life. Calculus and Probability for Life Scientists*. Pacific Grove: Brooks/Cole.
- AGENES, F., ROSADO, M. M. & FREITAS, A. A. (1997). Independent homeostatic regulation of B cell compartments. *Eur. J. Immunol.* **27**, 1801–1807.
- ANDERSON, R. M. & MAY, R. M. (1991). *Infectious diseases of humans. Dynamics and Control*. Oxford: Oxford U.P.
- ARDITI, R. & GINZBURG, L. R. (1989). Coupling in predator-prey dynamics: Ratio-dependence. *J. theor. Biol.* **139**, 311–326.
- ARDITI, R. & GINZBURG, L. R. (2012). *How Species Interact: Altering the Standard View on Trophic Ecology*. Oxford: Oxford U.P.
- BEDDINGTON, J. R. (1975). Mutual interference between parasites or predators and its effect on searching efficiency. *J. Anim. Ecol.* **51**, 597–624.
- BELAIR, J., MACKAY, M. C. & MAHAFFY, J. M. (1995). Age-structured and two-delay models for erythropoiesis. *Math. Biosci.* **128**, 317–346.
- BEREC, L., ANGULO, E. & COURCHAMP, F. (2007). Multiple Allee effects and population management. *Trends Ecol. Evol.* **22**, 185–191.
- BEVERTON, R. J. H. & HOLT, S. J. (1957). In: *On the dynamics of exploited fish populations*, vol. 19 of *Fish. Invest. Ser. 2*. London: Her majesty’s stationery office.

- BOERLIJST, M. C., OUDMAN, T. & DE ROOS, A. M. (2013). Catastrophic collapse can occur without early warning: examples of silent catastrophes in structured ecological models. *PLoS One* **8**, e62033.
- BOETTIGER, C., BODE, M., SANCHIRICO, J. N., LARIVIERE, J., HASTINGS, A. & ARMSWORTH, P. R. (2016). Optimal management of a stochastically varying population when policy adjustment is costly. *Ecol. Appl.* **26**, 808–817.
- BOETTIGER, C. & HASTINGS, A. (2012). Quantifying limits to detection of early warning for critical transitions. *J. R. Soc. Interface* **9**, 2527–2539.
- BOETTIGER, C. & HASTINGS, A. (2013). Tipping points: From patterns to predictions. *Nature* **493**, 157–158.
- BOHANNAN, B. J. M. & LENSKI, R. E. (1997). Effect of resource enrichment on a chemostat community of bacteria and bacteriophage. *Ecology* **78**, 2303–2315.
- BOHANNAN, B. J. M. & LENSKI, R. E. (1999). Effect of Prey Heterogeneity on the Response of a Model Food Chain to Resource Enrichment. *Am. Nat.* **153**, 73–82.
- BORGHANS, J. A. M., DE BOER, R. J. & SEGEL, L. A. (1996). Extending the quasi-steady state approximation by changing variables. *Bull. Math. Biol.* **58**, 43–63.
- BRITAIN, D. M., TOWN, J. P. & WEINER, O. D. (2022). Progressive enhancement of kinetic proofreading in T cell antigen discrimination from receptor activation to DAG generation. *Elife* **11**.
- BUSS, L. F., PRETE, JR, C. A., ABRAHIM, C. M. M., MENDRONE, JR, A., SALOMON, T., DE ALMEIDA-NETO, C., FRANÇA, R. F. O., BELOTTI, M. C., CARVALHO, M. P. S. S., COSTA, A. G., CRISPIM, M. A. E., FERREIRA, S. C., FRAJI, N. A., GURZENDA, S., WHITTAKER, C., KAMAURA, L. T., TAKECIAN, P. L., DA SILVA PEIXOTO, P., OIKAWA, M. K., NISHIYA, A. S., ROCHA, V., SALLES, N. A., DE SOUZA SANTOS, A. A., DA SILVA, M. A., CUSTER, B., PARAG, K. V., BARRAL-NETTO, M., KRAEMER, M. U. G., PEREIRA, R. H. M., PYBUS, O. G., BUSCH, M. P., CASTRO, M. C., DYE, C., NASCIMENTO, V. H., FARIA, N. R. & SABINO, E. C. (2021). Three-quarters attack rate of SARS-CoV-2 in the Brazilian Amazon during a largely unmitigated epidemic. *Science* **371**, 288–292.
- CASTRO, M. & DE BOER, R. J. (2020). Testing structural identifiability by a simple scaling method. *PLOS Comput. Biol.* **16**, e1008248.
- CASWELL, H. (1976). Community structure: A neutral model analysis. *Ecological Monographs* **46**, 327–354.
- CICIN-SAIN, L., MESSAOUDI, I., PARK, B., CURRIER, N., PLANER, S., FISCHER, M., TACKITT, S., NIKOLICH-ZUGICH, D., LEGASSE, A., AXTHELM, M. K., PICKER, L. J., MORI, M. & NIKOLICH-ZUGICH, J. (2007). Dramatic increase in naive T cell turnover is linked to loss of naive T cells from old primates. *Proc. Natl. Acad. Sci. U.S.A.* **104**, 19960–19965.
- COHEN, J. E. (1995). Population growth and earth's human carrying capacity. *Science* **269**, 341–346.
- CORNEJO, O. E., ROZEN, D. E., MAY, R. M. & LEVIN, B. R. (2009). Oscillations in continuous culture populations of *Streptococcus pneumoniae*: population dynamics and the evolution of clonal suicide. *Proc. Biol. Sci.* **276**, 999–1008.

- CUI, W., MARSLAND, R. & MEHTA, P. (2021). Diverse communities behave like typical random ecosystems. *Phys. Rev. E* **104**, 034416.
- DAL BELLO, M., LEE, H., GOYAL, A. & GORE, J. (2021). Resource-diversity relationships in bacterial communities reflect the network structure of microbial metabolism. *Nat. Ecol. Evol.* **5**, 1424–1434.
- DE BOER, R. J. (2012). Which of our modeling predictions are robust? *PLoS. Comput. Biol.* **8**, e1002593.
- DE BOER, R. J. & PERELSON, A. S. (1995). Towards a general function describing T cell proliferation. *J. theor. Biol.* **175**, 567–576.
- DEANGELIS, D. L., GOLDSTEIN, R. A. & O'NEILL, R. V. (1975). A model for trophic interaction. *Ecology* **56**, 881–892.
- DEN BRABER, I., MUGWAGWA, T., VRISEKOOP, N., WESTERA, L., MOGLING, R., DE BOER, A. B., WILLEMS, N., SCHRIJVER, E. H., SPIERENBURG, G., GAISER, K., MUL, E., OTTO, S. A., RUITER, A. F., ACKERMANS, M. T., MIEDEMA, F., BORGHANS, J. A., DE BOER, R. J. & TESSELAAR, K. (2012). Maintenance of peripheral naive T cells is sustained by thymus output in mice but not humans. *Immunity* **36**, 288–297.
- DERCOLE, F., FERRIÈRE, R. & RINALDI, S. (2002). Ecological bistability and evolutionary reversals under asymmetrical competition. *Evolution*. **56**, 1081–1090.
- DIEKMANN, O., HEESTERBEEK, H. & BRITTON, T. (2012). *Mathematical tools for understanding infectious disease dynamics*. Princeton University Press.
- DIEKMANN, O., HEESTERBEEK, J. A. & METZ, J. A. (1990). On the definition and the computation of the basic reproduction ratio  $R_0$  in models for infectious diseases in heterogeneous populations. *J. Math. Biol.* **28**, 365–382.
- ETIENNE, R. S. (2007). A neutral sampling formula for multiple samples and an 'exact' test of neutrality. *Ecol. Lett.* **10**, 608–618.
- FERRIERE, R. & LEGENDRE, S. (2013). Eco-evolutionary feedbacks, adaptive dynamics and evolutionary rescue theory. *Philos. Trans. R. Soc. Lond. B Biol. Sci.* **368**, 20120081.
- FRECKLETON, R. P., WATKINSON, A. R., GREEN, R. E. & SUTHERLAND, W. J. (2006). Census error and the detection of density dependence. *J. Anim. Ecol.* **75**, 837–851.
- FUSSMANN, G. F., ELLNER, S. P., SHERTZER, K. W. & HAIRSTON, JR, N. G. (2000). Crossing the hopf bifurcation in a live predator-prey system. *Science* **290**, 1358–1360.
- GADHAMSETTY, S., COORENS, T. & DE BOER, R. J. (2016). Notwithstanding circumstantial alibis, cytotoxic T cells can be major killers of HIV-1-infected cells. *J. Virol.* **90**, 7066–7083.
- GADHAMSETTY, S., MAREE, A. F. M., BELTMAN, J. B. & DE BOER, R. J. (2017). A Sigmoid Functional Response Emerges When Cytotoxic T Lymphocytes Start Killing Fresh Target Cells. *Biophys. J.* **112**, 1221–1235.
- GANUSOV, V. V. (2016). Strong Inference in Mathematical Modeling: A Method for Robust Science in the Twenty-First Century. *Front. Microbiol.* **7**, 1131.
- GANUSOV, V. V., PILYUGIN, S. S., DE BOER, R. J., MURALI-KRISHNA, K., AHMED, R. & ANTIA, R. (2005). Quantifying cell turnover using CFSE data. *J. Immunol. Methods.* **298**, 183–200.

- GARDNER, M. R. & ASHBY, W. R. (1970). Connectivity of large, dynamical (cybernetic) systems: critical values for stability. *Nature* **228**, 784.
- GAUSE, G. F. (1934). Experimental analysis of Vito Volterra's mathematical theory of the struggle for existence. *Science* **79**, 16–17.
- GELLNER, G., MCCANN, K. & HASTINGS, A. (2023). Stable diverse food webs become more common when interactions are more biologically constrained. *Proc. Natl. Acad. Sci. U.S.A.* **120**, e-2082906176.
- GERITZ, S. A. & KISDI, E. (2004). On the mechanistic underpinning of discrete-time population models with complex dynamics. *J. theor. Biol.* **228**, 261–269.
- GILLESPIE, D. (1977). Exact stochastic simulation of coupled chemical reactions. *J. Phys. Chem.* **81**, 2340–2361.
- GILLESPIE, D. T. (2007). Stochastic simulation of chemical kinetics. *Annu. Rev. Phys. Chem.* **58**, 35–55.
- GINZBURG, L. R. & AKÇAKAYA, H. R. (1992). Consequences of ratio-dependent predation for steady-state properties of ecosystems. *Ecology* **93**, 1536–1543.
- GOLDFORD, J. E., LU, N., BAJIĆ, D., ESTRELA, S., TIKHONOV, M., SANCHEZ-GOROSTIAGA, A., SEGRÈ, D., MEHTA, P. & SANCHEZ, A. (2018). Emergent simplicity in microbial community assembly. *Science* **361**, 469–474.
- GRIME, J. P. (1997). Biodiversity and ecosystem function: the debate deepens. *Science* **277**, 1260–1261.
- HANKSI, I. (1997). Be diverse, be predicatable. *Nature* **390**, 440–441.
- HANKSI, I. (1998). Metapopulation dynamics. *Nature* **396**, 41–49.
- HASSELL, M. P. (1975). Density-dependence in single-species populations. *J. Anim. Ecol.* **44**, 283–295.
- HASSELL, M. P., LAWTON, J. H. & MAY, R. M. (1976). Patterns of dynamical behaviour in single-species populations. *J. Anim. Ecol.* **45**, 471–486.
- HASTINGS, A. (1997). *Population biology: concepts and models*. New York: Springer.
- HASTINGS, A. & POWELL, T. (1991). Chaos in a three-species food chain. *Ecology* **72**, 896–903.
- HAYFLICK, L. (1988). Why do we live so long? *Geriatrics* **43**, 77–79.
- HAZENBERG, M. D., OTTO, S. A., STUART, J. W., VERSCHUREN, M. C., BORLEFFS, J. C., BOUCHER, C. A., COUTINHO, R. A., LANGE, J. M., DE WIT, T. F., TSEGAYE, A., VAN DONGEN, J. J., HAMANN, D., DE BOER, R. J. & MIEDEMA, F. (2000). Increased cell division but not thymic dysfunction rapidly affects the T-cell receptor excision circle content of the naive T cell population in HIV-1 infection. *Nat. Med.* **6**, 1036–1042.
- HEFFERNAN, J. M., SMITH, R. J. & WAHL, L. M. (2005). Perspectives on the basic reproductive ratio. *J. R. Soc. Interface* **2**, 281–293.
- HIROTA, M., HOLMGREN, M., VAN NES, E. H. & SCHEFFER, M. (2011). Global resilience of tropical forest and savanna to critical transitions. *Science* **334**, 232–235.

- HOGEWEG, P. & HESPER, B. (1978). Interactive instruction on population interactions. *Comput. Biol. Med.* **8**, 319–327.
- HOLLING, C. S. (1959). The characteristics of simple types of predation and parasitism. *Can. Entomol.* **91**, 385–399.
- HOPFIELD, J. J. (1974). Kinetic proofreading: a new mechanism for reducing errors in biosynthetic processes requiring high specificity. *Proc. Natl. Acad. Sci. U.S.A.* **71**, 4135–4139.
- HUBBELL, S. P. (1979). Tree dispersion, abundance, and diversity in a tropical dry forest. *Science* **203**, 1299–1309.
- HUBBELL, S. P. (2001). *The Unified Neutral Theory of Biodiversity and Biogeography. Monographs in Population Biology*. Princeton: Princeton U.P.
- HUISMAN, G. & DE BOER, R. J. (1997). A formal derivation of the “Beddington” functional response. *J. theor. Biol.* **185**, 389–400.
- HUISMAN, J., JOHANSSON, A. M., FOLMER, E. O. & WEISSING, F. J. (2001). Towards a solution of the plankton paradox: the importance of physiology and life history. *Ecology Letters* **4**, 408–411.
- HUISMAN, J. & WEISSING, F. J. (1999). Biodiversity of plankton by species oscillations and chaos. *Nature* **402**, 407–410.
- HUTCHINSON, G. E. (1961). The paradox of the plankton. *The American Naturalist* **95**, 137–145.
- JACOB, F. & MONOD, J. (1961). Genetic regulatory mechanisms in the synthesis of proteins. *J. Mol. Biol.* **3**, 318–356.
- JAMES, G., WITTEN, D., HASTIE, T. & TIBSHIRANI, R. (2014). *An Introduction to Statistical Learning: With Applications in R*. Springer Publishing Company.
- JIANG, W., MANIV, I., ARAIN, F., WANG, Y., LEVIN, B. R. & MARRAFFINI, L. A. (2013). Dealing with the Evolutionary Downside of CRISPR Immunity: Bacteria and Beneficial Plasmids. *PLoS. Genet.* **9**, e1003844.
- KAUNZINGER, C. M. K. & MORIN, P. J. (1998). Productivity controls food-chain properties in microbial communities. *Nature* **395**, 495–497.
- KRAMER, A. M., DENNIS, B., LIEBHOLD, A. M. & DRAKE, J. M. (2009). The evidence for allee effects. *Population Ecology* **51**, 341.
- LANDER, A. D., GOKOFFSKI, K. K., WAN, F. Y., NIE, Q. & CALOF, A. L. (2009). Cell lineages and the logic of proliferative control. *PLoS. Biol.* **7**, e15.
- LAW, R. & BLACKFORD, J. C. (1992). Self-assembling food webs - a global viewpoint of coexistence of species in Lotka-Volterra communities. *Ecology* **73**, 567–578.
- LEVIN, B. R., MOINEAU, S., BUSHMAN, M. & BARRANGOU, R. (2013). The population and evolutionary dynamics of phage and bacteria with CRISPR-mediated immunity. *PLoS. Genet.* **9**, e1003312.
- LEVINS, R. (1969). Some demographic and genetic consequences of environmental heterogeneity for biological control. *Bull. Ent. Soc. Am.* **15**, 237–240.

- LEVINS, R. & CULVER, D. (1971). Regional Coexistence of Species and Competition between Rare Species. *Proc. Nat. Acad. Sci USA*. **68**, 1246–1248.
- LI, T. A. & YORKE, J. A. (1975). Period three implies chaos. *Amer. Math. Monthly* **82**, 985–992.
- LIAO, C., WANG, T., MASLOV, S. & XAVIER, J. B. (2020). Modeling microbial cross-feeding at intermediate scale portrays community dynamics and species coexistence. *PLOS Comput. Biol.* **16**, e1008135.
- LIPSITCH, M., COHEN, T., COOPER, B., ROBINS, J. M., MA, S., JAMES, L., GOPALAKRISHNA, G., CHEW, S. K., TAN, C. C., SAMORE, M. H., FISMAN, D. & MURRAY, M. (2003). Transmission dynamics and control of severe acute respiratory syndrome. *Science* **300**, 1966–1970.
- LOTKA, A. J. (1913). A natural population norm. *J. Wash. Acad. Sci.* **3**, 289–293.
- LUCKINBILL, L. S. (1973). Coexistence in laboratory populations of *Paramecium aurelia* and its predator *Didinium nasutum*. *Ecology* **54**, 1320–1327.
- MACARTHUR, R. H. (1972). *Geographical Ecology*. New York: Harper & Row.
- MACARTHUR, R. H. & WILSON, E. O. (1967). *The Theory of Island Biogeography*. Princeton, NJ: Princeton University Press.
- MALKA, R., WOLACH, B., GAVRIELI, R., SHOCHAT, E. & ROM-KEDAR, V. (2012). Evidence for bistable bacteria-neutrophil interaction and its clinical implications. *J. Clin. Invest.* **122**, 3002–3011.
- MARSLAND, R., CUI, W. & MEHTA, P. (2020). A minimal model for microbial biodiversity can reproduce experimentally observed ecological patterns. *Scientific Reports*. **10**, 3308.
- MATSUDA, H. & ABRAMS, P. A. (1994). Runaway evolution to self-extinction under asymmetrical competition. *Evolution*. **48**, 1764–1772.
- MAY, R. M. (1972). Will a large complex system be stable? *Nature* **238**, 413–414.
- MAY, R. M. (1974). *Stability and complexity in model ecosystems*, vol. 6 of *Monographs in population biology*. Princeton, New Jersey: Princeton University Press, second edn.
- MAY, R. M. (1977). Thresholds and breakpoints in ecosystems with a multiplicity of stable states. *Nature* **269**, 471–477.
- MAY, R. M. (2004). Uses and abuses of mathematics in biology. *Science* **303**, 790–793.
- MAYNARD SMITH, J. & SLATKIN, M. (1973). The stability of predator-prey systems. *Ecol.* **54**, 384–391.
- MCCANN, K., HASTINGS, A. & HUXEL, G. R. (1998). Weak trophic interactions and the balance of nature. *Nature* **395**, 794–798.
- MCCAULEY, E., NISBET, R. M., MURDOCH, W. W., DE ROOS, A. M. & GURNEY, W. S. C. (1999). Large-amplitude cycles of *Daphnia* and its algal prey in enriched environments. *Nature* **402**, 653–656.
- MCKEITHAN, T. W. (1995). Kinetic proofreading in T-cell receptor signal transduction. *Proc. Natl. Acad. Sci. U.S.A.* **92**, 5042–5046.

- MCLEAN, A. & MAY, R. M. (2007). *Theoretical Ecology: Principles and Applications*. Oxford: Oxford University Press.
- MONOD, J. (1949). The growth of bacterial cultures. *Annual Review of Microbiology* **3**, 371–394.
- MURDOCH, W. W., KENDALL, B. E., NISBET, R. M., BRIGGS, C. J., MCCAULEY, E. & BOLSER, R. (2002). Single-species models for many-species food webs. *Nature* **417**, 541–543.
- MYLIUS, S. D. & DIEKMANN, O. (1995). On evolutionarily stable life histories, optimization and the need to be specific about density dependence. *Oikos* **74**, 218–224.
- NEUTEL, A. M., HEESTERBEEK, J. A. & DE RUITER, P. C. (2002). Stability in real food webs: weak links in long loops. *Science* **296**, 1120–1123.
- NEUTEL, A. M., HEESTERBEEK, J. A., VAN DE KOPPEL, J., HOENDERBOOM, G., VOS, A., KALDEWAY, C., BERENDSE, F. & DE RUITER, P. C. (2007). Reconciling complexity with stability in naturally assembling food webs. *Nature* **449**, 599–602.
- NINIO, J. (1975). Kinetic amplification of enzyme discrimination. *Biochimie*. **57**, 587–595.
- NOWAK, M. A. & MAY, R. M. (2000). *Virus dynamics. Mathematical principles of immunology and virology*. Oxford: Oxford U.P.
- NOY-MEIR, I. (1975). Stability of grazing systems: an application of predator-prey graphs. *J. Ecology* **63**, 459–483.
- O'DWYER, J. P. (2018). Whence lotka-volterra? conservation laws and integrable systems in ecology. *Theoretical Ecology* pp. 1874–1738.
- PANFILOV, A. V., TEN TUSSCHER, K. H. W. J. & DE BOER, R. J. (2025). *Matrices, Linearization, and the Jacobi matrix*. EBook: <http://tbb.bio.uu.nl/rdb/books/math.pdf>.
- PHAIBOUN, A., ZHANG, Y., PARK, B. & KIM, M. (2015). Survival kinetics of starving bacteria is biphasic and density-dependent. *PLoS. Comput. Biol.* **11**, e1004198.
- PIANKA, E. R. (1974). Niche overlap and diffuse competition. *Proc. Natl. Acad. Sci. U.S.A.* **71**, 2141–2145.
- PIMM, S. L. (1980). Properties of food webs. *Ecology* **61**, 219–225.
- POSFAI, A., TAILLEFUMIER, T. & WINGREEN, N. S. (2017). Metabolic Trade-Offs Promote Diversity in a Model Ecosystem. *Phys. Rev. Lett.* **118**, 028103.
- POST, W. M. & PIMM, S. L. (1983). Community assembly and food web stability. *Math. Biosci.* **64**, 169–192.
- RAM, Y., DELLUS-GUR, E., BIBI, M., KARKARE, K., OBOLSKI, U., FELDMAN, M. W., COOPER, T. F., BERMAN, J. & HADANY, L. (2019). Predicting microbial growth in a mixed culture from growth curve data. *Proc. Natl. Acad. Sci. U.S.A.* **116**, 14698–14707.
- RANKIN, D. J. & LOPEZ-SEPULCRE, A. (2005). Can adaptation lead to extinction? *Oikos* **111**, 616–619.
- RAPPOLDT, C. & HOGEWEG, P. (1980). Niche packing and number of species. *Am. Nat.* **116**, 480–492.
- RICHARDS, F. J. (1959). A Flexible Growth Function for Empirical Use. *Journal of Experimental Botany* **10**, 290–301.

- RIETKERK, M. & VAN DE KOPPEL, J. (1997). Alternate stable states and threshold effects in semi-arid grazing systems. *Oikos* **79**, 69–76.
- ROBERTS, A. (1974). The stability of a feasible random ecosystem. *Nature* **251**, 608.
- RODRIGUEZ-SANCHEZ, P., VAN NES, E. H. & SCHEFFER, M. (2020). Neutral competition boosts cycles and chaos in simulated food webs. *R. Soc. Open. Sci.* **7**, 191532.
- ROSENZWEIG, M. L. (1971). Paradox of enrichment: destabilization of exploitation ecosystems in ecological time. *Science* **171**, 385–387.
- SABINO, E. C., BUSS, L. F., CARVALHO, M. P. S., PRETE, JR, C. A., CRISPIM, M. A. E., FRAJI, N. A., PEREIRA, R. H. M., PARAG, K. V., DA SILVA PEIXOTO, P., KRAEMER, M. U. G., OIKAWA, M. K., SALOMON, T., CUCUNUBA, Z. M., CASTRO, M. C., DE SOUZA SANTOS, A. A., NASCIMENTO, V. H., PEREIRA, H. S., FERGUSON, N. M., PYBUS, O. G., KUCHARSKI, A., BUSCH, M. P., DYE, C. & FARIA, N. R. (2021). Resurgence of COVID-19 in Manaus, Brazil, despite high seroprevalence. *Lancet* **397**, 452–455.
- SCHEFFER, M. (1991). Fish and nutrients interplay determines algal biomass - a minimal model. *Oikos* **62**, 271–282.
- SCHEFFER, M. (2009). *Critical Transitions in Nature and Society*. Princeton: Princeton U.P.
- SCHEFFER, M., BASCOMPTE, J., BROCK, W. A., BROVKIN, V., CARPENTER, S. R., DAKOS, V., HELD, H., VAN NES, E. H., RIETKERK, M. & SUGIHARA, G. (2009). Early-warning signals for critical transitions. *Nature* **461**, 53–59.
- SCHEFFER, M., CARPENTER, A., FOLEY, J. A., FOLKE, C. & WALKER, B. (2001). Catastrophic shifts in ecosystems. *Nature* **413**, 591–596.
- SCHEFFER, M., CARPENTER, S. R., LENTON, T. M., BASCOMPTE, J., BROCK, W., DAKOS, V., VAN DE KOPPEL, J., VAN DE LEEMPUT, I. A., LEVIN, S. A., VAN NES, E. H., PASCUAL, M. & VANDERMEER, J. (2012). Anticipating critical transitions. *Science* **338**, 344–348.
- SCHEFFER, M. & DE BOER, R. J. (1995). Implications of spatial heterogeneity for the paradox of enrichment. *Ecology* **76**, 2270–2277.
- SCHEFFER, M., RINALDI, S., KUZNETSOV, Y. A. & VAN NES, E. H. (1997). Seasonal dynamics of *Daphnia* and algae explained as a periodically forced predator-prey system. *Oikos* **80**, 519–532.
- SCHEFFER, M. & VAN NES, E. H. (2006). Self-organized similarity, the evolutionary emergence of groups of similar species. *Proc. Natl. Acad. Sci. U.S.A.* **103**, 6230–6235.
- SCHIRM, S., ENGEL, C., LOEFFLER, M. & SCHOLZ, M. (2013). A biomathematical model of human erythropoiesis under erythropoietin and chemotherapy administration. *PLoS. One.* **8**, e65630.
- SHENK, T. M., WHITE, G. C. & BURNHAM, K. P. (1998). Sampling-variance effects on detecting density dependence from temporal trends in natural populations. *Ecological Monographs* **68**, 445–463.
- SMITH, J. A. & MARTIN, L. (1973). Do cells cycle? *Proc. Natl. Acad. Sci. U.S.A.* **70**, 1263–1267.

- SOETAERT, K. (2009). *rootSolve: Nonlinear root finding, equilibrium and steady-state analysis of ordinary differential equations*. R package 1.6.
- SOETAERT, K. & HERMAN, P. M. (2009). *A Practical Guide to Ecological Modelling. Using R as a Simulation Platform*. Springer. ISBN 978-1-4020-8623-6.
- SOETAERT, K. & PETZOLDT, T. (2010). Inverse modelling, sensitivity and Monte Carlo analysis in R using package FME. *Journal of Statistical Software* **33**, 1–28.
- SOETAERT, K., PETZOLDT, T. & SETZER, R. W. (2010). Solving differential equations in R: Package deSolve. *Journal of Statistical Software* **33**, 1–25.
- SPRAGGE, F., BAKKEREN, E., JAHN, M. T., B N ARAUJO, E., PEARSON, C. F., WANG, X., PANKHURST, L., CUNRATH, O. & FOSTER, K. R. (2023). Microbiome diversity protects against pathogens by nutrient blocking. *Science* **382**, eadj3502.
- STENSETH, N. C., CHAN, K., TONG, H., BOONSTRA, R., BOUTIN, S., KREBS, C. J., POST, E., O'DONOGHUE, M., YOCOZ, N. G., FORCHHAMMER, M. C. & HURRELL, J. W. (1999). Common Dynamic Structure of Canada Lynx Populations Within Three Climatic Regions. *Science* **285**, 1071–1073.
- TEXTOR, J., HENRICKSON, S. E., MANDL, J. N., VON ANDRIAN, U. H., WESTERMANN, J., DE BOER, R. J. & BELTMAN, J. B. (2014). Random migration and signal integration promote rapid and robust T cell recruitment. *PLOS Comput. Biol.* **10**, e1003752.
- TILMAN, D. (1980). Resources: a graphical-mechanistic approach to competition and predation. *The American Naturalist* **116**, 362–393.
- TILMAN, D. (1982). *Resource competition and community structure*, vol. 17 of *Monographs in population biology*. Princeton, New Jersey: Princeton University Press.
- TILMAN, D., LEHMAN, C. L. & THOMSON, K. T. (1997). Plant diversity and ecosystem productivity: theoretical considerations. *Proc. Natl. Acad. Sci. U.S.A.* **94**, 1857–1861.
- TILMAN, D., MAY, R. M., LEHMAN, C. L. & NOWAK, M. A. (1994). Habitat destruction and the extinction debt. *Nature* **371**, 65–66.
- VERAART, A. J., FAASSEN, E. J., DAKOS, V., VAN NES, E. H., LURLING, M. & SCHEFFER, M. (2012). Recovery rates reflect distance to a tipping point in a living system. *Nature* **481**, 357–359.
- VOISINNE, G., LOCARD-PAULET, M., FROMENT, C., MATURIN, E., MENOITA, M. G., GIRARD, L., MELLADO, V., BURLET-SCHILTZ, O., MALISSEN, B., GONZALEZ DE PEREDO, A. & RONCAGALLI, R. (2022). Kinetic proofreading through the multi-step activation of the ZAP70 kinase underlies early T cell ligand discrimination. *Nat. Immunol.* **23**, 1355–1364.
- VOLTERRA, V. (1926). Fluctuations in the abundance of a species considered mathematically. *Nature* **118**, 558–560.
- WALKER, M., HALL, A., ANDERSON, R. M. & BASANEZ, M. G. (2009). Density-dependent effects on the weight of female *Ascaris lumbricoides* infections of humans and its impact on patterns of egg production. *Parasit. Vectors.* **2**, 11.
- WEITZ, J. S. (2015). *Quantitative Viral Ecology: Dynamics of Viruses and Their Microbial Hosts*. Princeton University Press.

- WIESER, R. J. & OESCH, F. (1986). Contact inhibition of growth of human diploid fibroblasts by immobilized plasma membrane glycoproteins. *J. Cell Biol.* **103**, 361–367.
- WINTER, C., BOUVIER, T., WEINBAUER, M. G. & THINGSTAD, T. F. (2010). Trade-offs between competition and defense specialists among unicellular planktonic organisms: the "killing the winner" hypothesis revisited. *Microbiol. Mol. Biol. Rev.* **74**, 42–57.
- WOODCOCK, S., VAN DER GAST, C. J., BELL, T., LUNN, M., CURTIS, T. P., HEAD, I. M. & SLOAN, W. T. (2007). Neutral assembly of bacterial communities. *FEMS. Microbiol. Ecol.* **62**, 171–180.
- YODZIS, P. (1978). *Competition for space and the structure of ecological communities*. Berlin: Springer-Verlag.
- YODZIS, P. (1989). *Introduction to Theoretical Ecology*. New York: Harper & Row.
- YOSHIDA, T., ELLNER, S. P., JONES, L. E., BOHANNAN, B. J., LENSKI, R. E. & HAIRSTON, JR, N. G. (2007). Cryptic population dynamics: rapid evolution masks trophic interactions. *PLoS. Biol.* **5**, e235.
- YOSHIDA, T., JONES, L. E., ELLNER, S. P., FUSSMANN, G. F. & HAIRSTON NELSON G, J. (2003). Rapid evolution drives ecological dynamics in a predator-prey system. *Nature* **424**, 303–306.